Anti-myeloperoxidase associated glomerulonephritis: a study of innate immune activation

Hamad Al Nuaimi

A thesis submitted to the University of Birmingham for the degree of Doctor of Philosophy

Department of Immunity and Infection

Supervisors:

Professor Mark Little

Professor Caroline Savage

2011

Abstract

ANCA-associated vasculitis (AAV) is characterised by macrophage and neutrophil infiltration at the site of injury. Animal models have been used to study the disease and to try different treatment approaches. The aim of this study was to investigate the involvement of the innate immune system in AAV. This was done by looking at different innate immune system components such as macrophages and neutrophils.

There were a large number of CD68+ cells in the crescent region of the kidney following treatment with anti-MPO antibodies and LPS. Serial section staining has shown that these cells are more likely to be classically activated macrophages. Furthermore, gene expression studies have confirmed the up regulation of genes associated with classically activated macrophages such as calprotectin. In addition, there was an up regulation of genes associated with macrophages accumulation such as CCR2 and CX3CR1. These macrophages could be involved in secreting TGF-β, which was up regulated, which can lead to an increase in extracellular matrix such as collagen. Blocking macrophage accumulation was evaluated using anti-mouse CCR2 which was effective in depleting GR1+ blood monocytes. However, there was no significant difference on the disease outcome following treatment with anti-mouse CCR2. This suggests a lesser role of macrophages in the development of vasculitis or that disease was mild and so an effect could not be identified.

In addition, I investigated the variability in ANCA-induced neutrophil degranulation from healthy donors. I purified human neutrophils from healthy donors and treated them with different ANCA IgG samples. I found that these neutrophils responded differently to the same ANCA IgG as measured by neutrophil degranulation using ELISA. I tried to study the resulting metabolites using mass spectrometry but there was a considerable degree of technical variation which prevented making final conclusions. However, this was a novel approach and provided me with good ideas on how to take it further. I also looked at the

effect of pre-treating neutrophils with simvastatin. I found a significant reduction in ANCA-induced neutrophil degranulation following treatment with a statin.

In conclusion, preventing macrophage infiltration did not have an effect on the development of the disease in mice. This could be because the disease was mild or because resident macrophages are more important than infiltrating ones. In addition, the microarray experiment has provided interesting results that could be used to find common pathways in mouse, rat and human. It also provided more information on genes that are upregulated in the kidney following AAV induction. This could be used to arrange the genes into pathways and biological processes to study the involvement of macrophages and other components of the innate immune system. Finally, simvastatin significantly reduced ANCA-induced neutrophil degranulation.

Acknowledgements

This work was funded by the General Health Authority in Abu Dhabi, United Arab Emirates.

I have been greatly supported in this work by my supervisors Professor Mark Little (now at Trinity College Dublin) and Professor Caroline Savage (FRCP FMedSci).

Immunoglobulin G (IgG) and murine myeloperoxidase were purified with the help of Dr. Gregg Wallis (University of Birmingham).

At the start of my PhD, anti-MPO antibodies were kindly donated to me by Dr. Peter Heeringa (University Medical Centre Groningen, The Netherland).

I had a lot of support from Dr. Margaret Goodall (University of Birmingham) on culturing WEHI cells.

I would like to thank everyone in our group for their help and support during my PhD.

I am very grateful to my family, and especially to my parents and my wife, for help and support throughout my PhD.

Table of Contents

List of Figures:

List of Tables

Abbreviations

AAV	ANCA-associated vasculitis
MPO	Myeloperoxidase
ANCA	Anti-neutrophil cytoplasm antibodies
WG	Wegener's granulomatosis
PR3	Proteinase 3
cANCA	Cytoplasmic anti neutrophil cytoplasm antibodies
pANCA	Perinuclear anti-neutrophil cytoplasm antibodies
FNGN	Focal necrotising glomerulonephritis
LAMP-2	Lysosomal membrane protein-2
NTN	Nephrotoxic nephritis
NCGN	Necrotising and crescentic glomerulonephritis
TNF-α	Tumor necrosis factor alpha
Fc	Fragment crystalline
Fab	Fragment antibody binding
FcγR	Fc gamma receptor
IgG	immunoglobulin
MCP-1	Monocyte chemoattractant protein 1
CCR2	Chemokine receptor 2
GBM	Glomerular basement membrane
LPS	Lipopolysacharide
TGF-β	Transforming growth factor beta

Publications Arising from This Thesis

Papers

- Al-Ani B, Al Nuaimi H, Savage C, Little M, Shimizu A, Fujita E, Nagasaka S.

  The Beneficial Effects of Statin Therapy May Not Apply to All Forms of Crescentic Glomerulonephritis. *Correspondence, Am J Pathol. 2011 May; 178(5):2447.*

- Little M, Al-Ani B, Ren SY, Al Nuaimi H, Alpers CE, Savage C, Duffield JS.

  Anti-Proteinase 3 Anti-Neutrophil Cytoplasm Autoantibodies Recapitulate Systemic Vasculitis in Mice with a Humanized Immune System. *PLoS One. 2012 Jan; 7(1):e28626*

Abstracts

- Al-Ani B, Al Nuaimi H, Smith S, Young SP, Savage C, Little MA.

  Remission, relapse and renal scarring in EAV. *15th International Vasculitis/ANCA Workshop; Clinical and Experimental Immunology, May 2011. P124, volume 164.*

- Little MA, Al-Ani B, Ren SY, Al-Nuaimi H, Alpers CE, Savage C, Duffield JS.

  Human anti-PR3 ANCA recapitulate systemic vasculitis in mice with a humanized immune system. *15th International Vasculitis/ANCA Workshop; Clinical and Experimental Immunology, May 2011. P124, volume 164.*

- Harper L, Williams J, De Jong AM, Al Nuaimi H, Pallan L, Sarween N, Jesky E, Holden N, Savage C, Little M.

  Relative impact of ANCA source and neutrophil donor on the neutrophil response to ANCA stimulation. *XIVth international Vasculitis and ANCA Workshop. APMIS. June 2009.* P123, volume 117

- Sangha G, Al-Ani B, Al-Nuaimi H, Mukherjee S, Salama A, Pusey C, Little M.

  Absence of myeloperoxidase renal deposition in rat experimental autoimmune vasculitis. *XIVth international Vasculitis and ANCA Workshop. APMIS. June 2009. P88, volume 117*

1. Introduction

1.1. Autoimmunity

The immune system plays an essential role in providing protection from invading micro-organisms. The ability of the immune system to recognise and kill these micro-organisms while preventing harm to body elements (self-antigens) is called self-tolerance. Deficiency in this mechanism can lead to autoimmunity. Autoimmune diseases are characterised by chronic inflammation that can effect specific or multiple organs such as systemic lupus erythematosus (SLE) and systemic vasculitis (Thomas 2010). Furthermore, these systemic autoimmune diseases have vascular involvement with or without immune complex deposition and autoantibodies directed against self autoantigens. The development of such diseases could be the result of different factors, including genetic factors. Different animal studies have described a genetic defect in negative selection which results in the presence of autoreactive T cells (Liston, Lesage et al. 2004; Jiang, Anderson et al. 2005). Autoantibodies are considered to have significant value in the clinical field because they are used as a biomarkers for classification, diagnosis and disease progression (von Muhlen and Tan 1995). Systemic vasculitis is one of these autoimmune disorders and I will discuss small vessel vasculitis in this report.

1.2. The glomerulus

The kidneys are important organs in the human body and have several functions which include regulation of electrolytes, regulation of blood pressure, and maintenance of acid-base balance. The kidneys receive about 20% of the cardiac output via the renal artery which enters the kidney at the renal hilus (figure 1.1). The blood goes through the glomerular capillaries where it gets filtered. Furthermore, the glomerulus consists of the capillary endothelium, the glomerular basement membrane, and podocytes. The endothelial cells of

the capillary prevent blood cells and platelets from coming into contact with the basement membrane which allows filtration of molecules depending on their molecular size, charge, and shape. The glomerular filtration rate is around 125 ml/min, and molecules with a molecular weight less than 7,000 pass freely through the filters. Furthermore, some of the solutes that get filtered in the kidneys are reabsorbed in the proximal tubules, such as protein (Lote 2000). In anti-neutrophil cytoplasm antibody (ANCA)-associated vasculitis, the glomerulus is affected which results in its loss of function as a filtering unit.

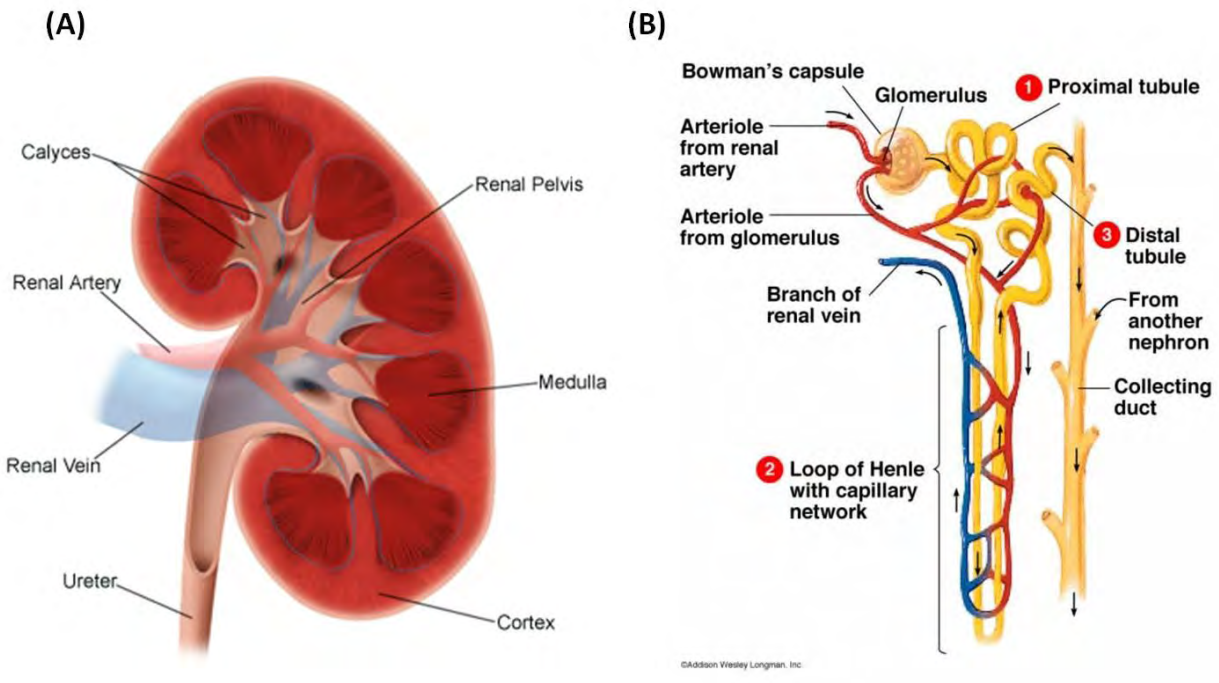

Figure 1.1: Kidney anatomy. This figure shows a cross section of the kidney (A). The functional unit of the kidney which is the nephron (B). Blood is filtered in the nephrons which are very important in regulating blood pressure, blood volume, and acid-base balance. (A) obtained from http://www.childrenshospital.org/az/Site1318/mainpageS1318P0.html and (B) obtained from http://biology-forums.com/index.php?topic=2926.0.

1.2.1. The glomerular endothelium

The endothelial cells of the glomerulus are involved in permeability and regulate the transport of fluid and solutes from the blood. In addition, they form the initial barrier to filtration. The glomerular capillaries are involved in the filtering of fluid and solutes, but not

oxygen and nutrient exchange like in other vascular beds. In addition, these glomerular endothelial cells contain small pores called fenestrae that are 60 to 80 nm in diameter which are involved in the filtration process. The glomerular capillary consists of a fenestrated endothelium, along with podocytes and the basal lamina or glomerular basement membrane; these structures form a filtration slit that filters the blood (Aird 2007) (figure 1.2 B). We are interested in the glomerulus because it is the most affected part of the kidney in ANCA-associated crescentic glomerulonephritis.

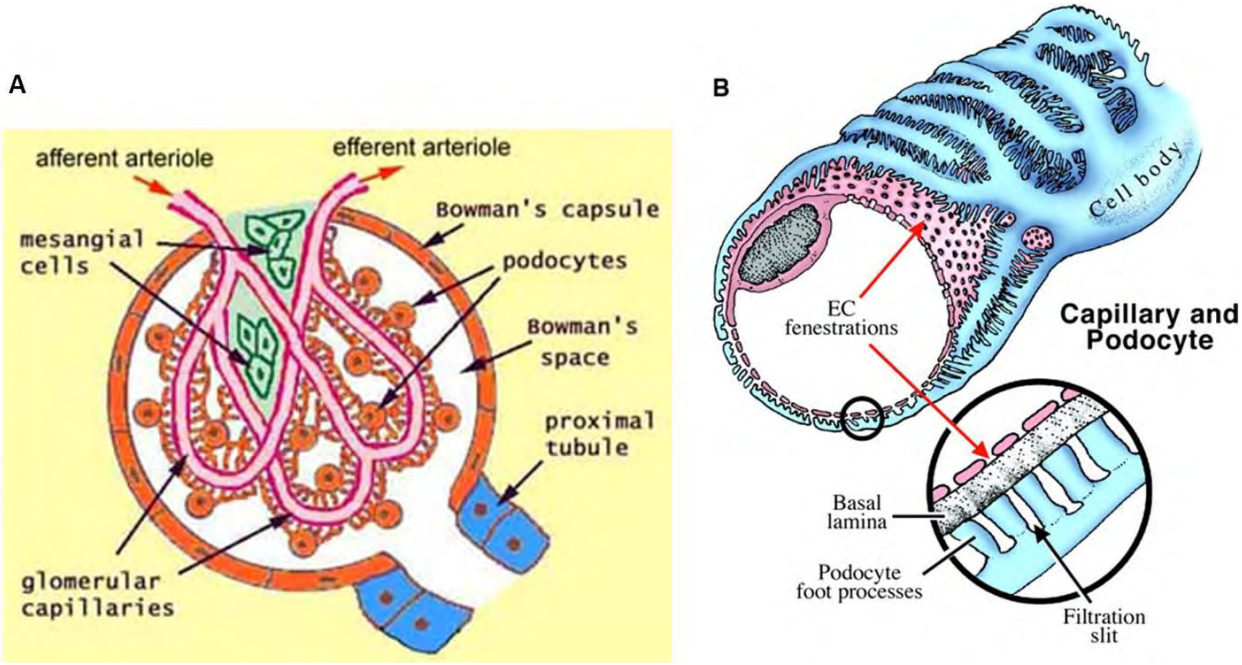

Figure 1.2: Structure of the glomerulus. (A) the filtering unit of the kidney is the glomerulus. The blood enters the glomerular capillaries through the afferent arteriole where it gets filtered and then leaves the glomerulus via the efferent arteriole. (B) Cross section of the glomerular capillary showing the filtration unit which consists of fenestrated endothelial cells, the basal lamina, and podocytes which form the filtration slit. (A) Adapted from http://www.siumed.edu/~dking2/crr/rnguide.htm. (B) Adapted from Aird et al., Circ Res. 2007;100;174-90.

1.3. Primary vasculitis

1.3.1 Types of primary systemic vasculitis

Inflammation of blood vessel walls is a feature of a disease known as vasculitis, which is classified according to the size of blood vessels affected (figure 1.3). Giant cell arteritis and

Takayasu's arteritis are both examples of large vessel vasculitis. Medium vessel vasculitis includes polyarteritis nodosa and Kawasaki disease. Finally, small vessel vasculitis is usually tightly associated with the presence of antineutrophil cytoplasm antibodies (ANCA). This type of systemic vasculitis is the focus of this research project.

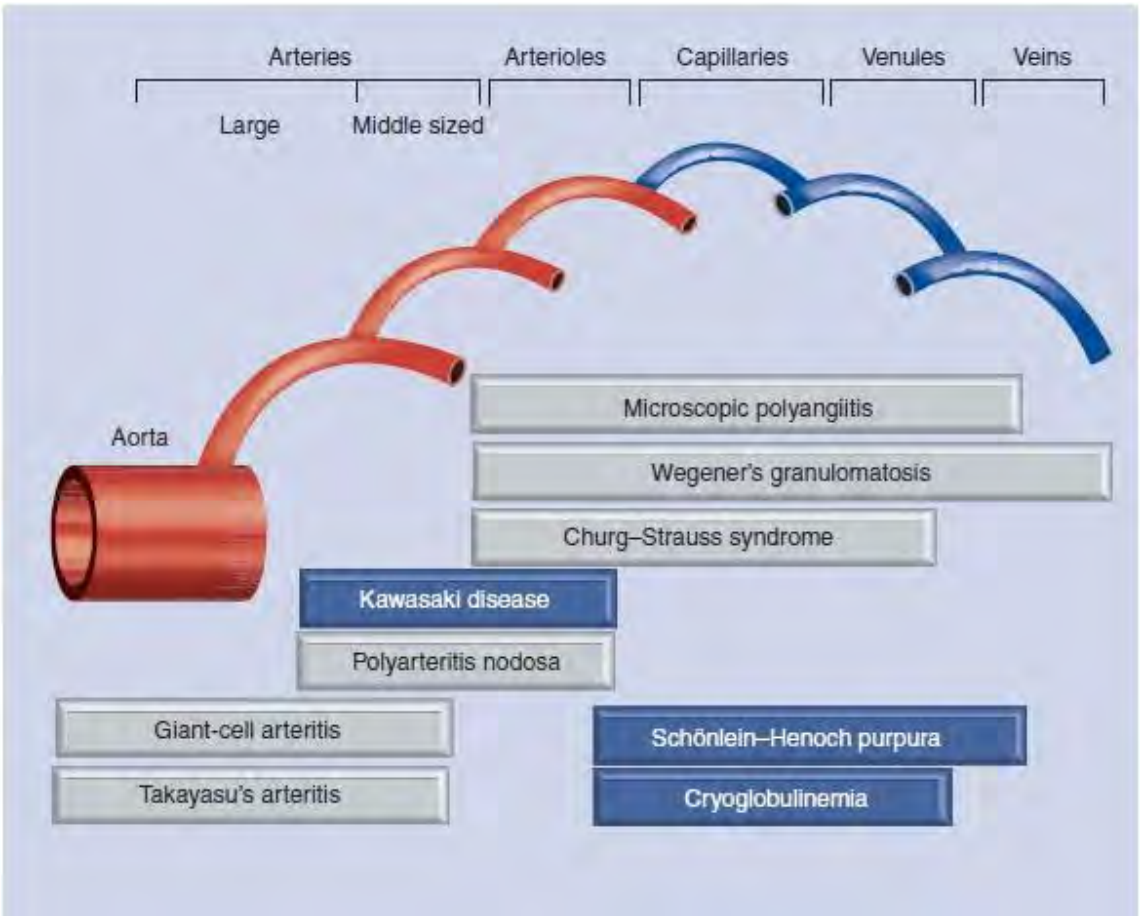

Figure 1.3: Types of systemic vasculitis. The different types of systemic vasculitis are divided according to the size of blood vessels affected. Adapted from Jennette et al. Arthritis Rheum 1994;37:187-92.

Wegener's granulomatosis (WG) is the most common type of small vessel vasculitis in the UK; the upper respiratory tract and lungs are usually affected in these patients. A high percentage of these patients also suffer from kidney disease, which can lead to renal failure. Necrotising and crescentic glomerulonephritis can often be seen in Wegener's granulomatosis. In addition, some patients with this disease develop alveolar necrotising capillaritis in the lung. Other parts of the body, such as the gut, skin, peripheral nervous

system, and eye can also be affected in this disease. Anti-neutrophil cytoplasm antibodies against proteinase 3 (PR3) are found in about 95% of patients with Wegener's granulomatosis, although it can be hard to detect ANCA if the disease is limited to the upper respiratory tract.

Microscopic polyangiitis and Churg-Strauss syndrome are also examples of small vessel vasculitis (Savage, Harper et al. 2000). Microscopic polyangiitis is similar to Wegener's granulomatosis, but upper respiratory tract disease is rare in microscopic polyangiitis. Glomerulonephritis is common in people suffering from this type of small vessel vasculitis, which is indistinguishable from that observed in Wegener's granulomatosis. ANCA are present in this type of small vessel vasculitis and are usually directed against myeloperoxidase (MPO). Churg-Strauss syndrome is usually associated with asthma and renal failure is relatively uncommon. ANCA directed against MPO are found in 50% of these patients. Approximately 20% of the patients with this disease have ANCA against PR3.

1.4. Anti-neutrophil cytoplasm antibody-associated vasculitis: understanding the causes of the disease and current therapy

Anti-neutrophil cytoplasmic antibodies (ANCA) are autoantibodies directed, in small vessel vasculitis, against the constituents of neutrophils and the lysosomes of monocytes (Chen and Kallenberg 2010). Anti-neutrophil cytoplasm antibodies were first described in 1982 (Davies, Moran et al. 1982) and they have proven to be invaluable for the diagnosis and monitoring of disease activity (van der Woude, Rasmussen et al. 1985). These autoantibodies are classified as cANCA or pANCA depending on the pattern of staining by indirect immunofluorescence on ethanol-fixed neutrophils (figure 1.4). For example, cANCA show a cytoplasmic staining pattern and most patients with cANCA have ANCA directed against PR3. On the other hand, pANCA show a perinuclear staining pattern and patients with pANCA have antibodies directed against MPO in small vessel vasculitis (Miller, Basu et al. 2008). A lot of work has gone into investigating what triggers the immune system to

produce these autoantibodies. There are several hypotheses about what causes the production of these antibodies, including a possible role of environmental factors, bacterial infection, and genetic factors in initiating the disease.

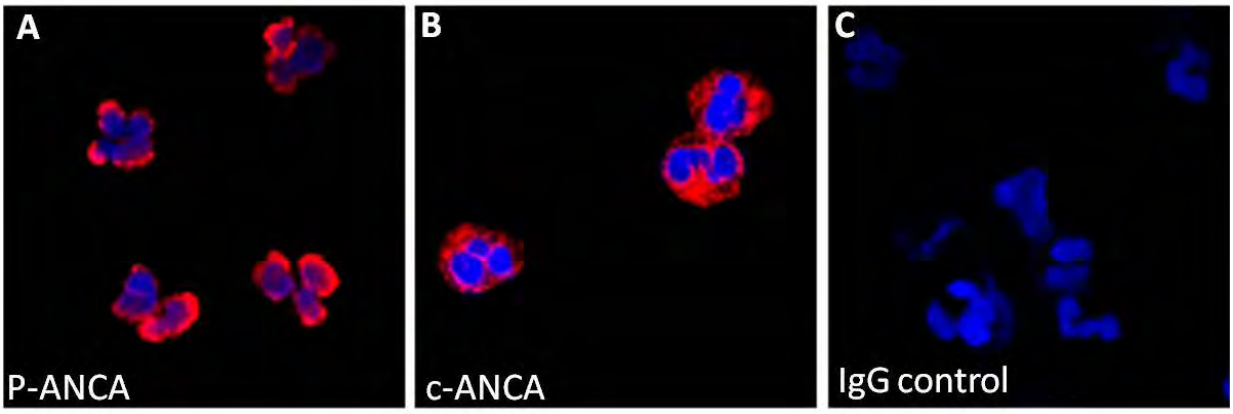

Figure 1.4: Binding of ANCA to neutrophils. Immunostaining of human neutrophils with plasma from vasculitis patients and IgG from a disease control. Neutrophils were isolated from human blood and then cytospins were made. Then, PR3-ANCA, MPO-ANCA, or normal IgG were added to each cytospin. This was followed by adding anti human IgG (red) and DAPI to stain the nucleus (blue). Perinuclear staining (A) and cytoplasmic staining (B) represent the interaction of MPO-ANCA and PR3-ANCA with human neutrophils. Adapted from (Al-Ani 2010).

1.4.1. Potential factors that could cause ANCA-associated vasculitis

1.4.1.1. Environmental factors: silica

Silica exposure has been associated with some autoimmune diseases such as systemic lupus erythematosus, rheumatoid arthritis, scleroderma, and ANCA-associated vasculitis (Hogan, Satterly et al. 2001). In addition, silica has been associated with rapidly progressive glomerulonephritis, and silica exposure in ANCA-associated vasculitis was first reported in the 1990s. It has been found that MPO is the predominant targeted antigen by ANCA in patients with ANCA-associated vasculitis following the exposure to silica. Furthermore, most of these patients were clinically diagnosed as having microscopic polyangiitis. In addition, it has been reported in several case-control studies that 22 to 46% of patients with ANCA-associated vasculitis were previously exposed to silica (de Lind van Wijngaarden, van Rijn et al. 2008). It is not completely understood how silica exposure may be involved in the development of ANCA-associated vasculitis, but several in vitro studies have suggested that

silica exposure could trigger the immune response and cause inflammatory reactions. For example, Leigh et al. have shown that intratracheal instillation of silica results in accelerated apoptosis of neutrophils in a dose-dependent manner (Leigh, Wang et al. 1997).

1.4.1.2. Bacterial infections

Bacterial infection is thought to play a role in stimulating the production of ANCA and the development of ANCA-associated vasculitis (figure 1.5). For example, the initiation and relapse of WG has been associated with bacterial infection, in particular with *Staphylococcus aureus* (*S. aureus*) (Holle and Gross 2009). In addition, there was an increase in the relapse rate in association with chronic nasal carriage of *S. aureus* in patients with WG (Stegeman, Tervaert et al. 1994). There are several hypotheses related to the mechanism underlying the increased risk of relapse by *S. aureus* in patients with WG. One of these theories is that T and/or B cells may be activated by superantigens from *S. aureus* (Popa, Stegeman et al. 2002). In addition, B cells may be activated polyclonally by the bacterium cell-wall components of *S. aureus* which could lead to the persistence of ANCA. Furthermore, direct stimulation of neutrophils by *S. aureus* is another possibility which could result in increased expression of PR3 on the surface of neutrophils (Kallenberg and Tadema 2008). Recently, a study described the presence of complementary proteins to PR3 which could, possibly, be related to *S. aureus*. In this study, Pendergraft et al. were able to identify a complementary protein to PR3, which is translated from the antisense DNA strand encoding for PR3. They suggested that the complementary peptides initiate the production of antibodies which results in producing antibodies called anti-idiotypic antibodies. As a result, these antibodies will react with the original antigen, which is PR3 in this case. In addition, the authors showed that immunising mice with complementary PR3 resulted in the production of antibodies to cPR3 and to PR3 itself. They also showed strong homology between peptides from cPR3 and peptides from *S. aureus* which could mean that an infection resulted in molecular mimicry and initiation of the disease (Pendergraft, Preston et al. 2004).

Molecular mimicry has been investigated in other types of ANCA-associated diseases such as pauci-immune focal necrotising glomerulonephritis (FNGN) which typically occurs in the context of a systemic small vessel vasculitis. Kain et al. found that patients with FNGN have ANCA directed against lysosomal membrane protein-2 (LAMP-2). In addition, they also found that 93% of 84 individuals had autoantibodies to human LAMP-2. Furthermore, rats that were injected with antibodies to human LAMP-2 developed FNGN. In addition, they found that these autoantibodies recognised two major human LAMP-2 epitopes, P_{41-49} and $P_{331-341}$. They showed that one of these epitopes had 100% homology to bacterial FimH. In addition, immunising rats with a recombinant FimH fusion protein resulted in the induction FNGN and the production of autoantibodies to rat and human LAMP-2. Also, they showed that most patients with FNGN in their study had a FimH-expressing bacterial infection. These studies have shown the possible relationship between bacterial infection and the development of autoimmune diseases (Kain, Exner et al. 2008).

1.4.1.3. Genetic factors

Genetic factors have been suggested to have an effect on the susceptibility of autoimmune diseases and ANCA-associated vasculitis (figure 1.5). Different studies have identified some genes that could be associated with an increased incidence of AAV. For example, some studies have suggested associations between MHC loci and WG; these include HLA-B50, HLA-DR9, HLA-DQw7, HLA-DR3, and HLA-DR1 (Papiha, Murty et al. 1992; Spencer, Burns et al. 1992; Cotch, Fauci et al. 1995). Furthermore, the activity of PR3 is inhibited by α_1-antitrypsin, and it is thought to limit the damage done to local tissues. Polymorphisms in the gene encoding for α_1-antitrypsin, including the Z and S alleles, reduce the function of this protein. Griffith et al. has shown an association between the presence of the Z and S alleles with cANCA and pANCA-positive vasculitis, respectively (Griffith, Lovegrove et al. 1996). Recently, Aitman et al. screened for susceptibility loci in a nephrotoxic nephritis (NTN) rat model and they were able to identify two major trait loci on chromosomes 13 and 16 (known as crescentic glomerulonephritis 1 and 2, Crgn 1, and Crgn

2). Furthermore, these two loci were associated with crescent formation and proteinuria. One of the genes found in the Crgn1 region is the gene encoding the Fc receptor (Fcgr3), which is also known as FcyRIII. In humans, a copy number polymorphism in Fcgr3 is associated with glomerulonephritis (Aitman, Dong et al. 2006). This finding has been linked recently to ANCA-associated vasculitis. Little et al. have shown resistance in non-WKY rats in developing vasculitis following immunisation with human MPO (Little, Smyth et al. 2009). They showed that these different rat strains developed a high titre of anti-MPO antibodies but they did not develop the disease. This further demonstrates the role of genetic variation in susceptibility to ANCA-associated vasculitis.

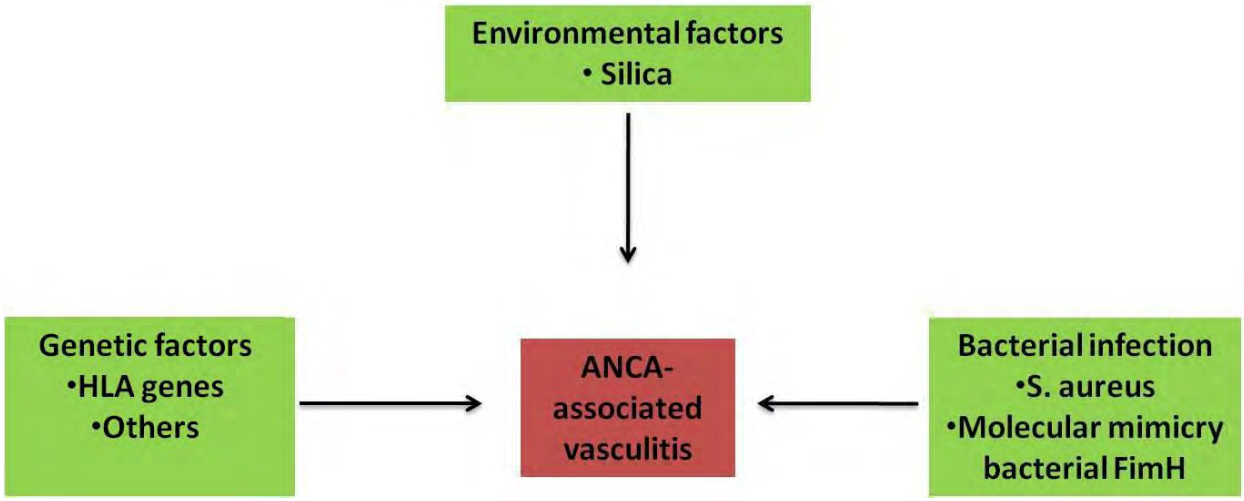

Figure 1.5: Potential aetiologic factors in AAV. Genetic factors, environmental factors, and bacterial infection are thought to be involved in triggering ANCA-associated vasculitis.

1.4.2. Epidemiology of vasculitis

The incidence of vasculitis varies in different parts of the world and according to the age group studied. For example, Kawasaki disease is most common in Asia in children under five with an incidence rate of 90/100,000. On the other hand, giant cell arteritis is more common in elderly Caucasians with an incidence rate of 53/100,000. Wegener's granulomatosis is more common than Churg-Strauss syndrome and microscopic polyangiitis in Europe, except for Spain which has a higher incidence of microscopic polyangiitis. These data were obtained from studies done in Norway, UK, Germany, and Spain (Koldingsnes

and Nossent 2000; Watts, Lane et al. 2001). The annual incidence of ANCA-associated vasculitis (AAV) in Europe is 10-20/million/year (Watts and Scott 2003). Furthermore, AAV can affect individuals from different age groups, but older people are more susceptible.

1.4.3. Current therapeutics of ANCA-associated vasculitis (AAV)

Considerable morbidity and mortality can be caused by AAV, with 20% of patients at five years developing end-stage renal failure (Booth, Almond et al. 2003). The chance for survival was very slim before introduction of cyclophosphamide (CYP) and steroid treatment in the early 1970s. As a result, remission can be achieved now in over 90% of patients with generalised WG by six months, and the survival rates at five years are around 75% (Matteson, Gold et al. 1996; Jayne, Rasmussen et al. 2003). However, the relapse rates are still high and up to 50% over five years (Westman, Bygren et al. 1998). Treatment of AAV can be divided into the initial immunosuppression stage to induce remission and follow-up treatment to prevent relapse. For example, CYP and steroids are used to induce remission in severe disease. However, these treatments are associated with increased risk of treatment-related morbidity and mortality. Other treatments include glucocorticoids, plasma exchange, methotrexate (MTX), mycophenolate mofetil (MMF), and rituximab (RTX) used as induction therapy. In addition, long-term immunosuppression treatment is usually required for the maintenance of remission in ANCA-associated vasculitis. These treatments include a low dose of glucocorticoids together with a second agent such as azathioprine, methotrexate, or mycophenolate mofetil. Finally, biological therapies such as TNF-α blockade using infliximab and B-cell depletion using RTX have been successful in some cases (Hamour, Salama et al. 2010).

In this chapter, I will give an introduction to ANCA-associated vasculitis and the involvement of the innate immune system in the development of this disease. In addition, I will mention animal models of ANCA-associated vasculitis.

1.5. Antineutrophil cytoplasmic autoantibodies (ANCA)

1.5.1. ANCA as a pathogenic factor in vasculitis: clinical evidence

Many studies have suggested that ANCA have an important role in the development of vasculitis and that they are not just a serologic marker of disease or an epiphenomenon. It has been suggested that ANCA are the primary pathogenic factor in the development of these diseases for several reasons (Jennette, Xiao et al. 2006). There is some clinical evidence to support the pathogenic role of ANCA in pauci-immune small-vessel vasculitis, including the presence of a high percentage of ANCA in these patients and a correlation between disease activity and ANCA titre. In addition, clinical remission is usually accompanied by a decrease in ANCA levels (Falk, Nachman et al. 2000; Savage 2001). Furthermore, Boomsma et al. showed that an increase in the ANCA titre in WG patients predicts relapse with 79% sensitivity and 68% specificity (Boomsma, Stegeman et al. 2000). On the other hand, this evidence does not prove that ANCA have a pathogenic role in the development of this disease. For example, Finkielman et al. could not confirm the association between disease activity and ANCA titre. They did not find an association between the rate of relapse and the increase in ANCA levels and the decrease in ANCA after treatment did not associate with a shorter time of remission (Finkielman, Merkel et al. 2007). The case for the pathogenic potential of ANCA was strengthened when a newborn child developed glomerulonephritis and pulmonary haemorrhage after delivery following placental transfer of ANCA from the mother, who had microscopic polyangiitis (Bansal and Tobin 2004; Schlieben, Korbet et al. 2005). This is the only definite proof of the potential pathogenicity of anti-MPO antibodies (or a co-expressed antibody) in humans.

1.5.2. In vitro evidence

The pathogenicity of ANCA in vitro was based on the discovery by Falk et al. that showed the ability of ANCA to stimulate primed neutrophils to release reactive oxygen species and

other enzymes (Falk, Terrell et al. 1990). ANCA antigens are found in the cytoplasm of unstimulated neutrophils, although some antigens are found on the surface of neutrophils. The amount of the antigens that are expressed on the surface of neutrophils is determined by genetic factors and high expression is a risk factor for developing ANCA-associated vasculitis (Schreiber, Busjahn et al. 2003; Schreiber, Luft et al. 2004). In addition, the binding of ANCA to neutrophils could result in the activation of the complement system (figure 1.6). Schreiber et al. has shown that the supernatant from neutrophils that were activated by ANCA activated the alternative pathway of the complement immune system, resulting in the production of C5a. In addition, ANCA were able to induce neutrophil activation after priming with C5a and this process was abrogated when the C5a receptor on neutrophils was blocked (Schreiber, Xiao et al. 2009). Furthermore, it has been shown that ANCA can stimulate neutrophil-induced cytotoxicity toward endothelial cells (Ewert, Jennette et al. 1992). In addition, Radford et al. have shown that ANCA induce firm integrin-mediated adhesion of rolling neutrophils in a flow assay (Radford, Savage et al. 2000). This was confirmed by an in vivo experiment where it was shown that MPO-ANCAs reduced the rolling of leucocytes and induced adhesion and migration across the endothelium. This was inhibited by blocking Fcγ receptors and β2 integrins (Nolan, Kalia et al. 2008). Little et al. have shown ANCA-enhanced leucocyte-vessel wall interactions in vivo (Little, Smyth et al. 2005). In addition, ANCA-activated neutrophils have been shown to induce the generation of neutrophil extracellular traps (NETs), which contain the autoantigens MPO and PR3. These NETs can cause damage to endothelial cells by adhering to them and can result in the activation of plasmacytoid dendritic cells and autoreactive B cells, thus contributing to the production of ANCA at the site of inflammation (Kessenbrock, Krumbholz et al. 2009). Furthermore, it has been suggested that MPO-ANCA have a pathogenic role, not only via the activation of neutrophils and monocytes, but also by activating MPO itself. The activation of MPO by ANCA in vitro results in the production of hypochlorous acid (HOCL); the by-products of this activation resulted in the lysis of endothelial cells (Guilpain, Servettaz et al. 2007). In conclusion, there are several lines of in vitro evidence to suggest that ANCA are pathogenic.

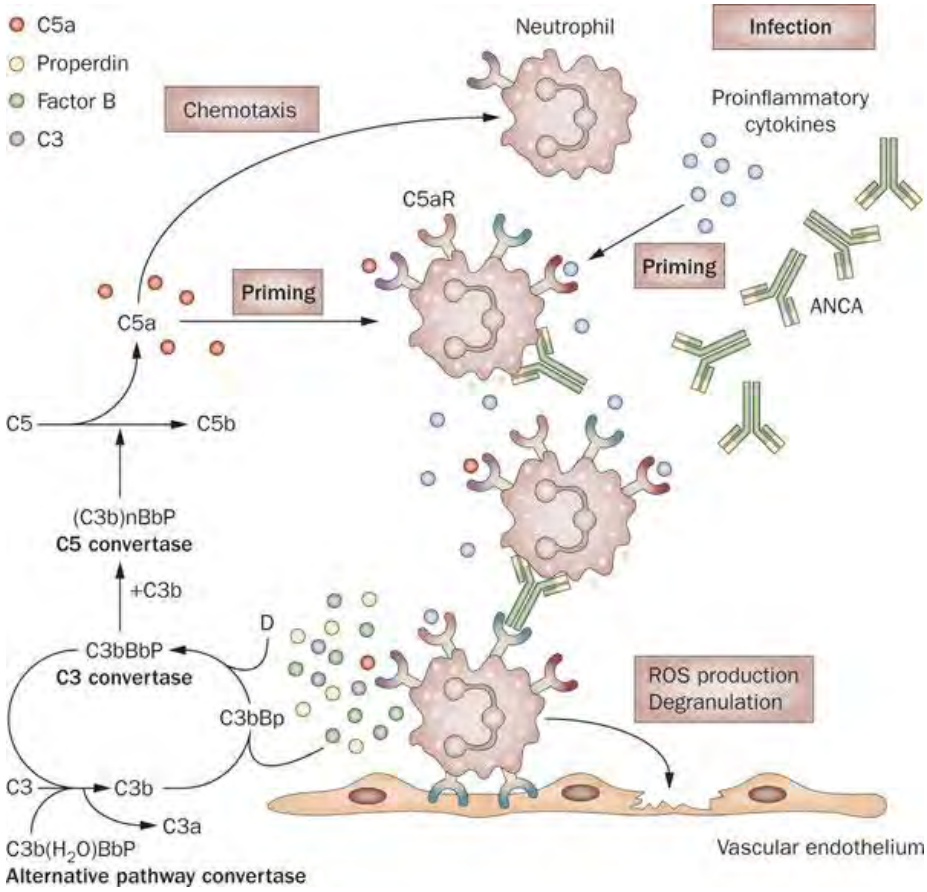

Figure 1.6: Proposed complement involvement in AAV pathogenesis. Activated neutrophils express ANCA antigens on their surfaces. This results in the binding of ANCA to neutrophils that adhere to the endothelium, causing neutrophils to release reactive oxygen species and resulting in damage to the endothelium. This could also result in the activation of the alternative complement pathway by factors released by neutrophils. (Chen and Kallenberg 2010)

1.6. ANCA and neutrophils

1.6.1. The role of neutrophils in ANCA-associated diseases

Neutrophils play a major role in the pathogenesis of different ANCA-associated diseases such as necrotising and crescentic glomerulonephritis (NCGN) (Xiao, Heeringa et al. 2005). There is a correlation between the number of activated neutrophils and the severity of renal injury (Brouwer, Huitema et al. 1994). In addition, activated neutrophils have been found in affected glomeruli in NCGN patients (Brouwer, Huitema et al. 1994). These neutrophils may cause damage to endothelial cells and they could release inflammatory cytokines which would attract more effector cells (Rarok, Limburg et al. 2003). Mice can be protected from

MPO antibody-induced NCGN if neutrophils are depleted (Xiao, Heeringa et al. 2005). These results suggest that neutrophils are important in the development of MPO-induced NCGN and that neutrophils are key early effector cells. The activation of neutrophils by ANCA IgG has been reported in many in vitro studies. The Fc part of these autoantibodies bind to the surface of neutrophils, while they bind to antigens through the antigen-binding site (Kettritz, Jennette et al. 1997; Williams, Ben-Smith et al. 2003). ANCA have the ability to stimulate and induce neutrophils to travel through endothelial monolayers and induce them to injure these endothelial cells (Savage, Pottinger et al. 1992; Radford, Savage et al. 2000; Radford, Luu et al. 2001).

1.6.2 Neutrophil priming and ANCA binding

Studies have shown that ANCA are directed against two major antigens that are found in the granules of neutrophils and lysosomes of monocytes: MPO, which is an enzyme involved in the generation of reactive oxygen species, and PR3, which is a serine protease (Heeringa and Tervaert 2004). ANCA bind to MPO and PR3 on the surface of neutrophils (Mulder, Heeringa et al. 1994). However, these antigens are found inside the cells. Neutrophils have to be stimulated in order for them to express these antigens on the cell surface and it has been shown that treating these cells with tumour necrosis factor alpha (TNF-α) in vitro triggers these antigens to travel to the surface of the cell. Neutrophils are usually primed in vivo to prepare them for the appropriate response to different stimulus. In addition, this state of preactivation can be achieved or induced in response to different proinflammatory cytokines such as TNF-α (Csernok, Ernst et al. 1994; Reumaux, Vossebeld et al. 1995), transforming growth factor-β1 (Csernok, Szymkowiak et al. 1996), and granulocyte macrophage-colony stimulating factor (Hellmich, Csernok et al. 2000) that are released during inflammation or tissue damage. For example, the level of TNF-α in systemic vasculitis has been reported to be increased (Deguchi, Shibata et al. 1990; Noronha, Kruger et al. 1993). Furthermore, neutrophil activation by TNF-α results in the degranulation of specific

granules and secretory vesicles (Luedke and Humes 1989) and the upregulation of cell-surface expression of many molecules such as MPO and PR3.

The binding of ANCA to antigens on the cell surface results in the activation of these neutrophils (Figure 1.7). The activation of these cells causes an increase in adhesion and migration of these cells through endothelium. In addition, MPO and PR3 are released as a result of neutrophil activation and bind to the surrounding tissues, potentially causing more damage. Furthermore, neutrophils secrete pro-inflammatory cytokines which attract more effector cells and cause further damage to endothelial cells. ANCA bind to neutrophil Fcγ receptors via the Fc portion; these antibodies also use F(ab')2 portions to bind to the antigen on the surface of these neutrophils (Day, Hewins et al. 2003). Furthermore, neutrophils predominantly express FcγRIIa (CD32) and FcγRIIIb (CD16) and these receptors differ in their ability to bind IgG and in their affinity to different subclasses of IgG (van de Winkel and Capel 1993; Dijstelbloem, van de Winkel et al. 2001). For example, FcγRIIa interacts with monomeric IgG2 and has high affinity to the IgG3 subclass (van de Winkel and Capel 1993), which is over-expressed in patients with ANCA-associated vasculitis during active disease (Jayne, Weetman et al. 1991). In addition, this receptor is also found to be involved in triggering the neutrophil oxidative burst. As a result, blocking FcγRIIa with monoclonal antibodies results in the abrogation of oxygen radical release in response to ANCA stimulation (Porges, Redecha et al. 1994; Reumaux, Vossebeld et al. 1995). However, blocking of FcγRIIa resulted only in partial blockade of the oxidative burst after stimulating neutrophils with ANCA in vitro, which suggests the involvement of other mechanisms as well (Mulder, Heeringa et al. 1994; Kettritz, Jennette et al. 1997). Another receptor expressed on neutrophils is FcγRIIIb, which has ten-fold higher density of expression than FcγRIIa (Hulett and Hogarth 1994). Its role in neutrophil activation is still not clear, but it is been suggested that it is involved in triggering the neutrophil response in the initial stage of activation (Kocher, Edberg et al. 1998). Furthermore, molecules other than FcγRs have been suggested to be involved in neutrophil activation by ANCA. For example, it has been shown

that F(ab')2 fragments alone are capable of stimulating primed neutrophils to produce oxygen radicals (Kettritz, Jennette et al. 1997). However, signals from both Fab_2 and FcγR could be required to produce full ANCA response.

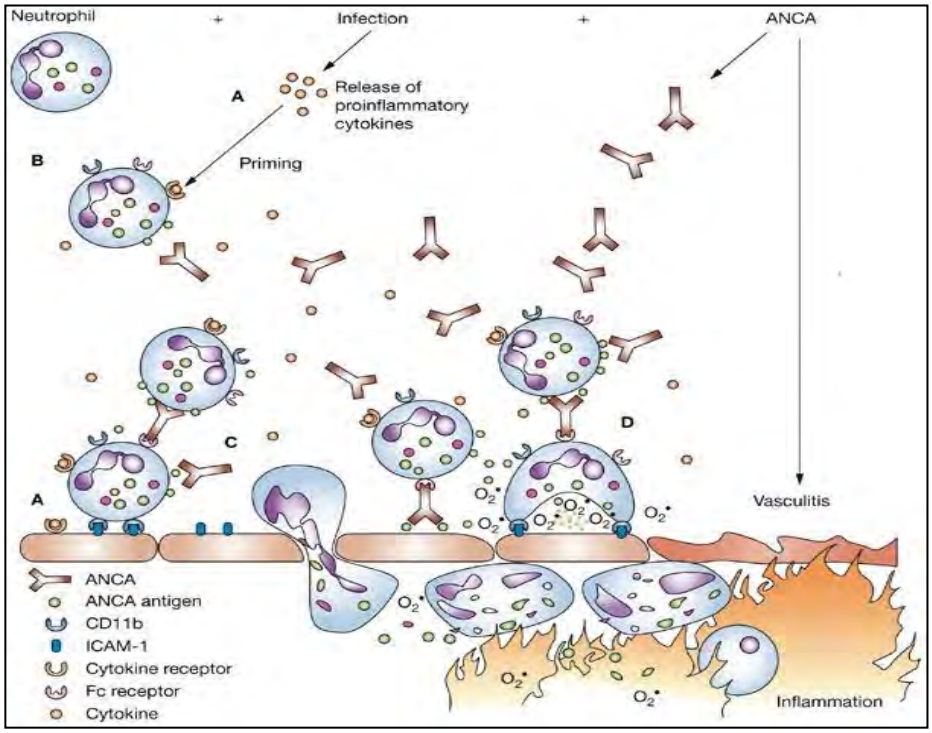

Figure 1.7: The pathogenesis of endothelial injury in ANCA-associated vasculitis. Adapted from: Mechanism of Disease: Pathogenesis and Treatment of ANCA-associated Vasculitides. Cees, G. M. Kalleenberg, P. Heeringa and C. A. Stegeman. Nature Clinical Practice Rheumatology (2006) 2, 661-670.

1.6.3. Signal transduction pathways involved in neutrophil activation by ANCA

We know, from previous studies, that the binding of ANCA to antigens on the surface of neutrophils results in neutrophil degranulation. Although the pathways involved in this process have not been fully elucidated, there are different ways that ANCA could activate neutrophils. As mentioned earlier, the binding of both ANCA F(ab')2 and Fc portions are required to induce effective neutrophil degranulation. It has been suggested that β2 integrin (CD11b/CD18) could help to propagate the signal by interacting with the Fcγ receptor. In addition, the signal transduction pathway initiated by F(ab')2 binding to the antigens would be different from that initiated by the Fc portion binding to the Fc receptor (Williams, Kamesh

et al. 2005). For example, the F(ab') portion of the antibody can activate G proteins and the RAS p21 protein activator. On the other hand, tyrosine kinases such as sarcoma virus kinases, Syk, phosphatidylinositol-3 kinase, protein kinase B, and protein kinase C are thought to be activated when the Fc portion of the antibody bind to its Fc receptor (Williams, Ben-Smith et al. 2003; Williams, Kamesh et al. 2005). The activation of tyrosine kinase pathways is thought to cause a respiratory burst via the activation of NADPH oxidase. Both of these pathways are thought to be important because G protein and tyrosine kinase pathways converge on the GTPase RAS p21 protein activator (Williams, Ben-Smith et al. 2003).

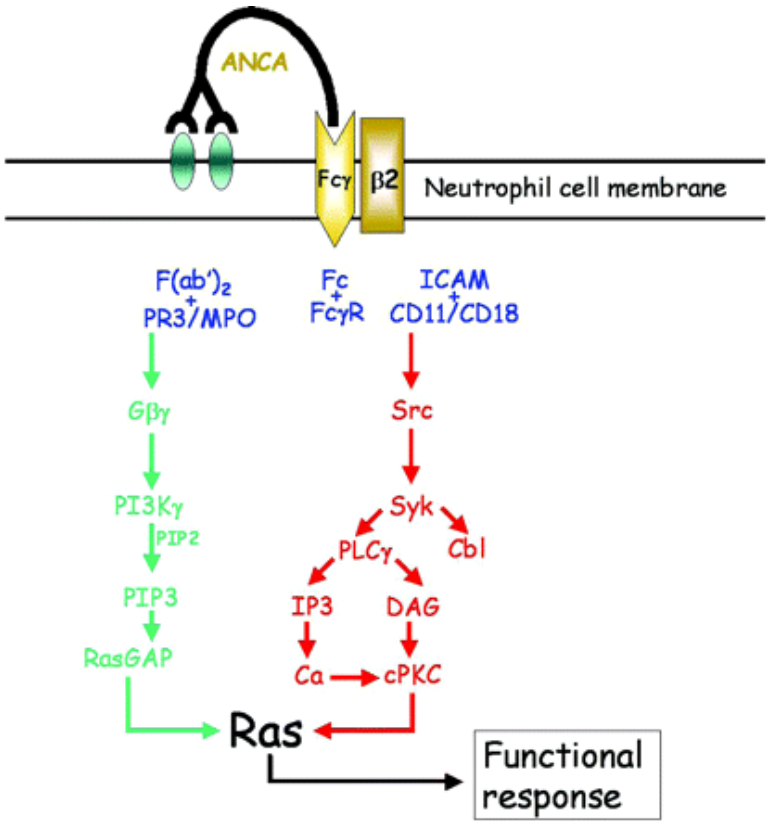

Figure 1.8: Proposed signalling pathways following neutrophil activation by ANCA F(ab)2 and whole IgG. The cross-linking of MPO or PR3 on the surface of neutrophils with Fc receptor results in intracellular signalling which causes a functional response. Morgan M. D. (2006)

The p38 mitogen-activated protein kinase (p38 MAPK) pathway is an inflammatory pathway suggested to be involved in ANCA-mediated neutrophil activation (Kettritz, Schreiber et al. 2001). Kettriz et al. have shown a reduction in ANCA-mediated neutrophil

activation in vitro as a result of p38 MAPK activation inhibition. In addition, patients with ANCA-associated glomerulonephritis are found to have activated p38 MAPK in the glomerular lesions. On the other hand, p38 MAPK inhibition in vivo resulted in only a moderate reduction in crescentic glomeruli (van der Veen, Chen et al. 2011). This suggests the involvement of other pathways that contribute to disease activity.

1.6.4. Neutrophil degranulation in response to ANCA IgG

Part of my project was to study the variability in ANCA-induced neutrophil degranulation. For that reason, I think it is important for me to be knowledgeable on how ANCA induce neutrophil degranulation and the effect of this process on the induction of vasculitis.

Neutrophils play an important role in host defence. Different types of granules are found inside neutrophils; they contain proteases, antimicrobial proteins, and components of the respiratory burst (Faurschou and Borregaard 2003). These granules also contain membrane-bound receptors for bacterial products and endothelial adhesion molecules. Neutrophil granules are classified as peroxidase-positive (azurophil) granules and peroxidase-negative granules that can be divided into specific (secondary) and gelatinase (tertiary) granules (Faurschou and Borregaard 2003). In addition, neutrophils contain secretory vesicles that contain membrane-associated receptors that are needed in the first stages of the neutrophil-mediated response; these vesicles have the highest ability for extracellular release. Mobilisation of granules and secretory vesicles can be achieved in vitro by increasing the level of calcium in the intracellular region (Sengelov, Kjeldsen et al. 1993). In addition, ligation of CD11b/CD18, L-selectin, and the fMLP receptor have been shown to increase cytosolic calcium concentration (Ng-Sikorski, Andersson et al. 1991; Sengelov, Kjeldsen et al. 1993; Laudanna, Constantin et al. 1994).

Different studies have demonstrated the ability of ANCA to induce neutrophil degranulation in vitro (Falk, Terrell et al. 1990). In addition, it has been shown that ANCA

IgG induce neutrophil degranulation in a dose-dependent manner. Furthermore, neutrophil degranulation was enhanced when neutrophils were primed with TNF-α (Falk, Terrell et al. 1990). The consequences of this activation by ANCA are that neutrophils degranulate and release PR3, MPO, and elastase which could result in the lysis of endothelial cells (Ewert, Jennette et al. 1992; Savage, Pottinger et al. 1992). It is believed that MPO, which is highly cationic, is released from neutrophils after stimulation by ANCA, binds to the endothelium via electrostatic interactions, creates a binding site for ANCA and results in cellular cytotoxicity (Savage, Gaskin et al. 1993). Furthermore, endothelial cell detachment and cytolysis is caused by PR3 and elastase release by ANCA-stimulated neutrophils (Savage, Gaskin et al. 1993; Ballieux, Hiemstra et al. 1994). In addition, apoptosis of endothelial cells can also by induced by PR3 and elastase (Yang, Kettritz et al. 1996; Taekema-Roelvink, van Kooten et al. 1998). Also, the oxidative burst results in the release of H_2O_2 and halide ions that MPO reacts with to produce highly active reactive oxygen species (Johnson, Couser et al. 1987), which are involved in endothelial cell detachment. Furthermore, Eiserich et al. have demonstrated the involvement of MPO in the formation of nitric oxide-derived inflammatory oxidants (Eiserich, Hristova et al. 1998). These results show the injury that can be caused by the enzymes released by activated neutrophils. In addition, it has been shown that PR3-ANCA from patients with WG can significantly inhibit the proteolytic activity of PR3 and interfere with its binding to α1-antitrypsin, which is a physiological PR3 inhibitor (van de Wiel, Dolman et al. 1992). This extensive activation of neutrophils will eventually lead to apoptosis and these cells should be cleared by macrophages. One of the important molecules involved in the recognition of apoptotic cells by macrophages is phosphatidylserine. It has been shown that activation of neutrophils by ANCA after priming with TNF-α accelerates apoptosis and results in delayed externalisation of phosphatidylserine (PS) (Harper, Ren et al. 2000). Externalisation of PS is considered to be an early feature of apoptosis in response to different stimuli. As a result, the delay in PS externalisation could result in a delay in clearing apoptotic cells because they are not recognised by macrophages.

1.7. Myeloperoxidase (MPO)

Myeloperoxidase is considered to be one of the major antigens in ANCA-associated vasculitis. In addition, ANCA-associated vasculitis is induced in all animal models using anti-MPO antibodies. Myeloperoxidase is a haemoprotein which is highly expressed in neutrophils, and accounts for up to 5% of the total cell protein content. It is thought to have a role in the host defence (Eiserich, Baldus et al. 2002). It has a molecular weight of about 144 kDa and disulphide bridges between its two identical subunits (Furtmuller, Zederbauer et al. 2006). Each one of these subunits is made up of a light and heavy polypeptide chain (Andrews, Parnes et al. 1984). Furthermore, it is believed that MPO is released into the extracellular space during neutrophil activation where it catalyses the formation of hypochlorous acid (HOCL), which is a microbicidal agent, and other oxidising species using hydrogen peroxide (H_2O_2) (Winterbourn, Vissers et al. 2000). Myeloperoxidase has been suggested to be involved in micro-organism killing because, in the presence of MPO inhibitors or neutrophils from individuals with an MPO-deficiency, a reduction in the killing rate was observed (Klebanoff 1970; Lehrer 1971; Koch 1974). Different studies have been performed to identify the target epitopes of ANCA on MPO. There is a strong homology between mouse and human MPO sequences, which is estimated to be around 90% (Erdbrugger, Hellmark et al. 2006). Despite this strong homology, most human ANCA against MPO do not bind to mouse MPO. This led Erdbrugger et al. to focus on the area of heterogeneity between mouse and human MPO and try to identify target epitopes for ANCA. They found that serum from patients with anti-MPO antibodies did not bind to the MPO light chain. In addition, serum from these patients bound to only one or two regions of MPO (Erdbrugger, Hellmark et al. 2006).

These findings describe the importance of neutrophils in the pathogenesis of ANCA-associated vasculitis. I wanted to investigate why some patients develop severe vasculitis while the disease in other individuals is moderate. People in our lab have previously shown

variability in ANCA-induced neutrophil degranulation from healthy donors. I decided to investigate this further by looking at neutrophil degranulation from several healthy donors to the same ANCA IgG.

1.8. Cytokines and chemokines in ANCA-associated vasculitis

Cytokines:

We know that cytokines are secreted by different cells and that they play an important role in immunity; each of these cytokines produces a specific cellular response. Some cytokines play an important role in ANCA-associated diseases. For example, tumour necrosis factor (TNF-α) is required for priming neutrophils in vitro in order to stimulate them with ANCA (Falk, Terrell et al. 1990; Radford, Lord et al. 1999). Little et al. investigated the effect of blocking TNF-α, using an anti-rat TNF-α antibody, in an animal model of ANCA-associated systemic vasculitis and showed that these antibodies reverse anti-MPO antibody-associated glomerulonephritis in rats (Little, Bhangal et al. 2006). They also showed that treating rats that suffer from experimental autoimmune vasculitis (EAV) with anti-TNFα can inhibit the ANCA-induced exaggerated adhesion in response to CXCL1. This chemokine has been shown in previous studies by the same group to facilitate the adhesion and transmigration response in response to ANCA (Little, Smyth et al. 2005). Furthermore, blocking TNF-α in rats using a soluble TNF-α receptor has been shown to reduce crescent formation (Karkar, Smith et al. 2001). Therefore, TNF-α seems to be important and to play a role in the pathogenesis of vasculitis in this animal model.

Another cytokine thought to play a role in the pathogenesis of ANCA is IL-18. It has been reported that IL-18 can prime neutrophils in vitro. IL-18 was found in patients with ANCA-associated systemic vasculitis (ASV) and the expression of this cytokine was seen in the biopsies of these patients. In addition, IL-18 priming of ANCA-induced superoxide production was not inhibited by an anti-TNFα antibody which inhibited TNF-α priming of ANCA-induced

superoxide production. In the same study, it was demonstrated that interstitial macrophages contain IL-18 suggesting a possible role of these cells in AAV (Hewins, Morgan et al. 2006).

In addition, Cook et al. have shown that IL-4 reduces proteinuria, fibrinoid necrosis, and macrophage infiltration among other effects in crescentic glomerulonephritis (nephrotoxic nephritis) model (Cook, Singh et al. 1999). Crescentic glomerulonephritis in these animals was induced using nephrotoxic serum. Furthermore, they showed that IL-4 treatment reduced glomerular ICAM-1 expression, which is known to be involved in macrophage infiltration. They suggested that the action of IL-4 protection is through reducing macrophage infiltration to the site of injury and preventing further damage. Having said that, they had also started IL-4 treatment after glomerular inflammation was established; no effect on macrophage infiltration was seen, but a reduction in injury was achieved. They suggest that IL-4 could affect macrophage-mediated injury because they have shown a reduction in cells expressing iNOS and sialoadhesin which are markers of macrophage activation.

Chemokines:

The role of IL-8 has been also investigated in ANCA-associated vasculitis. IL-8 is a neutrophil chemoattractant chemokine (Yoshimura, Matsushima et al. 1987), and is believed to stimulate neutrophil degranulation and the production of reactive oxygen species (Peveri, Walz et al. 1988). Furthermore, Cockwell et al. have shown that ANCA can stimulate the production of IL-8 in vitro (Cockwell, Brooks et al. 1999). They demonstrated an effect of IL-8 on neutrophil transmigration.

Chemokines such as RANTES (Regulated on Activation Normal T cell Expressed and Secreted) and monocyte chemoattractant protein-1 (MCP-1) have been reported to be upregulated in a murine model of crescentic glomerulonephritis where the disease was induced using nephrotoxic serum. They have shown that blocking RANTES and MCP-1 resulted in decreased accumulation of mononuclear phagocytes and T-lymphocytes. Also,

the blocking of these chemokines resulted in partial attenuation of proteinuria. In addition, MCP-1 blockade resulted in decreased formation of glomerular crescents and deposition of collagen I. However, macrophage infiltration was only inhibited by 50% as a result of MCP-1 blockade (Lloyd, Minto et al. 1997). In addition, Ohlsson et al. have shown an increased level of urinary MCP-1 in patients with ASVV (Ohlsson, Bakoush et al. 2009). They were able to show a strong correlation between urinary-MCP-1 excretion and disease outcome.

Van der Veen et al. have looked at chemokine expression in a mouse model of crescentic glomerulonephritis (ANCA-associated vasculitis model). They were able to produce a list of genes that were up regulated in renal disease using microarray techniques. They found that chemokines such as CXCL2 and the chemokine receptor CXCR2 were upregulated on day 1 of the experiment. On the other hand, chemokines such as CCL2 and the chemokine receptor CCR2 were found to be upregulated when the mice were sacrificed at day 7 (van der Veen, Petersen et al. 2009). Blocking the action of CXCR2 did not affect the outcome of the disease and did not prevent neutrophil accumulation. CXCR2 is expressed on neutrophils which have an important role in ANCA-associated vasculitis. As a result, this study suggests that neutrophils are recruited to the glomeruli by a chemoattractant other than CXCR2 ligands (such as CXCL1, CXCL2, and CXCL5).

I am interested in studying some of these chemokines and cytokines, especially those involved in macrophage infiltration to the glomeruli. It is important to identify these chemokines which could help in finding a way to block macrophage infiltration and studying the effect of this process on the disease development.

1.9. In vivo models of ANCA-associated vasculitis

Animal models have been useful tools in studying many human diseases. This is because mice can be used to induce diseases that resemble some human diseases. Studying these diseases in mice helps researchers observe the full immune response similar to how it

happens in humans. Until recently, animal models have not provided adequate evidence about the pathogenic role of ANCA in vasculitis (Heeringa, Brouwer et al. 1998). However, in groundbreaking experiments in 2002, Xiao et al. conducted a series of experiments to investigate the pathogenesis of ANCA in a murine model using MPO knockout (MPO-/-) C57BL/6J mice (Figure 1.9). These mice were immunised with MPO and developed anti-MPO antibodies. These antibodies were then injected into wild type and immune-deficient mice. They found that these recipient mice developed pulmonary haemorrhagic capillaritis, crescentic and necrotising glomerulonephritis and systemic necrotising arteritis. The pathology in these mice was similar to human ANCA-associated vasculitis. Some of these mice received anti-MPO splenocytes while the others received anti-MPO antibodies. All mice developed glomerular crescents and necrosis. On the other hand, mice that received anti-BSA antibodies did not develop glomerulonephritis (Xiao, Heeringa et al. 2002). This animal model, called murine experimental vasculitis, provided evidence that these anti-MPO antibodies are pathogenic because mice that received anti-MPO antibodies developed crescentic glomerulonephritis and small-vessel vasculitis.

I used this model to help me understand the importance of macrophages in the development of ANCA-associated vasculitis. Tissues were also used to understand more about the disease and the role of the immune system.

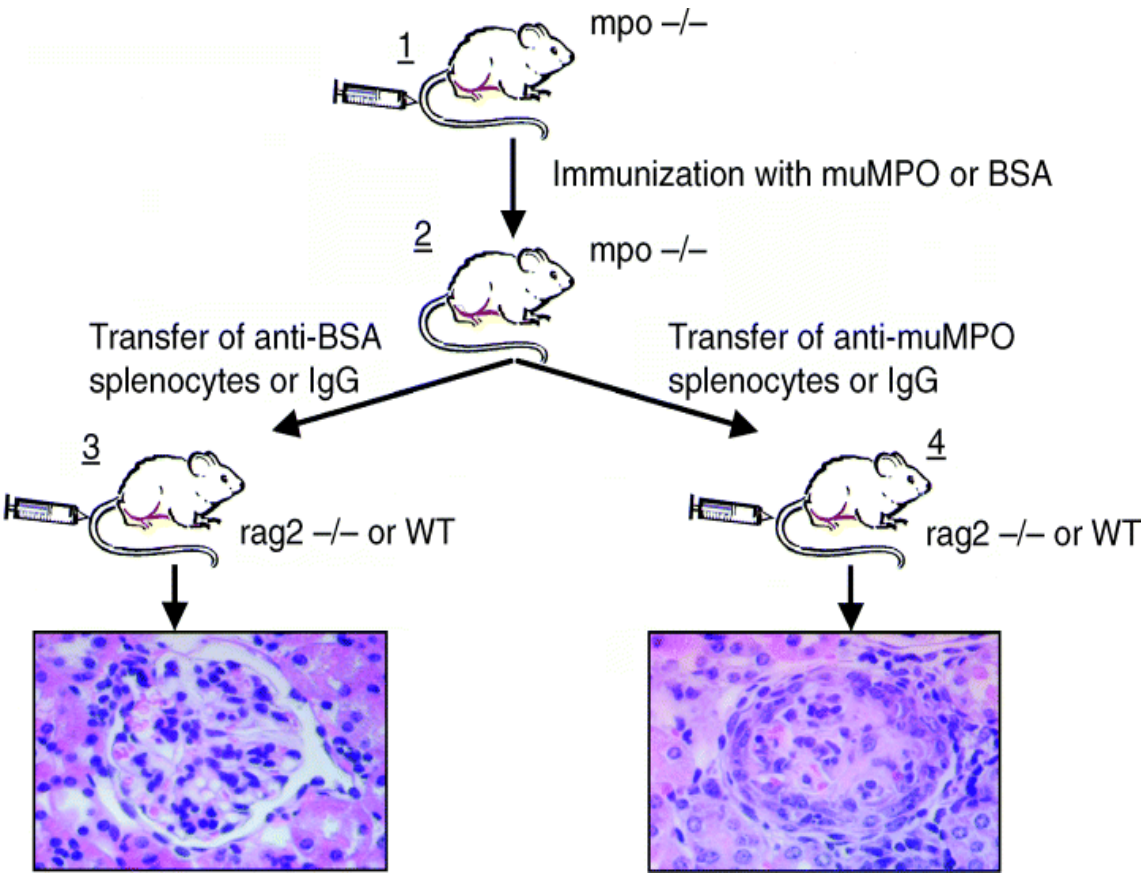

Figure 1.9: The design of experiment that was used to induce vasculitis in mice. MPO-/- mice were used in this experiment to raise anti-MPO antibodies. These antibodies were then injected in wild type mice and they developed vasculitis. Adapted from Kidney International (2004) 65, 1564-1567.

In addition, Little et al. were able to induce vasculitis in WKY rats using human MPO (hMPO), termed experimental autoimmune vasculitis (figure 1.10). They showed that immunising these rats with hMPO resulted in the generation of anti-MPO antibodies that cross-reacted with rat MPO. Furthermore, they showed that the severity of the disease was hMPO antigen dose-dependent because all the immunised rats had crescentic nephritis and lung haemorrhages when the dose was increased to 1600 µg/kg. In addition, they showed that the addition of pertussis toxin and lipopolysaccharide resulted in establishing the disease in all animals using less hMPO for immunisation. On the other hand, non-WKY strains did not develop vasculitis despite the fact that those strains developed high titres of anti-hMPO antibodies. They were able to show in this model, using intravital microscopy, that the anti-MPO antibodies were able to convert rolling neutrophils into firmly adhered

neutrophils which resulted in necrotising vasculitis after these cells invaded into the vascular wall (Little, Smyth et al. 2005; Little, Smyth et al. 2009).

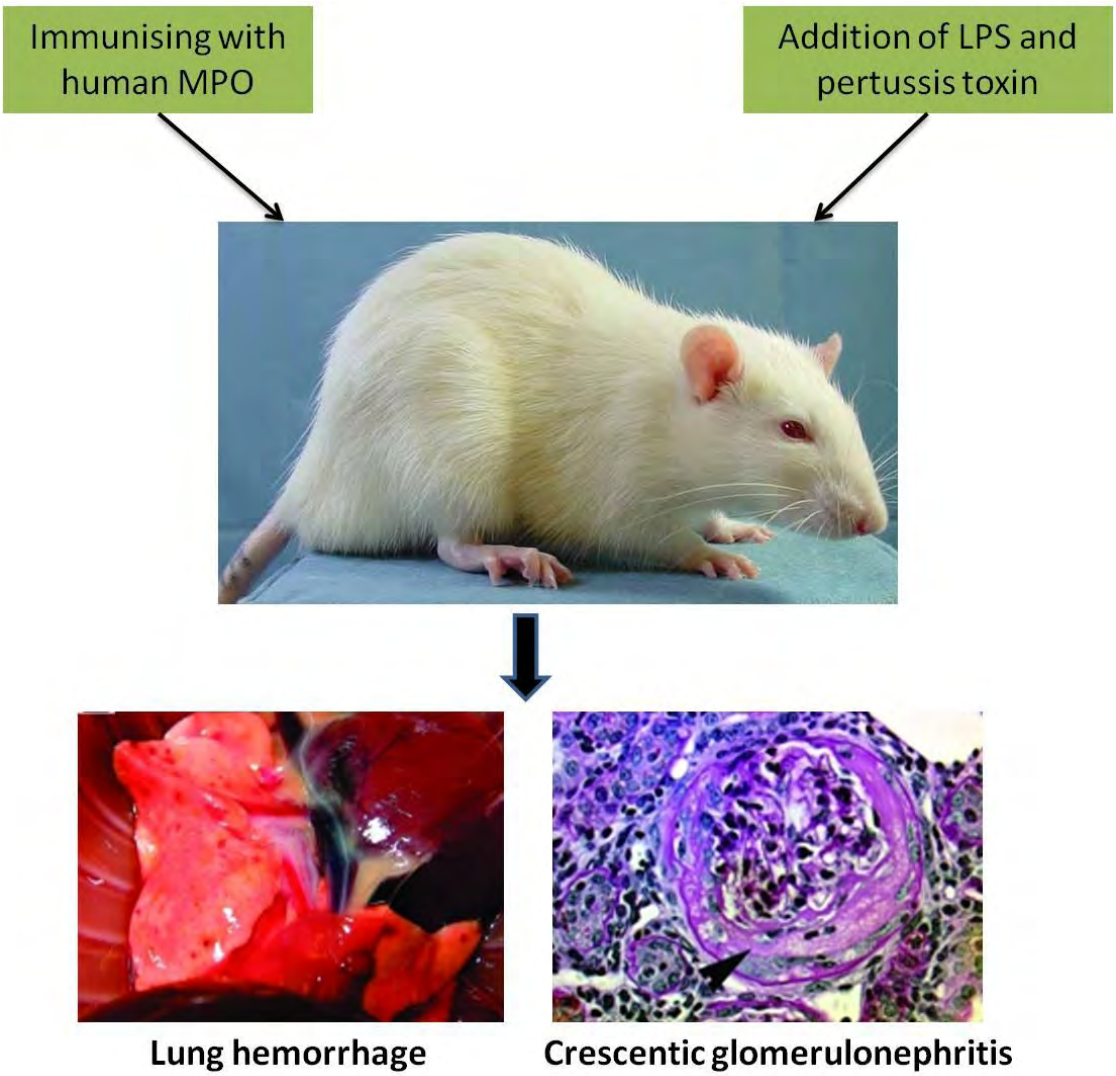

Figure 1.10: Experimental autoimmune vasculitis model. Rats are immunised with human MPO and the immune system is boosted with addition of LPS and pertussis toxin. These rats develop lung haemorrhage and crescentic glomerulonephritis after 8 weeks.

In contrast, finding an animal model of PR3 ANCA has proven to be more difficult. Different studies have been performed to try and establish an animal model of PR3-mediated disease, including immunisation of PR3-deficient mice with recombinant murine PR3. These mice developed anti-PR3 antibodies, but they did not induce vasculitis following passive transfer of the antibodies into wild type mice (Pfister, Ollert et al. 2004). Furthermore, van der Geld et al. immunised rats with human-mouse chimeric PR3 and they

were able to induce antibodies to rat PR3, but again the rats did not develop vasculitis (van der Geld, Hellmark et al. 2007).

The animal models that we have today depend on antibodies against MPO, which is thought to be, along with PR3, the main antigen in ANCA-associated vasculitis. Recently, Kain et al. were able to induce pauci-immune focal necrotising glomerulonephritis in rats by immunising them with rabbit IgG specific to lysosomal-associated membrane protein-2 (LAMP-2) (Kain, Exner et al. 2008). This work indicates the presence of other potential antigens that are involved in the pathogenesis of vasculitis.

In an effort to improve the mouse model of vasculitis, Xiao et al. have proposed, at a vasculitis and ANCA workshop (Lund, Sweden, 2009), a new mouse strain that is very susceptible to vasculitis (Xiao 2009). They used 129S6 mice that were shown to develop severe disease following injection with anti-MPO antibodies. It was not clear why this strain was more susceptible, but it could be due to genetic factors, as seen in the rat model where only the WKY strain develops the disease. Furthermore, they suggested that these mice develop 69% crescents compared to 8.56% crescents in C57BL/6J mice following injection with anti-MPO antibodies so we decided to use these mice in some of my work.

1.10. Macrophages and monocytes

Macrophages have long been suggested to play a role in the development of ANCA-associated vasculitis. Part of my project was to look at the effect of depleting macrophages on the development of vasculitis in mice. Therefore, I will talk about the origin of these cells and their role in the immune system. In addition, I will mention some of the previous work targeting macrophages in other types of crescentic glomerulonephritis.

1.10.1. Macrophage origin and different types of monocytes

The innate immune system is the first line of defence against infections; the cellular arm of this system includes specialised cells called phagocytes. These cells have many functions, including internalising and digesting bacteria and other cells, and also the secretion of inflammatory mediators that can kill bacteria and other infectious agents. Furthermore, these cells are able to scavenge toxic compounds and also stimulate cells from the adaptive immune system if needed. Monocytes represent about 10% of human leucocytes and 4% of mouse leucocytes (Auffray, Sieweke et al. 2009). One of the important functions of these monocytes is the renewal of some tissue macrophages and dendritic cells (DCs) (Geissmann, Jung et al. 2003; Auffray, Sieweke et al. 2009). These monocytes develop in the bone marrow from hematopoietic stem cells and they go through several progenitor stages, including the common myeloid progenitor (CMP), the granulocyte/macrophage progenitor (GMP), and the macrophage/DC progenitor (MDP) (Fogg, Sibon et al. 2006; Iwasaki and Akashi 2007). The growth factor CSF-1 is very important in the development of the blood monocytes and it is been shown that mice deficient in CSF-1R and CSF-1 demonstrate reduced numbers of blood monocytes (Cecchini, Dominguez et al. 1994; Dai, Ryan et al. 2002). One of the myeloid progenitors is MDP which is a cell in the bone marrow that expressed CSF-1R and also the chemokine receptor CX3CR1; this cell type gives rise to spleen conventional dendritic cells (cDCs), monocytes, and several macrophage subsets (Fogg, Sibon et al. 2006; Varol, Landsman et al. 2007; Waskow, Liu et al. 2008).

The migration of monocytes from the bone marrow to the blood is very important during inflammation. Recent studies have demonstrated the importance of CCR2 and its ligands CCL2 and CCL7 in the movement of inflammatory monocytes from the bone marrow to the blood (Serbina and Pamer 2006). In humans, these blood monocytes can be identified by specific markers such as the CSF-1 receptor and CX3CR1. Furthermore, these blood monocytes can be divided into three subsets defined by the expression of CD14 and CD16

(Auffray, Sieweke et al. 2009). Human CD14+CD16- monocytes express high levels of CCR2 and low levels of CX3CR1 and represent 80-90% of blood monocytes. In addition, these subsets are reported to produce IL-10 in response to LPS in vitro (Frankenberger, Sternsdorf et al. 1996; Geissmann, Jung et al. 2003). On the other hand, CD16+ monocytes express low levels of CCR2 and high levels of CX3CR1 and produce TNF-α in response to LPS in vitro (Belge, Dayyani et al. 2002; Geissmann, Jung et al. 2003).

Mouse blood monocytes and human monocytes have some typical morphological features. Mouse monocytes are identified by the expression of CD115 and other markers such as CD11b, F4/80, and variable expression of Ly6c antigen. Furthermore, mouse monocytes can be divided into different subsets depending on the expression of Ly6C (GR1+) and other chemokine receptors. Similar to human CD14+ monocytes, CD115+Ly6C+ mouse monocytes express CCR2 and low levels of CX3CR1 chemokine receptors (Geissmann, Jung et al. 2003). Unlike human CD14 monocytes, mouse Ly6c monocytes have the ability to produce TNF-α and IL-1 during infection and are known as inflammatory monocytes (Geissmann, Jung et al. 2003; Serbina and Pamer 2006; Nahrendorf, Swirski et al. 2007) (figure 1.11). These cells are the source of inflammatory monocytes (Geissmann, Jung et al. 2003) and resident macrophages and DCs in the lung, skin, and digestive tract (Ginhoux, Tacke et al. 2006; Landsman and Jung 2007; Landsman, Varol et al. 2007; Jakubzick, Tacke et al. 2008). The second type of mouse blood monocyte are the CD115+ Ly6C- monocytes, which are known to express high levels of CX3CR1 and lack the expression of CCR2 (Geissmann, Jung et al. 2003; Sunderkotter, Nikolic et al. 2004). These cells have a longer half-life and are found in inflamed and resting tissues after adaptive transfer (Geissmann, Jung et al. 2003).

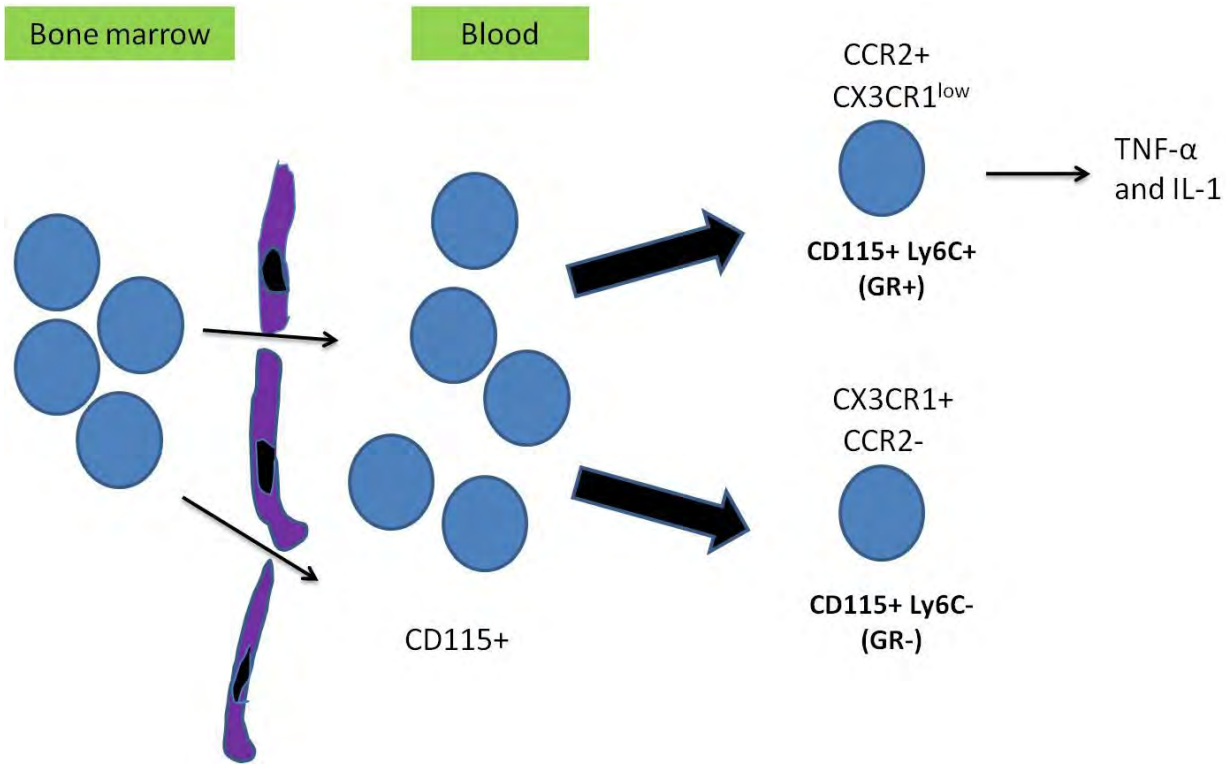

Figure 1.11: Mouse blood monocytes. Mouse monocytes express CD115 and can be divided into two subsets. Some of these monocytes are Ly6C+ and express CCR2 and low levels of CX3CR1. The second subset is Ly6C- monocytes which lack CCR2 expression but express CX3CR1.

CCR2 is the chemokine receptor for MCP-1 and has been mentioned previously to have a role in the development of crescentic glomerulonephritis. Blood monocytes that express CCR2 differentiate into inflammatory macrophages and dendritic cells. This receptor has an important role in macrophage recruitment to the site of injury. Furuichi et al. have shown protection from renal injury in an ischaemia reperfusion model in CCR2 deficient mice. In addition, they showed a reduction in the number of interstitial infiltrated macrophages (Furuichi, Wada et al. 2003). For these reasons, I decided to investigate the possibility of using anti-mouse CCR2 antibody to block or reduce macrophage infiltration into the glomerulus.

1.10.2. Monocytes and macrophages as part of the innate immune system

Monocytes are found in the bone marrow, blood, and spleen and they do not proliferate in a steady state (Auffray, Sieweke et al. 2009; Swirski, Nahrendorf et al. 2009). They express

different chemokine receptors that allow them to migrate to the tissue during infection, express pathogen recognition receptors, are involved in clearing cells and toxic molecules and also produce inflammatory cytokines. Furthermore, they differentiate to macrophages and inflammatory DCs during inflammation (Serbina, Jia et al. 2008) (figure 1.12). Macrophages are an important part of the immune system and are found in lymphoid and non-lymphoid tissues. In addition, they are known to be involved in tissue homeostasis by clearing apoptotic cells and also by producing growth factors. Furthermore, they express different ranges of pathogen recognition receptors and are able to produce inflammatory cytokines (Gordon 2002).

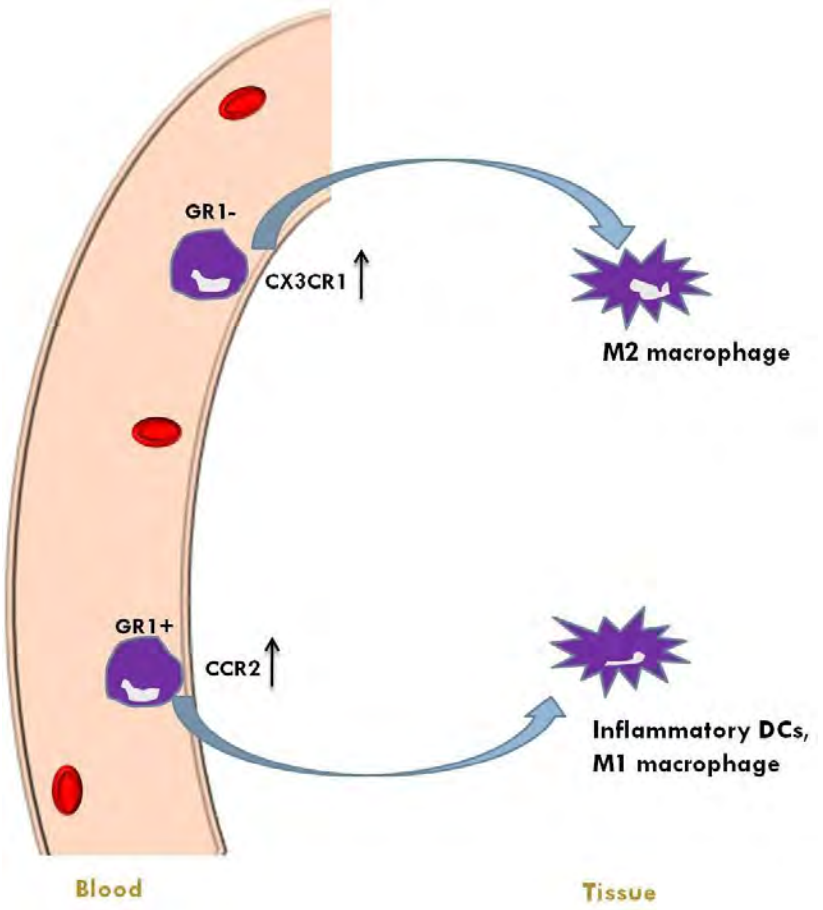

Figure 1.12: The origin of tissue macrophages and DCs. As shown in the diagram, tissue macrophages arise from Ly6c+ (Gr1+) monocytes and from Ly6c- (Gr1-) monocytes during inflammation. Gr1+ monocytes are known as inflammatory monocytes and have been suggested to be the source of M1 macrophages and inflammatory DCs. On the other hand, Gr1- blood monocytes are thought to be the source of M2 tissue macrophages.

1.11. Macrophages and renal disease

1.11.1. The role of macrophages in renal disease

ANCA-associated vasculitis is characterised by glomerular crescent formation. The involvement of macrophages in this disease and in the progression of the disease has been identified by different groups. The involvement of macrophages was first reported in 1972 when large numbers of macrophages were found infiltrating glomerular lesions (Atkins, Holdsworth et al. 1976). Researchers then suggested that macrophages must have a role in the progression of the disease and in crescent formation (Cattell 1994). The infiltration of macrophages to the site of injury is also a common feature in experimental models of glomerulonephritis (Figure 1.13) (Schreiner, Cotran et al. 1978; Bagchus 1990; Hara, Batsford et al. 1991). For example, the use of anti-rabbit macrophage serum in anti-glomerular basement disease in rabbits helps to reduce the severity of the disease. In addition, it has been shown that protection from the disease can be achieved by inducing leucopoenia by nitrogen mustard, but injecting peritoneal macrophages can reconstitute the disease (Holdsworth, Neale et al. 1981; Holdsworth and Neale 1984). These results were confirmed by more recent work and it was demonstrated that the number of macrophages injected correlated with the severity of the disease (Ikezumi, Hurst et al. 2003). Furthermore, there are several examples of the involvement of macrophages in different types of renal diseases. For example, Diamond et al. have shown that a reduction in the number of glomerular and interstitial macrophages prevented progressive glomerular disease in a model of acute puromycin aminonucleoside nephrosis. The reduction in the number of macrophages was achieved by exposing the rats to a sublethal dose of X-irradiation (Diamond and Pesek-Diamond 1991). In addition, the involvement of macrophages has been investigated in a rabbit model of glomerulonephritis. The disease was induced using an anti-glomerular basement membrane (GBM) antibody and there was a reduction in histological lesions and proteinuria following treatment with sheep anti-rabbit macrophage serum. In addition, this treatment resulted in a reduction in the number of circulating

monocytes and also prevented macrophage accumulation in the glomeruli (Holdsworth, Neale et al. 1981). Furthermore, Tang et al. were able to reduce macrophage infiltration in glomeruli using anti MCP-1 antibodies in a rat model of glomerulonephritis. This reduction in macrophage infiltration resulted in a reduction in proteinuria (Tang, Qi et al. 1996). All of these findings suggest a role for macrophages in renal disease, but their involvement and their role in ANCA-associated vasculitis has not been fully investigated.

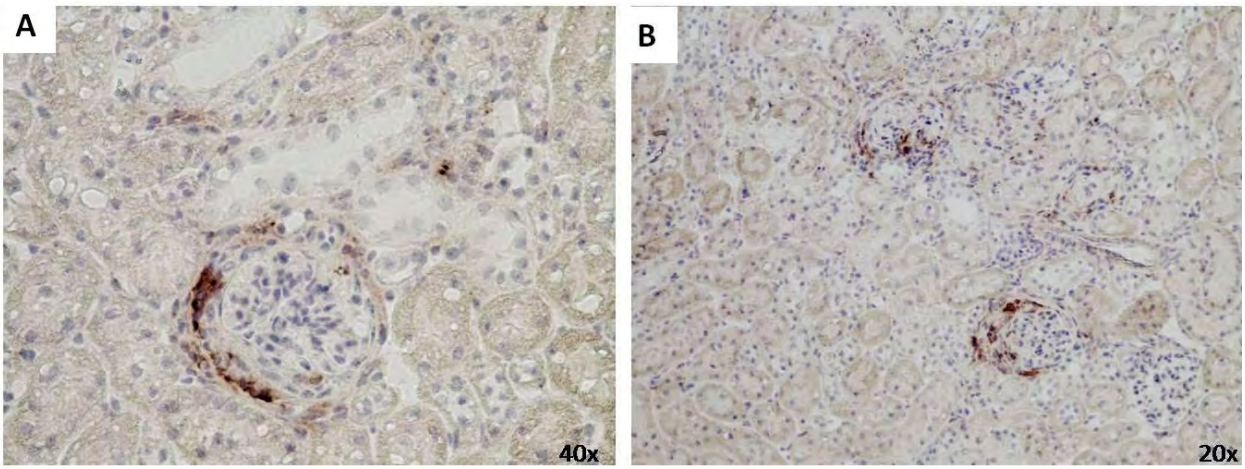

Figure 1.13: Macrophage infiltration in murine experimental vasculitis. CD68 staining shows macrophage accumulation in the crescent region of the glomeruli.

1.11.2. Potential mechanisms of glomerular injury by macrophages

As mentioned earlier, macrophages are present in inflamed glomeruli in different renal diseases. These macrophages have different functions that make them capable of increasing the severity of the disease. For example, macrophages are able to produce reactive oxygen and nitrogen species and different cytotoxic products. In addition, macrophages can secrete different pro-inflammatory cytokines at the site of inflammation (Kluth, Erwig et al. 2004) (figure 1.14). The production of reactive oxygen species by macrophages from nephritic glomeruli was seen in rabbits and rats (Boyce, Tipping et al. 1989; Cook, Smith et al. 1989). In addition, it has been shown that glomerular macrophages produce TNF-α in mice and rabbits with nephrotoxic nephritis (Boswell, Yui et al. 1988; Tipping, Leong et al. 1991). In addition, IL-1β has also shown to be produced by

macrophages and it was shown, in different disease models, that blocking this cytokine can lead to a reduction in glomerular inflammation (Kluth and Rees 1999).

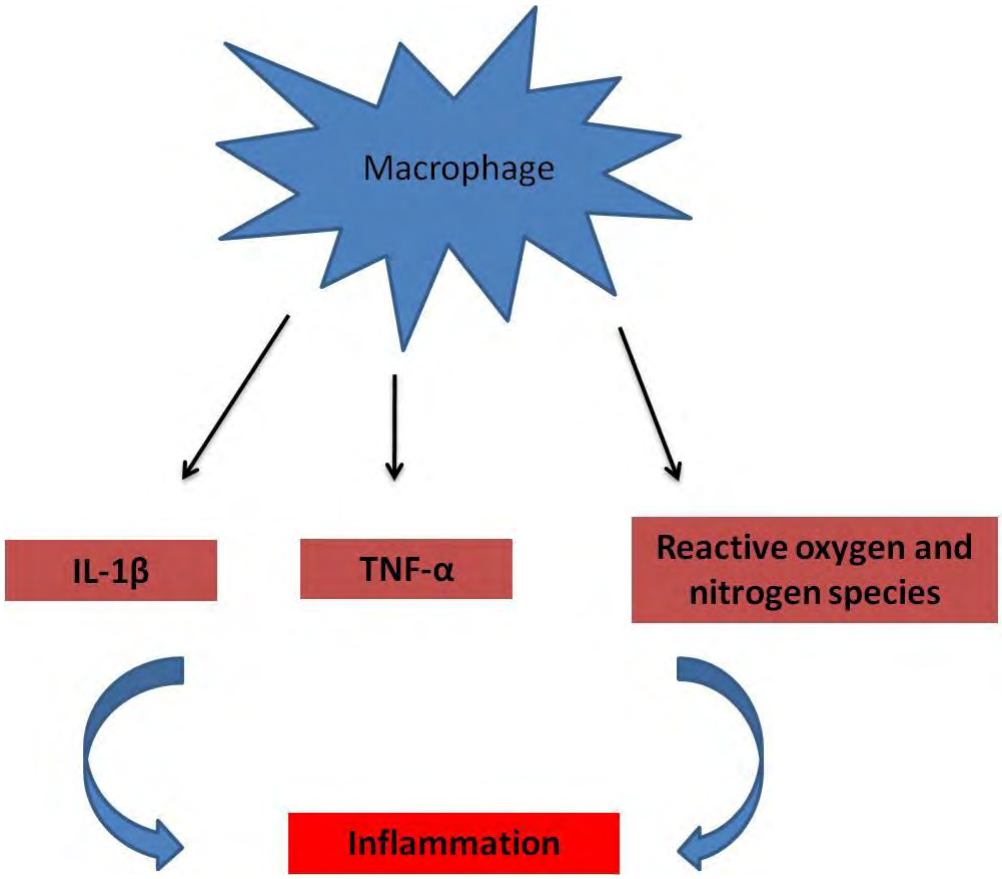

Figure 1.14: Potential role of macrophages in renal inflammation. Macrophages are capable of producing reactive oxygen and nitrogen species. Furthermore, macrophages can produce inflammatory cytokines such as TNF-α and IL-1β which can lead to inflammation and tissue injury.

1.11.3. The activation of macrophages and susceptibility to glomerulonephritis

Macrophages protect the body from microbial infection using different surface receptors. These receptors include Toll-like receptors (TLRs), scavenger receptors, and mannose receptors. These receptors are important for stopping microbial infection and recognise different microbial products. TLRs can recognise lipopolysaccharide (LPS) and also viral double-stranded RNA. Macrophages become classically activated when they receive two signals. The first signal is received when microbial products bind to the TLR and the second signal is received from T-helper cells or natural killer cells (Kluth, Erwig et al. 2004). These two signals lead to the classical activation of macrophages.

In addition, macrophages can be alternatively activated in the presence of IL-13 or IL-4 (Stein, Keshav et al. 1992; Doyle, Herbein et al. 1994). The alternative activation of macrophages causes these cells to increase their expression of different receptors such as MHC class II receptors and mannose receptors. Furthermore, alternative activation results in a reduction in nitric oxide production (Fenton, Buras et al. 1992) and it has been suggested that these cells are involved more in tissue repair than in killing intracellular organisms (Jakubzick, Choi et al. 2003).

Recently, different types of M2 macrophages have been identified such as type II activated macrophages with increased production of IL-10 and reduced production of IL-12 (Anderson and Mosser 2002). Cells that follow the type II activation pathway have been reported to favour the shift of immune response toward Th2 (Anderson and Mosser 2002).

It has been found that some rodent strains, such as WKY rats, are more susceptible to glomerulonephritis (Tam, Smith et al. 1999). On the other hand, Lewis rats have been found to be resistant to crescentic glomerulonephritis after injection with nephrotoxic serum. This susceptibility was found to be linked to two major quantitative trait loci, crescentic glomerulonephritis 1 and 2 (*Crgn1 and Crgn2*) (Aitman, Dong et al. 2006). It has been shown in a recent study that some transcripts located in the *Crgn2* congenic interval are upregulated in the glomeruli of WKY rats and downregulated in the glomeruli of LEW rats. The activator protein-1 (AP-1) transcription factor gene (*Jund*) is one of these transcripts and has been found to be upregulated in the glomeruli of WKY rats compared to LEW rats. This gene has been found to have an important role in macrophage activation because knockdown of this gene resulted in a significant reduction in macrophage activation in WKY rats (Behmoaras, Bhangal et al. 2008). These findings support the fact that macrophages have an important role in the pathogenesis of glomerulonephritis.

1.12. Macrophages and their heterogeneity in renal injury and repair

Macrophages are recruited to the site of inflammation in response to chemokines and they differentiate into two distinct subsets. In response to the disease state, macrophages can either be classically activated (M1) or alternatively activated (M2), depending on what they are exposed to (Martinez, Sica et al. 2008). For example, macrophages will differentiate toward M1 subtype when they are exposed to IFN-γ and LPS and these cells are known to produce IL-12 and IL-23. Interleukin-23 is reported to have a role in renal allografts and autoimmune diseases (Chen and Wood 2007). Traditionally, macrophages are thought to have a resolving role in renal disease by clearing apoptotic cells and promoting wound healing, but ongoing injury suggests a pathological role of macrophages in tissue destruction and irreversible fibrosis in the kidney (Figure 1.15). In addition, members of the TGF-β superfamily have been linked to renal fibrosis and it has been reported that macrophages, among other cell types, are capable of synthesising TGF-β when renal fibrosis lesions are developing (Border and Noble 1994; Eddy 2005). In addition, Isaka and colleagues have shown that overexpression of TGF-β can lead to the development of glomerulosclerosis (Border and Noble 1997). It has been shown that renal injury can be reduced by modulating the function and the phenotype of macrophages in models of renal diseases such as allograft injury (Yang, Reutzel-Selke et al. 2003), glomerulonephritis (Yokoo, Ohashi et al. 1999; Anders, Frink et al. 2003), and interstitial fibrosis (Nishida, Okumura et al. 2005). It has been proposed that changing the activation state of macrophages from M1 to M2 can help in reducing renal injury in renal diseases. For example, Wang et al. showed in adaptive transfer studies that injecting M2-polarised macrophages into mice with chronic renal disease resulted in a reduction in renal injury. This was an ex vivo study where they stimulated macrophages isolated from the spleen with IL-4 and IL-13 to obtain M2 macrophages (Wang, Wang et al. 2007).

Furthermore, the protective role of macrophages expressing hemeoxygenase-1 (HO-1) has been shown in different studies of autoimmunity and inflammatory activation (Roach, Moore et al. 2009; Tzima, Victoratos et al. 2009). In addition, expression of HO-1 in macrophages has been suggested to improve the outcome in hepatic and renal ischaemia-reperfusion injury (IRI) (Gueler, Park et al. 2007; Devey, Ferenbach et al. 2009). Ferenbach et al. were able to upregulate HO-1 expression on mouse macrophages using haem arginate (HA). They were able to demonstrate an improvement in renal function in a mouse model of acute kidney injury after treatment with HA. This protection was absent in animals that were treated with HA but had their macrophages depleted (Ferenbach, Nkejabega et al. 2011). This result shows a diverse role of macrophages in renal diseases. Some studies have demonstrated a protective role of macrophages while others have shown an inflammatory role.

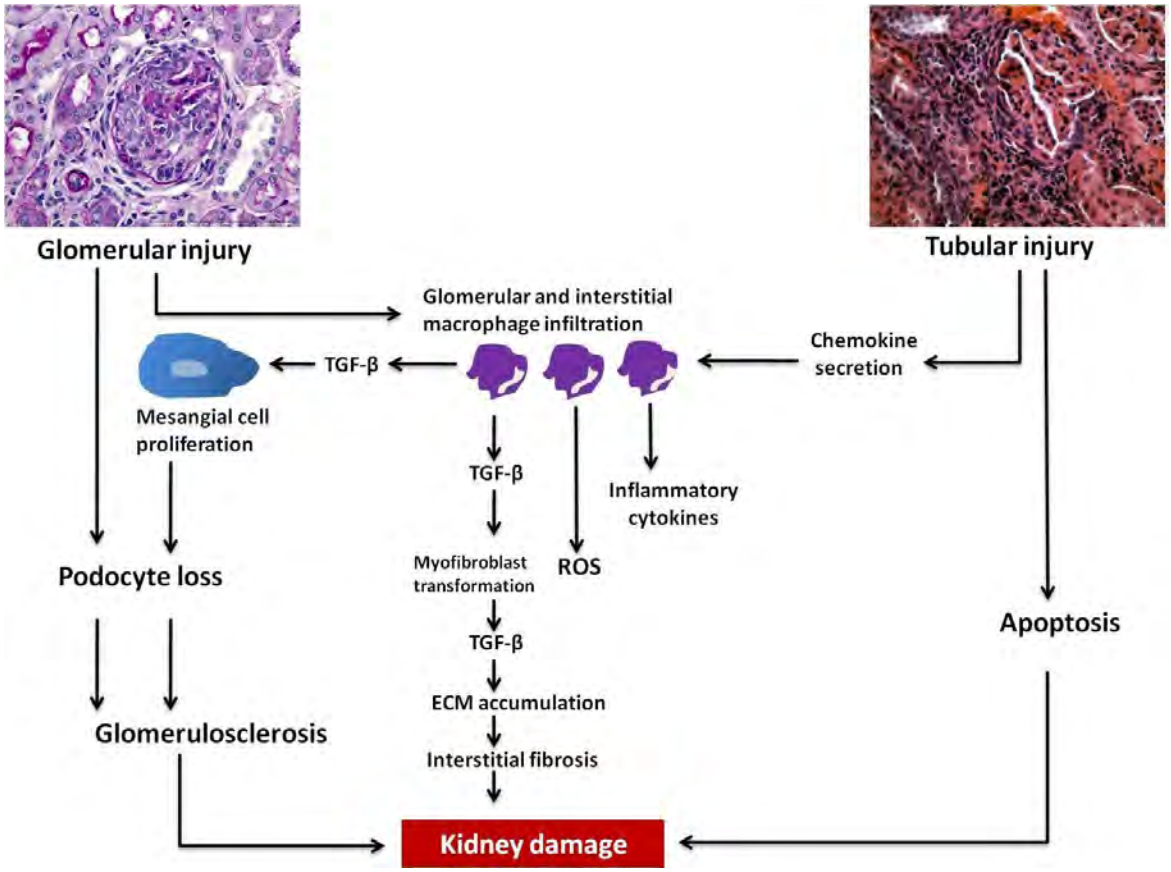

Figure 1.15: **The consequences of macrophage infiltration in renal disease leading to renal damage.** Macrophages infiltrate to the site of inflammation in response to glomerular and tubular injury. Macrophages that are recruited to sites of inflammation produce TGF-β and proinflammatory cytokines, causing more damage. Adapted from The Journal of Clinical Investigation (2008) 118:3522-3530.

1.13. Localisation and adhesion of macrophages in renal diseases

1.13.1. The importance of adhesion molecules in macrophage localisation

The involvement of macrophages in renal diseases requires the migration of these cells to the site of inflammation. This process involves lectin interaction, which results in the rolling of monocytes. This rolling allows the binding of VLA-4 to vascular cell adhesion molecule (VCAM) and LFA-1 to intracellular adhesion molecule (ICAM-1). The binding of these adhesion molecules is an important step in macrophage migration (Springer 1994). It has been found, in WKY rats with nephrotoxic nephritis, that macrophage infiltration can be reduced when the adhesion molecules ICAM-1 or LFA-1 are blocked (Nishikawa, Guo et al. 1993). In addition to adhesion molecules, chemokines play an important role in directing macrophages to the site of inflammation.

1.13.2. Chemokines and macrophage localisation

Macrophages follow a chemotactic gradient that leads them to the site of inflammation. Different chemokines play a key role in macrophage accumulation. These include MCP-1 and its receptor CCR2 which are present in different diseases such as ANCA-associated vasculitis and other causes of crescentic glomerulonephritis (Rovin, Rumancik et al. 1994; Segerer, Cui et al. 2000). The level of this chemokine has been used in different studies to indicate the severity of the disease. For example, the level of urinary MCP-1 has been found to correlate with the severity of renal injury in some studies (Rovin, Doe et al. 1996; Saitoh, Sekizuka et al. 1998; Wada T, Furuichi K et al. 1999). In addition, additional chemokines such as MIP-1β, MIP-1α, and RANTES have been identified in different diseases such as crescentic glomerulonephritis and lupus nephritis (Cockwell, Howie et al. 1998; Wada T, Furuichi K et al. 1999).

The role of chemokines in controlling the function of leucocytes is more complex since the functions of different chemokines overlap. This means that in the absence of one chemokine, another chemokine might have the ability to replace it. However, blocking the action of these chemokines using antibodies has proven to be a good approach to studying their effects. For example, blocking MCP-1 in mice with nephrotoxic nephritis results in a reduction in crescent formation, macrophage infiltration, and proteinuria (Tang, Qi et al. 1996; Wada T, Yokoyama H et al. 1996; Lloyd, Dorf et al. 1997). In addition, it has been shown that vMIP-II, which is a chemokine analogue produced by herpes virus 8, is able to reduce proteinuria, crescent formation, and macrophage infiltration in mice with crescentic glomerulonephritis (Chen, Bacon et al. 1998). This is because vMIP-II can block MCP-1, MIP-1α, RANTES, and MIP-1β. The blockade of these chemokines seems to affect macrophage infiltration and might have an effect on the progression of different renal diseases.

1.14. Depletion of macrophages

1.14.1. Liposomal clodronate

Macrophage depletion is important in the study of the role of macrophages in different diseases because it allows us to see their role in disease development. One of these methods is clodronate administration, which is used to treat osteolytic bone diseases (Jordan, van Rooijen et al. 2003). It has been found that once clodronate is incorporated into liposomes then it can be used to deplete macrophages (van Rooijen and van Nieuwmegen 1984; Claassen, Van Rooijen et al. 1990). Clodronate works by inducing apoptosis in macrophages after it has been taken up by these cells (Naito, Nagai et al. 1996; van Rooijen, Sanders et al. 1996) (figure 1.16). The type of injection has been found to affect the type of macrophages that are going to be depleted. For example, intravenous injection will result in depleting hepatic and splenic macrophages. On the other hand, injection into tissue will result in the depletion of macrophages in this tissue and the draining lymph nodes (van Rooijen, Kors et al. 1989). Van Rooijen at el. have shown that depleting macrophages using this method does not result in the secretion of pro-inflammatory cytokines by these cells when they undergo apoptosis (van Rooijen and Sanders 1997). In addition, liposomal clodronate has been found to affect macrophages and phagocytic dendritic cells, but not neutrophils or lymphocytes (van Rooijen, Kors et al. 1989; Van Rooijen and Sanders 1994; Alves-Rosa, Stanganelli et al. 2000).

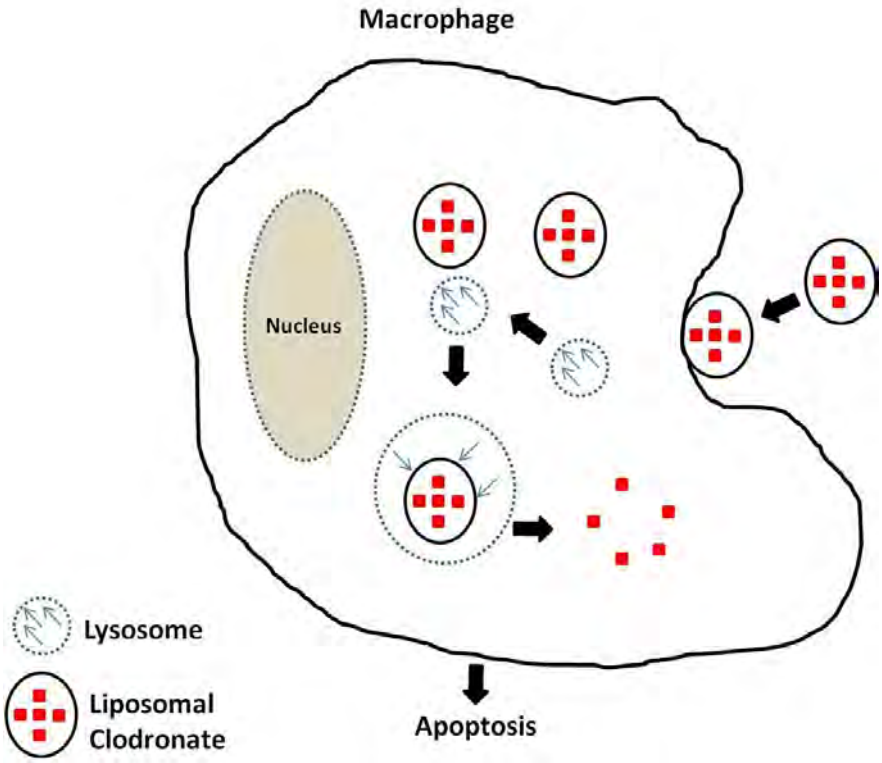

Figure 1.16: Mechanism of macrophage depletion using liposomal clodronate. Liposomal clodronate is taken up by the macrophage through endocytosis. Then, the bilayers of the liposome are disrupted by phospholipases from lysosomes. This results in the release of clodronate, causing cell death.

1.14.2. Diphtheria toxin in CD11b-DTR mice

Another method of depleting macrophages involves using diphtheria toxin (DT) to deplete macrophages. Duffield et al. achieved this by generating transgenic mice that express the human diphtheria toxin receptor (DTR) under the control of the CD11b promoter, thereby leading to its expression on circulating monocytes. They used human DTR because mice respond poorly to DT. This allowed them to deplete macrophages by intravenous injection of minute quantities of DT (Duffield, Tipping et al. 2005). They used this method to test the effect of depleting macrophages on crescentic glomerulonephritis in mice. They found that following DT injection in mice, the percentage of resident macrophages in the kidney dropped by 98%. Depleting macrophages resulted in a reduction in the number of cellular glomerular crescents (Duffield, Tipping et al. 2005). In addition, renal function showed

improvement after depleting macrophages. Duffield et al. showed that renal injury and fibrotic scarring were reduced following macrophage depletion (Duffield, Tipping et al. 2005).

1.14.3. The role of CCR2 in macrophage accumulation

CCR2 is a chemokine receptor for MCP-1; it has been shown that MCP-1/CCR2 signalling is involved in crescentic glomerulonephritis in humans (Segerer, Cui et al. 2000). The role of CCR2 in macrophage infiltration in kidney disease models has been investigated by different groups. For example, Furuichi et al. have shown a reduction in the number of macrophages infiltrating the kidney interstitium in CCR2 deficient mice after ischaemia-reperfusion (Furuichi, Wada et al. 2003). Furthermore, they used a CCR2 antagonist and showed a reduction in the number of infiltrating cells and in tubular necrosis. In a different study, Kitagawa et al. showed a significant reduction in renal pathology after treatment with a CCR2 antagonist in the unilateral ureteral obstruction (UUO) model (Kitagawa, Wada et al. 2004). In addition, the number of F4/80 positive cells was reduced after treatment with a CCR2 antagonist and most of these cells were positive for CCR2. These studies demonstrated the ability of anti-CCR2 antibodies to reduce macrophage infiltration which can be used in our model.

1.15. The aim of the project

The aim of my work was to study the innate immune system in ANCA-associated vasculitis. I also aimed to establish a mouse model of AAV in Birmingham and to work to improve this model. I focused on two cell types of the innate immune system: macrophages and neutrophils. I aimed to study the phenotype of macrophages in the injured kidney following treatment with anti-MPO antibodies. In addition, I studied the role of macrophages in AAV by blocking macrophage infiltration to the kidney following disease induction. My hypothesis was that macrophages are important in the development of the disease and blocking their recruitment should protect animals from developing severe disease.

Furthermore, I looked at gene expression in the kidney using mouse and rat models of AAV. The aim of this work is to help in the search for genes associated with macrophage activation (classical and alternative activation). It also provided a basis on which to study the pathways involved in disease induction such as complement pathways. In addition, was interesting to see if the mouse and rat models of AAV were similar and if the upregulated genes were similar. Finally, I performed some experiments to study the variability in ANCA-induced neutrophil degranulation. Previous work in our lab has shown that there is variation in the ability of ANCA to induce neutrophil degranulation from healthy donors. I studied the metabolites present following neutrophil degranulation to identify why we see this variability.

1.16. Experimental questions and hypothesis

My hypotheses are:

- Macrophages are involved in tissue injury in AAV and blocking their recruitment can improve disease outcome.
- Macrophages that are recruited to the glomeruli are classically activated macrophages.
- Variability in ANCA-induced neutrophil degranulation is due to variability in donors and the ANCA source.

Questions to be answered:

- Can we improve the mouse model of AAV by finding a reliable source of MPO for immunisation?
- What are the phenotypes of macrophages in the glomeruli?
- Does blocking macrophage recruitment prevent or reduce renal injury in AAV?
- What genes are upregulated in the kidney of mice with MEV?
- What are the sources of variation in ANCA-induced neutrophil degranulation?

Chapter 2

2. General Materials and Methods

This chapter describes the general methods used throughout my PhD. I have also included some of the techniques that I optimised during my work. I have included all specific methods in the relevant result chapters.

Neutrophils that are used in my experiment were taken from healthy donors with their consent.

2.1. Animals, reagents, and antibodies

2.1.1. Animals

Most mice had a C57BL/6 (B6) background and 129SvEv mice were used in one experiment. Myeloperoxidase heterozygous (MPO+/-) mice were kindly donated to us by Dr. Peter Heeringa (University Medical Centre, Groningen, the Netherlands). These mice were maintained by the Biomedical Services Unit (BMSU) at the University of Birmingham. The heterozygous mice were mated to establish an MPO-knockout (MPO-/-) colony. I immunised the MPO-/- mice with MPO when they were 10 weeks old. We also used 129S6/SvEv mice (Taconic, New York USA). All procedures were performed according to the Home Office Regulations for Animal Experimentation under the project licence of Dr. Mark Little.

2.1.2. Reagents

Company	Reagents
Sigma-Aldrich, Poole, Dorset, UK	SIGMAFAST OPD tablets, methyl α-D-mannopyranoside, hexadecyltrimethylammonium bromide (CTAB), rat serum, mouse serum, normal horse serum, SIGMAFAST 3,3'-diaminobenzine tablets

	(DAB), penicillin-streptomycin, L-glutamine solution, rabbit serum, E-toxate kit, lipopolysaccharides from *Escherichia coli* 026:B6 (LPS), SIGMAFAST p-nitrophenyl phosphate tablets (p-NPP), Freund's incomplete adjuvant, goat serum, manganese (II) chloride tetrahydrate, McCoy's 5A medium, ethidium bromide solution, phenylmethanesulphonyl fluoride, 250 units ready Taq DNA polymerase.
Qiagen, Crawley, West Sussex, UK	DNeasy blood and tissue kit, RNeasy micro kit.
Carl Zeiss Ltd., Welwyn Garden City, Hertfordshire, UK.	MembraneSlide NF 1.0 PEN.
Thermo Scientific, Epsom, Surrey, UK.	Cap strip-strips of 8-120 strips of 8 ultra-clear, 1-Step PNPP, Slide-A-Lyzer dialysis cassettes, 20 K, 0.5-3 ml capacity.
Applied Biosystems, Warrington, UK	LCM staining kit.
Lonza, Wokingham, Berkshire, UK	PBS 10x w/o Ca, Mg, QCL-1000 CHROMOGENIC LAL 120 TESTS.
Invitrogen, Paisley, UK	SlowFade Antifade kit, Agarose
GE Health Care, Little Chalfont, Buckinghamshire, UK	Percoll, Amersham Hyperfilm ECL, HiTrap SP Sepharose HP 5 ml.
Bunzl Healthcare, Coalville, Leics, UK	BD Connecta™ Plus Stopcock, 10 cm.
LGC Standards, Teddington, Middlesex, UK	WEHI-3
Surgipath Europe Limited, Bretton, Peterborough, UK	Mayers haematoxylin.
Gamidor Technical Services Ltd, Didcot, Oxfordshire, UK	Diff-Quick.
Bioline, London, UK	dNTP Master mix.
Promega, Southampton, UK	Blue/orange loading dye, 100 bp DNA ladder, nuclease-free water.
R&D Systems Europe,	Recombinant mouse MPO.

Abingdon, UK	
Insight Biotechnology Limited, Middlesex, UK	MPO heavy chain (L-20) blocking peptide.

2.1.3. Antibodies

I purchased and used the following antibodies in my experiments:

Company	Antibody
ABD Serotec, Oxford, UK	Rat anti-mouse CD68, rat anti-mouse CD206, rat anti-mouse CD206:FITC, rat IgG2a negative control:FITC, goat anti-rat IgG:HRP (mouse adsorbed), rat IgG2a negative control
Invitrogen, Paisley, UK	Alexa 488 goat anti-rabbit IgG, anti-fluorescein/Oregon green goat IgG fraction, Alexa Fluor conjugate, Alexa 594 goat anti-rat IgG, Alexa 488 goat anti-mouse IgG.
Vector Labs, Peterborough, UK	Biotinylated rabbit anti-rat IgG, Texas red streptavidin, rabbit unconjugated anti-rat IgG (H+L) mouse adsorbed, fluorescein rabbit anti-rat IgG, rabbit biotinylated anti-goat IgG (H+L)
Abcam, Cambridge, UK	MHC class II IA+IE antibody, rat IgG secondary antibody.

2.2. In vitro methods

2.2.1. Culturing WEHI cells as a source of murine MPO

Murine WEHI-3 cells (a murine myeloid cell line, ATCC) were used as a source of murine MPO, which is not commercially available. These cells were frozen in liquid nitrogen in 1 ml of medium with DMSO. The cells were stored in a liquid nitrogen tank and directly

transferred to a water bath at 37°C prior to use. Then, McCOY5A medium with 10% FCS, 5% penicillin/streptomycin, 5% HEPES, and 5% L-glutamine was used to culture these cells. The WEHI cells were added to a T75 flask drop by drop and then 15 ml of medium was added to the cells. The next day, the cells were transferred to a new flask and the following day they were split into two T75 flasks. The cells were incubated for two days and then spun down; the pellet was resuspended and 9 ml of medium was added to the cells. The cells were then transferred to a large flask containing 300 ml of medium. In early cultures, these large culture flasks were used to propagate the WEHI cells. I subsequently investigated the feasibility of using a rolling bioreactor instead of static flasks. With the assistance of Dr. Margaret Goodall, I started culturing these cells using bioreactors (Greiner Bio-One Ltd., UK). The bioreactors have two separate chambers or sections that are separated by a membrane that allows fluid exchange (figure 2.1). The cells were resuspended in 40 ml of medium with 10% FCS and 400 ml of medium without FCS was added to the top chamber. The medium in the top chamber was replaced twice a week and the cells were harvested from the bottom chamber once a week using a 50 ml Luer-Lock syringe (Medisave, Dorset, UK). I left about 5 ml of cells in the lower chamber and added 40 ml fresh medium with 10% FCS. The cells that were harvested were spun down and washed in PBS and then stored at -80ºC.

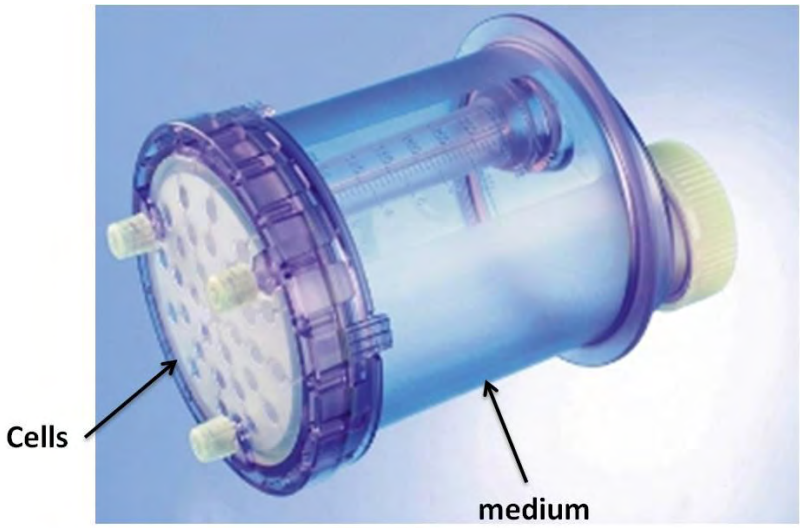

Figure 2.1: bioreactor or culturing WEHI cells. Cells are added to the bottom chamber with FCS and medium is added to upper chamber.

The MPO content of the cells was periodically estimated using an MPO activity assay. Cells (at a concentration of 1 million cells per 50 µl) were spun down and 0.3% Triton was added to the pellet. The cells were incubated with Triton for 10 min at room temperature. Then, the cells were spun down and added to an ELISA plate and 100µl of o-Phenylenediamine (OPD) substrate was added to each well. After this, I incubated the cells for 30 min and then the plate was read at 450 nm. This was done for both cell samples cultured under static and rolling conditions over a long period of time to ensure that MPO production did not decline over time.

2.2.2. Neutrophil isolation for use in degranulation experiments

I also investigated the variability in ANCA-induced neutrophil degranulation in healthy neutrophil donors using ANCA IgG. This followed on from a previous project that provided preliminary data to suggest that the neutrophil phenotype is more important than the source of IgG in determining neutrophil responses to ANCA. In order to optimise my technique, I started isolating neutrophils from human blood using a Percoll solution to prepare gradients for neutrophil separation. I first prepared a 100% solution (22.5 ml Percoll + 2.5 ml 1.5 M saline), from which I then prepared 81% (8.1 ml 100% solution + 1.9 ml PBS), 70% (7 ml

100% solution + 3 ml PBS), and 55% (5.5 ml 100% solution + 4.5 ml PBS) solutions. Then, blood was taken and slowly added to a 50 ml tube containing 5 ml of the anticoagulant ACD (4.2 g disodium hydrogen citrate, 5 g D-glucose, 200 ml pyrogen-free water). After this, I mixed blood with an equal volume of 2% Dextran (9 g NaCl, 20 g Dextran T500, and 1 L pyrogen-free water) and inverted the mixture several times. I spun down the mixture at 25 g for 10 min. While the blood was spinning, I prepared the gradient in a 15 ml white-top conical tube. First, I added 4.5 ml of the 81% solution to the bottom of the tube, being careful not to leave drops on the side of the tube. Then, I balanced a 21G needle on a 5 ml syringe near the top of the 81% solution and made sure that the opening of the needle was facing the wall of the tube so that the solution would not drip from the needle. Then, I added 3 ml of the 70% solution to the syringe and left it to flow through and run down the side of the tube onto the top of the bottom layer. Then, the syringe was removed without moving the tube.

After spinning the blood for 10 min, the supernatant was removed to new tubes, leaving behind all of the red blood cells, and spun at 150 g for 7 min. The pellet was resuspended and 3 ml of 55% Percoll solution was added to it. I balanced a 19G needle on a 5 ml syringe near the top layer of the gradient. A sample was then drawn into the syringe, left to flow as before, and spun down at 1500 g for 45 min. Two clear layers were separated by the gradient. I used a sterile transfer pipette to remove the top layer (monocytes). The bottom layer contained neutrophils, which were transferred to a fresh 15 ml tube, which was filled with PBS to dilute the Percoll solution. The tube was spun down at 400 g for 5 min; this was repeated twice. Then, the pellet was resuspended in HBH ready for use. I determined neutrophil viability and purity using trypan blue and Diff-quick staining on cytospins, respectively.

2.2.3. Neutrophil degranulation assay

I looked at the effect of different ANCA samples on the degranulation of neutrophils from different donors. The degranulation of MPO from neutrophils was measured by ELISA. Neutrophils were isolated using the Percoll gradient and the cells were resuspended at 2.5 ×

10^6 cells/ml of HBH. In order to prime these neutrophils, the cells were incubated with 80 U/ml of TNF-α (2 µl/ml of cells) in the presence of cytochalasin B (5 µg/ml of cells) for 15 min at 37ºC. The ANCA IgG samples were spun down at 13,000 rpm (to remove any debris formed during storage) for 1 min and were then diluted to 1 mg/ml in HBH. N-formyl-methionine-leucine-phenylalanine (fMLP) was used as a positive control and was diluted 1:2,000 in HBH (final concentration 1 µM). Following this, 100 µl (2.5×10^5 cells) of stimulated neutrophils were added to each well of a round-bottomed 96-well plate. Then, I added 25 µl of either normal or ANCA IgG to the wells and 25 µl of the positive control was added to one well. The final concentration of IgG in each well was 200 µg/ml. The plates were incubated at 37ºC for 15 min. Next, the plates were spun down at 1500 rpm for 5 min and 75 µl of the supernatant was transferred to a flat-bottomed 96-well plate. Then, I added 100µl of the OPD substrate to each well and the plates were incubated at room temperature for 30 min. Finally, I stopped the reaction by adding 100 µl of acetic acid and the plates were read at 450 nm.

2.2.4. Superoxide release

This assay was done by Dr. Julie Williams in parallel with my degranulation assay.

The ability of ANCA IgG to stimulate superoxide production was measured by the superoxide dismutase-inhibitable reduction of ferricytochrome C as described elsewhere (Radford, Lord et al. 1999). Neutrophils were resuspended at 2×10^6/ml in HBH. Then, they were primed with 2 ng/ml TNF-α and 5 mg/ml cytochalasin B for 15 min at 37ºC. The cells were then stimulated with 1µM N-formyl-methionyl-leucyl-phenylalanine (fMLP), which was used as a positive control, or 200 µg/ml of IgG (MPO-ANCA, PR3-ANCA or normal IgG). The release of superoxide was then measured over 120 min.

2.2.5. Flow cytometry

Confirming monocyte depletion in mice

For this experiment, 50 µl of blood was taken from each mouse and placed into a tube with 5 µl of 50 mM EDTA. After this, antibodies were added to the bottom of 1 ml Eppendorf tubes in the dark. For double staining, two antibodies or their isotype control antibodies were added to the same Eppendorf tubes. Next, 20-30µl of blood was added to each tube containing the antibodies or isotypes. After vortexing, the tubes were incubated in the dark for 15-20 min. Then, I added 1 ml of 1× FACS lysis buffer (cat no. 349202, BD biosciences, UK) and incubated them in the dark for 15 min. The samples were then transferred to FACS tubes, 2 ml of cold PBS was added to each tube and the tubes were spun at 1,000 rpm for 5 min. Finally, the supernatant was poured off and the pellet was resuspended in 500 µl PBS. The samples were then put on ice and analysed using a FACSCalibur flow cytometer (BD biosciences, Oxford, UK); the data were analysed using FlowJo.

2.2.6. Immunohistochemistry and immunofluorescence staining

Immunostaining of frozen sections

Mouse kidneys were frozen in OCT compound after culling the animal and stored at -80ºC until sectioning; 5 µm thick sections were prepared using a cryostat. The sections were collected on Superfrost plus glass adhesion microscope slides (Fisher Scientific, Leicestershire, UK). The sections were left to air dry for 2 h or overnight and stored at -80ºC until use. On the day of staining, the slides were taken out of the freezer and left to thaw at room temperature for 15 min. They were then fixed in ice-cold acetone for 15 min in the fridge before being taken out and left to dry; a circle was then drawn around each section using a wax pen (S2002, Dako, UK). The sections were rehydrated in PBS for 5 min and then blocked with 0.3% hydrogen peroxide in methanol for 30 min in a humidity chamber. Following this, the sections were washed three times in PBS for 5 min each. Then, I blocked non-specific binding with 10% horse serum (shown to be a good blocking agent during

optimisation) in PBS for 20 min. Next, I tapped off the serum and added a primary antibody to each section at a dilution of 1:100 in PBS/2% horse serum and incubated them for 2 h at room temperature or overnight in the cold room. Then, the sections were washed three times in PBS for 5 min each before a secondary antibody was added to each section at a 1:200 dilution in PBS/2% horse serum and incubated for 45 min at room temperature in a humidity chamber. Then, the slides were washed as described above. Next, an ImmPRESS anti-rabbit (peroxidase) kit (MP-7401-15, Vector Lab, UK) was added to each section (two drops on each section) and they were incubated for 30 min and then washed as described above. The staining was then visualised using DAB (Sigma, Dorset, UK) for 10 s and the reaction was stopped by immersing the slides in water. Then, the slides were washed under running water for 5 min. Counterstaining was then performed by immersing the slides in Mayer's haematoxylin (01582E, Surgipath Europe Limited, UK) for 1 min and washed under running water for 5 min. After this, the slides were immersed in sodium bicarbonate for 1 min and were washed under running water for 10 min. Next, the sections were dehydrated in 75% and 100% ethanol for 20 s each and moved to xylene for 2 min. Finally, the slides were mounted using Immu-mount (Thermo Scientific, Surrey, UK) and left overnight to dry.

Immunostaining of paraffin sections

I started by removing the paraffin and rehydrating the sections by immersion in xylene and 100% ethanol for 5 min each. Next, peroxidase activity was blocked by 1% hydrogen peroxide in water for 15 min. After this, the antigens were retrieved by microwaving the sections for 20 min in 10 mM citrate buffer. The sections were washed with gentle agitation in TBS for 5 minutes (three times). The sections were then blocked with casein solution (Vector Labs, Peterborough, UK) that was kindly donated to me by Dr. Gary Reynolds (University of Birmingham, UK) for 10 min. Then, the sections were incubated with a primary antibody or negative control and placed in an incubation chamber for 1 h. After this, the sections were washed in TBS 0.025% Triton by gentle agitation twice for 5 min each. Rabbit anti-rat IgG (Vector Labs, Peterborough, UK), diluted at 1:200 in TBS, was added to the

sections. The sections were then placed in an incubation chamber for 15 min. After washing, I applied the ImmPRESS anti-rabbit Ig kit (Vector Labs, Peterborough, UK) for 30 min by adding 100 µl of the kit to each slide. After this, I washed the sections with TBS-Tween (six times) for 5 min each. The sections were visualised using ImmPACT DAB (Vector Labs, Peterborough, UK) for 5 min. The sections were counterstained in haematoxylin for 1 min and washed under warm running water for 10 min to allow the colour of the stain to develop. Then, the sections were rehydrated by immersing them in 100% ethanol and then xylene for 5 min each. Finally, DPX mounting medium was used to mount the sections and they were left to dry before being examined.

Quantitative assessment using Aequitas 1A

I analysed the immunohistochemical staining using Aequitas 1A (DDL, Cambridge, UK). I started by taking five random images at 10× magnification from each kidney section. Images were taken from control and diseased animals. Then, I took one of the control images and used it to adjust the threshold. This threshold was used to analyse all of the images. The software gave a percentage of positive staining; this percentage was the percentage of positive staining in that area (the whole image). I analysed the percentage of positive staining in the glomeruli by selecting glomeruli only and then measuring the positive staining as a percentage of the area of glomeruli.

2.2.7. Measuring the endotoxin level in LPS

Lipopolysaccharide (LPS) (Sigma Aldrich, UK) was used to help induce vasculitis in mice. In order to give the same amount of active LPS to each mouse, I needed to measure the endotoxin level in the commercial LPS preparation. The E-Toxate kit (Sigma Aldrich) was used to calculate specific endotoxin activity. E-Toxate is prepared from a lysate of the circulating amoebocytes of the horseshoe crab. This lysate forms a gel when exposed to endotoxins such as LPS, depending on the concentration of the endotoxin. All tubes used in this experiment were autoclaved and then baked for 4 h at 200ºC. The E-Toxate multiple test

vials and endotoxin standard were re-constituted in the appropriate volume of endotoxin-free water (Sigma Aldrich, UK). The endotoxin standard was vigorously mixed for 2 min and then it was vortexed for 30 s at 10-min intervals over a 30 min period. After this, different dilutions of the endotoxin standard were prepared using endotoxin-free water (Table 2.1). In addition, serial dilutions of stock LPS were made in order for a negative result to be achieved (Table 2.2). Then, the sample, water, and endotoxin standard dilution were added directly to the bottom of the tubes. Endotoxin-free water was used as a negative control. After this, the endotoxin detection solution was added to each tube by inserting a pipette just above the contents and allowing the solution to flow down the side of tube. Next, the contents of the tubes were gently mixed, the mouths of the tubes were covered using Parafilm, and the tubes were incubated at 37ºC for 1 h. Then, the tubes were slowly removed from the incubator and inverted by 180º to check for evidence of gel formation. The formation of a hard gel was considered a positive result. The endotoxin level of the LPS was calculated by multiplying the inverse of the greatest dilution of LPS found to be positive by the lowest concentration of the endotoxin standard found to be positive.

Table 2.1: Different dilutions of endotoxin standard.

Tube no.	Endotoxin	Endotoxin-free water (ml)	Final conc. (EU/ml)
1	0.2 ml endotoxin std. stock soln.	1.8	400
2	0.2 ml from tube no. 1	1.8	40
3	0.2 ml from tube no. 2	1.8	4
4	0.3 ml from tube no.3	2.1	0.5
5	1 ml from tube no. 4	1	0.25
6	1 ml from tube no.5	1	0.125
7	1 ml from tube no. 6	1	0.06
8	1 ml from tube no. 7	1	0.03
9	1 ml from tube no.8	1	0.015

Table 2.2: Different dilutions of LPS.

Tube No.	LPS	Endotoxin-free water	Dilution factor	Expected concentration (3,300,000 EU/ml stock)
A1	10µl LPS stock	990µl	1/100	33,000 EU/ml
A2	10µl from tube no. A1	990µl	1/10,000	330 EU/ml
A3	100µl from tube no. A2	900µl	1/100,000	33 EU/ml
A4	100µl from tube no. A3	900µl	1/1,000,000	3.3 EU/ml
A5	100µl from tube no. A4	900µl	1/10,000,000	0.33 EU/ml
A6	100µl from tube no. A5	900µl	1/100,000,000	0.033 EU/ml
A7	100µl from tube no. A6	900µl	1/1,000,000,000	0.0033 EU/ml

2.3. Protein Methods

2.3.1. MPO purification from WEHI-3 cells

After 6 months of continuous culturing and harvesting of WEHI cells, I started isolating MPO from these cells. I estimated the number of cells to be 5×10^{10}. There were 8.2×10^{8} cells in a 1 ml pellet (based on early counting estimates using a Coulter counter). I used a method similar to that of Xiao et al. (Xiao, Heeringa et al. 2002). The pellets were resuspended in buffer A (6.7 mM sodium phosphate, pH 6.0; 1 mM $MgCl_2$; 3 mM NaCl; 0.5 mM PMSF); 5 ml of buffer A was added to each 1 ml pellet. After this, the cells were lysed by Dounce homogenisation and then they were spun down in an ultracentrifuge at 25,000 rpm for 25 min. The supernatant, which had a green colour, was dialysed against buffer B (100 mM sodium acetate, pH 6.3; and 100 mM NaCl) overnight; I called this SN1. Buffer A was added to the pellet (P1) and incubated overnight to obtain any residual MPO.

The next day, concanavalin-A (Amersham Pharmacia Biotech, UK) was washed with buffer B con-A (100 mM sodium acetate, pH 6.3; 100 mM; 1 mM $CaCl_2$; 1 mM $MgCl_2$; and 1 mM $MnCl_2$). The material from the dialysis tubes was then added to the con-A pellet at a

ratio of 50 ml SN1 to 1.5 ml of con-A and incubated overnight end-over-end. After this, P1 was spun down at 25,000 rpm for 20 min and dialysed against buffer B overnight.

The next day, the mixture from SN1 and con-A was spun down and the supernatant (SN2) was re-incubated with con-A and incubated overnight. The MPO was eluted from the con-A using buffer B elution (100 mM sodium acetate, pH 6.3; 100 mM NaCl; 1 mM $CaCl_2$; 1 mM $MgCl_2$; 1 mM $MnCl_2$; and 750 mM methyl α-D-mannopyranoside), which was added to the pellet and incubated overnight end-over-end in a cold room.

I used the same con-A extraction with the methyl α-D-mannopyranoside elution for the P1 and SN2 samples and stored all samples at -80^{o}C until I was ready to perform the final purification step using a Mono- cation exchange column (GE Healthcare, UK). When I was ready to run the samples through this column, the samples were dialysed against buffer D (50 mM sodium acetate, pH 8.5-9; and 100mM NaCl). Then, I washed the Mono-S column with buffer D and buffer E (50 mM sodium acetate, pH 8.5-9; and 1 M NaCl) and finally I equilibrated it with buffer D. Then, I loaded the sample into the column with buffer D and eluted with buffer E. I checked the absorbance of the purified fraction at A280 and A430. The concentration of MPO was calculated using the following formula: [MPO] = (A430/0.178) × 0.144. Then, the MPO was dialysed with PBS overnight and then stored at -80ºC.

MPO was also isolated from human blood using a similar protocol in order to optimise my technique before MPO was isolated from WEHI cells.

2.3.2. Purification of IgG

2.3.2.1. Affinity chromatography of mouse serum

I purified IgG from mouse serum using protein G affinity chromatography. The column was packed using protein G matrix (Sigma, Dorset, UK) in a XK16 × 20 column (GE Healthcare, UK). The serum was first centrifuged at 10,000-15,000 rpm for 10 min to remove any debris that might have formed during storage. The column was first washed with a

loading buffer (20 mM sodium phosphate, pH 7.0). Then, the sample was loaded by injection using a syringe at a flow rate of 0.5 ml/min. The entire process was run using an AKTA Prime Plus chromatography system (GE Healthcare, UK) with a PC for visualisation of the results. When the entire sample was loaded, the machine was switched to the elution buffer (0.1 M glycine, pH 2.7). The pH of the sample was neutralised using a neutralisation buffer (Tris-HCl, pH 9.0), which was added to the collection tubes before I started eluting the IgG from the column. The size of the fractions was 1-2 ml. The IgG concentration was calculated using the formula: (C= A 280/1.35). Samples were injected into 20 K Slide-A-Lyzer dialysis cassettes using a needle and syringe and dialysed against PBS overnight. The purity of the anti-MPO antibody was checked using SDS-PAGE.

2.3.2.2. Purification of human IgG from plasma exchange fluid

Human IgG was purified from plasma exchange fluid (PEX) for use in the degranulation experiments. The purification process was similar to the one mentioned above with some modifications. Plasma exchange fluid that is normally discarded was obtained from patients with systemic vasculitis and stored at -20ºC. Serum was prepared by adding 1 ml of 1 M $CaCl_2$ to 50 ml of PEX and left to clot overnight at 4ºC. The next day, the sample was spun down at 2,000 g for 15 min and the supernatant was collected and filtered through syringe filters. After this, the serum was diluted 1:1 with PBS before loading it into the column. I used a 5 ml HiTrap protein G HP column (GE Healthcare, UK) for this process. The column was washed with 4-5 column volumes of PBS by injecting PBS into the column using a 50 ml syringe; the flow-through was discarded. The serum was injected into the column (10 ml) and the column was then washed with PBS as previously described. After this, IgG was eluted from the column by injecting 20 ml of 0.1 M glycine pH 2.7 and the flow-through was collected and neutralised by adding 0.75-1 ml of 1 M Tris pH 9.0. Next, the samples were dialysed in sterile PBS by loading the samples into dialysis tubes (Medicell International, London, UK) and stirring them at 4ºC overnight. The next day, the samples were concentrated down using vivaspins (Appleton Woods, Birmingham, UK). These vivaspins

were first washed by adding 5 ml of PBS to the upper chamber and spinning them at 5,000 rpm for 5 min at 4ºC. Then, the samples were loaded into the vivaspins and spun down until approximately 1 ml was left in the upper chamber. I removed the samples from the upper chamber using a syringe and needle and washed the membrane by trituration. Finally, the sample was filtered by passing it through a 0.2 µm syringe filter. The concentration of IgG was measured using a spectrophotometer.

2.3.3. SDS-PAGE and Western blot

2.3.3.1. SDS-PAGE

SDS-PAGE and Western blot were performed to confirm the presence and the purity of MPO (murine MPO and human MPO). The SDS-polyacrylamide gels were prepared by first pouring the 10% resolving gel between glass plates, leaving 2-3 cm at the top. Then, an upper layer of water was added to the top of the gel to prevent it from drying out. The gel was left to polymerise for 30 min. Then, I poured off the top layer of water and the remaining space was filled with the stacking gel. The comb was inserted and the gel was left to polymerise for 30 min. After this, the gels were placed onto a holder/electrode and transferred to a running tank, which was filled with 1× running buffer. Then, 1.6 µg or less of MPO was diluted 1:1 in loading buffer (without β-mercaptoethanol (β-ME)). For reducing conditions, the samples were diluted 1:1 in a loading buffer containing β-ME and boiled at 95°C for 5 min. After this, the samples were loaded into the wells and a protein standard ladder was added to the first well. Two gels were made: one reduced and the other non-reduced. Then, the gels were stained with Coomassie Blue overnight. The next day, the gels were destained and photographed.

2.3.3.2. Western blot

Proteins were transferred from the gel to nitrocellulose and blocked with a blocking buffer (10% non-fat dried milk in TBS-T) for 3 h. Then, the blot was covered with rabbit anti-human

MPO antibody diluted 1:100 in blocking buffer for human MPO and mouse anti-mouse MPO for mouse MPO and incubated overnight. Then, the blot was incubated with goat anti-rabbit Ig HRP secondary conjugate (Biosource, UK) diluted 1:1000 in blocking buffer for human MPO, and with goat anti-mouse immunoglobulin/HRP (DAKO, UK) for mouse MPO. I used the chemiluminescent method to detect MPO by incubating my Western blot with a substrate (Amersham, UK) and the light was detected by photographic film.

2.3.4. ELISA techniques

2.3.4.1. Anti-MPO ELISA

The antibody level in the serum of MPO immunised MPO-/- mice was measured by an anti-MPO ELISA. The serum was obtained from the mice by leaving the blood to clot overnight at 4ºC and then spinning it down at 4,000 rpm for 10 min. The concentration of murine MPO was made up to 2 µg/ml using 0.015 M carbonate buffer (0.795 g Na_2CO_3, 1.465 g $NaHCO_3$, 500 ml water, pH 9.6). Then, 100 µl of the murine MPO was added to each well of 96-well ELISA plates and incubated overnight at 4ºC. The next day, serum samples from immunised mice were serially diluted in blocking buffer (PBS + 1% BSA + 0.1 % Tween 20) in triplicates. The plates were washed three times using PBS-Tween. I then added 100 µl of a diluted sample, in triplicate, to each well and incubated it for 60 min at 37ºC. The plate was washed three times in PBS-T and 100 µl of a secondary antibody (anti-mouse IgG alkaline phosphatase developed in goat, Sigma Aldrich, UK) diluted 1:30,000 in blocking buffer was added to each well and incubated for 45 min at 37ºC. Then, the plate was washed three times and 100 µl of the substrate was added to each well (p-nitro-phenylphospate tablets, Sigma Aldrich, UK) and incubated at room temperature for 30 min. The plate was read at 405 nm.

A log dilution of 1:10,000 was performed in order to determine the anti-MPO antibody titre. The titre was estimated as the dilution that resulted in a 50% drop in the OD value

using non-linear fit with the following equation: $Y=OD^{Bottom} + (OD^{Top}-OD^{Bottom})/(1+10^{((Log_{EC50}-X))})$. A positive control was used for each ELISA experiment, consisting of serum from MPO-/- mice immunised with WEHI MPO. In addition, a negative control was also used, consisting of serum from MPO-/- mice immunised with BSA.

2.4. Molecular techniques (genotyping, arrays)

2.4.1. Mouse genotyping

2.4.1.1. DNA isolation

The DNA was extracted from murine tissue using a DNeasy Blood and Tissue kit (Qiagen, West Sussex, UK). I added 180 µl of ATL buffer to each tissue sample in Eppendorf tubes. This buffer is a lysis buffer which works by breaking open the membrane and of the cell and the nucleus. After this, 20 µl of proteinase K was added to each Eppendorf tube, which is important for denaturing hydrolytic enzymes and also for keeping the DNA intact. The samples were mixed by vortexing and then incubated at 56°C overnight using a heat block. The next day, the samples were mixed by vortexing and then 200 µl of AL buffer and 200 µl of ethanol were added to each sample and mixed by vortexing. Then, the samples were transferred to a DNeasy Mini spin column in a 2 ml collection tube and I centrifuged the sample at 8,000 rpm for 1 min. This allowed proteins and other cytoplasmic components to pass through and it also allowed the DNA to stick to the membrane in the column. The columns were then washed twice using AW1 and AW2 buffers. Finally, an elution buffer (AE) was used to collect the DNA from the membrane of the column. I added 0.5 ml of the AE buffer to each column and incubated them at room temperature for 1 min. The samples were then centrifuged at 8,000 rpm for 1 min and the DNA was eluted and collected in Eppendorf tubes.

2.4.1.2. PCR preparation

Polymerase chain reaction (PCR) was used to amplify the DNA and MPO primers were used to ensure that only MPO was amplified. The PCR master mix was prepared; it

contained Ready TAQ polymerase (Sigma, IBR store, University of Birmingham, UK), buffer (Sigma, IBR store, University of Birmingham, UK), dNTP Master Mix (Bioline Products, IBR store, University of Birmingham, UK), MPO primers (Alta Bioscience, University of Birmingham, UK), and nuclease-free water (Promega Products, University of Birmingham, UK).

The samples were then subjected to PCR using the specific settings shown in Chapter 3. Then, the samples were subjected to gel electrophoresis in order to identify MPO-/- mice.

2.4.2. Affymetrix array

2.4.2.1. Microdissection

We wanted to study gene expression in glomeruli and tubules from mouse and rat models of ANCA-associated vasculitis. The laser microdissection technique was used to microdissect glomeruli from frozen kidney sections. I started by preparing sections from frozen kidneys. The kidneys were transferred from -80°C to a cryostat on dry ice, although they were not allowed to defrost. Then, I prepared 8 μm-thick sections from these tissues using the cryostat. I cleaned the blade and all the brushes using RNaseZap. The sections were then transferred to membrane slides (Zeiss, Germany). Each slide was then kept inside the cryostat for 2 min and a second tissue sample was added to the same slide. In order to do this, I put my finger behind the area where the new section would stick in order to defrost that area and allowed the tissue to stick without allowing the first section to defrost. Then, the sections were transferred to a storage box that contained silica gel (to remove any moisture) on dry ice.

The sections were then stored at -80°C until I was ready for microdissection. On the day of microdissection, the sections were kept on dry ice and I stained one slide at a time. I used cresyl violet stain for visualisation. The sections were taken out of dry ice and quickly moved (without allowing them to defrost) to 95% ethanol for 30 s. Then, they were transferred to 75% ethanol for 30 s and then 50% ethanol for 25 s. Next, I drained off any excess ethanol

and marked the edges of each slide with a barrier pen in order to keep the dye in place. Then, I added 300 µl of cresyl violet stain directly onto the tissue for 1 min. After this, I removed the excess dye and transferred the slide to 75% ethanol for a short period of time, then to 100 ethanol for 30 s. I then left the slides to dry at room temperature for 5 min. The sections were quickly transferred for laser microdissection. I started laser microdissection and the microdissected tissues were collected on collection caps containing 30 µl of lysis buffer (diluted with 1:100 β-ME). When the microdissection was finished, I removed the cap and added 10 µl of lysis buffer and mixed the contents. The cap was then replaced on the micro-tube and the tube was tapped to force the sample to the bottom of the tube. Then, the sample was centrifuged at 4,000 rpm for 15 s. The sections were used for microdissection for no longer than 45 min to prevent RNA degradation. Then, the tissues that were collected were stored in lysis buffer at -80°C until RNA extraction.

2.4.2.2. RNA extraction from microdissected tissues

I extracted total RNA from microdissected tissues stored in 30 µl of lysis buffer using an RNeasy micro kit (Qiagen, UK). Eight kidney sections from each animal were microdissected in order to obtain 400 glomeruli (50 glomeruli from each section). I pooled these samples together and I adjusted the sample volume to 350 µl with RLT buffer containing β-ME. After this, the sample was mixed by vortexing for 30 s. Next, I added 1 volume of 70% ethanol (350 µl) to the homogenised lysate and the sample was mixed well by pipetting (no centrifuging). Then, I transferred the sample, including any precipitate that may have formed to an RNeasy MinElute spin column placed in a 2 ml collection tube. I gently closed the lid and centrifuged the sample for 15 s at 10,000 rpm. The flow-through was then discarded from the lower chamber. Subsequently, I added 350 µl RW1 buffer (a wash buffer that contains ethanol) to the RNeasy MinElute spin column. The lid was gently closed and the sample was centrifuged for 15 s at 10,000 rpm in order to wash the spin column membrane (the flow-through was discarded). I added 10 µl DNase I stock solution (to remove any DNA from the sample) to 70 µl RDD buffer and I mixed the mixture by gently inverting the tube.

Then I added the DNase I incubation mix (80 µl) directly to the RNeasy MinElute spin column membrane and placed the tube on the bench top for 15 min. Then I washed the column by adding 350 µl RW1 buffer to the RNeasy MinElute spin column and centrifuged the sample as described previously. The RNeasy MinElute spin column was placed in a new 2 ml collection tube. Then, I added 500 µl Buffer RPE to the spin column and centrifuge as previously described. I washed the column again by adding 500 µl of 80% ethanol to the RNeasy MinElute spin column. Then, I centrifuged for 2 min at 10,000 rpm to wash the spin column membrane and I discarded the flow-through and collection tube. I placed the RNeasy MinElute spin column in a new 2 ml collection tube, opened the lid of the spin column and centrifuged at full speed for 5 min. This was done to make sure that the membrane was dry before eluting the RNA because ethanol can affect downstream applications. Finally, I placed the RNeasy MinElute spin column in a new 1.5 ml collection tube and added 14 µl RNeasy-free water directly to the centre of the spin column membrane before centrifuging for 1 min at full speed to elute the RNA.

2.4.2.3. RNA amplification step

The RNA samples were processed by the College of Medical and Dental Sciences Affymetrix Microarray Service (Dr. John Arrand). The RNA was amplified using an ExpressArt C&E Nano kit (AMSBIO, UK) in two amplification steps (figure 2.2). I will describe the protocol that was used to amplify the total RNA.

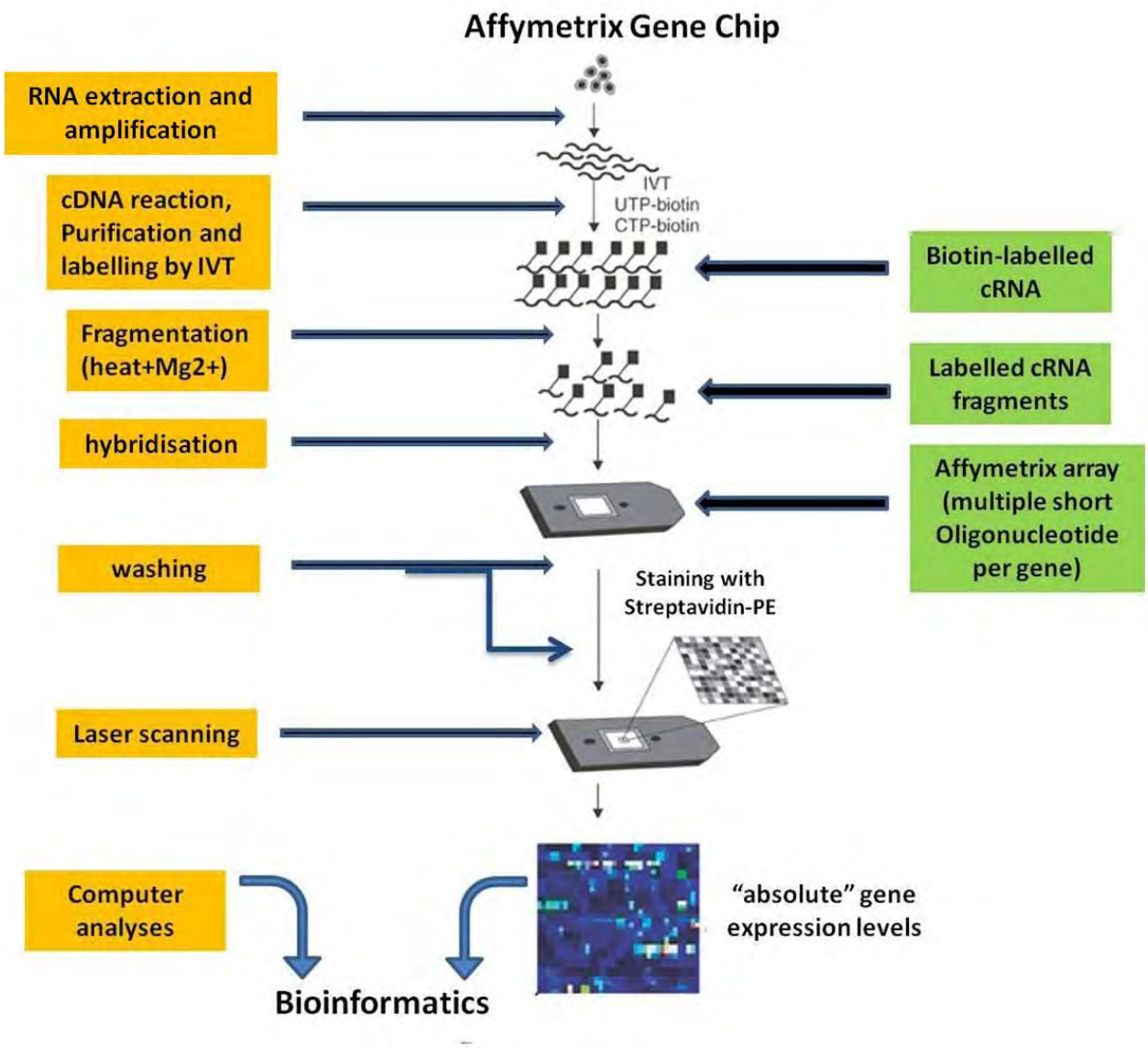

Figure 2.2: Affymetrix array procedure. RNA was amplified, followed by biotin labelling, fragmentation, and hybridisation to mouse or rat genome arrays. This was then followed by washing, staining and scanning according to standard Affymetrix protocols. Adapted from Staal et al. Leukaemia. 2003 Jul; 17(7):1324-32.

2.4.2.4. First strand cDNA synthesis

The procedure started by preparing the first strand cDNA synthesis Mix1. Then, 4 µl of Mix1 was added to 4 µl of each RNA sample. This was followed by 4 min incubation at 65ºC in a thermocycler with a heating lid. After this, the samples were cooled down to 37ºC. During that time, the first strand cDNA synthesis Mix2 was prepared at room temperature.

Then, 8 µl of Mix2 was added to each sample and mixed well. Next, the samples were run in a thermocycler using the following settings:

37ºC/ for 45 min

45ºC/ for 15 min

50ºC/ for 5 min

70ºC/ for 10 min

4ºC/ Hold

The samples were removed from the thermocycler and the tubes were centrifuged and kept on ice.

First Strand cDNA Synthesis (Mix1)	
H_2O	2.4 µl
dNTP Mix	0.8 µl
Primer A	0.8 µl

First Strand cDNA Synthesis (Mix2)	
DEPC-H2O	3.2 µl
5× RT Buffer	3.2 µl
RNase Inhibitor	0.8 µl
RT Enzyme	0.8 µl

2.4.2.5. Template DNA synthesis

The second strand DNA synthesis mix (Mix3) was prepared in the given order in a 1.5 ml reaction tube. Then, 104 µl of Mix3 was added to the first strand reaction on ice and the sample was gently mixed by pipetting. The samples were then incubated in a thermocycler at 16ºC for 2 h. After this, the samples were removed from the thermocycler and kept on ice. Finally, the samples were centrifuged to collect the liquid and then they were quickly moved to the purification step.

Second Strand DNA Synthesis (Mix3)	
H_2O	73.0 µl
Polymerase buffer	24.0 µl
dNTP Mix	2.4 µl
Polymerase A	3.2 µl
Polymerase B	0.8 µl
Polymerase C	0.8 µl

2.4.2.6. Purification of template DNA with spin columns

The purification step started by adding 246 µl of Mix4 to each template DNA reaction (120 µl from the previous step). The samples were gently mixed by pipetting. Then, the column was prepared by inserting DNA purification spin columns into collection tubes. Samples were then transferred onto each column and centrifuged for 1 min at 10,000 rpm. The flow-through was discarded and the column was re-inserted in the same collection tube. Then, the columns were washed with 200 µl washing buffer and centrifuged as previously described. The washing step was repeated again. After this, the flow-through was discarded and the column centrifuged again for 1 min at 10,000 rpm. Finally, the template DNA was eluted by inserting the columns in fresh 1.5 ml reaction tubes and then adding 10 µl of elution buffer to the columns. After this, the columns were incubated for 2 min and centrifuged for 1 min at 10,000 rpm. The purified template DNA was now ready for in vitro transcription.

Purification (Mix4)	
Binding Buffer	244 µl
Carrier DNA	2 µl

2.4.2.7. Amplification via in vitro transcription

First of all, the samples for in vitro transcription (Mix5) were prepared at room temperature. Then, 10 µl of Mix5 was added to the template DNA obtained in the previous step. The transcription was then incubated overnight at 37ºC in a thermocycler with the heating lid adjusted to 45ºC. Next, 1 µl DNase was added to each reaction and thoroughly mixed. The mixture was then incubated at 37ºC for 15 min.

***In vitro* Transcription (Mix5)**	
NTP Mix	6.6 µl
10× Buffer	1.7 µl
RNA Polymerase	1.7 µl

2.4.2.8. Amplified RNA purification using RNA spin columns

The purification step was started by adding 987 µl of Mix6 to each in vitro transcription reaction and thoroughly mixing. Then, 700 µl of this mixture was transferred into a spin column and centrifuged for 30 s at 10,000 rpm and the flow-through was discarded. The remaining mixture was then transferred to the column and centrifuged as previously described. Next, the column was washed by adding 500 µl of wash buffer 1 and centrifuged as previously described. This was followed by a second washing step by adding 500 µl of wash buffer 2 and centrifuging as previously described. Then, 500 µl of 80% ethanol was added to the column and centrifuged. The flow-through was discarded and the column was centrifuged again for 1 min at maximum speed to remove residual salts from the spin column matrix. Finally, the column was inserted into a fresh 1.5 ml reaction tube and the RNA was eluted from the column by adding 30 µl of RNase-free water (pre-heated to 95ºC). The column was incubated for 2 min and then centrifuged for 1 min at maximum speed. The eluted sample was then reapplied to the column and treated as before. The RNA was now in a total volume of 30 µl and was used for the second amplification step.

aRNA Purification (Mix6)	
RNA LB Buffer	340 µl
RNA DeS Buffer	87 µl
100% Ethanol	560 µl

2.4.2.9. Second amplification round

Amplified RNA was again reverse transcribed into cDNA to produce high yields of aRNA via a second round of amplification because the starting quantity of RNA was low.

First strand cDNA synthesis

The amplified RNA was used for a second amplification step. First, 5 µl of Mix2-1 was added to 25 µl of each RNA (for smaller volumes, the final volume was adjusted to 30 µl with water). Then, the samples were incubated at 65ºC in a thermocycler for 4 min before being cooled to 37ºC. Then, 20 µl of Mix2-2 was added to each sample; this was mixed well by gently flicking the tube. Then, the samples were incubated in a thermocycler using the following settings:

37ºC/ 45 min
45ºC/ 15 min
50ºC/ 5 min
37ºC/ hold

This was followed by adding 5 µl of Mix2-3 while the samples were in a thermocycler, and they were incubated using the following settings:

37ºC/ 5 min
80ºC/ 15 min
37ºC/ hold

Finally, 5 µl of RNase Mix2-4 was added to first strand cDNA reaction and the reaction was incubated at 37ºC for 20 min.

First Strand cDNA Synthesis (Mix2-1)	
dNTP Mix	2.5 µl
Primer B	2.5 µl

First Strand cDNA Synthesis (Mix2-2)	
DEPC-H_2O	8.4 µl
5 × RT Buffer	10.0 µl
RNase Inhibitor	0.8 µl
RT Enzyme	0.8 µl

Primer Erase (Mix2-3)	
DEPC-H_2O	3 µl
5× Extender Buffer	1 µl
Primer Erase	1 µl

RNase (Mix2-4)	
DEPC-H_2O	3 µl
5× Extender Buffer	1 µl
RNase	1 µl

Template cDNA synthesis

The procedure started by adding 35 µl of Mix2-5 to each first strand cDNA synthesis reaction; the samples were then incubated in a thermocycler using the following settings:

96ºC/ 1 min

37ºC/ 1 min

Following this, 20 µl of Mix2-6 was added to each sample and this was mixed well by gently flicking the tube. Then, incubation was continued as follows:

37ºC/ 30 min

65ºC/ 15 min

4ºC/ Hold

Second Strand cDNA Synthesis (Mix2-5)	
DEPC-H_2O	10.0 µl
5× Extender Buffer	10.0 µl
Primer C	12.5 µl
dNTP Mix	2.5 µl

Extender Enzyme B (Mix2-6)	
DEPC-H_2O	18 µl
5× Extender Buffer	1 µl
Extender Enzyme B	1 µl

Purification of template DNA with spin columns

First, 236 µl of Mix2-7 was added to each template DNA reaction and this was gently mixed. The sample with then transferred to the column and it was centrifuged for 1 min at 10,000 rpm. The flow-through was discarded and the column was washed by adding 200 µl washing buffer to the column and then centrifuged as previously described. This washing step was repeated again. Then, the flow-through was discarded and the column was centrifuged as before. Next, the columns were inserted into fresh 1.5 ml reaction tubes and 10 µl of an elution buffer was added to each column. The columns were incubated for 2 min and then they were centrifuged as previously described.

Purification (Mix2-7)	
Binding Buffer	234 µl
Carrier DNA	2 µl

Amplification via *in vitro* transcription

First, the *in vitro* transcription mix was prepared as shown in the table below. Then, 10 µl of transcription Mix5 was added to the template DNA. The samples were then incubated overnight at 37ºC in a thermocycler with the heating lid adjusted to 45ºC.

In vitro Transcription (Mix5)	
NTP Mix	6.6 µl
10× Buffer	1.7 µl
T7 RNA Polymerase	1.7 µl

Synthesis of biotin-labelled cRNA

The labelling process was started by transferring template cDNA to an RNase-free microfuge along with the other reaction components, as shown in the table below. These reagents were carefully mixed and the mixture was collected at the bottom of the tube by a brief 5 s of microcentrifugation. Following this, the samples were incubated at 37ºC for 16 h.

Reagent	Volume
Template cDNA	12 µl
RNase-Free Water	8 µl
10× IVT Labelling Buffer	4 µl
IVT Labelling NTP Mix	12 µl
IVT Labelling Enzyme Mix	4 µl
Total Volume	40 µl

Cleanup of biotin-labelled cRNA

It is essential to remove any unincorporated nucleotide triphosphate (NTPs) so that the concentration and the purity of the cRNA can be accurately measured. First, 60 µl of RNase-free water was added to each sample and mixed by vortexing for 3 s. Then, 350 µl of IVT cRNA Binding Buffer was added to the sample and they were mixed by vortexing for 3 s. Next, 250 µl of 100% ethanol was added to the samples and mixed well by pipetting. Following this, the samples were transferred to the IVT cRNA clean-up spin columns and were centrifuged for 15 s at 10,000 rpm. The flow-through was discarded and the column was transferred to a new collection tube. The columns were then washed by adding 500 µl of IVT cRNA wash buffer to the spin columns. The columns were then centrifuged as previously described. Following this, 500 µl of 80% ethanol was added to the spin column

and centrifuged as previously described. The columns were then dried by centrifuging for 5 min at maximum speed while leaving the cap open. Then, the columns were transferred to new 1.5 ml collection tubes and the cRNA was eluted by adding 11 µl of RNase-free water to the column and then centrifuging it for 1 min at maximum speed. This elution step was repeated again by adding 10 µl of RNase-free water.

Fragmentation of cRNA for target preparation

The fragmentation process of cRNA has been shown to be critical for obtaining optimal assay sensitivity. A fragmentation buffer is used for this process, which has been optimised to break down full-length cRNA to 35 to 200 base fragments. The following fragmentation reaction mixture was used:

Component	volume
cRNA	20 µg (1 to 21µl)
5× Fragmentation Buffer	8 µl
RNase-Free Water	To a final volume of 40 µl

The reaction mix was incubated at 94ºC for 35 min; the samples were then kept on ice following incubation. The cRNA samples were then stored at -20°C until the time of hybridisation.

Hybridisation

The DNA microarray is a chip or solid surface that has microscopic DNA spots. Each DNA spot contains probes which are picomoles of specific DNA sequences. These are short sections of a gene that are used to hybridise a cDNA or cRNA sample. Hybridisation between two DNA strands is the core principle behind DNA microarray (figure 2.3). The hybridisation cocktail was prepared as shown below:

Component	Final Concentration
Fragmented cRNA	15 µg
Control Oligonucleotide B2 (3 nM)	5 µl
20x Eukaryotic Hybridisation Controls	15 µl
Herring Sperm DNA (10 mg/ml)	3 µl
BSA (50 mg/ml)	3 µl
2× Hybridisation Buffer	150 µl
DMSO	30 µl
H_2O	To a final volume of 300 µl
Final Volume	300 µl

The hybridisation cocktail was then heated to 99ºC for 5 min in a heat block. The probe array was filled with 1× hybridisation buffer and incubated at 45ºC for 10 min with rotation. Following this, the hybridisation cocktail was transferred to a 45ºC heat block for 5 min. The hybridisation cocktail was centrifuged at maximum speed for 5 min to remove any insoluble material. After this, the buffer was removed from the probe array cartridge and replaced with 200 µl of the hybridisation cocktail. Next, the probe was placed in the hybridisation oven at 45ºC for 16 h. This was followed by washing, staining and scanning, according to the standard Affymetrix protocol.

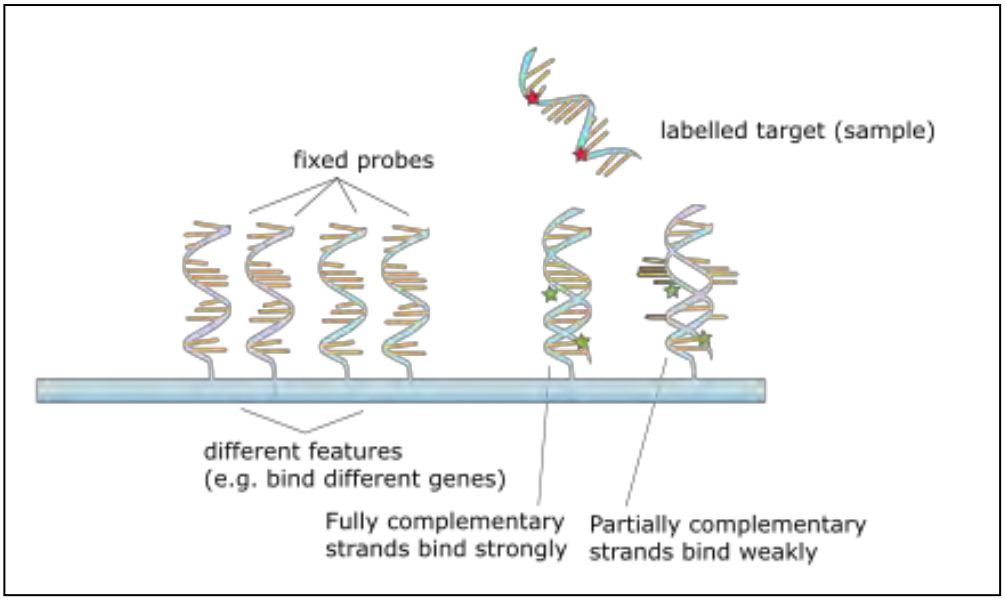

Figure 2.3: Hybridisation process. The labelled complementary RNA samples were added to an Affymetrix chip that contained different probes. The sample was then bound to the complementary sequence on the chip. Fully complementary strands bind strongly whereas partially complementary strands bind weakly and are washed away in the washing step. www.thefullwiki.org/Gene_chip_technology

2.5. In vivo experiments

2.5.1. Generating anti-MPO antibodies

MPO-/- mice were immunised with MPO or other antigens such as BSA, recombinant MPO, MPO peptides, and MPO heavy chain to raise specific antibodies. They were immunised when they were 8-10 weeks old. We started the immunisation process by injecting the mice with 10 µg of MPO in complete Freud's adjuvant on day 10. They were boosted with 5 µg of MPO in incomplete Freud's adjuvant on days 21 and 36. All of the injections were s.c. injections. The tails of the mice were bled after the first boost to check for anti-MPO antibodies. The mice were sacrificed on day 42 and blood was collected via cardiac puncture. The blood was stored at 4ºC overnight. Then, the blood was centrifuged at 2,000 rpm for 5 min and the serum was removed and stored at -80°C.

2.5.2. Murine Experimental Vasculitis

The mice were injected with anti-MPO antibodies to induce crescentic glomerulonephritis. The specific treatment protocols are described in the relevant chapters. The mice were then injected with 1,500 EU/g of LPS 1 h after the first injection of anti-MPO antibodies via i.p. injections. The urine was collected on days 1 and 6 and the mice were sacrificed on day 6. Blood was collected via cardiac puncture. In addition, kidney, lung, liver and spleen tissues were also collected. They were snap frozen by embedding the tissue in OCT and then immersing it in iso-pentane in liquid nitrogen. Some of the tissues were also stored in 10% formalin saline for histological processing and analysis.

2.5.3. Tissue collection and histological analysis

The disease in these experiments was assessed by histological analysis and also by immunohistochemical staining. After culling the animals, I collected the kidney, liver, spleen and lung tissues and immediately fixed them in formalin for histological evaluation. In addition, the tissues were also snap frozen. Formalin-fixed tissues were sent to the histology department where they were sectioned. Periodic acid Schiff-stained and H&E sections were prepared and used to quantify crescentic glomerulonephritis. The histological scoring in these experiments was performed without any knowledge of the experimental conditions, and the sections were assessed by myself and Prof. Mark Little. Glomeruli were scored blindly as normal, mild (evidence of cell infiltration and ubnormal glomeruli), and severe (evidence of necrosis, tuft disruption, and cresent formation).

Chapter 3
Murine experimental vasculitis: establishing and improving the model

3.1. Introduction

Since the discovery of ANCA in 1982 (Davies, Moran et al. 1982), a lot of work has gone into trying to understand the pathogenesis behind ANCA-associated vasculitis and if ANCA are really pathogenic. In vitro evidence has shown the ability of ANCA to stimulate neutrophils to degranulate and release reactive oxygen species (Falk, Terrell et al. 1990). The binding of ANCA to the antigens on the surface of neutrophils results in the adhesion and migration of leucocytes across the endothelium, which results in injury to endothelial cells and underlying tissues. These in vitro findings are very important to help understand the pathogenesis behind ANCA-associated vasculitis, but these findings need to be confirmed in vivo using animal models.

Animal models are considered to be a great tool in science and help in understanding the biology of different human diseases. Until recently, there was no animal model of vasculitis to help study the effect of ANCA on neutrophils and monocytes. We needed an animal model that resembles the human disease with circulating ANCA and crescentic glomerulonephritis, with no or little immune complex deposition. There were many attempts to produce an animal model of vasculitis, including the attempt by Brouwer et al. (Brouwer, Huitema et al. 1993) to induce crescentic glomerulonephritis in rats. Initially, they were not able to induce necrotising crescentic glomerulonephritis after immunising the rats with human MPO, even though these rats produced anti-MPO antibodies. However, subsequent administration of a neutrophil extract including MPO in combination with hydrogen peroxide (H_2O_2) resulted in severe crescentic glomerulonephritis. In this model, immune complexes were reported to be present shortly after kidney perfusion, but they seemed to disappear when kidney injury was at its peak. In a different study, Yang et al. found an association

between the degree of kidney injury in this model and the amount of IgG immune complex deposits, which suggests the involvement of immune complex deposition in the injury and not anti-MPO antibodies. This finding argues against this being a good model of AAV because immune deposition is absent in this disease, as shown by different investigators.

The possibility of ANCA having a potentially pathogenic effect in ANCA-associated vasculitis was addressed by a model developed in 2002. Xiao et al. were able to produce a reliable model of ANCA-associated vasculitis with no immune deposition by immunising MPO knockout mice with murine MPO, purified from WEHI cells, and then injecting mouse splenocytes or IgG from these immunised mice into Rag2-/- mice or wild type mice (Xiao, Heeringa et al. 2002). Rag2-deficient mice developed severe renal lesions following injection of splenocytes from mice immunised with murine MPO and they also developed circulating anti-MPO antibodies. In addition, intravenous injection of anti-MPO antibodies into wild type or Rag2-/- mice resulted in the development of renal injury similar to that seen in humans, albeit much milder.

Like all other animal models, this model needed to be modified to resemble the human disease because the disease in this model is moderate compared to human disease. One of the approaches to try and aggravate the disease was by using bacterial lipopolysaccharide (LPS). The idea came following experimental evidence indicating an association between infection and ANCA in vasculitis. Huugen et al. tested this hypothesis and they were able to increase renal injury in mice following anti-MPO IgG administration (Huugen, Xiao et al. 2005). The severity of injury was LPS dose-dependant and they found that the minimum dose of LPS needed to induce significant increase in renal injury was 0.5 μg/g (1,500 EU/g).

In addition, Little et al. produced a rat model of vasculitis by immunising rats with human MPO (Experimental Autoimmune Vasculitis); these rats produced antibodies in response to the immunisation that cross-reacted with rat MPO (Little, Smyth et al. 2009). In an effort to improve their model, they increased the dose of MPO and they were also able to induce

disease in all the animals when they added pertussis toxin and killed *Mycobacterium tuberculosis*. It has been shown in these two models that another proinflammatory signal, beside ANCA, is necessary to induce full-blown disease. For example, the importance of LPS could be due to the increased level of TNF-α as shown in other murine models (Huugen, Xiao et al. 2005). TNF-α is a cytokine involved in systemic inflammation and it has been shown that priming human neutrophils with TNF-α is necessary to induce the respiratory burst in response to ANCA IgG. Indeed, blocking TNF-α in mouse model of vasculitis attenuated crescent formation (Huugen, Xiao et al. 2005). Little et al. have also shown a protective role of anti-TNF-α in a rat model where there was a reduction in albuminuria, crescent formation and lung haemorrhage (Little, Bhangal et al. 2006). The effect of TNF-α seen here could be through the involvement in leucocyte adhesion and transmigration because Little et al. have shown a reduction in leucocyte adhesion and transmigration following TNF-α treatment in vivo.

One of the difficulties of the mouse model of ANCA-associated vasculitis is finding a reliable source of murine MPO. Unlike the rat model of vasculitis where the disease is induced by immunising the rats with human MPO, which is available commercially, the mouse model requires immunisation of MPO-/- mice with murine MPO to generate anti-MPO antibodies. The current source of murine MPO is WEHI-3 cells which are myelomonocytic leukaemia, macrophage-like, Balb/C mouse cells. These cells are used by different groups as a source of murine MPO which can be used to raise anti-MPO antibodies in MPO-/- mice and then induce disease in WT mice (Xiao, Heeringa et al. 2002; Huugen, Xiao et al. 2005; Xiao, Heeringa et al. 2005). Culturing these cells is extremely time-consuming and a large quantity of cells is required to produce a sufficient yield of murine MPO to immunise MPO-/- mice and raise anti-MPO antibodies. Another cell line that is being investigated now as a source of MPO is an IL-3 dependent cell line, 32Dc13. These cells have been found to express similar amounts of mouse MPO as mouse neutrophils following stimulation with mouse granulocyte colony stimulating factor (G-CSF) (Guchhait, Tosi et al. 2003). In

addition, the possibility of using recombinant mouse MPO was investigated by Apostolopoulos et al. (Apostolopoulos, Ooi et al. 2006). When the MPO-/- mice were immunised with the recombinant MPO, they produced anti-MPO antibodies that were found to react with native mouse MPO isolated from 32Dc13 cells.

The aim of this work was to establish a mouse model of ANCA-associated vasculitis in our institute and find new ways to improve it. I looked at different ways to improve this model and, especially when it comes to finding a good source of MPO antigen to generate anti-MPO antibodies. As it stands, the model is not used by many researchers because of its high costs and because the disease is moderate. As a result, I spent a lot of time trying to find a reliable source of MPO because the current approach required culturing and harvesting a large quantity of WEHI cells. This method of generating MPO is costly and time-consuming. Therefore, I investigated the possibility of using recombinant mouse MPO or MPO multi-antigenic peptides to raise anti-MPO antibodies that react with native mouse MPO and induce disease in mice. In addition, the current approach of generating anti-MPO antibodies requires using a large number of MPO-/- mice for immunisation. I decided to do an experiment that could potentially lead to using fewer mice. I performed a maternal transfer experiment where a mother mouse immunised with MPO was mated with a WT male to produce heterozygous offspring that could potentially develop vasculitis. If the offspring developed vasculitis, fewer mice would be required for the experiment because there would be no need to immunise large numbers of MPO-/- mice with MPO to raise anti-MPO antibodies. In the end, the disease in this model was moderate and I decided to use LPS to aggravate the disease.

3.2. Methods

3.2.1. Mice Genotyping

When I first started my PhD, I had to establish an MPO-/- colony to raise anti-MPO antibodies. We started the colony by mating MPO+/- mice; 25% of the litters were expected to be MPO-/-. To identify the MPO-/- mice, I had to genotype all the litters by extracting DNA from tissues that were obtained from these mice and then running the samples on PCR with MPO primers.

DNA isolation

DNA was isolated from animal tissues as previously described in Chapter 2. We mated MPO heterozygous mice to produce MPO knockout mice. In order to identify MPO knockout mice, I extracted DNA from all the animals. DNA was extracted from ear clippings that were obtained from all newborn mice and the DNA samples were then used for genotyping as described below.

PCR preparation

PCR was used to amplify the DNA, and MPO primers were used to ensure that only MPO was amplified. PCR mix was prepared containing Ready TAQ polymerase, buffer, dNTP Master Mix, MPO1 (5' TGA-CAC-CTG-CTC-AGC-TGA-AT 3'), MPO2 (5' TGC-AGG-CAG-CTG-GTC-TCG-CA- 3'), MPO3 (5' CTA-CCG-GTG-GAT-GTG-GAA-TGT- 3'), and nuclease-free water. The concentrations of these reagents are shown in Table 3.1.

Table 3.1: Preparing PCR mix.

Reagent	Volume	Stock concentration	Final concentration
10* Buffer	5 µl	**-**	1×
dNTP	5 µl	10 mM	1 mM
MPO1	2.5 µl	10 µM	0.5 µM
MPO2	2.5 µl	10 µM	0.5 µM
MPO2	2.5 µl	10 µM	0.5 µM
TAQ	2.5 µl	**-**	0.05 unit/µl
Water	30 µl	**-**	**-**

After that, samples were run on PCR using the settings shown in Table 3.2. The primers anneal to the target DNA and amplify it; these products can be seen as bands when run on 2% gel electrophoresis. When the MPO-/- mice were identified, they were mated to establish the MPO-/- colony.

Table 3.2: PCR setting for mice genotyping.

Temperature (	Time	Number of cycles
95	5 min	1
94	1 min	35
60	1 min	35
72	1 min	35
72	5 min	1
10	Hold	-

Confirming MPO-/- mice by indirect immunofluorescence

In order to be completely sure that I had correctly identified the MPO-/- mice, I used indirect immunofluorescence to confirm MPO-/- mice. I sacrificed two wild type, four heterozygous, and one MPO-/- mice. Blood was collected from these mice by cardiac puncture, from which I created mixed leucocyte cytospins. Each slide had two spots; one spot was coated with 20 µl (100 µg/ml) of murine anti-BSA (a kind gift from Sarah Nolan) and the second spot was incubated with 20 µl (100 µg/ml) murine anti-MPO antibody (kindly provided by Dr. Peter Heeringa). The slides were incubated for 30 min in a moist chamber. Then, the slides were washed three times in PBS. Next, 20 µl of anti-mouse IgG FITC (1:20, Dako, UK) was added to each spot and incubated for 30 min. Slides were then washed and images were acquired with a fluorescent microscope.

3.2.2. Pilot experiment to evaluate the possibility of inducing AAV in mice (MEV1)

I decided to perform a pilot experiment to test the feasibility of inducing vasculitis in mice and also to test the efficacy of liposomal clodronate in depleting macrophages. The aim of this experiment was to make sure that we had a good animal model on our hands to use in future experiments. Six wild type mice on a C57BL/6J background were used in this experiment and divided into two groups (Table 3.3). All animals were treated with the intravenous anti-MPO antibodies, purified as described in the methods section, in an effort to induce systemic vasculitis.

We started by injecting these mice intravenously (IV) with either 100 µl clodronate or 100 µl saline 48 hours prior to the first anti-MPO antibody injection (day -2). In addition, these mice were injected with either clodronate or saline on days 0, 2, 4, and 7 (Figure 3.1). All the mice received 50 µg/g anti-MPO antibodies intravenously on days 0 and 3 (Figure 3.1). These mice were put in metabolic cages to collect urine on day 8 and sacrificed on day 9. Blood was obtained by cardiac puncture. Kidney, liver, spleen, and lung were stored in

formalin for later sectioning and staining, and the same tissues were snap-frozen in liquid nitrogen and stored at -80°C.

Table 3.3: Mice that were used in the MEV1 experiment. Mice treated with clodronate (red) or saline (black).

Mouse	Age (weeks)	Sex	Weight	Group
1	16	M	30.2g	1
2	16	M	33.3g	2
3	16	F	22.7g	1
4	16	F	22.5g	2
5	12	M	25.0g	1
6	10	M	24.7g	2

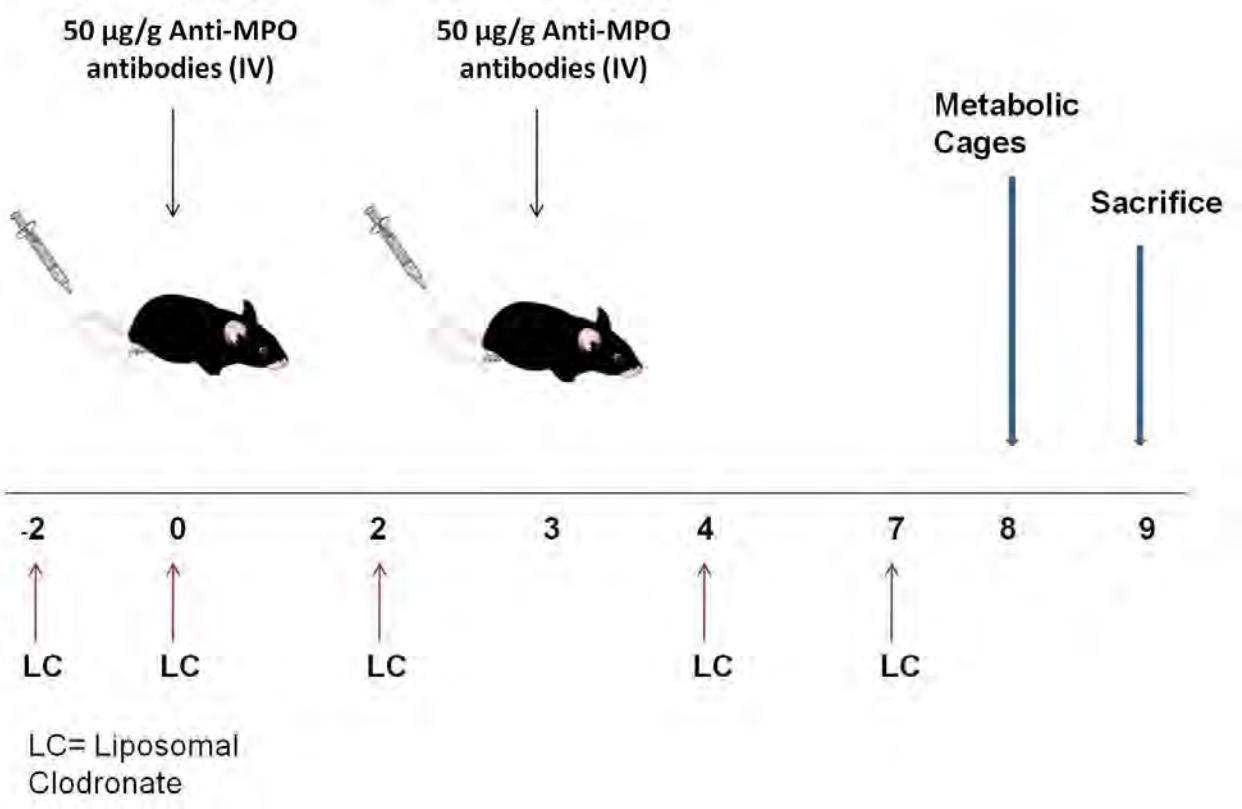

Figure 3.1: **The design of the pilot MEV experiment.** Mice were injected with 50 µg/g of i.v. anti-MPO antibody on days 0 and 3. Some of the mice received 100 µl of liposomal clodronate (LC) on days -2, 0, 2, 4, and 7.

3.2.3. Using anti-MPO antibodies and LPS to induce vasculitis in mice (MEV2)

As MEV1 was characterised by relatively mild vasculitis, I embarked on a second experiment using an adjusted protocol that made use of an additional LPS step. We decided

to use LPS to stimulate the immune system in mice and produce more severe disease. LPS was measured as previously described and stored at -80°C. On the day of the experiment, LPS was taken and diluted to 1,500 EU/g in water for injection. I used 10 mice in this experiment (figure 3.2): five were injected with 75 µg/g anti-MPO antibodies and five with 75 µg/g anti-BSA antibodies. I was not able to give 75 µg/g in one day because of limitations of the project licence. As a result, the mice received an i.v. injection of 50 µg/g on day 0 and 25 µg/g on day 3 of either anti-BSA or anti-MPO antibody. In addition, mice received LPS (1,500 EU/g IP) 1 hour after the first antibody injection on day 0. Mice were put in metabolic cages on day 5 for urine collection and they were culled on day 6. The urine was tested for haematuria on days 1 and 6 using multistix for urinalysis. Kidney, lung, liver, and spleen sections were obtained from all of these mice at day 6 and they were either fixed in formalin or snap frozen in liquid nitrogen for use in the histological analysis.

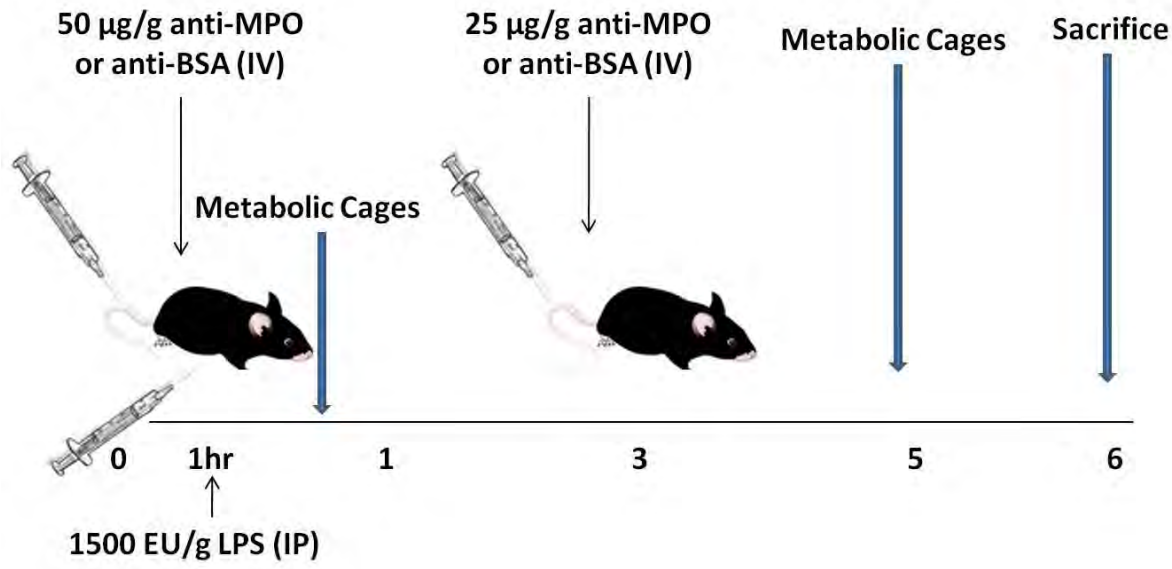

Figure 3.2: Experimental design of MEV2. Mice received 75 µg/g of either anti-MPO (n=5) or anti-BSA (n=5) antibodies on day 0 and 3 through i.v. injection. All the mice received 1,500 EU/g of LPS through i.p. injection on day 3. Urine was collected on day 1 and 6 and mice were culled on day 6.

3.2.4. Alternative approaches to raising anti-MPO antibodies

I investigated the possibility of finding another source of MPO to generate anti-MPO antibodies. I used three approaches to raise anti-MPO antibodies: multi-antigenic MPO peptides, recombinant mouse MPO, and MPO heavy chain. All of these are commercially available and could make the model more accessible if they work.

3.2.4.1. Induction of MEV using antibodies raised against MPO multi-antigenic peptides

In an effort to use an alternative to the laborious and expensive approach of purifying native MPO from cells, I tried to use MPO peptides to raise anti-MPO antibodies. Three MPO peptides were recommended by the Binding Site (Dr. Phil Stubbs) and produced by Alta Bioscience at the University of Birmingham. The sequences of the three peptides used here are as follows:

Peptide	Sequence
1	VTCPPNDKYRTITGHCNNRR-(MAPs)
2	PAEYEDGVSMPFGWTPGVNRNG-(MAPs)
3	LNCETSCLQQPPCFPLKIPPND- (MAPs)

We selected these peptides for the following reasons: VTCPPNDKYRTITGHCNNRR-(MAPs) was selected as it is at the N-terminus of the MPO light chain. LNCETSCLQQPPCFPLKIPPND-(MAPs) was selected as it is at the N-terminus of the MPO heavy chain. These were selected by the Binding Site because from previous use of peptide MAPs, it was found that N-terminal sequences often give a good antibody response, with antibodies recognising the target protein. PAEYEDGVSMPFGWTPGVNRNG-(MAPs) was selected as it covers a “loop” region in the X-ray structure of the protein. As there is no published X-ray structure of mouse MPO, human MPO was used and sequence alignment was performed using the GCC package. This sequence was extended beyond this loop with

the aid of hydrophilicity, surface probability and flexibility predictions (using the "peptidestructure" programme, part of the GCC Wisconsin package). Exposed loops are a good target for antibodies on the surface of a protein. All the peptides were synthesised as 8-branch multi-antigenic peptides (MAPs). Eight copies of the sequence were synthesised directly onto a poly-lysine core. This increases the molecular size of the peptide, overcoming the need for a carrier protein, and avoiding the generation of non-specific anti-carrier protein antibodies. Peptides were dissolved in 0.1 M acetic acid to a final concentration of 4 mg/ml. The three peptides were mixed before immunisation and the mice were divided into three groups (Figure 3.3). Each group received different concentrations of the MPO peptides to test the ability of these peptides to raise anti-MPO antibodies against native mouse MPO. Mice were immunised as described in the general methods section.

These doses of MPO peptides (40, 200, and 400 µg) were selected to induce a high level of anti-MPO antibodies. Brouwer et al. have demonstrated that immunising WKY rats with 10 µg of hMPO induced anti-MPO antibodies, but not vasculitis (Brouwer, Weening et al. 1993). However, Little et al. have shown that a greater dose of human MPO was required to induce vasculitis in rats and that a dose of 1,600 µg/kg reliably induced vasculitis. As a result, I decided to start with this dose to immunise MPO-/- mice with MPO peptides, which was around 40 µg for a mouse. In addition, I decided to use greater doses because this was the first time these peptides were used for immunisation and we did not know what to expect.

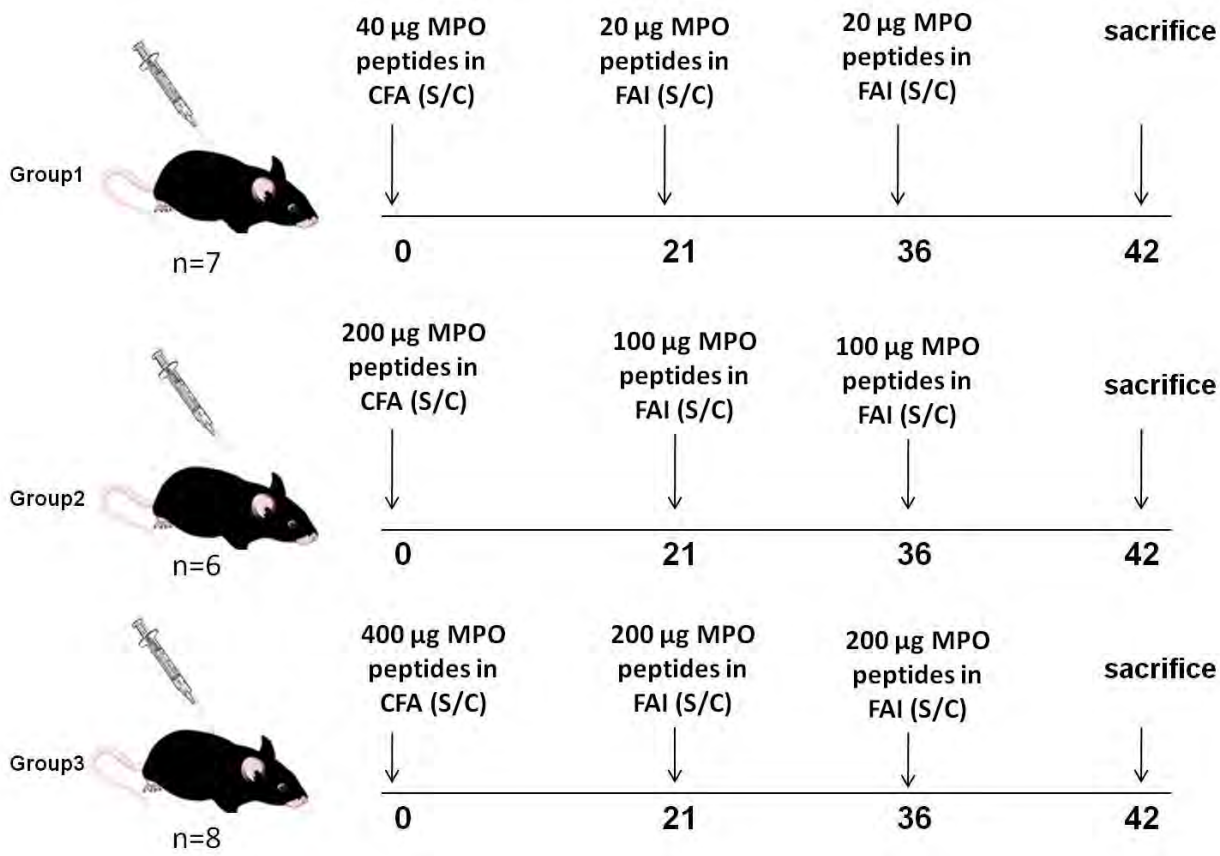

Figure 3.3: Immunising MPO-/- mice with multi-antigenic peptides. Mice were immunised with different doses of multi-antigenic peptides: 400 µg (n=8), 200 µg (n=6), 40 µg (n=7). These were the first doses on day 0 in complete Freund's adjuvant (S/C). They were boosted on days 21 and 36 in incomplete Freund's adjuvant.

In this experiment, I tried to test the ability of anti-MPO antibodies derived from MPO-/- mice that were immunised with multi-antigenic murine MPO peptides. I wanted also to compare them to anti-MPO antibodies from mice immunised with murine MPO. I used these antibodies to induce vasculitis in C57BL/6J mice using a comparable protocol to that used in MEV2. I used four mice in this experiment: two mice were injected with 75 µg/g of anti-MPO peptides and two mice were injected with 75 µg/g of anti-murine MPO antibodies. The mice also received 1,500 EU/g of LPS.

	Group 1	Group 2
No. of Mice	two mice	two mice
Treatment	• 75 µg/g anti-mMPO antibody on day 0 • 1,500 EU/g of LPS after 1 hour	• 75 µg/g anti-pMPO antibody on day 0 • 1,500 EU/g of LPS after 1 hour

3.2.4.2. Immunising with recombinant mouse MPO

I also tried using recombinant mouse MPO (R&D systems, Abingdon, UK). We decided to try this approach following a study by an Australian group where they immunised MPO-/- mice with recombinant mouse MPO; these mice mounted a significant antibody response to native mouse MPO (Apostolopoulos, Ooi et al. 2006), but this protocol was not used to induce disease in mice because they were only interested in producing the recombinant MPO. Mice were immunised with recombinant mouse MPO as previously described; 19 mice were used in this experiment. Mice were injected with 10 µg of recombinant MPO on day 0 in complete Freund's adjuvant and boosted on days 21 and 36 (Figure 3.4).

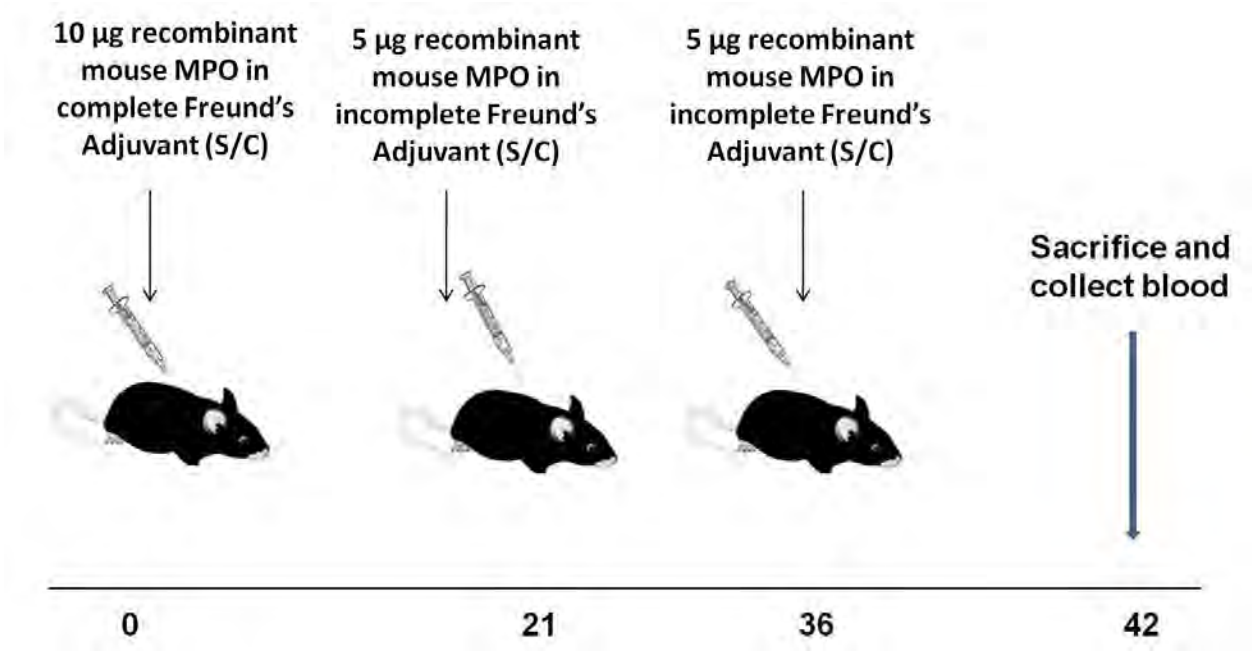

Figure 3.4: Immunising MPO-/- mice with recombinant MPO. MPO-/- mice (n=19) were immunised with recombinant mouse MPO. They received 10 µg (same dose used by Apostolopoulos et al.) in complete Freund's adjuvant on day 0 and were boosted (with half the dose) on days 21 and 36 in incomplete Freund's adjuvant.

3.2.4.3. Immunising with MPO heavy chain

I also tried immunising the mice with MPO heavy chain (Insight Biotechnology Limited, Middlesex, UK). This antibody was used previously by Kuligowski et al. (Kuligowski, Kwan et al. 2009) to raise anti-MPO antibodies in MPO-/- mice which were used to study neutrophil adhesion in vivo. Mice were divided into two groups. Mice in group 1 received 5 µg (the same dose used by Kuligowski et al.) of MPO on day 0 in complete Freund's adjuvant and were boosted on day 7 with 5 µg of MPO in incomplete Freund's adjuvant; they were culled on day 14 (this is the same immunisation protocol used by Kuligowski et al.). The mice in group 2 were immunised with 20 µg on day 0 in complete Freund's adjuvant and boosted with 5 µg on day 21 in incomplete Freund's adjuvant, and then were sacrificed on day 42 (Figure 3.5). Blood was collected from these mice by cardiac puncture.

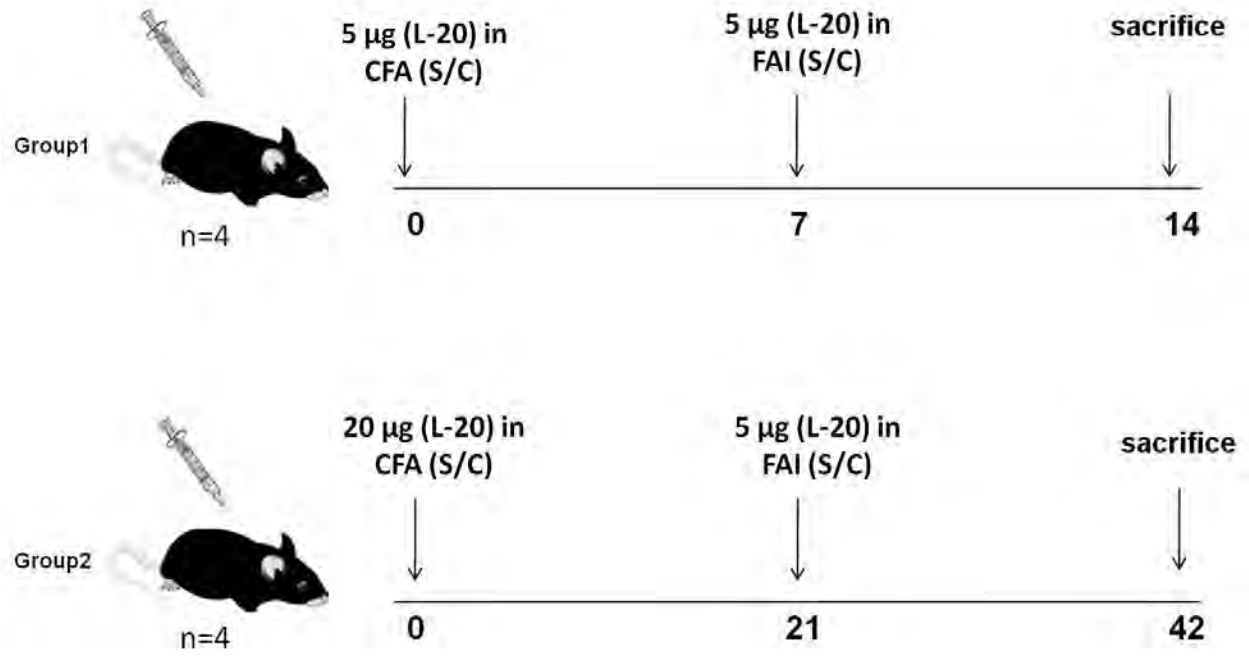

Figure 3.5: Immunisation with MPO heavy chain (L-20). Mice were divided into two groups. A: mice were immunised with 5 µg of L-20 at day 0 in complete Freund's adjuvant, boosted at day 7 and sacrificed at day 14. B: mice in group 2 were immunised with 20 µg at day 0, boosted on day 21 and sacrificed at day 42.

3.2.5. Induction of MEV by maternal trans-placental transfer of anti-MPO antibodies

In an effort to reduce the number of mice required and to remove the IgG purification step, we investigated the possibility of inducing vasculitis in newborn litters. In order to do that, we immunised MPO-/- females with MPO peptides and monitored the level of anti-MPO antibodies. We selected two females with the highest titre of anti-MPO antibodies as measured by ELISA. These females were mated with wild type males, which meant that all of the offspring should be heterozygous for MPO and express normal amounts of MPO. The offspring were sacrificed on day 21 to examine them for evidence of vasculitis. In addition, selected animals were sacrificed at earlier time points (day 2) to ascertain the kinetics of the passively transferred anti-MPO antibody (Figure 3.6).

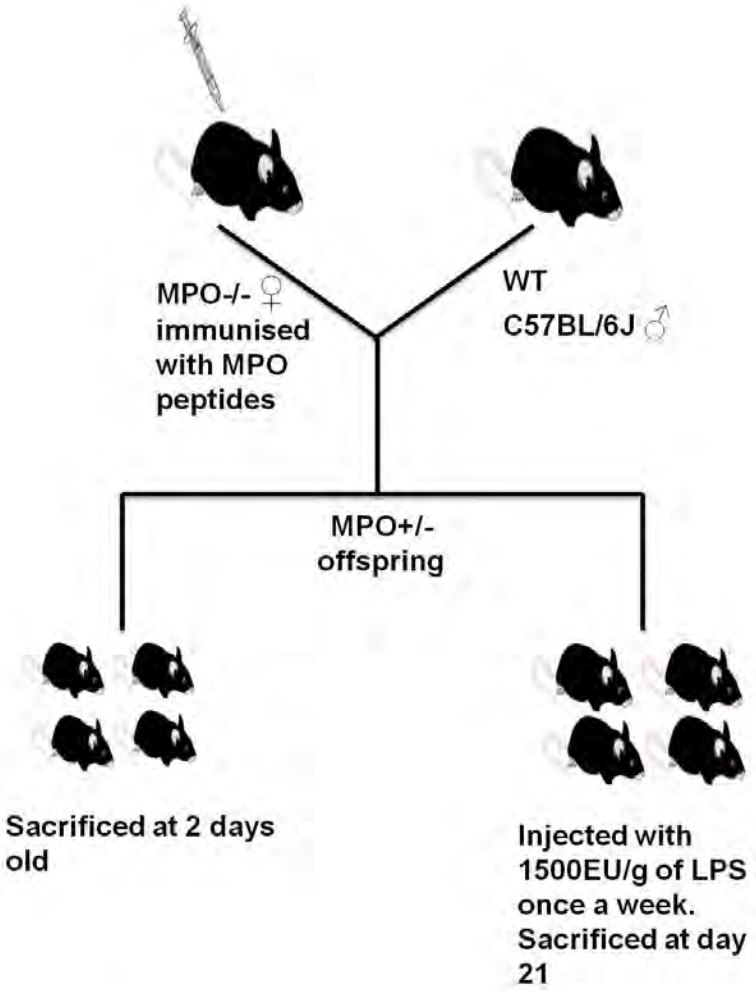

Figure 3.6: Induction of MEV by maternal trans-placental transfer of anti-MPO antibodies. MPO-/- females (n=2) that were immunised with 400 µg of multi-antigenic peptides were mated with WT males. The offspring were sacrificed either at day 2 or day 21; they received 1,500 EU/g of LPS once a week if they were sacrificed at day 21.

3.3. Results

3.3.1. Mice Genotyping

All the litters from mated MPO+/- pairs were genotyped using PCR. I used three MPO primers. If the size of the band was 400 kb, then the mouse was MPO-/- (Figure 3.7, B). On the other hand, MPO+/+ mice were identified by a band at 600 kb (Figure 3.7, C). MPO+/- mice had two bands at 600 and 400 (Figure 3.7, A). At the beginning, I did not get any results from genotyping the first batch, but after optimising my technique and using fresh samples, I was able to genotype all the mice. I started by trying to increase the amount of DNA in each well, but that did not work. Then I started changing the concentration of reagents such as dNTP, Taq polymerase, and MPO primers. There were still no clear bands, so I decided to extract DNA from fresh samples. I got strong bands when I used fresh samples; this meant that the DNA must have degraded in the old samples.

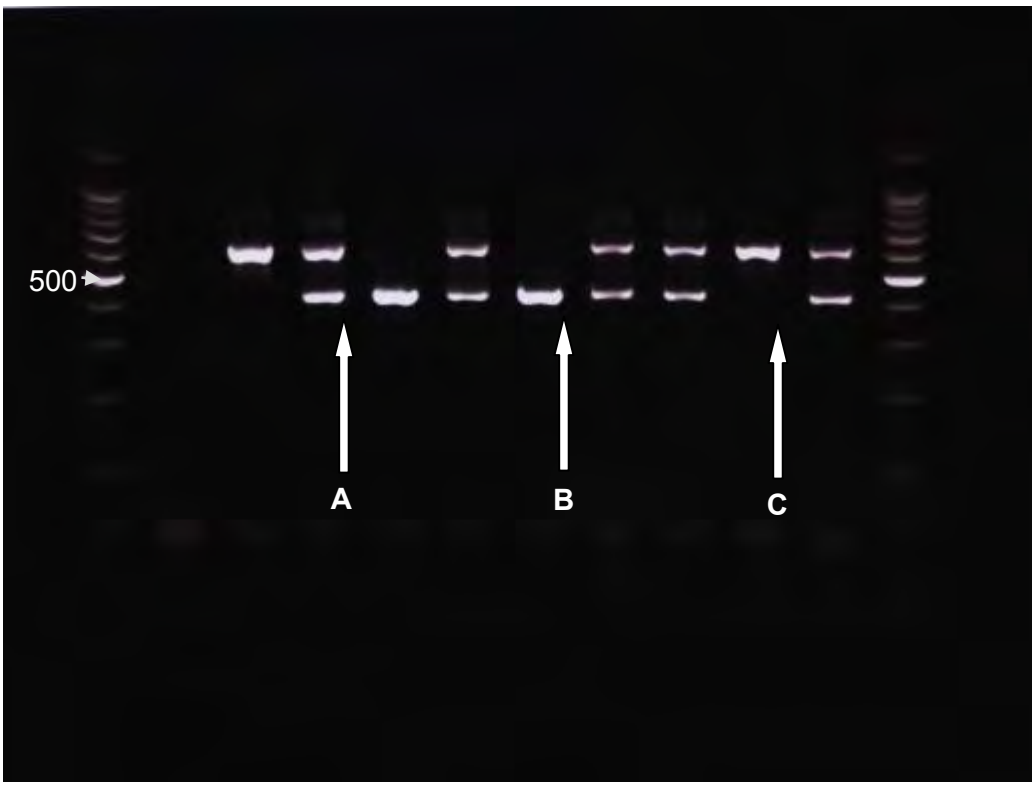

Figure 3.7: **Mouse genotyping using PCR.** PCR was effective in identifying the genotype of the mice. Two bands were produced from MPO+/- mice **(A)** and the sizes of these bands were 600 KD and 400 KD. MPO-/- mice were identified by one band with size of 400 KD **(B)**. On the other hand, a 600KD band was produced from MPO+/+ mice **(C)**.

3.3.2. Confirming MPO-/- mice

Indirect immunofluorescence on peripheral leucocyte cytospins was done to confirm the absence of MPO in MPO-/- mice. Anti-BSA antibody was used as the control. If MPO was present in neutrophils, then anti-MPO antibodies will bind to it and will give a bright green colour when stained with anti-mouse IgG-FITC. This was seen when leucocytes from MPO+/+ and MPO+/- mice were incubated with 100 µg/ml anti-MPO antibody and then stained with FITC (Figure 3.8, B and D). On the other hand, neutrophils from MPO-/- mice should not have any MPO and therefore no bright green fluorescence (Figure 3.8, F). MPO-/- mice were confirmed by both PCR and indirect immunofluorescence and these mice were used to establish an MPO knockout colony which was of sufficient size to begin the generation of anti-MPO antibodies.

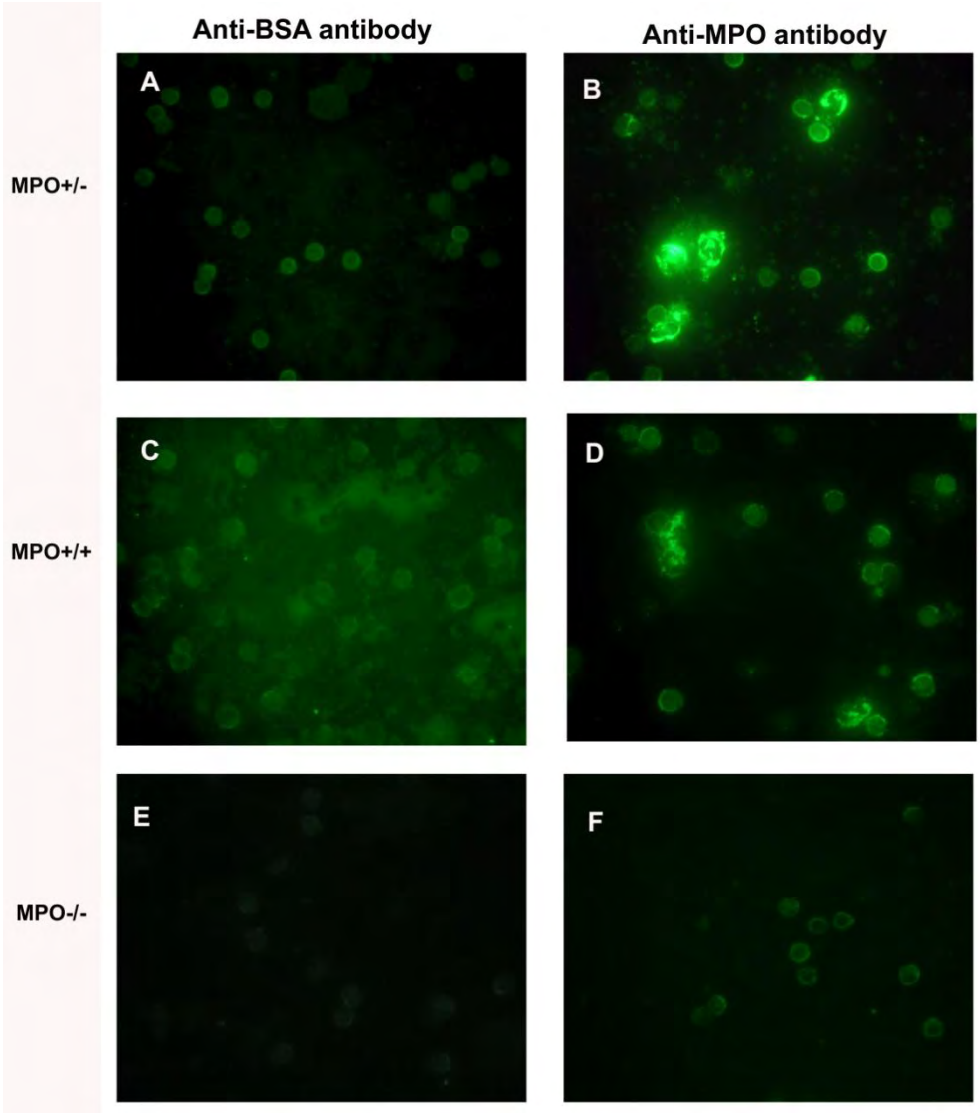

Figure 3.8: Indirect immunofluorescence to identify MPO-/- mice. A and B: mixed leucocytes from an MPO+/- mouse were incubated with **(A)** anti-BSA antibodies and **(B)** with anti-MPO antibodies. **C** and **D**: mixed leucocytes from an MPO+/+ mouse were incubated with anti-BSA antibodies **(C)** and with anti-MPO antibodies **(D)**. E and F: mixed leucocytes from an MPO-/- mouse were incubated with anti-BSA antibodies **(E)** and with anti-MPO antibodies **(F)**. Anti-mouse IgG-FITC was used for staining.

3.3.3. MPO activity assay and culturing WEHI Cells

An MPO activity assay was used to determine the presence and the concentration of MPO in WEHI cells because I needed to confirm the presence of MPO in these cells before we started isolating MPO from them. This was also done to make sure that the concentration of MPO did not drop over time. The assay was also used to compare the MPO concentration in WEHI cells that were cultured under two different conditions (static and rolling conditions). MPO from human leucocytes (Calbiochem, UK) was used to create a standard curve, which

was used to estimate the concentration of MPO from WEHI cells. The MPO concentration/million cells was measured once a week from WEHI cells that were cultured under either static or rolling conditions. The MPO concentration was relatively higher when WEHI cells were cultured under rolling conditions compared to the MPO concentration from WEHI cells that were cultured under static conditions (Figure 3.9, A). We also found that it was markedly less expensive to culture these cells using bioreactors because less medium and FCS was required (results not shown). In addition, the cell yield was higher when cells were cultured under rolling conditions.

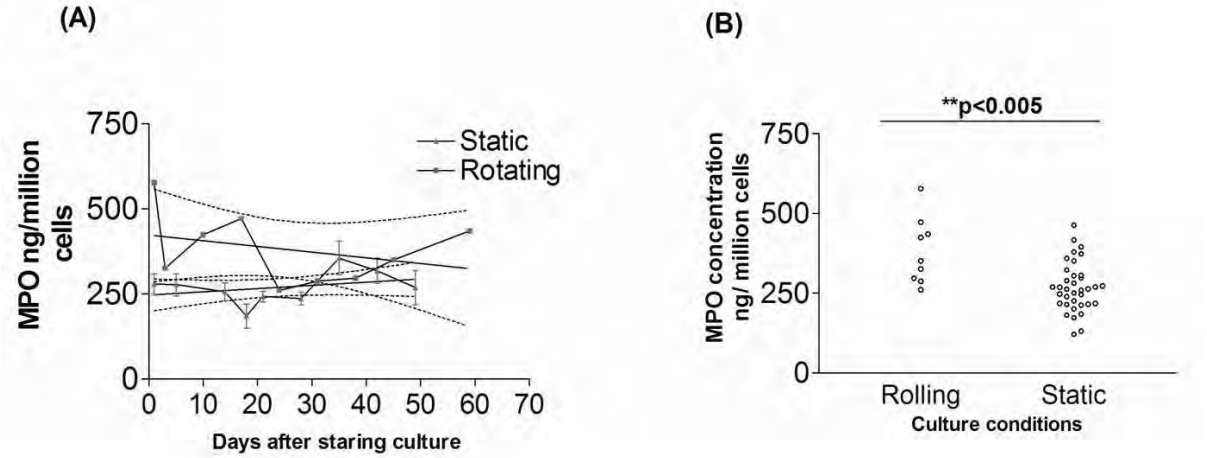

Figure 3.9: WEHI cells under static and rolling conditions. The MPO concentration in WEHI cells that were cultured under static and rolling conditions was monitored during cell culture using an MPO activity assay. **A:** MPO concentration (ng/million cells) over time from WEHI cells under static and rolling conditions. **B:** comparing the MPO concentration in ng/million cells from WEHI cells that were cultured under static and rolling conditions; these tests were done on different days. A t-test was used to determine statistical significance.

3.3.4. Optimisation of MPO isolation from WEHI cells

Following con-A extraction as described in the general methods section, I loaded my samples onto the Mono-S column. I first loaded all eluate 1 from all samples (SN1, SN2, P1, and P2) and I pooled eluates 2 and 3 together from all samples and loaded them in the second run. Most of the MPO was in the first run, and it was identified by the high green peak (Figure 3.10, A) which represents the absorbance at A430. On the other hand, samples in the second run had only tiny amounts of MPO, as shown by the small peak (Figure 3.10, B). Most of the MPO was collected in eluate which had the highest A430 value.

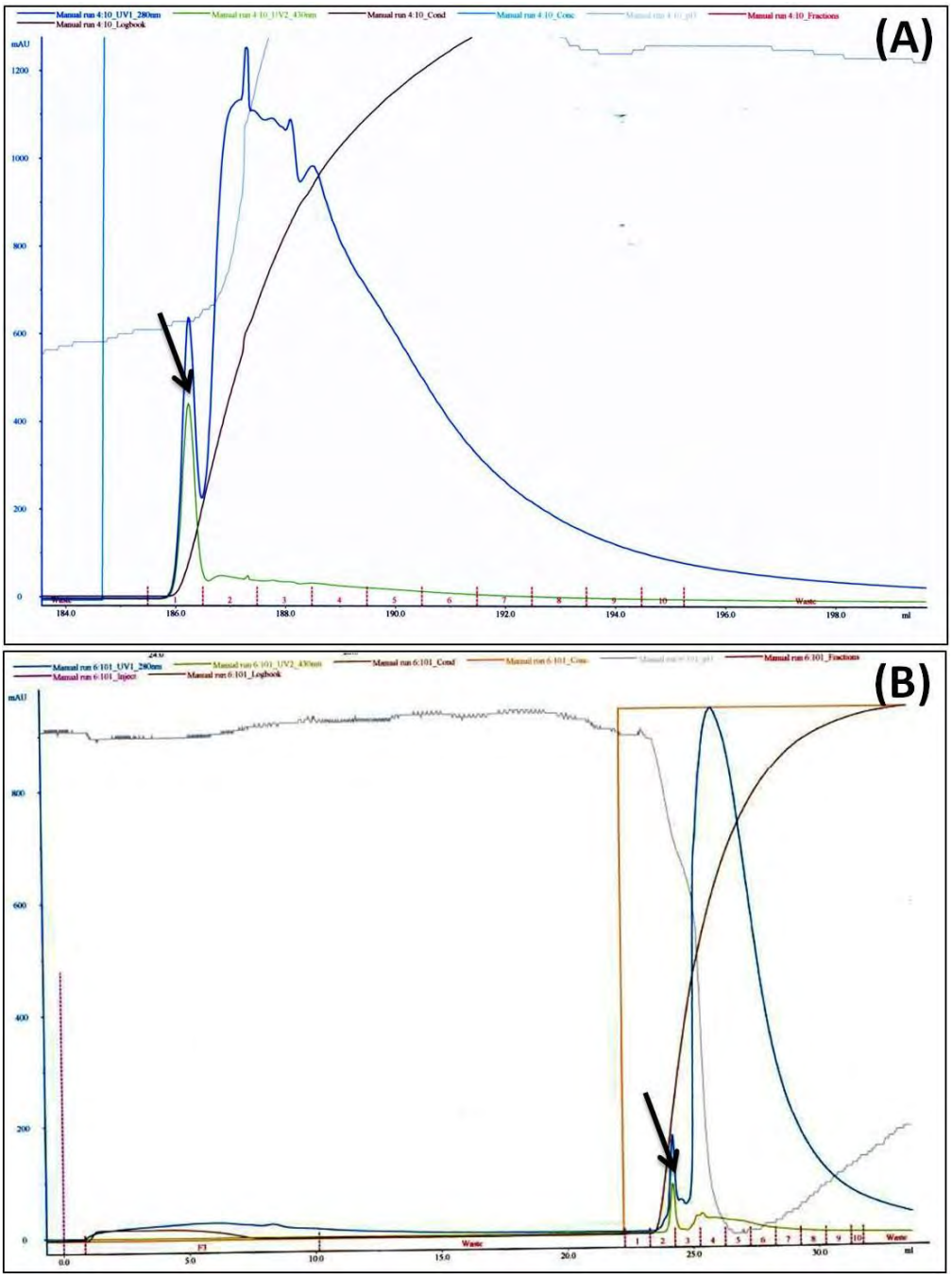

Figure 3.10: MPO isolation from WEHI cells using the Mono-S column. The green peak in the graph shows the dissociation of MPO from the column and it also shows the absorbance at A430. Most of the MPO was collected in eluate 1 (E1), as shown by the green peak. The blue peak represents the total protein absorbance at A280.

SDS-PAGE and Western blot were performed to assess the purity of the MPO (Figure 3.11). The first run contained all E1 samples. The second run contained E2 and 3 from all samples. Most of the MPO was in the first run, as shown by the strong band of E1, which was supported by the green colour and the absorbance at A430 and A280. Other elution

fractions had some MPO in addition to many contaminants. The band in E1 had a similar size to the control commercial human MPO.

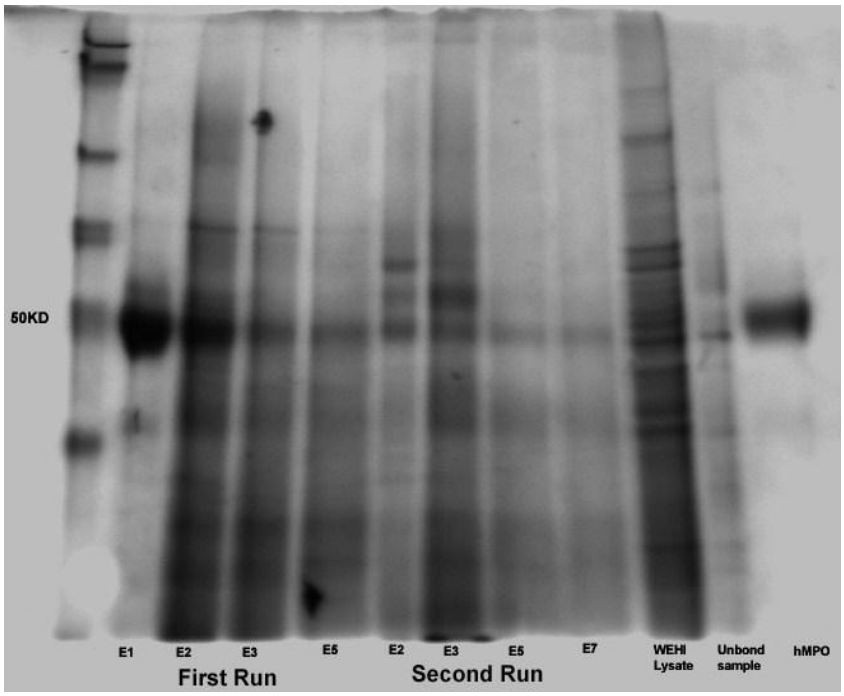

Figure 3.11: SDS-PAGE for murine MPO. This figure shows the SDS-PAGE that was done for different elution fractions from two separate runs in the Mono-S column. E1-E5 in the first run are different elution fractions that were collected after eluting the MPO from the column after loading the first batch. E2-E7 in the second run are different elution fractions that were collected after eluting the MPO from the Mono-S column after loading the second batch. E1 in the first run had most of the MPO, as shown by the strong band at 50 kD, which had similar size to hMPO. WEHI lysate is the supernatant from WEHI cells that were lysed with 0.3% triton. The unbound sample is the run-through that was collected from the column and did not bind to the column.

3.3.5. Immunising MPO-/- mice with murine MPO

MPO knockout mice were immunised with murine MPO isolated from WEHI cells to raise anti-MPO antibodies. Day 42 serum was pooled together from all MPO-immunised mice and then I used anti-MPO ELISA to measure the level (Figure 3.12, A) and titre (Figure 3.12, B) of anti-MPO antibodies. The titre of anti-MPO antibodies (EC_{50}) was 679.4.

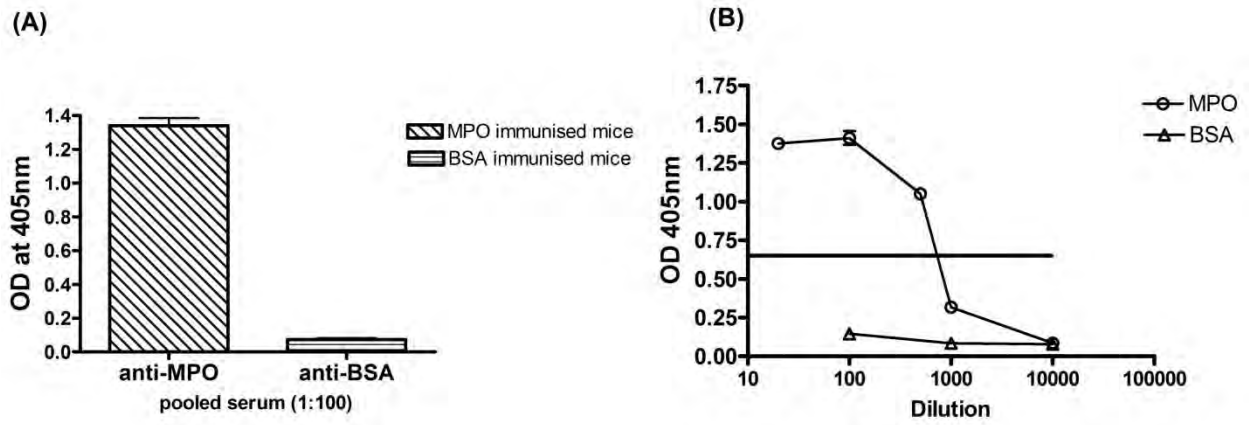

Figure 3.12: The level of anti-MPO antibodies in MPO-/- mice. Mice were immunised with MPO or BSA and the production of anti-MPO antibodies was detected in the serum using an anti-MPO ELISA. A high level of anti-MPO antibodies was detected in the pooled serum from MPO-immunised mice compared to BSA-immunised mice at 1:100 dilution (A). The titre of anti-MPO antibodies was calculated using non-linear regression analysis (B). The anti-MPO titre was 679.

3.3.6. Anti-MPO antibody (IgG) isolation from mouse serum

We used murine MPO to immunise MPO-/- mice and to generate anti-MPO antibodies. Blood was obtained from the immunised mice on day 42 and then serum was collected after leaving the blood to clot. Serum was then run on a protein G column. A sample chromatogram from protein G affinity chromatography is depicted in Figure 3.13.

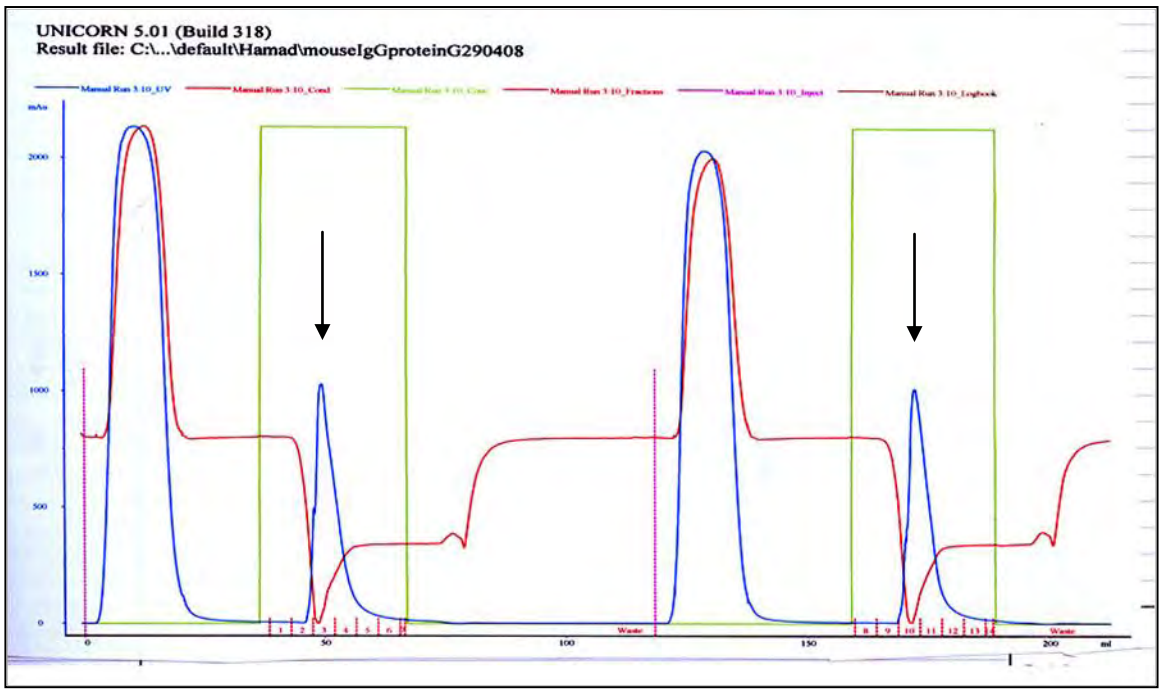

Figure 3.13: IgG isolation from murine serum using protein-G column. The red line represents the pH. When the elution buffer was added to the column, the pH dropped and IgG started to dissociate from the column. The small blue peak (arrow) represents the dissociation of the IgG from the column after adding the elution buffer, and eluates were collected at this point. This graph represents two runs and the two small peaks represent the dissociation of IgG from the column from the two runs.

SDS-PAGE was done to confirm the presence of IgG. One band at 160 kD appeared on a non-reduced gel (Figure 3.14, A) and the heavy chain and light chain were seen on the reduced gel (Figure 3.14, B), thereby confirming the presence of acceptably pure IgG, which means that there was no contamination of other proteins.

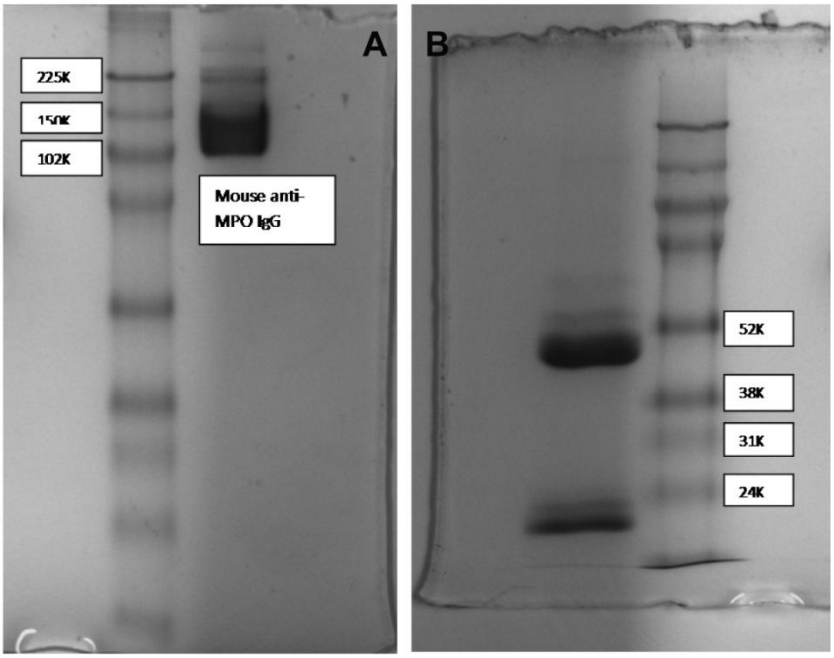

Figure 3.14: SDS-PAGE for anti-MPO antibody. A: non-reduced SDS-PAGE and **B:** reduced SDS-PAGE. In the reduced one, there is one band at about 160 kD. On the other hand, there are two bands on the reduced one and these bands are about 50 kD (heavy chain) and 20 kD (light chain). The results from this confirm the presence and the purity of IgG.

3.3.7. Pilot experiment to evaluate the possibility of inducing AAV in mice (MEV1)

After confirming that I had generated high titres of anti-MPO antibodies, I passively transferred these into wild type recipients. Urine was collected from all of the mice in the MEV1 experiment on day 8 and was tested for haematuria using a dipstick. One mouse from the saline group had blood present in the urine and the other mice from the control group showed traces of blood. On the other hand, mice from the clodronate-treated group showed negative results when tested for blood in the urine (Table 3.4).

Table 3.4: Testing for blood in urine using dipstick. Mice in clodronate treated group showed negative results.

Mouse	Treatment	Haematuria
17	Liposomal clodronate	No urine
23	Saline	+2
24	Liposomal clodronate	Negative
27	Saline	Trace
39	Liposomal clodronate	Negative
59	Saline	Trace

3.3.7.1. Monitoring anti-MPO antibodies level in MEV1

The level of passively transferred anti-MPO antibodies in the mice that were used in the MEV1 experiment was also measured using anti-MPO ELISA. I included serum from WKY rats immunised with human MPO to the plate coated with murine MPO. These rats develop glomerulonephritis when they are immunised with hMPO and produce anti-MPO antibodies. I found that these antibodies cross-reacted with murine MPO. On the other hand, human MPO-ANCA did not react with murine MPO. I was able to detect anti-MPO antibodies in the mice that were injected with anti-MPO antibodies (Figure 3.15, A). A dilution curve was also constructed to calculate the antibodies titre, which was (71-92) (Figure 3.15, B). This represents the point where the dilution resulted in 50% drop of OD value compared to the highest OD.

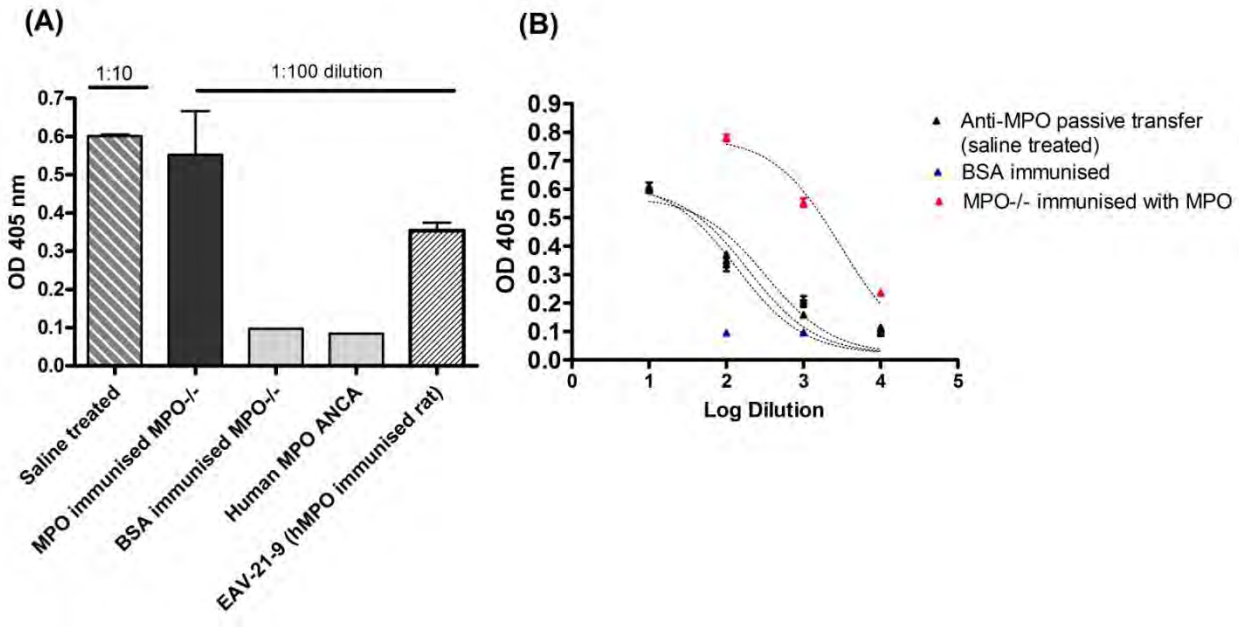

Figure 3.15: Measuring anti-MPO antibodies in MEV1 mice. All the mice received the same concentration of anti-MPO antibodies and then either received clodronate or saline. **A:** Anti-MPO antibodies level in MEV1 mice and in MPO-/- mice immunised with MPO, MPO-/- mice immunised with BSA, human ANCA, and serum from a rat immunised with hMPO. **B:** Dilution curve to calculate antibody titres using non-linear regression analysis.

3.3.7.2. Histology analysis from pilot experiment

We expected that crescents would appear in 5% of the glomeruli in the kidneys from the mice not receiving clodronate. However, most of these mice were healthy and showed only mild glomerulonephritis (Figure 3.16, D). Only one mouse (from the saline-treated group) had evidence of crescents. None of the clodronate-treated mice displayed glomerulonephritis. (Figure 3.16, A). I also saw abnormal glomeruli in both groups, but this was relatively more frequent in the control group (Figure 3.16, C).

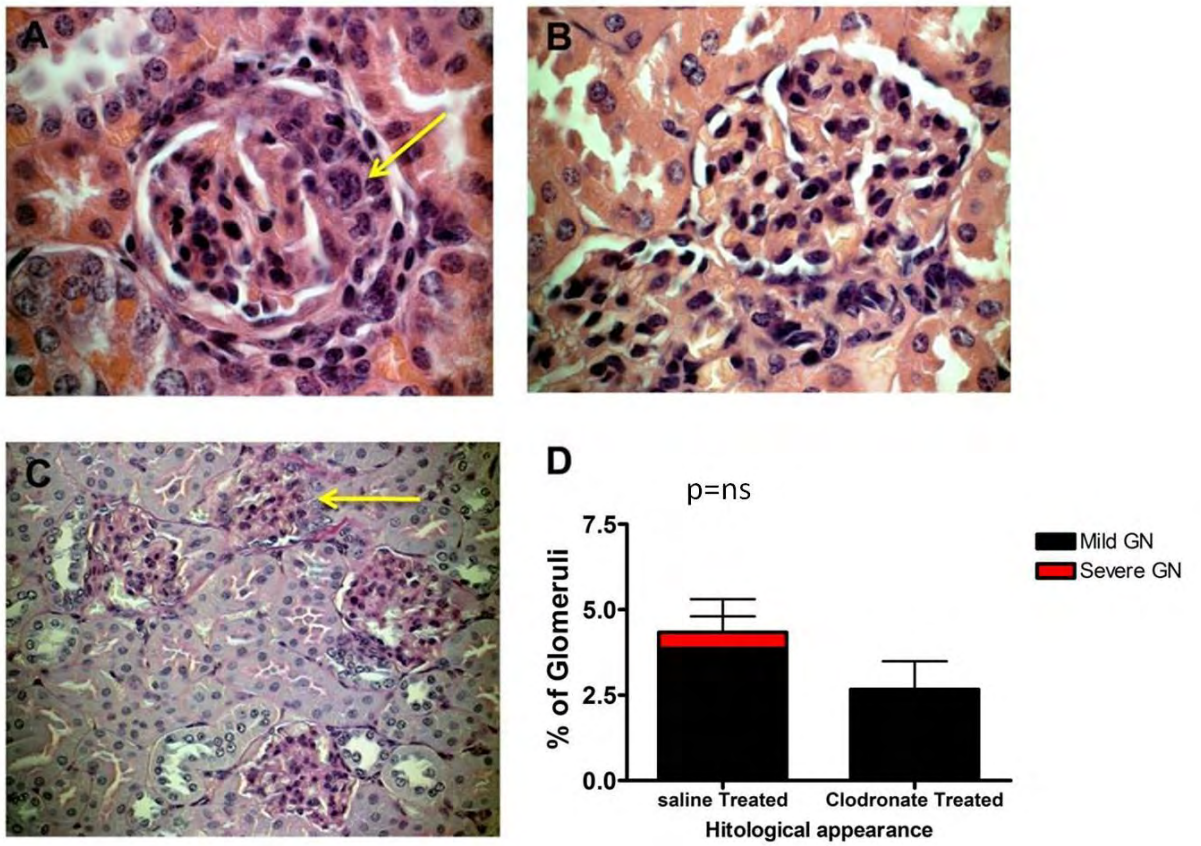

Figure 3.16: Histological appearance of glomeruli in the MEV1 experiment. All the mice in this experiment received two doses of anti-MPO antibody. Some of these mice received liposomal clodronate to deplete macrophages (n=3), while the others received saline and were used as the control (n=3). **A:** Crescent formation in glomeruli was seen in one of the mice that received saline. **B:** Normal glomerulus from a mouse that received clodronate. **C:** Abnormal glomeruli were seen in the kidney of a mouse that received saline. **D:** This graph represents the histological appearance of the kidneys in all six mice that were used in this experiment. The p value represent the difference in cresent formation between the two groups (Mann-Whitney test)

3.3.8. Induction of AAV using anti-MPO antibodies and LPS (MEV2)

Mice in the MEV2 experiment received 75 µg/g of either anti-MPO or anti-BSA antibody and all received 1,500 EU/g of LPS. I collected urine from all the mice in MEV2 on days 1 and 6 to assess kidney function. All the mice that received anti-MPO antibodies had haematuria on days 1 and 6; the score was between +3 to +4 on day 1 and between 0 to +4 on day 6. On the other hand, all the mice that received anti-BSA antibodies had negative haematuria on days 1 and 6, except for one mouse (Figure 3.17, A). There was a significant difference in the albumin:creatinine ratio between anti-MPO- and anti-BSA-treated mice (Figure 3.17, B). All the mice that received anti-MPO antibodies developed crescentic glomerulonephritis (Figure 3.18, A). On the other hand, none of the mice that received anti-

BSA antibody developed crescentic glomerulonephritis. The percentage of crescents in the mice that were injected with anti-MPO antibody was variable with a mean percentage of crescentic glomeruli of 13.4% (4%-30%). In addition, glomerular necrosis was seen in some of the mice that received anti-MPO antibody (Figure 3.18, B). On the other hand, most of the glomeruli from the mice that received anti-BSA antibody were normal (Figure 3.18, C).

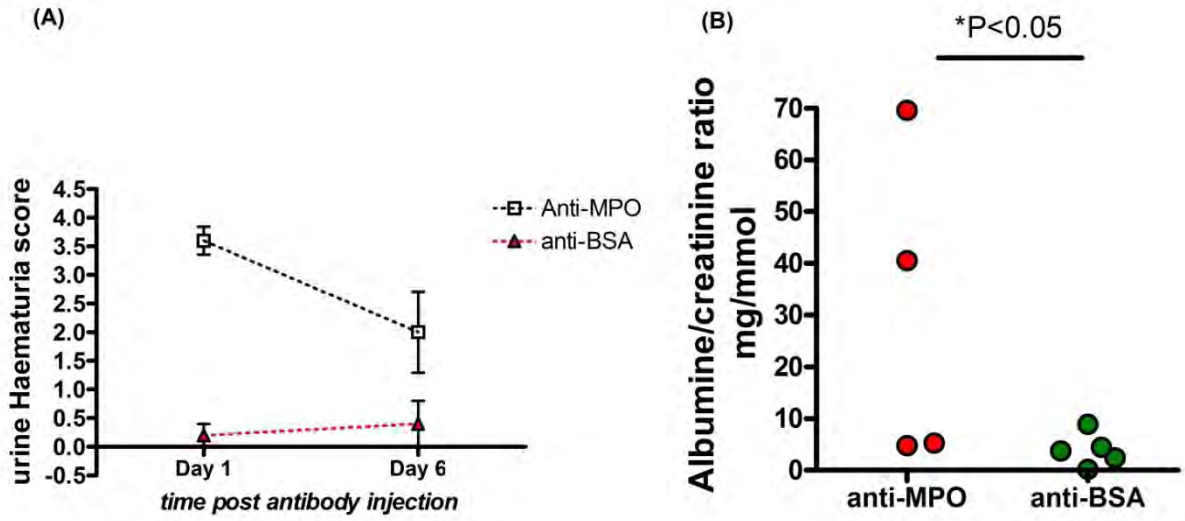

Figure 3.17: Urine analysis in MEV2. All the mice that received anti-MPO antibodies (n=5) (75 µg/g) had haematuria on days 1 and 6 compared to only one mouse that had haematuria from the anti-BSA-treated mice (n=5) (A). In addition, there was a significant difference ($p<0.05$) between anti-MPO- and anti-BSA-treated mice in the albumin:creatinine ratio (B). One tailed t-test (Mann-Whitney test).

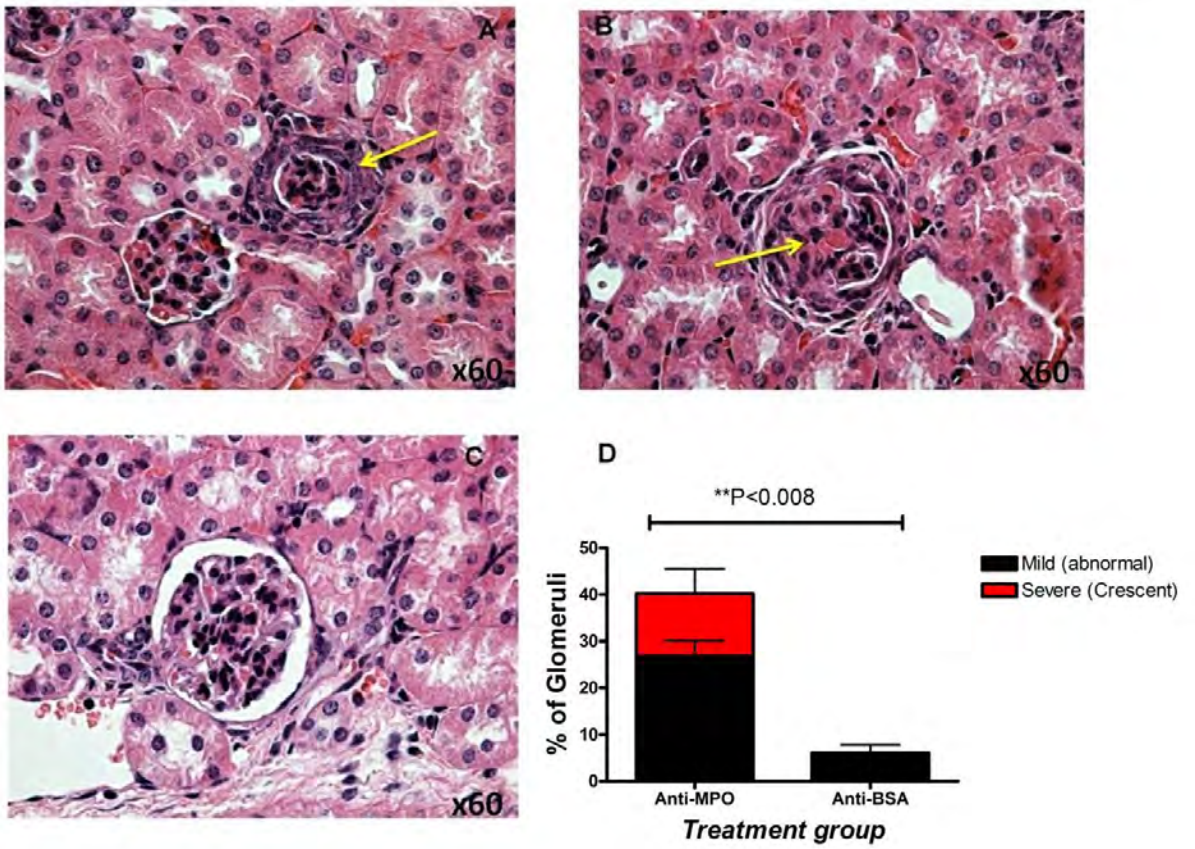

Figure 3.18: Histological analysis of kidney sections from MEV2 (H&E stain). Mice received 75 µg/g of either α-MPO or α-BSA antibody i.v. **A:** Crescentic glomerulonephritis (arrowhead) in a mouse injected with 75 µg/g of α-MPO antibody (n=5). **B:** Glomerular necrosis (arrowhead) in a mouse injected with 75 µg/g of α-MPO antibody. **C:** Normal appearing glomerulus in a mouse injected with 75 µg/g of α-BSA antibody (n=5). **D:** Statically significant differences between groups in the percentage of crescents were assessed by a t-test (Mann-Whitney test).

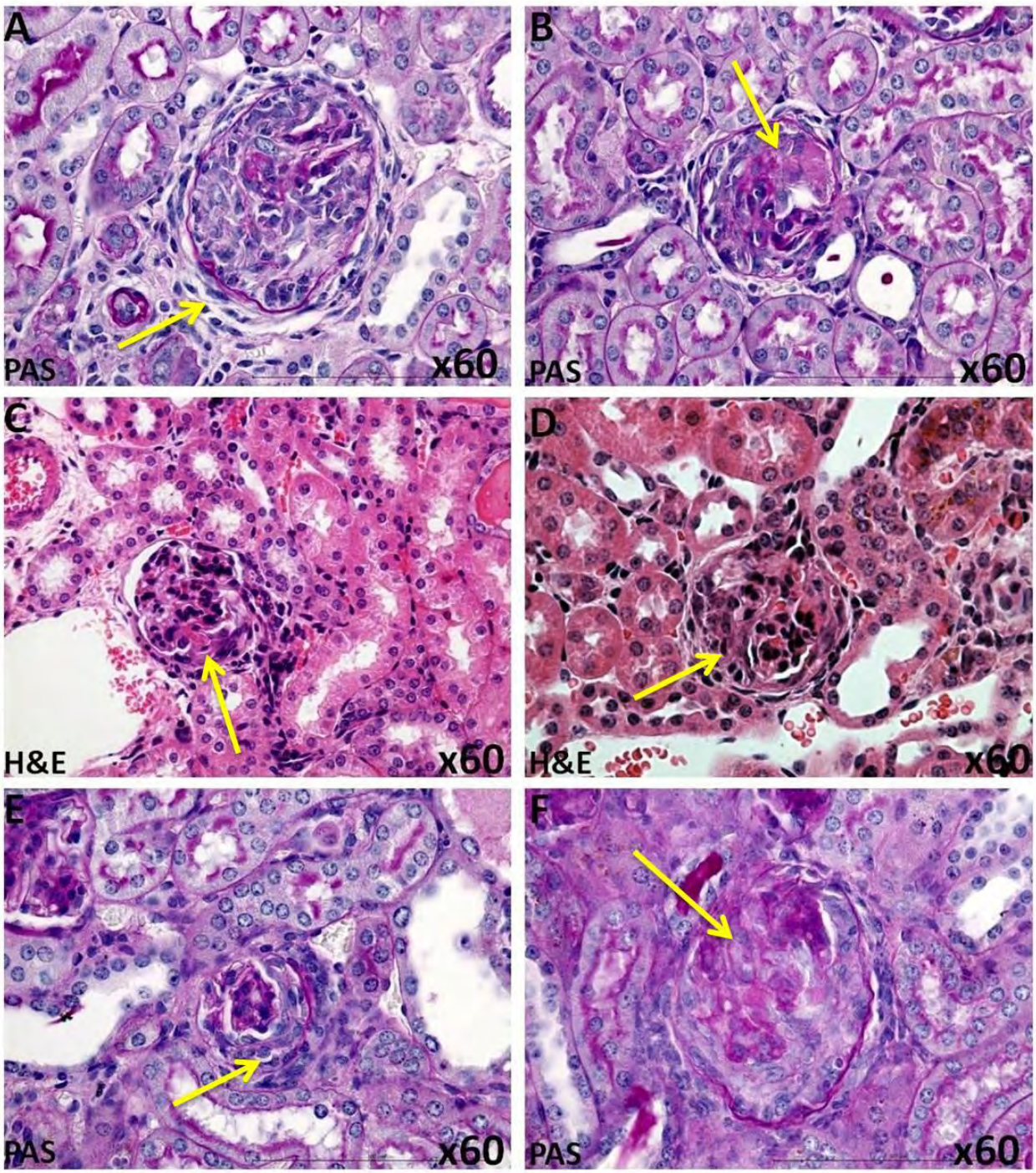

Figure 3.19: Further histological sections from anti-MPO- and LPS-treated mice. Histological sections from mice that were injected with 75 µg/g of anti-MPO antibodies and 1,500 EU/g of LPS. These mice developed severe crescentic glomerulonephritis and necrosis. PAS staining (A, B, E, and F), and H&E staining (C and D).

Immunohistochemical staining

Macrophage infiltration in the kidney was identified by CD68 immunohistochemistry staining. All mice that received anti-MPO antibodies had positive staining for CD68 (Figure

3.20, A and C) and none of the mice that received anti-BSA antibodies (Figure 3.20, D) had CD68 positive staining. CD68 positive cells in the kidney were found mainly in the crescent area in the glomeruli (Figure 3.20, A and C).

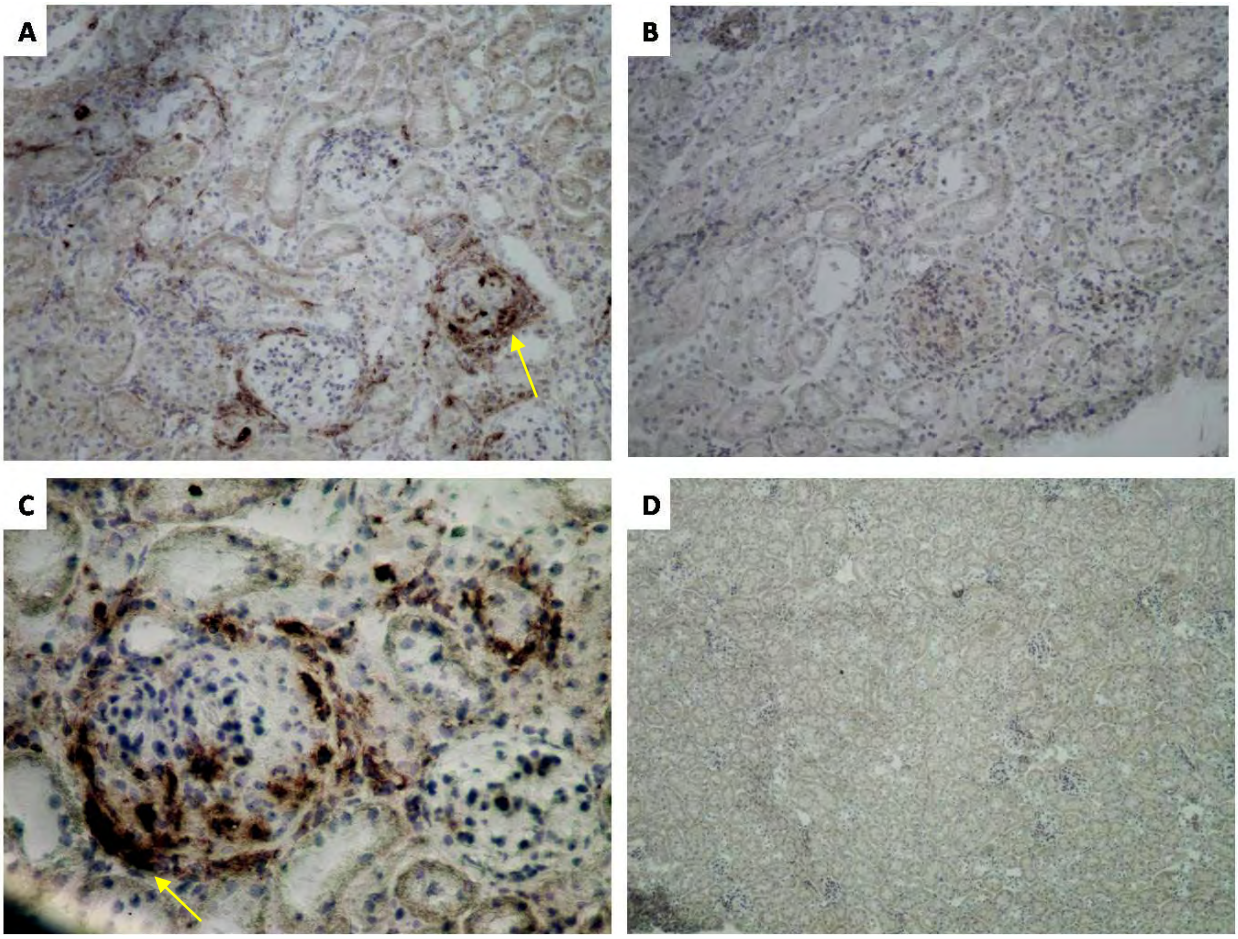

Figure 3.20: CD68 staining on MEV2 frozen kidney sections. Anti-MPO treated mice had positive staining for CD68 (A) and (C). CD68 positive cells were mainly found in the crescent area in the glomeruli (arrows). B: IgG2b negative control on kidney section from an anti-MPO treated mouse. D: anti-BSA treated mouse showing negative staining for CD68.

I counted the total number of CD68 positive cells in the kidney sections (in both in the glomeruli and tubulo-interstitium); there was a significant difference between the anti-MPO- and anti-BSA-treated mice (Figure 3.21, A). In addition, I found a positive correlation between the number of CD68 positive cells and percentage of crescents in the anti-MPO-treated mice (Figure 3.21, B).

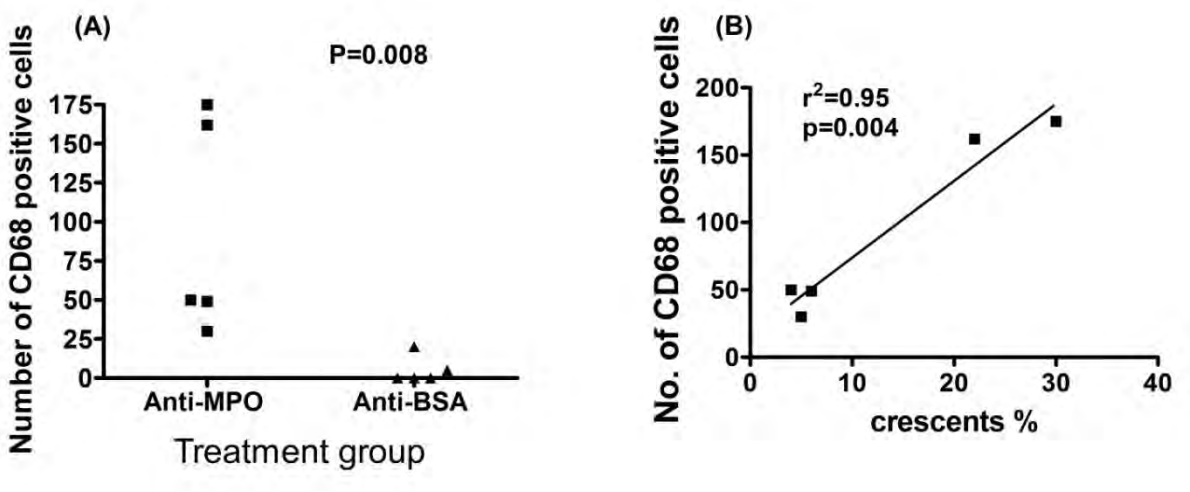

Figure 3.21: CD68 count in MEV2. The number of CD68 positive cells was counted using Aequitas 1A software. There was a significant difference between anti-MPO- (n=5) and anti-BSA-treated (n=5) mice in the number of CD68 positive cells (A) (two-tailed t-test (Mann-Whitney test)). Also, there was a positive correlation between the number of CD68 positive cells and the percentage of crescents in anti-MPO treated mice (B).

3.3.9. MEV6 and immunising mice with MPO peptides and recombinant MPO

Immunising MPO-/- mice with MPO peptides

Mice were immunised with MPO peptides to try and raise anti-MPO antibodies that cross-react with murine MPO. Three MPO peptides were used in this experiment and they were given at different doses. I performed an anti-MPO ELISA to check for anti-MPO antibodies in the serum of these mice. The plate was coated with murine MPO purified from WEHI cells. The titre of anti-MPO antibodies was EC_{50}= 40.64 at the (40+20 mg) dose, EC_{50}= 84.28 at the (200+100 mg) dose, and EC_{50}= 66.05 at the (400+200 mg) dose. The titre was low when the plate was coated with murine MPO as shown in Figure 3.22. I isolated IgG from these immunised mice and injected 75µg/g of antibody plus 15000EU/g of LPS into WT mice but they did not develop any disease on day 6.

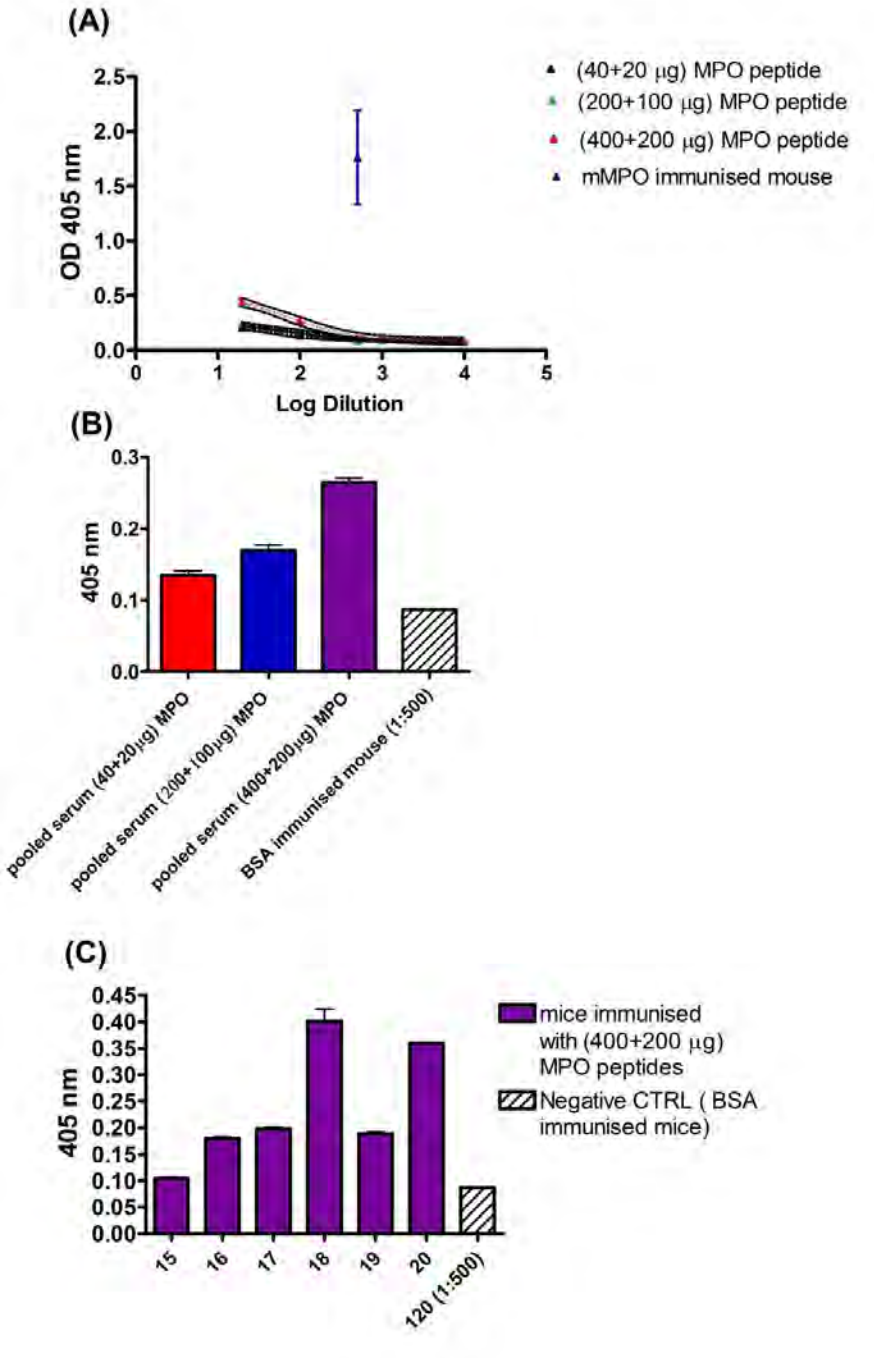

Figure 3.22: Anti-MPO ELISA on serum from MPO peptide-immunised mice. Mice were divided into three groups. Each group received a different concentration of MPO peptides on day 0 and were then boosted with half the dose on day 21. The level of anti-murine MPO antibodies generated by these mice was much less than that generated from a mouse immunised with murine MPO. A: The titre was calculated from the dilution curve using non-linear regression analysis. B: Pooled serum from the mice in the three groups and their OD value. C: Individual mice that were immunised with 400+200 μg of MPO peptides. Plate was coated with murine MPO.

Immunising MPO-/- mice with recombinant mouse MPO

Mice were immunised with recombinant mouse MPO to raise anti-murine MPO antibodies. In order to detect the anti-MPO antibodies generated by these mice, I coated two plates with either recombinant MPO or murine MPO. I used serum from MPO-/- mice that were immunised with murine MPO as a positive control and also used serum from mice that were injected with 75 µg/g of anti-MPO antibodies to induce vasculitis. There was a high titre of anti-recombinant MPO (plate coated with recombinant MPO) in the MEV6 mice serum (immunised with recombinant MPO) (Figure 3.23, A). On the other hand, the titre of anti-murine MPO in the serum from MEV6 was low and significantly less than that from anti-MPO antibodies injected mice (Figure 3.23, B).

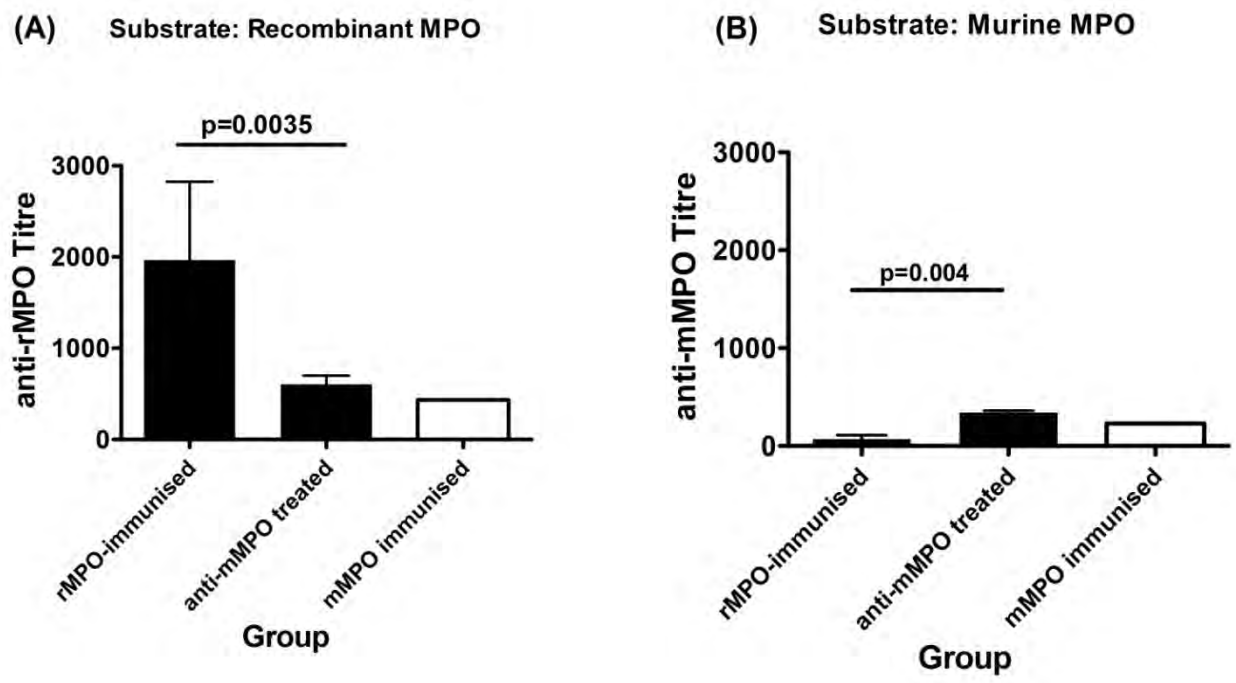

Figure 3.23: Titre of anti-recombinant and anti-murine MPO in MEV6. Plates were coated with either recombinant MPO (A) or murine MPO (B). A serial dilution was done to calculate the titre of anti-MPO antibodies. The titre was calculated from the log dilution by indicating the point where the OD value drops below 50% using non-linear regression analysis. There was no significant difference in the titre of anti-rMPO between rMPO immunised (MEV6) and anti-MPO treated mice (MEV2 and MEV8). However, there was a significant difference in the titre of anti-murine MPO between MEV6 and MEV2 or MEV8. Non-linear fit was used to calculate the titre. An unpaired t-test was used to analyse the differences between the groups.

Injecting WT mice with anti-rMPO antibodies

I used the anti-recombinant MPO generated by immunising MPO-/- mice with recombinant MPO to induce vasculitis in WT mice. Mice were injected with 50 µg/g of either anti-recombinant MPO or anti-BSA antibodies; they also received 1,500 EU/g of LPS. Mice were sacrificed on day 6 and blood was collected for anti-MPO ELISA. These mice had a detectable level of anti-rMPO antibodies with an antibody titre between 87-166 for all the animals that were treated with anti-rMPO antibodies (Figure 3.24). The histological sections from these mice looked normal and there were no crescents (Figure 3.25).

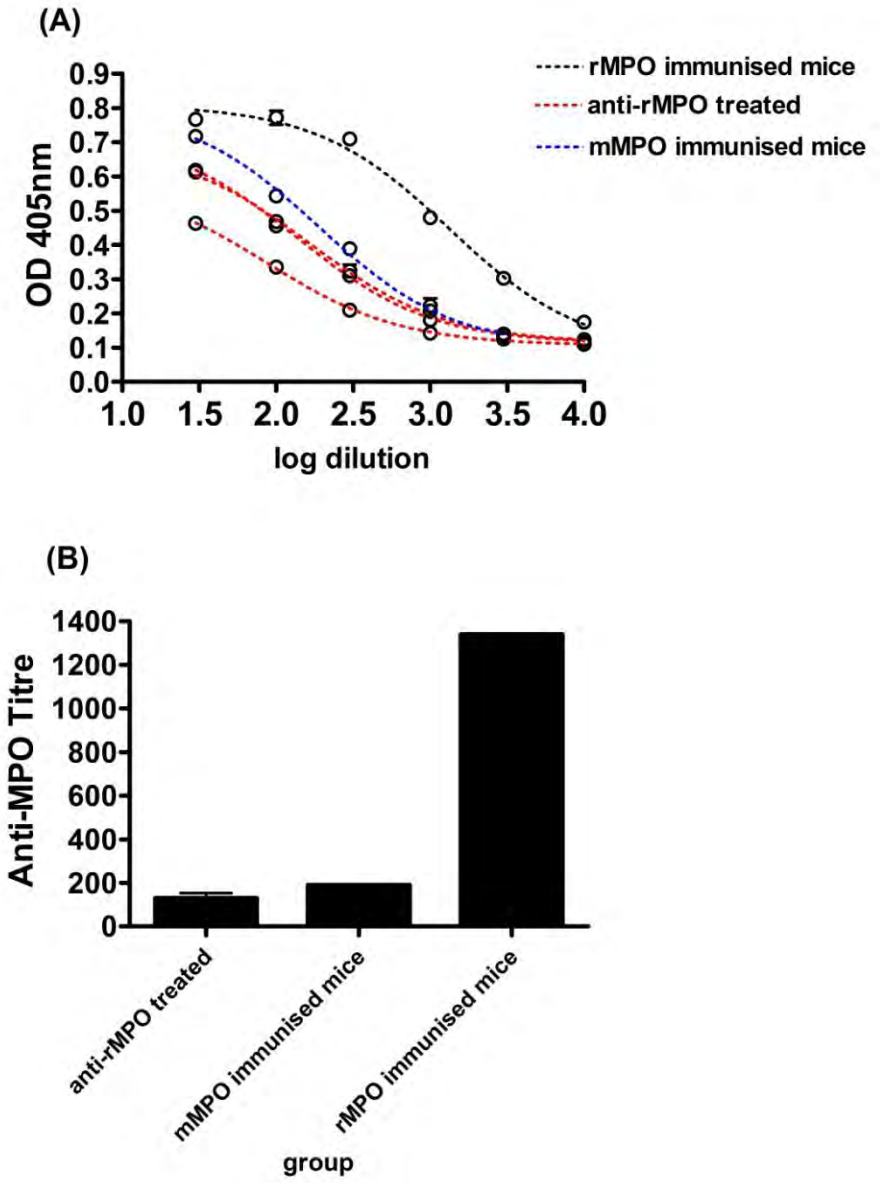

Figure 3.24: The level of anti-MPO antibodies in mice treated with anti-rMPO. A: Dilution curve to measure the titre of anti-rMPO antibodies at day 6 post antibody injection. The EC_{50} was between 87 and 166 in mice injected with anti-rMPO antibodies using non-linear regression analysis. B: The anti-MPO titre in mice injected with r-MPO compared to murine MPO-immunised mice and r-MPO-immunised mice that were used as the positive control. The plate was coated with rMPO.

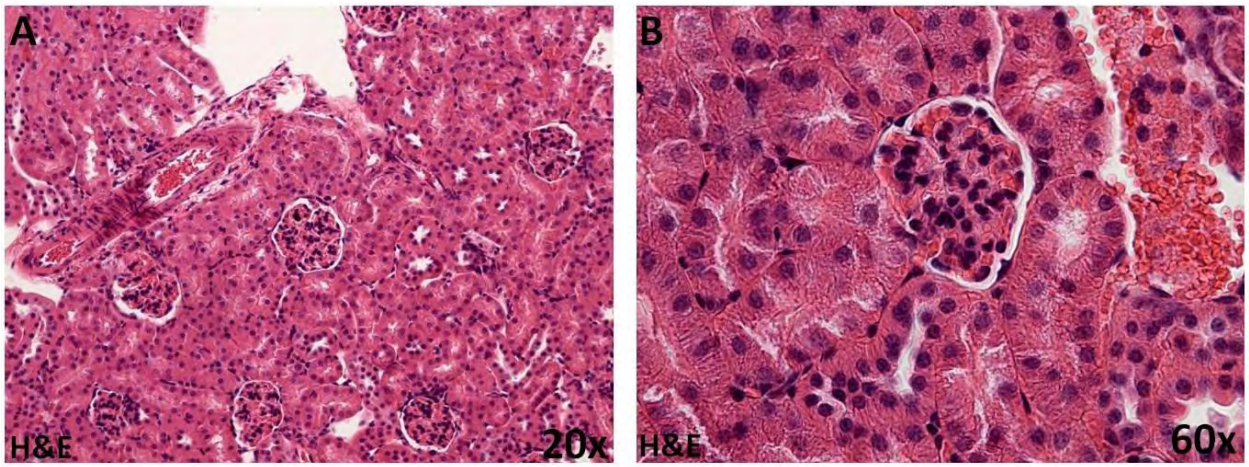

Figure 3.25: Histological sections from mice treated with anti-rMPO. Mice were treated with 50 µg/g of anti-rMPO; none developed crescents. A and B showing normal glomeruli from anti-rMPO treated mice at 20x and 60x.

Maternal transfer experiment (MEV4):

Two female MPO-/- mice that were immunised with MPO peptides (400+200mg) were mated with WT males. The newborn mice were either sacrificed on day 2 or day 21. The mice that were sacrificed at day 21 were injected with 1,500 EU/g of LPS once a week. I measured the level of anti-MPO peptides in these mice using an anti-MPO ELISA coated with MPO peptides. These newborn mice had a detectable level of anti-MPO peptides in the serum on day 2 and day 21. The titre of anti-MPO peptides was 1960 on day 2 and 2251 on day 21 (Figure 3.26). The histological sections from these newborn mice were normal and no crescents were seen (Figure 3.27).

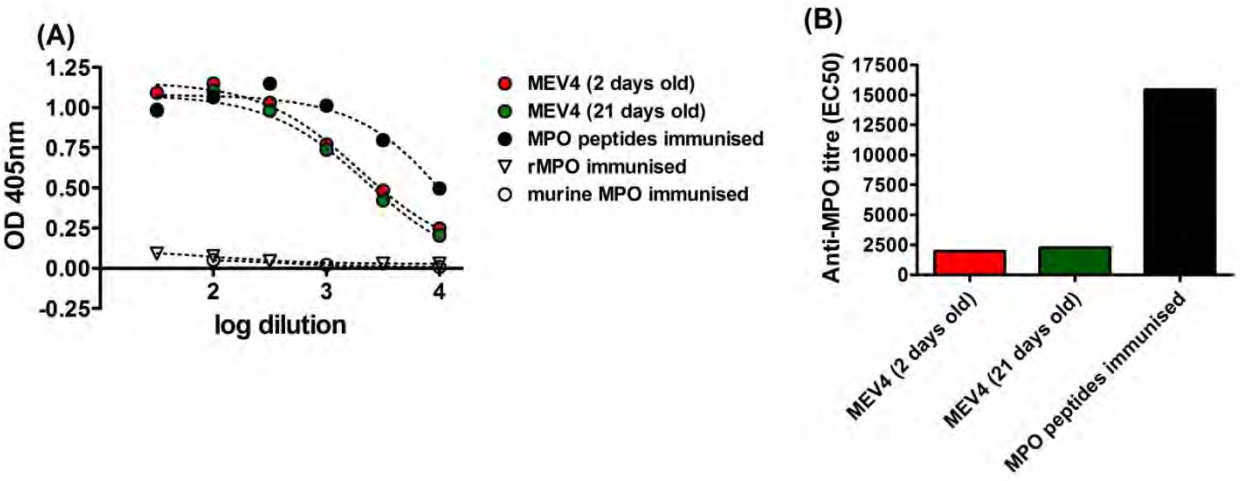

Figure 3.26: The level of anti-MPO peptides in maternal transfer experiment. A dilution curve was used to measure the titre of anti-MPO peptides in 2-day-old and 21-day-old mice from a mother immunised with MPO peptide (A). Pooled serum from MPO peptide-immunised mice, rMPO-immunised mice, and mMPO-immunised mice used as the positive control. Newborn mice had anti-MPO titre of 1960 on day 2 and 2251 on day 21 (B). Non-linear regression analysis. Plate was coated with MPO peptides.

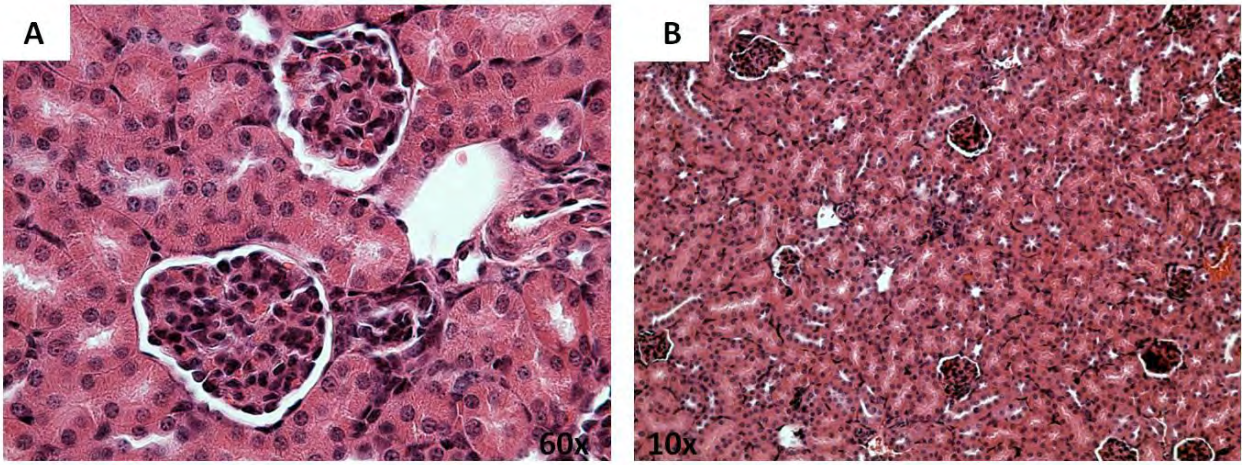

Figure 3.27: MEV4 histology results. Kidneys were fixed in formalin and sections were prepared and stained with H&E. The kidney sections from these mice were normal.

3.4. Discussion

The aim of this work was to induce AAV in mice using anti-MPO antibodies raised in MPO-/- mice and also to test different methods for generating anti-MPO antibodies. First, I injected six mice with 100 µg/g of anti-MPO antibodies; they also received either clodronate or saline. The disease was very mild and only one mouse had crescents, at a rate of 1.4%. I moved on to do another experiment using anti-MPO antibodies and LPS. I injected five mice with anti-MPO antibodies and five mice with anti-BSA antibodies; I also injected all the mice with 1,500 EU/g of LPS. Mice that received anti-MPO antibodies developed crescentic glomerulonephritis at a percentage of around 13%. Macrophages were present in the kidney and they were found mainly in the crescent region of the glomeruli, as shown by CD68 staining. We also looked at different approaches to generate anti-MPO antibodies. I immunised MPO-/- mice with MPO peptides, MPO heavy chain, or recombinant mouse MPO. Although I was able to detect anti-MPO antibodies after immunising the mice with these antigens, I was not able to induce disease in WT mice.

WEHI cells were previously used by Xiao et al. (Xiao, Schreiber et al. 2007) as a source of MPO which we need for immunising MPO-/- mice to produce anti-MPO antibodies. I started culturing these cells in large 1 litre flasks that required large volumes of medium and FCS. The yield was higher when cells were cultured using a bioreactor and less FCS was required compared to the other technique. Less FCS was required because a bioreactor has a membrane that separates the cells that were re-suspended in medium with FCS from the feeding medium (no FCS); this membrane allows fluid to pass through. On the other hand, I had to use medium with FCS when using flasks for cell culturing and that is why I required a large volume of FCS. My results showed that more MPO was present in the cells that were cultured in the bioreactor than in the static flasks. This could be because the cells change their phenotype when they stick to the bottom of the flask, possibly differentiating towards a macrophage phenotype. Therefore, for the remainder of the experiments, I used a rolling bioreactor to generate WEHI cells.

I decided to do a preliminary experiment to ensure the reproducibility of the model. In this case, I was only able to induce very mild glomerulonephritis and only one crescent was seen in one of the mice. This is clearly not sufficiently severe to allow us to address questions of pathogenesis. In contrast to my results, Xiao and colleagues were able to induce glomerulonephritis in all anti-MPO antibody treated mice (Xiao, Heeringa et al. 2002). One reason for this difference between my results and their results is that the titre of anti-MPO antibodies in my experiment was relatively low. Another explanation is that another stimulus was required for inducing severe glomerulonephritis and anti-MPO antibody alone was not sufficient in this experiment to induce severe glomerulonephritis. Although Xiao et al. did not use LPS in their experiment, we found it to be required in ours. These differences could be due to the animal house where the animals are kept. The animal house at the University of Birmingham is known to be very clean and many people here have struggled with their animal models. In a different study, it has been shown that systemic administration of bacterial lipopolysaccharide (LPS) increased disease severity compared to using anti-MPO antibody alone (Huugen, Xiao et al. 2005). These authors suggested that proinflammatory stimuli may be required along with ANCA to induce full disease in humans.

I started looking for explanations as to why I was not able to induce severe vasculitis in the pilot experiment. One explanation was that the mice did not receive the full dose or volume of anti-MPO antibodies and that could be due to a loss of antibodies during i.v. injection. Another explanation was that the antibodies were trapped in the spleen when they were injected intravenously. In order to find a good explanation, I decided to measure the level of anti-MPO antibodies in the serum of the mice that were used in the MEV1 experiment using ELISA to check for any differences in the level of anti-MPO antibodies. I was able to detect a sufficient amount of anti-MPO antibodies in the saline-treated mice. We concluded that we have to stimulate the immune system of these mice with LPS to augment the immune response.

In order to induce severe vasculitis, I used LPS, which was used by another group to aggravate anti-MPO antibody-induced glomerulonephritis (Huugen, Xiao et al. 2005). All the mice received LPS and they either received anti-MPO or anti-BSA antibody. All of the mice that received anti-MPO antibody developed crescentic glomerulonephritis. The mean percentage of crescentic glomeruli in these mice was 13.4%, in which some mice developed a high percentage of crescents while some mice developed fewer crescents. On the other hand, none of the mice that received anti-BSA antibody developed crescents or glomerular necrosis and most of the glomeruli were normal. A logical explanation for the effect of LPS on the immune system is that it results in an increase in the serum TNF-α level. Priming human polymorphonuclear leucocytes with TNF-α has been found to be required in vitro to induce the respiratory burst by ANCA. In addition, priming neutrophils with TNF-α in vitro results in the translocation of ANCA antigens to their surface. Blocking TNF-α in both rat and mouse models of ANCA-associated vasculitis resulted in a reduction crescent formation (Huugen, Xiao et al. 2005; Little, Bhangal et al. 2006). In addition, LPS could induce leucocyte and macrophage recruitment to the tissue, resulting in more severe disease.

I also investigated macrophage infiltration using CD68 staining. Positive staining was seen in all the mouse kidneys that were injected with anti-MPO antibodies. CD68 positive staining was found mainly in the crescent region of the glomeruli, and there was a positive association between the crescent percentages and the number of CD68 positive cells. In humans, CD68 positive macrophages are the dominant cell type infiltrating glomeruli (Weidner, Carl et al. 2004). Macrophage infiltration has been reported in previous studies of vasculitis. Huugen et al. have shown influx of CD45+ leucocytes and most of these were FA11+ macrophages. They also noticed an increase in the number of macrophages following administration of LPS. We have shown the ability to induce vasculitis in mice using anti-MPO antibodies and LPS and also shown the presence of macrophages in the site of injury.

In addition, I investigated the possibility of raising anti-MPO antibodies in MPO-/- mice using MPO peptides and recombinant MPO. I investigated giving different concentrations of MPO peptides: 40, 200, 400 μg. We found an increase in the level of anti-murine MPO in correlation with increasing the dose of MPO peptides as measured by anti-MPO ELISA. Although there was a detectable amount of anti-MPO antibodies generated by MPO-/- mice in response to MPO peptide immunisation, this was much less than that detected from mice immunised with murine MPO and I described the reason behind this in chapter 6.

I used two females from the group that were immunised with MPO peptides for the maternal transfer experiment. The aim of this experiment was to investigate the possibility of inducing vasculitis in newborn mice from MPO-/- mothers that were immunised with MPO peptides and were mated with WT males. The idea came after a study was published describing a newborn child from a mother with microscopic polyangiitis who developed glomerulonephritis and pulmonary haemorrhage (Bansal and Tobin 2004; Schlieben, Korbet et al. 2005). We sacrificed the newborn mice at different time points (day 2 and day 21) and some of these mice received LPS to stimulate the immune system. We were not able to see any evidence of vasculitis on the histological sections; however I was able to detect clear evidence of efficient antibody transfer. This does not mean that it is not possible to induce vasculitis in newborn mice from mothers immunised with MPO, but antibodies produces in this mice were specific to the MPO peptides and did not react with murine MPO. With further optimisation, I believe this approach holds promise for a reduction in the requirement for animals both in this model and in other models of autoantibody-driven disease; moreover, it removes the requirement for potentially wasteful IgG purification from serum.

In addition, we tried using recombinant mouse MPO to raise anti-MPO antibodies. A high titre of anti-recombinant MPO was achieved as shown by ELISA when the plate was coated with recombinant MPO. On the other hand, the level of anti-MPO antibodies was significantly less than that seen in mice injected with anti-murine MPO when the plate was coated with murine MPO. Antibodies purified from these mice were injected into WT mice, but they did

not develop the disease. This could be because anti-recombinant mouse MPO antibodies did not cross-react with murine MPO due to differences in the structure between native and recombinant MPO as described in chapter 6. This was seen when an ELISA plate was coated with murine MPO and there was a significant difference in the MPO titre when serum from anti-murine MPO-treated mice was compared to mice immunised with recombinant MPO.

In conclusion, optimising the animal model was one of my priorities before starting any further investigations. I tried different approaches to try and find a source of MPO that would make the model easier to work with. I was able to induce severe vasculitis in mice using anti-MPO antibodies and LPS, which was found to be required to induce severe disease.

Chapter 4
Macrophage Phenotyping and monocyte depletion in murine experimental vasculitis

4.1. Introduction

This chapter covers the work I did in trying to understand the role of macrophages in ANCA-associated vasculitis. This involved identifying macrophage phenotypes in the kidney by immunohistochemical staining following disease induction. In addition, I used a microarray approach to study upregulated genes in the kidney, especially those genes that are associated with macrophage activation. Finally, I investigated the effect of preventing macrophage infiltration in the kidney on disease development.

Macrophage infiltration to the site of injury is a common feature of ANCA-associated vasculitis. Atkins et al. reported the accumulation of large numbers of macrophages in necrotising/crescentic lesions (Atkins, Holdsworth et al. 1976). However, the phenotype of these macrophages has not been investigated in the mouse model of ANCA-associated vasculitis (MEV). Nevertheless, the role and type of macrophages has been investigated in other kidney diseases, such as ischaemic injury. For example, Lee et al. reported a switch in the macrophage phenotype during ischaemic kidney injury from the M1 phenotype to M2 (Lee, Huen et al. 2011). In addition, they showed an accumulation of M1 macrophages during the first 48 hours following injury, but M2 macrophages were dominant in later stages of the disease. These results suggest the involvement of both M1 and M2 macrophages in kidney injury and repair in ischaemic injury of the kidney. In addition, Ferenbach et al. showed a protective role of HO-1-positive macrophages in ischaemic-reperfusion injury (IRI) (Ferenbach, Nkejabega et al. 2011). These results show the variability of macrophage phenotypes in kidney injury. I believe that identifying macrophage phenotypes in AAV in mice is important, as it should help to identify whether they were inflammatory or anti-inflammatory and whether the depletion was beneficial or not.

I discussed the different macrophage subsets in Chapter 1, including M1 and M2 macrophages. If macrophages are involved in the pathogenesis of crescentic glomerulonephritis, then these would be expected to be M1 macrophages. On the other hand, M2 macrophages are mostly involved in repair and can be identified by the expression of specific M2 markers such as the mannose receptor (CD206) and CD163. I investigated the phenotype of macrophages in kidney sections from animals treated with anti-MPO antibodies.

The understanding of macrophages in AAV can be strengthened by studying gene expression and upregulation in the glomerulus using microarray analysis. The Affymetrix array works by loading labelled cDNA onto a microarray chip that contains thousands of genes, allowing complementary sequences to form strong bonds that can then be detected by laser scanning. The development of new scientific techniques and molecular biological tools has provided new directions for evaluating the pathophysiology of different diseases. Gene expression analysis has made it possible to study the expression of thousands of genes in a relatively short period of time using small amounts of starting materials. In mammalian tissues, some genes are upregulated or downregulated depending on a given disease process. Comprehensive gene expression analysis is possible and has been performed on different animal models of renal injury. For example, Yoshida et al. used microarray analysis to study gene expression in ischaemia-induced renal failure (Yoshida, Tang et al. 2002). They were able to identify upregulated and downregulated genes on both days 1 and 4. Using microarray analysis, they were able to identify several novel genes, such as serine protease inhibitors, that might be involved in kidney repair. I used this approach to identify upregulated genes in crescentic glomerulonephritis induced by anti-MPO antibodies in mice and rats.

I used this approach to look for genes that are upregulated in the glomeruli and tubules in the kidney in mouse and rat models of vasculitis. These two animal models develop the same disease, but it is induced by different methods. In mice, this disease is induced by the

passive transfer of anti-MPO antibodies into wild-type mice. On the other hand, rats are actively immunised with human MPO with an adjuvant and they produce anti-MPO antibodies that cross-react with rat MPO and cause vasculitis. The purpose of using the rat model here is to use mouse, rat and human microarray data for a web-based analysis that may facilitate the integration of data across species. Human data were obtained from our collaborators at the European Renal Cell Bank (ERCB) in Zurich (Dr. Clemens Cohen). Their data were obtained from microdissected glomeruli of vasculitis patients using Affymetrix array analyses. I used a similar approach to collect data from mouse and rat models of vasculitis. The aim of this study was to use the network analysis tool to generate a network of human, mouse and rat data sets and to then generate an overlay of the mouse and the rat model with the human data set. This analysis will be undertaken by our collaborators at the University of Michigan (Matthias Kretzler). This will then act as the starting point for biological analyses investigating which pathways and networks are model specific and which ones are common between species. This could lead to finding common transcriptional factors that are conserved between species.

Meanwhile, the data from the gene expression and upregulation analyses were used to study genes associated with macrophage activation, which could identify pathways associated with macrophage activation that result in kidney injury. Also, upregulated genes could be used to identify the type of macrophages that accumulate in the kidney and help strengthen the results on macrophage phenotyping.

As a result, the main question that I hoped to answer from the Affymetrix array study was: could these results be used to study the type of macrophages that accumulate in the kidney in order to help understand the effect of macrophage infiltration on the development of vasculitis? The second goal was to find common transcriptional factors or pathways in mice, rats and humans.

Macrophage depletion has been used as a technique for studying the role of macrophages in kidney injury (Duffield, Tipping et al. 2005). There are different methods for depleting macrophages, including the diphtheria toxin approach, liposomal clodronate and CCR2 blockade. Clodronate is used to treat osteolytic bone diseases (Jordan, van Rooijen et al. 2003). It has been found that once clodronate is incorporated into liposomes it can be used to deplete macrophages (van Rooijen and van Nieuwmegen 1984; Claassen, Van Rooijen et al. 1990). Clodronate works by causing macrophage apoptosis after it has been taken up by these cells (Naito, Nagai et al. 1996; van Rooijen, Sanders et al. 1996). The type of injection used has been found to affect the type of macrophages that will be depleted. For example, an intravenous injection will result in hepatic and splenic macrophages being depleted. On the other hand, tissue injection will result in the depletion of macrophages from this tissue and the draining lymph nodes (van Rooijen, Kors et al. 1989). Van Rooijen et al. showed that using this method to deplete macrophages does not result in the secretion of pro-inflammatory cytokines by these cells when they undergo apoptosis (van Rooijen and Sanders 1997). In addition, liposomal clodronate was found to affect macrophages and phagocytic dendritic cells, but not neutrophils or lymphocytes (van Rooijen, Kors et al. 1989; Van Rooijen and Sanders 1994; Alves-Rosa, Stanganelli et al. 2000).

The anti-mouse CCR2 antibody MC-21 has also been used to block CCR2 in mice (Mack, Cihak et al. 2001). Mack et al. showed that MC-21 blocked the binding of monocyte chemotactic protein (MCP)-1 to CCR2. In addition, MC-21 prevented monocyte infiltration in the model of thioglycollate-induced peritonitis. Furthermore, Bruhl et al. demonstrated the ability of MC-21 to deplete GR1+ cells from peripheral blood (Bruhl, Cihak et al. 2007). These cells differentiate into inflammatory macrophages, as I will explain below. MC-21 could be used to deplete GR1+ monocytes and to study its effect on the development of vasculitis. The purpose of this experiment was to determine whether the blockage of CCR2

prevents macrophage infiltration, as reported previously, as part of a study on the effects of macrophage depletion on disease development.

Mouse and human blood monocytes have typical morphological features and originate from the bone marrow. These monocytes can differentiate into macrophages and inflammatory DCs during inflammation (Serbina, Jia et al. 2008), and they are also involved in renewing tissue DCs and macrophages (Geissmann, Jung et al. 2003; Auffray, Sieweke et al. 2009). Mouse monocytes are divided into different subsets depending on their expression of receptors such as Ly6C (GR1). The GR1+ monocytes differentiate into inflammatory DCs and M1-type macrophages, whereas GR1- monocytes differentiate into M2-type macrophages (Auffray, Sieweke et al. 2009). The GR1+ monocytes express CCR2 and a low level of CX3CR1. On the other hand, GR1- monocytes lack the expression of CCR2. This chemokine receptor has been shown to be involved in monocyte migration from the bone marrow to the bloodstream (Serbina and Pamer 2006). This is a chemokine receptor for monocyte chemoattractant protein-1 (MCP-1), which has been shown to be involved in macrophage recruitment in several inflammatory models (Flory, Jones et al. 1993; Huffnagle, Strieter et al. 1995). This suggests the possibility of the involvement of CCR2 in monocyte trafficking during inflammation. Kurihara et al. showed that macrophage recruitment following inflammation is significantly lower in CCR2-deficient mice compared to wild-type mice (Kurihara, Warr et al. 1997). In addition, they found that the absence of CCR2 in these mice did not affect the recruitment of other cell types such as neutrophils and eosinophils, and that the defect was specific for macrophage recruitment. These results suggest an important role of CCR2 and its ligands in macrophage recruitment following inflammation. Furuichi et al. a reagent (RS-504393) that is a specific antagonist of CCR2. They found that the number of interstitial infiltrated cells and tubular necrosis was reduced in ischaemia-reperfusion injury following treatment with RS-504393 (Furuichi, Wada et al. 2003). This study and other studies showed the importance of CCR2 in macrophage recruitment. As a result, we decided to use antibodies to block the function of this receptor in order to eliminate macrophage

recruitment in the mouse model of vasculitis. This should allow for the effect of macrophage depletion on AAV in mice to be studied.

Disease severity in the mouse model of vasculitis is relatively mild compared to human vasculitis. We wanted to improve this model and induce a more severe disease, similar to the type seen in humans. Previously, we used C57Bl/6J mice in our model. However, Xiao et al. recently reported that they were able to increase the severity of the disease by using a different strain of mice (129S6) (Xiao 2009). They were able to increase crescent formation to 69%. For this reason, we decided to use this mouse strain in our experiment.

4.2. Methods

4.2.1. The macrophage phenotype in AAV in mice

I used kidney sections from mice that were treated with anti-MPO or anti-BSA antibodies to study macrophage phenotypes in crescentic glomerulonephritis. These mice only received anti-MPO or anti-BSA antibodies and LPS, and they were also used to study gene expression.

Different markers were used to stain for macrophages and also to identify their phenotype: CD68 was used to stain for macrophages and CD206 (mannose receptor) was used as an M2 marker (Chavele, Martinez-Pomares et al. 2010). I started by optimising the antibodies and performing serial dilutions to find the right concentration. Wild-type spleen sections were used to optimise staining. I also tried double staining (CD68+CD206), but this proved to be difficult because all of my primary antibodies were made in the same species (rat anti-mouse). I will describe some of the methods that I used.

First, frozen sections were fixed in acetone and re-hydrated in PBS as described in Chapter 2. Sections were blocked with 5% normal goat serum to block non-specific binding. Then, I added the first primary antibody (rat anti-mouse CD68) that was diluted by 1:100 in 2% horse serum in PBS (optimised to this dilution) and incubated for 1 hour. After this, sections were washed three times in PBS and incubated with a secondary antibody (Alexa Fluor 594 goat anti-rat IgG) for 45 minutes in the dark. Next, the sections were washed and blocked with 5% normal mouse serum for 30 minutes, washed again, and the second primary antibody (rat anti-mouse CD206) was added and diluted by 1:100. The sections were then incubated in the dark for 2 h. After this, the sections were washed in PBS and incubated with a secondary antibody (FITC rabbit anti-rat IgG) for 45 minutes. Finally, the sections were washed three times in PBS and mounted.

I could not get the double staining to work, so I used serial sections instead. The serial sections were prepared from frozen kidneys and three serial sections were placed onto one

slide. I selected three important markers to identify the type of macrophages in the kidney: CD68, CD206 (mannose receptor) and MHC class II. The CD68 marker is a general macrophage marker, whereas expression of the mannose receptor increases in alternatively activated macrophages. On the other hand, MHCII expression is increased in classically activated macrophages (Gordon and Taylor 2005). Staining for CD68, CD206, and MHCII was performed as previously described. Serial images of the same area were taken to analyse the staining.

Staining for T cells, neutrophils, and macrophages:

Frozen serial kidney sections were used to stain for different cell type in the kidney to compare macrophages to other cells in the kidney as shown below. The staining was done by MRC, UK. The procedure started by fixing the sections in 2% paraformaldehyde for 10 minutes on ice. The sections were then washed 3 times in PBS/0.1%Tween. The sections were incubated with quench for 15 minutes at 37ºC in oven and then washed in PBS. Then, sections were blocked with 5% normal goat serum for 30 minutes and then washed in PBS. This was followed by avidin blocking for 15 minutes and then washing the sections in PBS. After that, sections were incubated with biotin blocking for 15 minutes and then they were washed in PBS. Next, primary antibody was added using the dilution shown below and incubated for 1 hour at room temperature and then washed in PBS. Then secondary biotin goat anti-rat IgG (Jackson labs, UK) diluted 1:500 was added to each section and incubated at room temperature for 30 minutes and then wash in PBS. After that, sections were incubated with ABC kit for 30 minutes and then washed. Then procedure continued as previously described.

Antibody	Supplier	Dilution
F4/80 (macrophage marker)	ABD Serotec, UK	1:100
CD4 (T Cells)	//	1:100
CD8 (Cytotoxic T cells)	//	1:100
CD3 (mature T cells)	//	1:100
GR-1 (neutrophil marker)	//	1:200
Dectin-1	//	1:20

4.2.2. Affymetrix array and tissue preparation for laser microdissection

Tissues and animals

Tissues for the laser microdissection experiment were obtained from mouse and rat models of vasculitis. Mice tissues were obtained from mice treated with 75 μg/g of anti-MPO (n=5) or anti-BSA (n=5) and 1,500 EU/g of LPS and sacrificed on day 6. Rats were immunised with either human MPO (n=5) or human serum albumin (n=5) (this experiment was performed by Dr. Bahjat Al-Ani). The rats received 1 μg of pertussis toxin through an i.p. injection on day -5. Then, they received 3.2 mg/kg of MPO or HSA in complete Freund's adjuvant on day 0 by i.m. and s.c. injections. In addition, they received 1,500 EU/g of LPS on days 7, 28, 35 by i.p. injections. The rats were boosted with 100 μg/kg of MPO or HSA in weeks 3 and 5 and they were sacrificed in week 8. They also received pertussis toxin and LPS. These rats were then sacrificed after 8 weeks. The kidneys were collected from these animals for laser microdissection; they were kept in cryo tubes, snap frozen in liquid nitrogen and stored at -80°C.

This study was performed following work undertaken on human kidneys from ANCA-associated vasculitis patients to study gene expression and upregulation in glomeruli which was performed by our collaborators in Zurich (Dr. Clemens Cohen). For this reason, we tried to replicate their work as close as possible to allow us to compare the results. For human

crescentic glomerulonephritis, they used an HG-U 133 Plus 2.0 Affymetrix array; therefore, I used Affymetrix arrays that were similar to the one they used: these were Affymetrix rat genome 230 2.0 and mouse genome 430 2.0 arrays (Affymetrix UK Ltd., UK).

Optimising the microdissection technique

I optimised my technique before starting the actual work on laser microdissection. The aim of this work was to compare the results that we obtained from the animal models (rat and mouse) with the results that were obtained from human patients with AAV. We wanted to compare the results that we obtained from the animal models with the human results, which meant following the same protocol that was used for the human kidneys in order to minimise variations in the data. They started with 20 ng of total RNA; therefore, I decided to start with the same quantity. I microdissected glomeruli from wild-type mouse kidneys and tried to measure the RNA using the Nano-drop UV instrument, but the reading was not accurate and I also lost RNA during the process because I needed 2 µl of RNA to get a reading. I therefore decided to use a bioanalyser to measure the RNA concentration, which also measures the integrity of the RNA. I microdissected 250 glomeruli and extracted the RNA from these and also from a whole kidney section to use as a positive control. I obtained 13 ng of total RNA from 250 glomeruli, so we decided to microdissect 400 glomeruli, which gave a sufficient amount of starting RNA material for the experiment.

I also investigated the maximum time that I could store microdissected tissue before starting RNA extraction. We decided to microdissect glomeruli and tubules from four animals each week by doing one animal each day, which meant storing microdissected tissues in lysis buffer for a maximum of 4 days. I found that the quality of the RNA was not affected after 4 days, as measured by the bioanalyser and compared to tissues that were only stored for 1 day.

Preparing sections

Kidney tissues frozen in cryo vials were transferred to dry ice in the cryostat. The tissues were placed inside the cryostat and left for 10 minutes to equilibrate. All brushes were treated with RNase Zap to eliminate contamination. Then, I cut 8 µm-thick tissues and transferred them to a membrane slide (Carl Zeiss, UK). These are special glass slides covered with a thin membrane that can be easily cut together with the tissue, without affecting the morphological integrity. The slide was kept inside the cryostat for 2 minutes and the second section was transferred to the slide by keeping my finger on the slide where the section would be located. This was done to make the section stick to the cold slide. The slides were then transferred to a storage box on dry ice that contained silica gel to control the moisture level and stored at -80°C until they were ready for microdissection.

Staining with cresyl violet

I prepared 12 slides from each tissue; each slide had two sections. I used 10 mouse kidneys and 10 rat kidneys for this experiment. We had disease and control groups from each species. Five animals were from the disease group and these were either injected with anti-MPO antibodies and LPS (mouse) or immunised with human MPO with pertussis toxin and LPS (rat). The control groups contained five animals and these were either injected with anti-BSA and LPS (mouse) or immunised with human serum albumin with pertussis toxin and LPS (rat). This resulted in a total number of 20 animals. Kidney sections from these animals were used to microdissect 400 glomeruli and the interstitial tubules. These were divided into five groups as shown below. Each group contained four animals (two rats and two mice): mouse control, mouse disease, rat control, and rat disease.

Table 4.1: Mouse and Rat tissues that were used for microdissection. Kidney sections were prepared from control and disease groups.

Mouse tissues (anti-MPO treated)	Mouse tissues (anti-BSA treated)	Rat tissues (MPO immunised	Rat tissues (HSA immunised)
75 µg/g anti-MPO + 1,500 EU/g	75 µg/g anti-BSA + 1,500 EU/g	3.4 mg/kg MPO+LPS+pertussis	3.4 mg/kg HSA+LPS+pertussis
//	//	//	//
//	//	//	//
//	//	//	//
//	//	//	//

Table 4.2: Describing the type of tissues used each week for microdissection. Each week, two mouse (control and disease) and two rat (control and disease) tissue were used for microdissection.

Week 1	Week 2	Week 3	Week 4	Week 5
Anti-MPO-treated mouse	Anti-BSA treated mouse	MPO-immunised rat	HSA-immunised rat	MPO-immunised rat
MPO-immunised rat	HSA-immunised rat	Anti-MPO-treated mouse	Anti-BSA-treated mouse	Anti-MPO-treated mouse
Anti-BSA-treated mouse	Anti-MPO-treated mouse	HSA-immunised rat	MPO-immunised rat	HSA-immunised rat
HSA-immunised rat	MPO-immunised rat	Anti-BSA-treated mouse	Anti-MPO-treated mouse	Anti-BSA-treated mouse

It took one day for 400 glomeruli and interstitial tubules from one animal to be microdissected (12 hours). On the day of microdissection, I took the slides from one animal, which were stored in a small box, and transferred them onto dry ice. I stained one slide at a time and performed the microdissection and then did the next one using cresyl violet stain (figure 4.1), as previously described in Chapter 2.

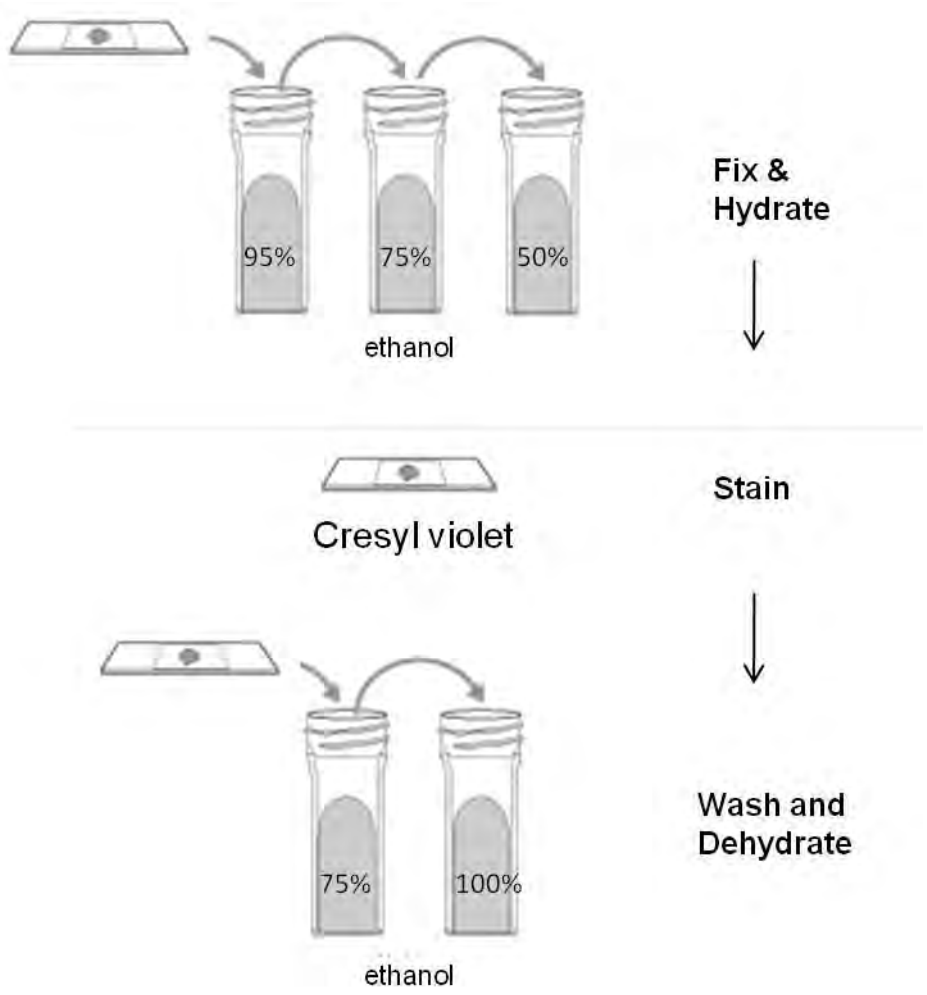

Figure 4.1: Cresyl violet staining. Sections were stained for visualisation before laser microdissection was started. The slides were fixed and hydrated in 95% (30 seconds), 75% (30 seconds), and 50% (25 seconds) ethanol. The sections were then stained for 1 minute with cresyl violet and then quickly washed in 75% ethanol and rehydrated for 30 seconds in 100% ethanol.

Laser microdissection and RNA extraction

The tissues were microdissected as previously described in Chapter 2. For each animal, I used eight slides to microdissect 400 glomeruli and four slides for the interstitium. Four tissues were microdissected each week (two mice and two rats), which resulted in the production of eight samples (glomeruli and tubules from each animal). The microdissected tissues were stored at -80°C until ready for RNA extraction (no more than 4 days stored at -80°C). The RNA was extracted as previously described in Chapter 2.

The RNA samples were processed by the College of Medical and Dental Sciences Affymetrix Microarray Service under the guidance of Dr. John Arrand. The quality of the RNA

was measured by a bioanalyser, which is an instrument used to measure the quality and quantity of total RNA. When eukaryotic RNA is broken down, it produces two distinct bands representing 18S and 28S. The quality of RNA is measured by the RNA integrity number (RIN), which is calculated using an Agilent software algorithm. This gives a number between 1 and 10, where 1 is considered degraded RNA and 10 indicates intact RNA. An RIN of 7 is considered good for working with microarray http://biomedicalgenomics.org/The_RNA_Integrity_Number.html. The RNA was amplified using an ExpressArt C&E Nano kit according to the manufacturer's instructions, followed by biotin labelling, fragmentation, hybridisation to the Affymetrix Rat Genome 230 2.0 or Mouse Genome 430 2.0 arrays, washing, staining, and scanning, all according to standard Affymetrix protocols. The protocol is described in Chapter 2.

The samples were analysed using Linear Model for Microarray Analysis (LIMMA) software (http://www.statsci.org/smyth/pubs/limma-biocbook-reprint.pdf) to find upregulated genes. The LIMMA software uses linear models to analyse data from microarray experiments. For upregulated genes in mouse and rat glomeruli, the P value was set to 0.05 and a two-fold change compared to the control group was required. In addition, PANTHER (Protein Analysis Through Evolutionary Relationships) software was used to separate these upregulated genes in different groups. I uploaded the symbols of upregulated genes to the PANTHER website at the following link http://www.pantherdb.org/tools/compareToRefListForm.jsp. Each list was compared to the reference list using the binomial test (Cho and Campbell 2000) for each molecular function, biological process, or pathway term in PANTHER.

4.2.3. Macrophage depletion using clodronate

I decided to investigate the possibility of using liposomal clodronate to deplete macrophages in a pilot experiment. Mice were treated with 100 µl clodronate on days -2, 0, 2, 4, and 7 relative to the first anti-MPO injection, as shown in Figure 4.2. Huang et al.

showed >95% elimination of macrophages 48 hours after clodronate administration, which is why I chose to administer clodronate every two days, in order to achieve macrophage depletion at all disease stages (Huang, Tipping et al. 1997). Clodronate was given through i.v. injections, except on day 0 where it was given through an i.p. injection for technical reasons. Macrophage depletion was assessed by CD68 immunohistochemical staining on paraffin sections from the kidney and spleen, as previously described. I also measured the anti-MPO antibody titre in the serum of these mice following clodronate treatment using an anti-MPO ELISA, as described in Chapter 2.

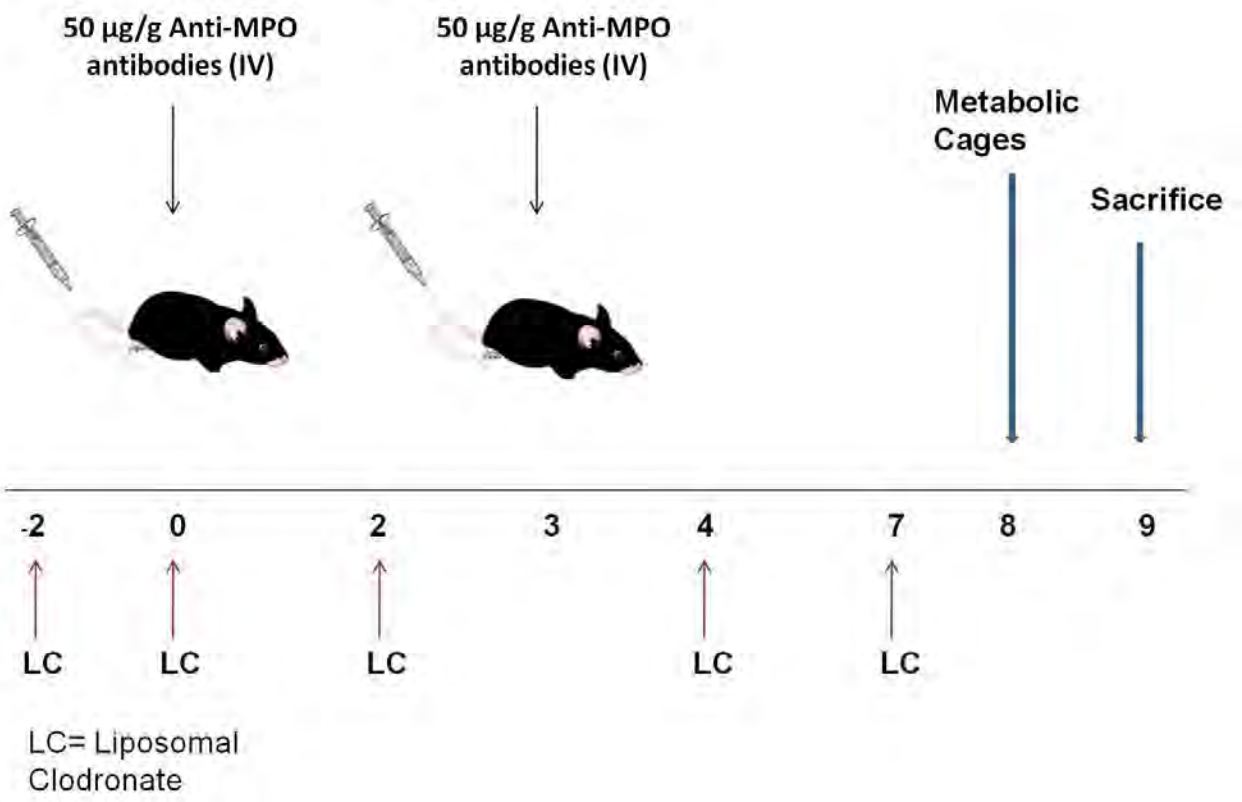

Figure 4.2: Macrophage depletion using clodronate. The mice were injected with liposomal clodronate on days -2, 0, 2, 4, and 7. The mice were sacrificed on day 9 and their blood was collected.

4.2.4. Depletion of CCR2+ monocytes to investigate role of monocyte recruitment in MEV

Clodronate affected the level of transferred antibodies, so we decided to use another method for depleting macrophages. We used anti-mouse CCR2 (MC-21; kindly donated by

Dr. Matthias Mack, Germany) to deplete Gr1+ monocytes. This antibody was produced when Chinese hamster ovary cells were transfected with murine CCR2 and then Wister rats were immunised with these cells (Mack, Cihak et al. 2001). The anti-mouse CCR2 antibody was shown to increase the level of interlukin-6 (IL-6) when introduced at a high dose (e.g. 50-100 µg), but it did not do so when given at a low dose (e.g. 10 µg). Therefore, I decided to use this antibody at 20 µg because this dose showed good depletion during the optimisation stage. I used a different strain of mice in this experiment than was previously used: 129 SvEv (Taconic, USA). The reason for using this strain was that it was reported to develop severe crescentic glomerulonephritis following the passive transfer of anti-MPO antibodies. Eight mice were used in this experiment and rat anti-mouse CCR2 antibody was used to deplete the blood monocytes (figure 4.3). The mice were divided into two groups and received 20 µg of either anti-mouse CCR2 antibody (MC-21, n=4) or rat IgG2b (isotype control, n=4) via i.p. injections from day -1 to day 5. All mice received 75 µg/g of anti-MPO antibody via an i.v. injection on day 0. Monocyte depletion was monitored using flow cytometry. Urine was collected on days 1 and 6 to check for haematuria. No haematuria detected on day 1, so we elected to give LPS to boost the immune response. The mice were culled on day 6 and tissues were collected and either snap frozen or fixed in a 10% formalin/saline solution.

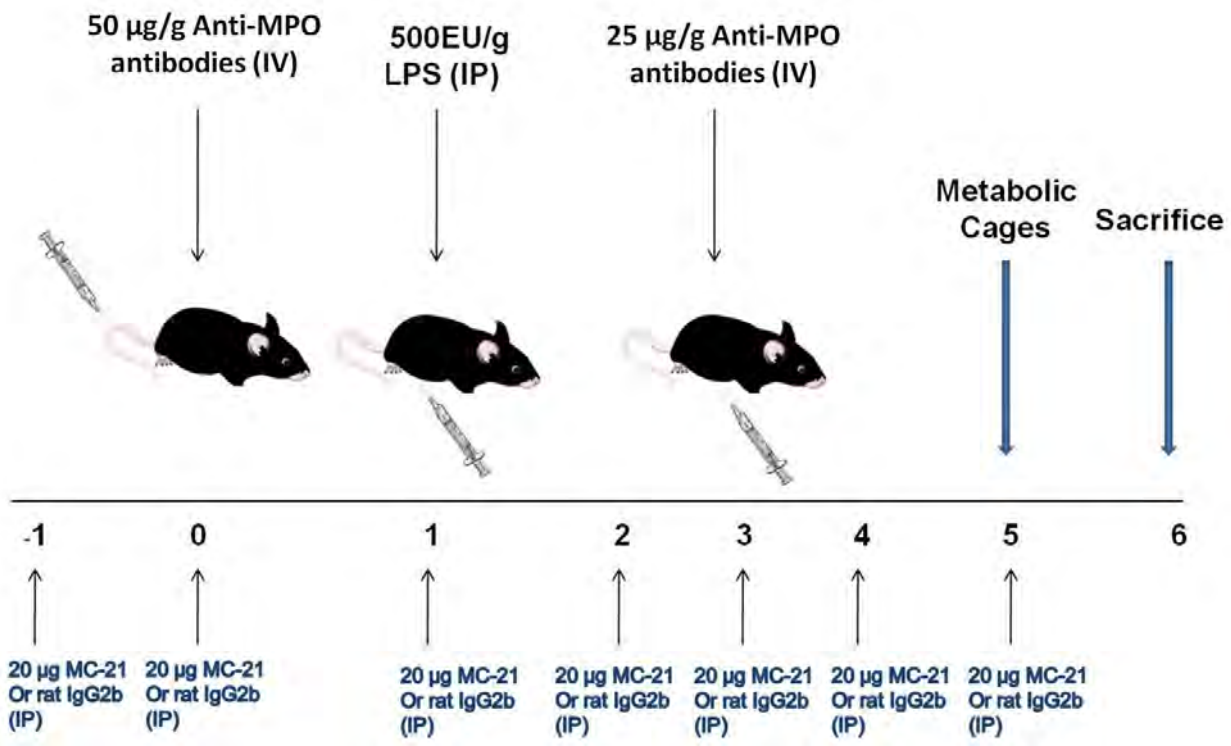

Figure 4.3: Experimental design for the monocyte depletion experiment. Monocytes were depleted in order to study their role in the induction of vasculitis. Mice were injected with 75 µg/g anti-MPO antibodies (n=8) and received 20 µg of either anti-mouse CCR2 (MC-21) or rat IgG2b from day -1 to day 5.

4.2.5. Monitoring monocyte depletion using flow cytometry

Blood was obtained from the mice treated with MC-21 to check for monocyte depletion, where 50µl of blood was taken on a daily basis by tail bleeding from all MC-21-treated mice (n=4), one mouse from the IgG2b-treated group and one untreated mouse. I stained for Ly-6G (GR1) and CD11b, which are expressed by monocytes that also express CCR2. The staining was performed as previously described in Chapter 2. The following antibodies were used: Alexa Fluor 647 anti-mouse Ly-6G (Gr1) (0.125µg), Alexa Fluor 488 anti-mouse CD11b (0.5µg), Alexa Fluor 647 rat IgG2b isotype control, and Alexa Fluor 488 rat IgG2b isotype control (eBioscience, UK).

Staining analysis

Immunohistochemical staining was analysed and quantified using Aequitas 1A software as described previously in Chapter 2. Briefly, the threshold of the grey scale was kept

constant and positive staining was expressed as a percentage of the image area (Balding, Howie et al. 2001).

.

4.3. Results

4.3.1. Macrophage phenotyping in AAV induced in mice

Macrophage infiltration into the injured kidney was investigated by IHC staining. Macrophages are identified by the CD68 marker and can be divided into classically activated (M1) or alternatively activated (M2) macrophages. M2 macrophages are identified by upregulation of the mannose receptor (CD206). I used serial sections to identify macrophage types as double staining was not possible. Positive CD68 staining was observed in the injured kidneys, with strong positive staining in the crescent region of the glomeruli (Figure 4.4, A, D, and J). The macrophages in the crescent region were most likely M1 macrophages as they did not express CD206, which is an M2 marker, as shown by the serial section staining (Figure 4.4). There was little or no staining of CD206+ cells in the glomeruli, but there was strong positive staining of CD206 on mesangial cells. On the other hand, MHC class II was found to be heavily expressed in the injured kidney and we also know that MHCII is upregulated in M1 macrophages but downregulated in M2 macrophages (Gordon and Taylor 2005). The MHCII marker was also expressed by other antigen presenting cells, which suggests the presence of other cells, such as dendritic cells (DCs), in the injured kidney. Positive staining of CD206 and MHCII was found in the control (anti-BSA treated) kidney sections (Figure 4.4, N and O).

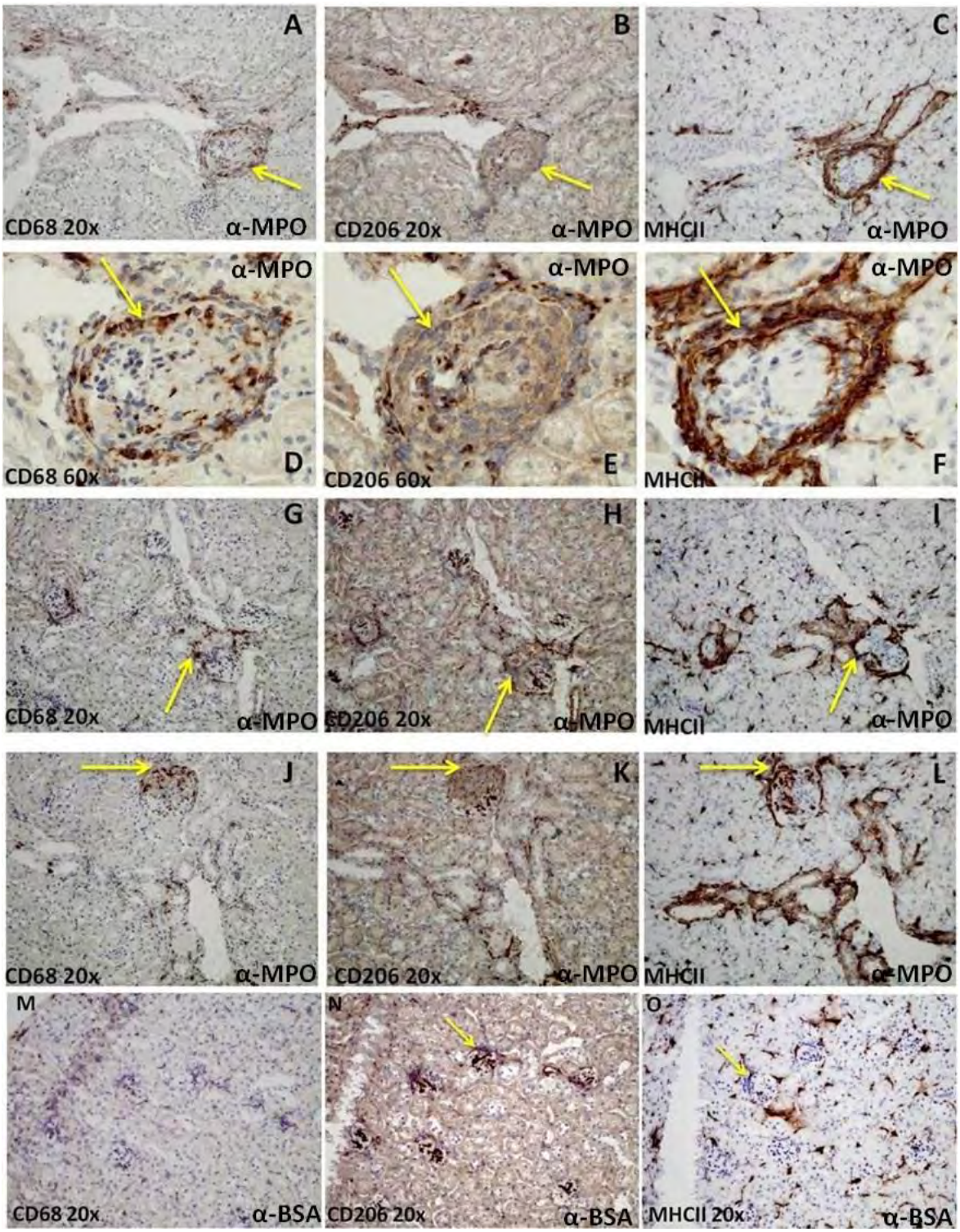

Figure 4.4: Immunohistochemical staining to identify the macrophage phenotype. Frozen kidney sections from mice treated with anti-MPO or anti-BSA antibodies and LPS. Each row represents serial sections of the same kidney and the same area stained for CD68, CD206, and MHCII. Arrows show the same area in each image in order to compare the staining. Sections M, N, and O are serial sections from mice injected with anti-BSA antibodies and stained with CD68, CD206, and MHCII, respectively.

Analysis of CD68, CD206, and MHCII staining

I analysed CD68 and CD206 staining in the kidney sections from anti-MPO and anti-BSA-treated mice. CD68-positive cells were found in the injured glomeruli and also in the interstitial region of the anti-MPO-treated mice. We found a significant difference between anti-MPO and anti-BSA-treated mice in the number of CD68-positive cells in both glomeruli and the interstitial compartment (figure 4.5 A and B). On the other hand, there was no significant difference between anti-MPO and anti-BSA in CD206 staining in the glomeruli, but there was a significant difference between them in the interstitial compartment (figure 4.5 C and D). This could be because mesangial cells in glomeruli have been reported to express CD206, and I found strong, positive staining of CD206 in mesangial cells. There was a strong positive staining of MHCII in anti-MPO treated mice (figure 4.6).

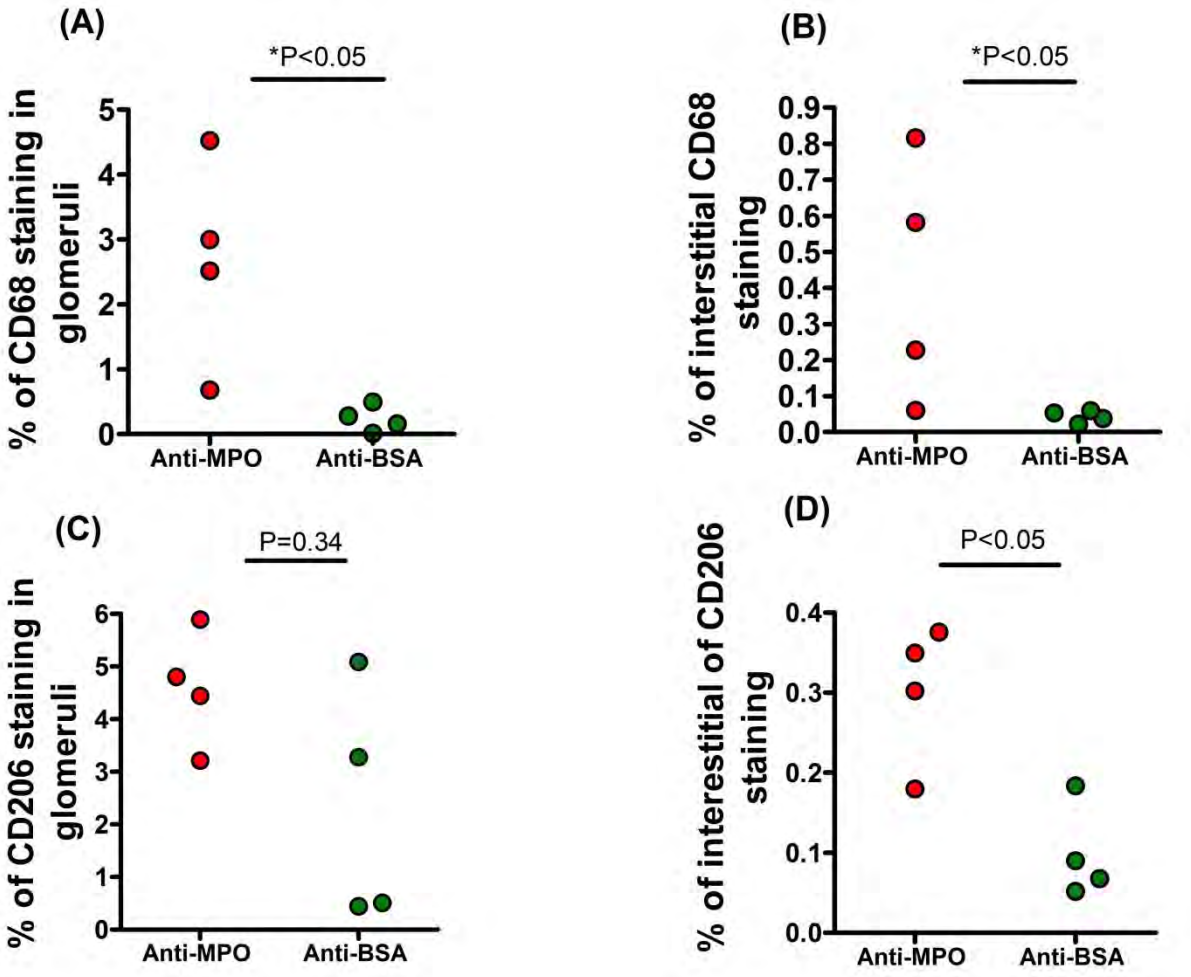

Figure 4.5: Staining analysis of CD68 and CD206. A significant difference was found between anti-MPO (n=4) and anti-BSA-treated (n=5) mice in the number of CD68-positive cells in both the glomeruli and interstitial compartments (A and B). Significant staining of CD206 only occurred in the interstitial compartment (D); t-test (Mann-Whitney test).

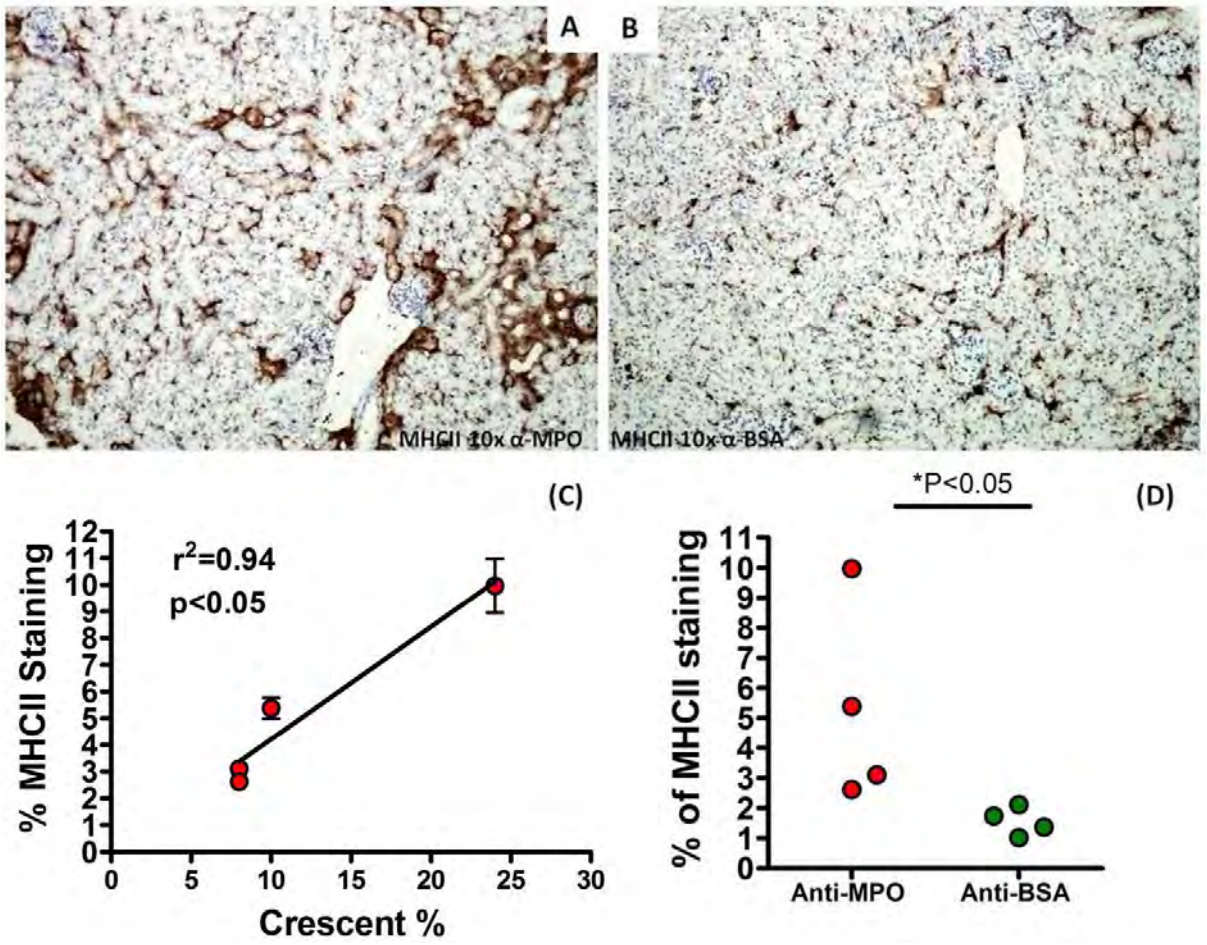

Figure 4.6: MHCII staining analysis. Kidney sections from α-MPO (A) and α-BSA (B)-treated mice with 1,500 EU/g of LPS. There was positive correlation between the percentage of MHCII staining and the crescent percentage (C) with r^2=0.85 and P<0.001, as measured by linear regression. A significant difference was found in MHCII staining between α-MPO and α-BSA-treated mice by measuring positive staining and taking the percentage of this staining to the whole area in the image. The t-test (Mann-Whitney test) was used for analysis (D).

4.3.2. Comparing the presence of other cell types to macrophages:

I investigated the presence of T cells and neutrophils using different markers and compared that to the presence of macrophages. There were very view CD4+ (T helper cells) and CD8+ (cytotoxic T cells and NK cells) cells (figure 4.7 D and C). In addition, there were almost no GR1+ cells (neutrophil) (figure 4.7 B) or CD3+ cell (mature T cells) (figure 4.7 E). Dectin-1 staining was also very low. However, there were a large number of macrophages in the kidney as shown by F4/80 staining (figure 4.7 A).

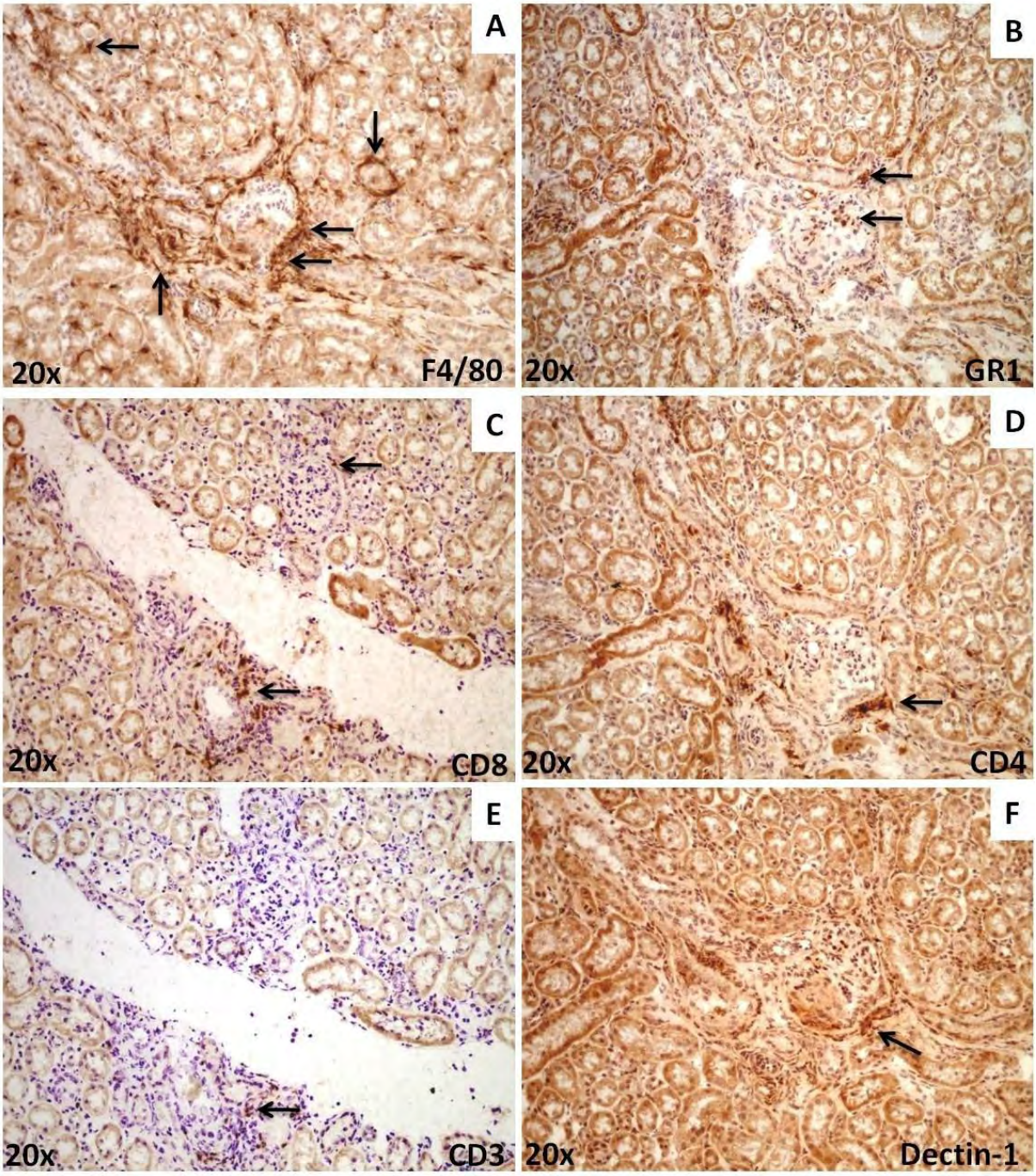

Figure 4.7: Immunohistochemistry results of different cell types in anti-MPO treated mice. These are serial section from mouse treated with anti-MPO antibodies. There were large number of F4/80+ macrophages in both glomeruli and tubules (A). There were very view CD8+ and CD4+ T cell (C and D). There were almost no CD3+ T cells or Gr1+ neutrophils (E and B).

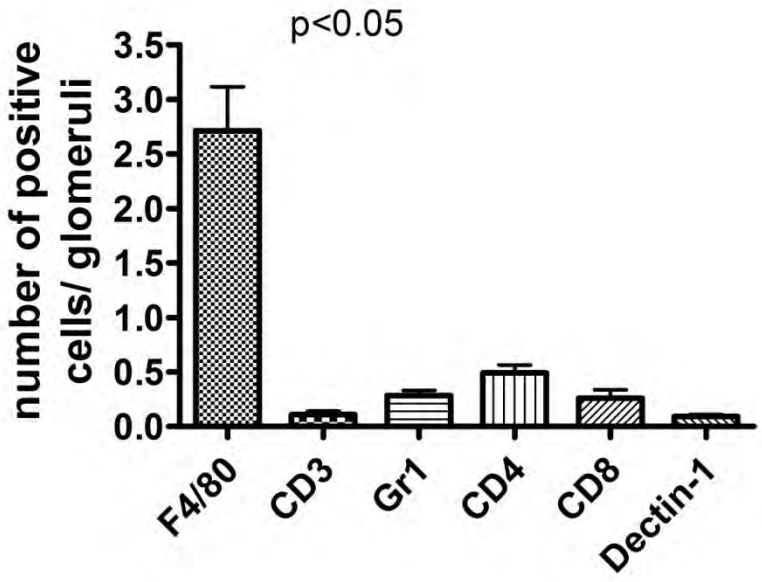

Figure 4.8: Staining analysis of different cells in the glomeruli. Manual count of positive staining in the glomeruli from anti-MPO treated mice. The dominating cells in both glomeruli and tubules were found to be F4/80+ macrophages. There were very few other cells. The p value represent the variation between groups (one way ANOVA).

4.3.3. Gene modulation in AAV in mice

One of the approaches that we used in an attempt to understand vasculitis was studying gene expression in kidney sections from anti-MPO-treated mice and comparing it to that in the tissues of anti-BSA-treated mice. A total of 400 glomeruli from anti-MPO and anti-BSA-treated mice and MPO and HSA-immunised rats was microdissected. This is a very difficult technique and required a lot of time and effort to microdissect the areas of interest without compromising RNA integrity.

RNA quality and quantity

Total RNA was extracted from laser microdissected tissues (Figure 4.9). I measured the quality and quantity of RNA using an Agilent bioanalyser (figure 4.10). All of the RNA samples used in this experiment had an RIN of 7 or above, which is considered good for microarray usage (table 4.3). The concentration of the RNA from microdissected glomeruli (from rats and mice) is shown in table 4.4.

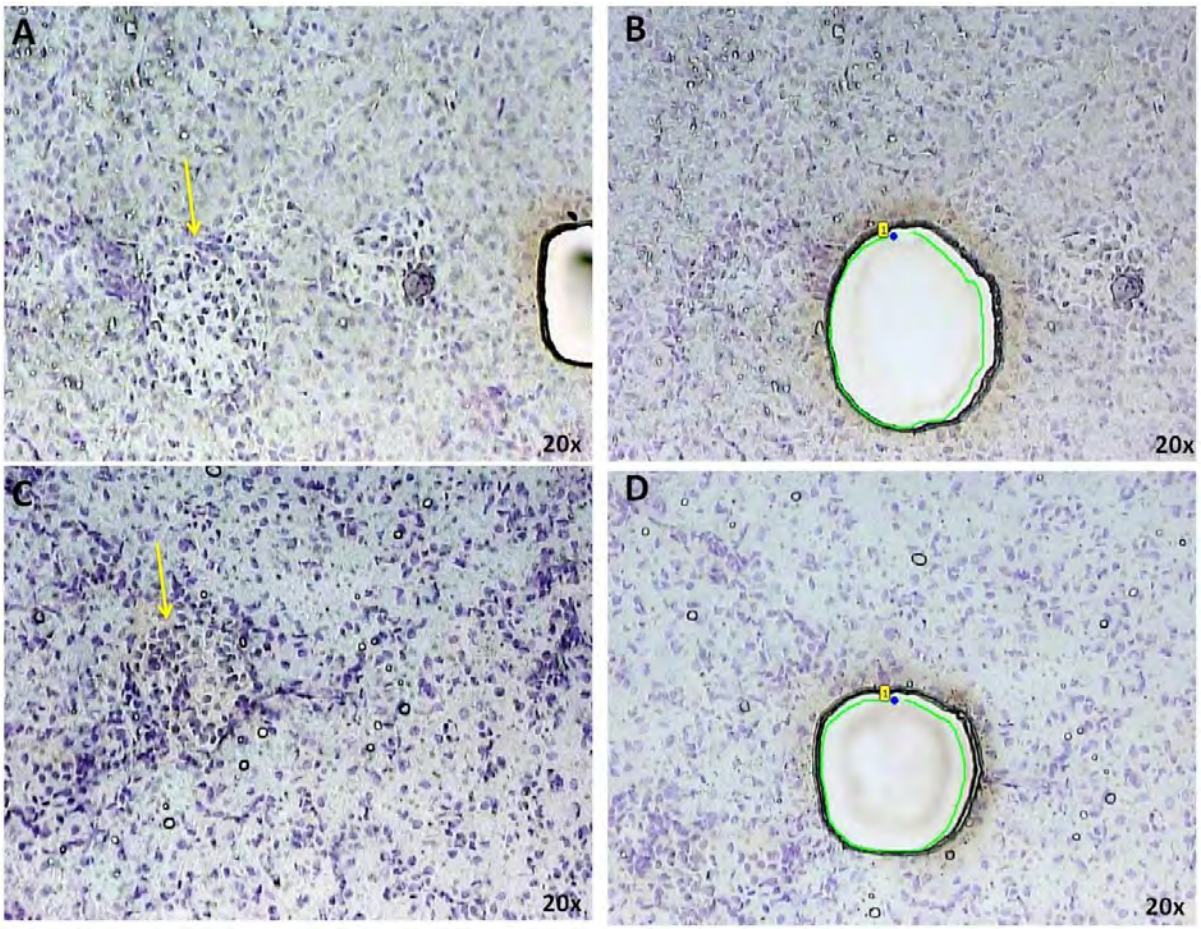

Figure 4.9: Laser microdissection. Glomeruli from rats (A) and mice (C) were microdissected. Kidney sections were prepared and stained with the cresyl violet stain for visualisation. (A) Rat section before cutting and (B) after cutting. (C) Mouse section before cutting and (D) after cutting.

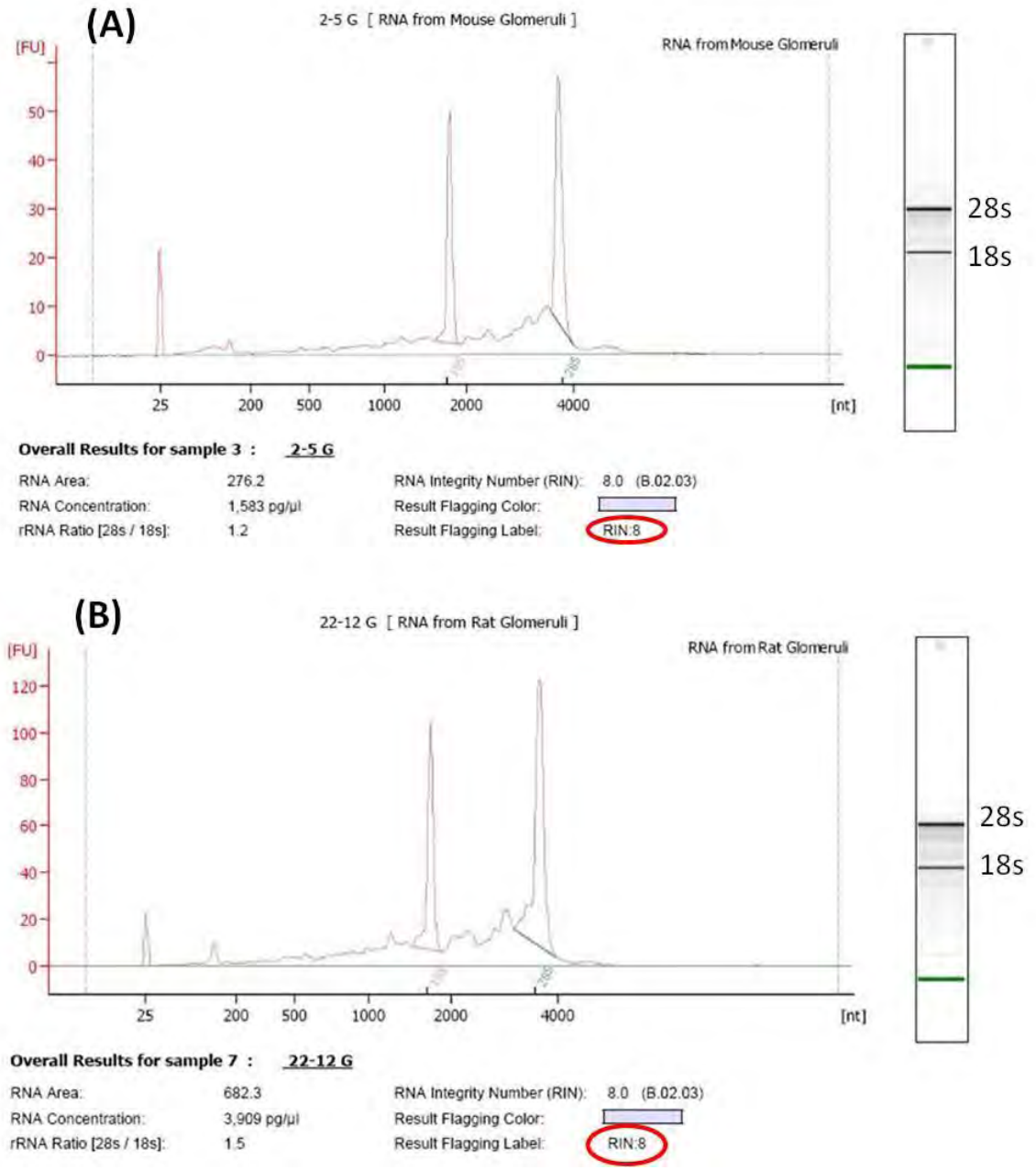

Figure 4.10: RNA quality and quantity. The RNA extracted from the microdissected glomeruli. A: The RNA from mouse glomeruli had clear bands at 28S and 18S with an RIN value of 8. B: The RNA from rat glomeruli had an RIN value of 8. The RNA fragments were separated by size, where the smaller fragments travelled faster. The software automatically compares unknown samples to ladder fragments in order to determine the concentration of unknown samples and to identify ribosomal RNA peaks. Two peaks and two bands are shown in each figure and they represent RNA fragments at 18S and 28S.

Table 4.3: RNA integrity number (RIN) for microdissected tissues from mouse and rat as measured by bioanalyser.

Mouse (α-MPO) RIN	Mouse (α-BSA) RIN	RAT (MPO-immunised) RIN	Rat (HSA-immunised) RIN
Glom	Glom	Glom	Glom
7.7	7.8	8.1	8.2
7.9	8.0	7.9	8.1
8.3	7.7	8.5	8.4
9.0	8.7	8.3	8.7
8.0	8.1	8.0	8.6

Table 4.4: RNA concentration of microdissected glomeruli.

Mouse (α-MPO) ng	Mouse (α-BSA) ng	RAT (MPO-immunised) ng	Rat (HSA-immunised) ng
Glom	Glom	Glom	Glom
16.02	32.60	46.48	27.19
42.93	14.31	89.18	51.48
20.67	20.65	45.85	21.54
6.74	8.05	52.84	40.81
18.99	17.96	46.91	31.23

Confirming the quality of the microdissections

The quality of the microdissections was investigated by looking at genes that are only expressed in the glomeruli or tubules. This was done to make sure that the microdissected glomeruli did not contain any tubules and vice versa. Nephrosis 1 (*Nphs1*) is one of the genes used to identify the quality and purity of microdissected glomeruli. The *Nphs1* gene is solely expressed in glomeruli and encodes a member of the immunoglobulin family of cell adhesion molecules that functions in the glomerular filtration barrier in the kidney. I found

that *Nphs1* was expressed in microdissected glomeruli but not in microdissected tubules in both the mouse (Figure 4.11, A) and rat (Figure 4.11, C), which confirms the purity of the microdissected glomeruli. On the other hand, the *Lrp2* gene encodes low-density lipoprotein-related protein 2 (*LRP2*) or megalin. This protein is solely found in tubules. I found that this gene was mainly expressed in microdissected tubules and less so microdissected glomeruli in both the mouse (Figure 4.11, B) and rat (Figure 4.11, D). However, there was some expression of *Lrp2* on the microdissected glomeruli because I microdissected a small area outside the glomeruli to avoid losing glomeruli, which resulted in contamination with of some tubules.

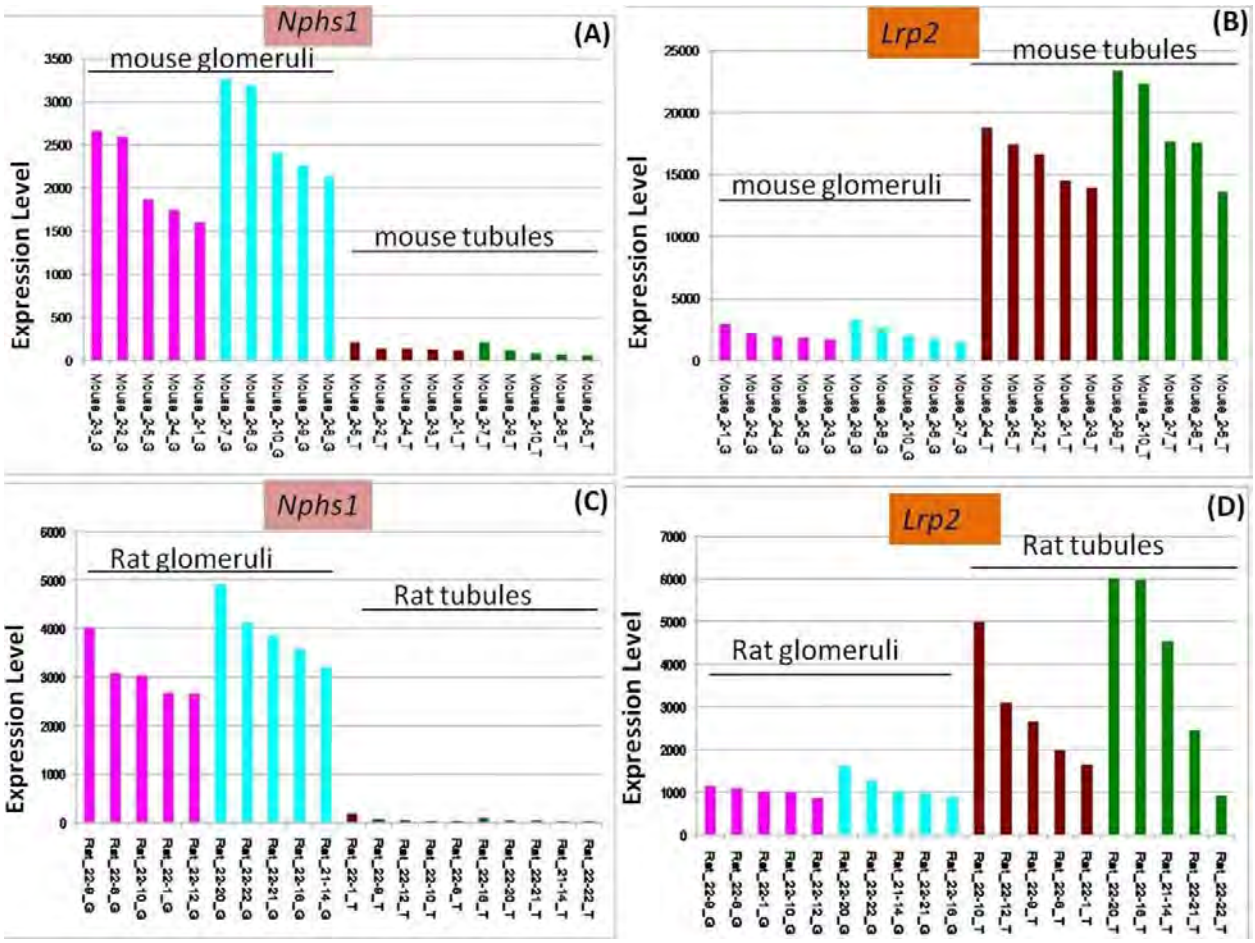

Figure 4.11: Confirming the quality and purity of the microdissections. Glomeruli and tubules were microdissected from rats and mice (control and diseased). The Nphs1 gene was used to identify the purity of the microdissected glomeruli. It was found to be expressed in microdissected glomeruli from the rat and mouse but not in microdissected tubules (A and C). The Lrp2 gene was used to identify the purity of microdissected tubules and was mainly found in the tubules of both the rat and mouse (B and D).

Analysis of microarray results

The microarray results were analysed using LIMMA software with the assistance of Dr. Wenbin Wei at the University of Birmingham. In order to eliminate any false results, we set the P value to 0.05, with at least two-fold changes between anti-MPO and anti-BSA groups. We identified 146 genes that were upregulated in mouse glomeruli and 139 genes that were upregulated in rat glomeruli (figure 4.12). I found 42 common genes that were upregulated in both the mouse and rat (Table 4.5). Some genes known to be biomarkers of kidney injury were upregulated. For example, lipocalin, which is also known as neutrophil gelatinase-associated lipocalin (*NGAL*), was found to be highly upregulated in mouse glomeruli with an 8.7-fold increase compared to and 3.7 in the rat model. In addition, Havcr1, which is also known as kidney injury molecule 1 (*Kim 1*), was highly upregulated in the mouse model with a 7.3-fold increase compared to 2.9 in the rat model. The Fibronectin 1 (Fn1) gene, which is associated with inflammation, was upregulated in both the rat and mouse with a 3.8-fold increase in the mouse and a 3.48-fold increase in the rat.

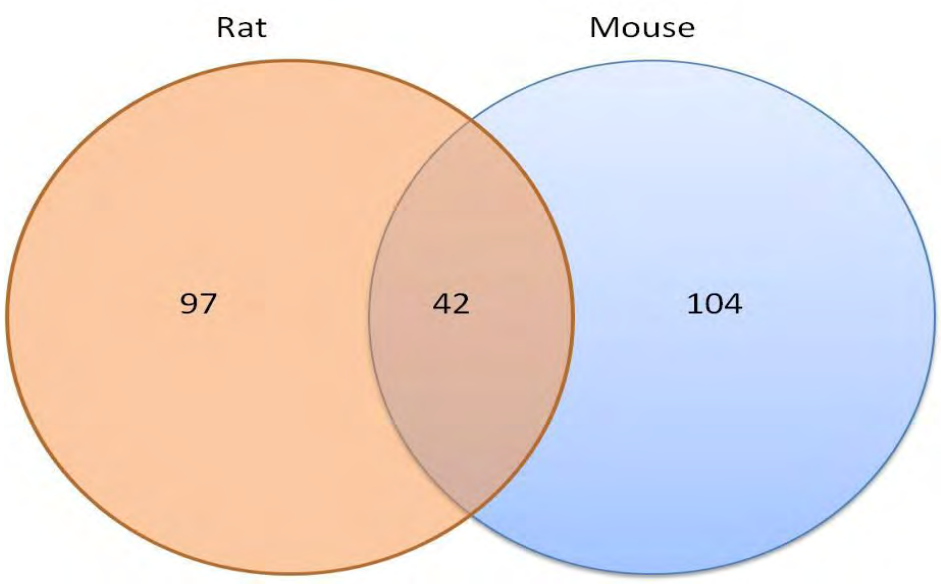

Figure 4.12: Common upregulated genes in both rat and mouse glomeruli. There were 139 genes upregulated in rat glomeruli and 146 genes upregulated in mouse glomeruli. There were 42 upregulated genes common to both the rat and mouse.

Table 4.5: Common upregulated genes in diseased mouse and rat glomeruli compared to the control groups of each species.

Mouse		Rat	
Gene	**Fold change**	**Gene**	**Fold change**
lipocalin 2, NGAL (LCN2)	8.7	lipocalin 2 (NGAL)	3.7
collagen, type III, alpha 1 (Col3a1)	4.9	collagen, type III, alpha 1 (Col3a1)	6.3
fibronectin 1	3.8	fibronectin 1	3.5
CD44 antigen	3.3	CD44 molecule	2.0
complement component 1, q subcomponent, alpha polypeptide (C1qa)	3.3	complement component 1, q subcomponent, A chain (C1qa)	2.9
complement component 1, q subcomponent, C chain (C1qc)	3.0	complement component 1, q subcomponent, C chain (C1qc)	2.2
early growth response 2 (Egr2)	2.9	early growth response 2 (Egr2)	2.5
C-type lectin domain family 7, member a (Clec7a)	2.8	C-type lectin domain family 7, member a (Clec7a)	3.4
Interleukin-33 (IL-33)	2.8	Interleukin-33 (IL-33)	2.3
B-cell leukaemia/lymphoma 2-related protein A1a (Bcl2a1a /// Bcl2a1b /// Bcl2a1d)	2.7	B-cell leukaemia/lymphoma 2-related protein A1d (Bcl2a1d)	2.0
collagen, type I, alpha 1 (Col1a1)	2.7	collagen, type I, alpha 1 (Col1a1)	2.5
histocompatibility 2, class II antigen A, alpha (H2-Aa)	2.6	RT1 class II, locus Ba (RT1-Ba)	2.6
membrane-spanning 4-domains, subfamily A, member 6D (Ms4a6d)	2.6	membrane-spanning 4-domains, subfamily A, member 11 (Ms4a11)	3.6
histocompatibility 2, class II antigen A, beta 1 (H2-Ab1)	2.6	RT1 class II, locus Bb (RT1-Bb)	2.6
Lysosomal-associated protein transmembrane 5 (Laptm5)	2.6	lysosomal-associated protein transmembrane 5 (Laptm5)	2.3
membrane-spanning 4-domains, subfamily A, member 6B (Ms4a6b)	2.5	membrane-spanning 4-domains, subfamily A, member 6B (Ms4a6b)	2.2
histocompatibility 2, class II antigen E beta (H2-Eb1)	2.4	RT1 class II, locus Db1 (RT1-Db1)	2.6
lectin, galactose binding, soluble 3 (Lgals3)	2.4	lectin, galactoside-binding, soluble, 3 (Lgals3)	3.6
serine (or cysteine) peptidase inhibitor,	2.3	serine (or cysteine) peptidase inhibitor,	3.9

clade E, member 1 (Serpine1)		clade E, member 1 (Serpine1)	
CD74 antigen (invariant polypeptide of major histocompatibility complex, class II antigen-associated) (CD74)	2.3	Cd74 molecule, major histocompatibility complex, class II invariant chain (CD74)	2.7
lysozyme 2 (Lyz2)	2.3	lysozyme 2 (Lyz2)	2.4
CD68 antigen (CD68)	2.2	CD68 molecule (CD68)	2.0
cathepsin S (Ctss)	2.2	cathepsin S (Ctss)	2.1
allograft inflammatory factor 1 (Aif1)	2.1	allograft inflammatory factor 1 (Aif1)	3.0
secreted phosphoprotein 1 (Spp1)	2.1	secreted phosphoprotein 1 (Spp1)	5.8
hepatitis A virus cellular receptor 1 (Havcr1)	2.0	hepatitis A virus cellular receptor 1 (Havcr1)	2.9
collagen, type VI, alpha 1 (Col6a1)	2.0	collagen, type VI, alpha 1 (Col6a1)	2.5
EGF-like module containing, mucin-like, hormone receptor-like sequence 1 (Emr1)	2.0	EGF-like module containing, mucin-like, hormone receptor-like 1 (Emr1)	2.3
coronin, actin binding protein 1A (Coro1a)	2.0	coronin, actin binding protein 1A (Coro1a)	2.1
ecotropic viral integration site 2a (Evi2a)	2.0	ecotropic viral integration site 2A (Evi2a)	2.1

Organising the genes according to their biological processes

I also studied the upregulated genes in tubules of the diseased mouse and rat compared to the control groups. I organised upregulated genes in mouse glomeruli according to their biological processes. I also included the upregulated genes in the glomeruli that were common to both the mouse and rat and also the upregulated genes in mouse tubules compared to the control. Some of the genes that were upregulated in mouse glomeruli are involved in macrophage activation, such as *Aif1*, *Col3a1*, *Col1a2,* and *Cd209a*. For example, *Aif1* is related to the inflammatory status of macrophages and it is also involved in the migration, survival, and pro-inflammatory properties of macrophages (Yang, Ho et al. 2005). Other genes were found to be involved in complement activation, as shown in Table 4.6. In addition, some of the genes identified are involved in antigen processing and presentation,

such as the MHCII gene. Furthermore, some of the genes found are related to cell adhesion, such as *CD44*, *Fn1*, *Havcr1*, *CD48,* and *CD209a*. We also identified genes that are involved in cell surface receptor-linked signal transduction, such as *CX3CR1*, *CCR2*, *CCL9,* and *Fn1*.

Table 4.6. Grouping of the upregulated genes according to their biological processes. The genes that were upregulated in mouse glomeruli and mouse tubules, and also the upregulated genes common to both mouse and rat glomeruli, were divided into different groups according to their biological processes.

Biological process	Diseased mouse vs. control (glomeruli)	Common to both mouse and rat G (glomeruli)
Macrophage activation	Collagen alpha-1(III) chain **(Col3a1)**, Collagen alpha-1(I) chain **(Col1a1)**, C-type lectin domain family 6 member A **(Clec6a)**, **Cxcl5**, Allograft inflammatory factor 1 **(Aif1)**, **Cxcl2** M1, Collagen alpha-1(VI) chain **(Col6a1)**, CD209 antigen-like protein A **(Cd209a)**, Arachidonate 5-lipoxygenase-activating protein **(Alox5ap)**, EGF-like module-containing mucin-like hormone receptor-like 1 **(Emr1)** **F4/80**M1/M2, Collagen alpha-2(I) chain **(Col1a2)**, CXCl9, Protein S100-A9 **(S100a9)** M1 Protein S100-A8 **(S100a8)** M1	Collagen alpha-1(III) chain **(Col3a1)**, Collagen alpha-1(I) chain **(Col1a1)**, Allograft inflammatory factor 1 **(Aif1)**, Collagen alpha-1(VI) chain **(Col6a1)**, EGF-like module-containing mucin-like hormone receptor-like 1 **(Emr1)**,
Complement activation	Complement C1q subcomponent subunit C **(C1qc)**, Collagen alpha-1(III) chain **(Col3a1)**, Complement C1q subcomponent subunit A **(C1qa)**, Collagen alpha-1(I) chain **(Col1a1)**, Collagen alpha-1(VI) chain **(Col6a1)**, Collagen alpha-2(I) chain **(Col1a2)**, Haptoglobin beta chain **(HP)**, Complement factor I light chain **(Cfi)**, Complement C1q subcomponent subunit B **(C1qb)**,	Complement C1q subcomponent subunit C **(C1qc)**, Collagen alpha-1(III) chain **(Col3a1)**, Complement C1q subcomponent subunit A **(C1qa)**, Collagen alpha-1(I) chain **(Col1a1)**, Collagen alpha-1(VI) chain **(Col6a1)**,
Cell Adhesion	Collagen alpha-1(III) chain **(Col3a1)**, Complement C1q subcomponent subunit C **(C1qc)**, C-type lectin domain family 7 member A (**Clec7a)**, CD44 antigen **(CD44)**, Hepatitis A virus cellular receptor 1 homolog **(Havcr1)**, Complement C1q subcomponent subunit A **(C1qa)**, Dipeptidyl-peptidase 1 light chain **(Ctsc)**, Cadherin-11 **(Cdh11)**, Collagen alpha-1(I) chain **(Col1a1)**, C-type lectin domain family 6 member	Collagen alpha-1(III) chain **(Col3a1)**, CD44 antigen **(CD44)**, Complement C1q subcomponent subunit C **(C1qc)**, C-type lectin domain family 7 member A **(Clec7a)**, Complement C1q subcomponent subunit A **(C1qa)**, Hepatitis A virus cellular receptor 1 homolog **(Havcr1)**, Collagen alpha-1(I) chain **(Col1a1)**, Fibronectin **(Fn1)**, Collagen alpha-1(VI) chain **(Col6a1)**, Cathepsin S **(Ctss)**, EGF-like module-containing mucin-like hormone receptor-like 1 **(Emr1)**, Sphingosine-1-phosphate phosphatase 1 **(Spp1)**, Galectin-3 **(Lgals3)**, Leucocyte

	A **(Clec4n)**, Collagen alpha-1(VI) chain **(Col6a1)**, Fibronectin **(Fn1)**, CD209 antigen-like protein A **(CD209a)**, Cathepsin S **(Ctss)**, CD48 antigen **(CD48)**, EGF-like module-containing mucin-like hormone receptor-like 1 **(Emr1)**, Collagen alpha-2(I) chain **(Col1a2)**, Sphingosine-1-phosphate phosphatase 1 **(Spp1)**, Galectin-3 **(Lgals3)**, Leucocyte common antigen **(Ptprc)**, Osteopontin **(Spp1)**, Fibrinogen gamma chain **(Fgg)**, Leucine-rich repeat LGI family member 2 **(Lgi2)**, Complement C1q subcomponent subunit B **(C1qb)**,	common antigen **(Ptprc)**,
Antigen processing and presentation	H-2 class II histocompatibility antigen, E-B beta chain **(H2-Eb1)**, H-2 class II histocompatibility antigen gamma chain **(CD74)**, Allograft inflammatory factor 1 **(Aif1)**, Cathepsin S **(Ctss)**, H-2 class II histocompatibility antigen, A-B alpha chain **(H2-Aa)**, H-2 class II histocompatibility antigen, A beta chain **(H2-Ab1)**,	H-2 class II histocompatibility antigen, E-B beta chain **(H2-Eb1)**, H-2 class II histocompatibility antigen gamma chain **(CD74)**, Allograft inflammatory factor 1 **(Aif1)**, Cathepsin S **(Ctss)**, H-2 class II histocompatibility antigen, A-B alpha chain **(H2-Aa)**, H-2 class II histocompatibility antigen, A beta chain **(H2-Ab1)**,
Cell surface receptor signal transduction	Membrane-spanning 4-domains subfamily A member 6D **(Ms4a6d)**, Mast cell surface glycoprotein Gp49A **(Gp49a)**, CX3C chemokine receptor 1 (**Cx3cr1)**, Hepatitis A virus cellular receptor 1 homologue **(Havcr1)**, CCL9 (31-101) **(CCL9)**, Ras-related protein Rab-32 **(Rab32)**, Cadherin-11 **(Cdh11)**, C-type lectin domain family 6 member A **(Clec4n)**, GCP-2(9-78) **(CxCl5)**, C-X-C chemokine receptor type 4 **(Cxcr4)**, Allograft inflammatory factor 1 **(Aif1)**, C-X-C motif chemokine 2 **(Cxcl2)**, Fibronectin **(Fn1)**, CD209 antigen-like protein A **(CD209a)**, CD48 antigen **(CD48)**, C3a anaphylatoxin chemotactic receptor **(C3ar1)**, EGF-like module-containing mucin-like hormone receptor-like 1 **(Emr1)**, Forkhead box protein I1 **(Foxi1)**, Leucocyte common antigen **(Ptprc)**, C-C chemokine receptor type 2 **(Ccr2)**, Leucine-rich repeat LGI family member 2 **(Lgi2)**,	Membrane-spanning 4-domains subfamily A member 6D **(Ms4a6d)**, Hepatitis A virus cellular receptor 1 homologue **(Havcr1)**, Allograft inflammatory factor 1 (Aif1), Fibronectin **(Fn1)**, EGF-like module-containing mucin-like hormone receptor-like 1 **(Emr1)**, Leucocyte common antigen **(Ptprc)**, Membrane-spanning 4-domains subfamily A member 6B **(Ms4a6b)**, Regulator of G-protein signalling 10 **(Rgs10)**,

	C-X-C motif chemokine 9 **(Cxcl9)**, Olfactomedin-4 **(Olfm4)**, Membrane-spanning 4-domains subfamily A member 6B **(Ms4a6b)**, Regulator of G-protein signalling 10 **(Rgs10)**, Suppressor of cytokine signalling 2 **(Socs2)**	

Gene organisation in the different pathways

These upregulated genes are involved in different pathways, as shown in Figure 4.13. Five genes were found to be related to T-cell activation: *CD74*, *H2-Aa*, *H2-DMa*, *H2-DMb1,* and *Vav1*. Furthermore, genes such as *Eif2s1*, *Aif1,* and *Bcl2a1a* are involved in the apoptosis signalling pathway. In addition, genes that are involved in inflammation mediated by the chemokine and cytokine signalling pathways include *Cxcr1*, *Ilf1f6*, *C3ar1*, *CCR2,* and *Vav1*. Also, *Fn1* and *Col3a1* are involved in the integrin signalling pathway.

Table 4.7: Grouping of the upregulated genes according to different pathways. Upregulated genes in mouse glomeruli and mouse tubules and the upregulated genes common to both mouse and rat glomeruli were divided into their different biological pathways.

Pathway	Diseased mouse vs. control (glomeruli)	Common to both mouse and rat (glomeruli)
Inflammation mediated by chemokine and cytokine signalling pathways	**Cx3cr1**, **Cxcr4**, Prostaglandin G/H synthase 2 **(ptgs2)**, **Col6a1**, **C3ar1**, Arachidonate 5-lipoxygenase-activating protein **(Alox5ap)**, **Ccr2**	**Col6a1**
Integrin signalling pathway	Collagen alpha-1(III) chain **(Col3a1)**, Collagen alpha-1(I) chain **(Col1a1)**, Fibronectin **(fn1)**, Collagen alpha-1(VI) chain **(Col6a1)**, Collagen alpha-2(I) chain **(Col1a2)**	Collagen alpha-1(III) chain **(Col3a1)**, Collagen alpha-1(I) chain **(Col1a1)**, Fibronectin **(fn1)**, Collagen alpha-1(VI) chain **(Col6a1)**
T-cell activation	H-2 class II histocompatibility antigen gamma chain **(CD74)**, H-2 class II histocompatibility antigen, A-B alpha chain **(H2-Aa)**, Leucocyte common antigen **(Ptprc)**	H-2 class II histocompatibility antigen gamma chain **(CD74)**, H-2 class II histocompatibility antigen, A-B alpha chain **(H2-Aa)**, Leucocyte common antigen **(Ptprc)**
Blood coagulation	Plasminogen activator inhibitor 1 **(Serpine1)**, Fibrinogen gamma chain **(Fgg)**	Plasminogen activator inhibitor 1 **(Serpine1)**
Apoptosis signalling pathway	Allograft inflammatory factor 1 **(Aif1)**, Bcl-2-related protein A1 **(Bcl2a1a)**	Allograft inflammatory factor 1 **(Aif1)**, Bcl-2-related protein A1 **(Bcl2a1a)**

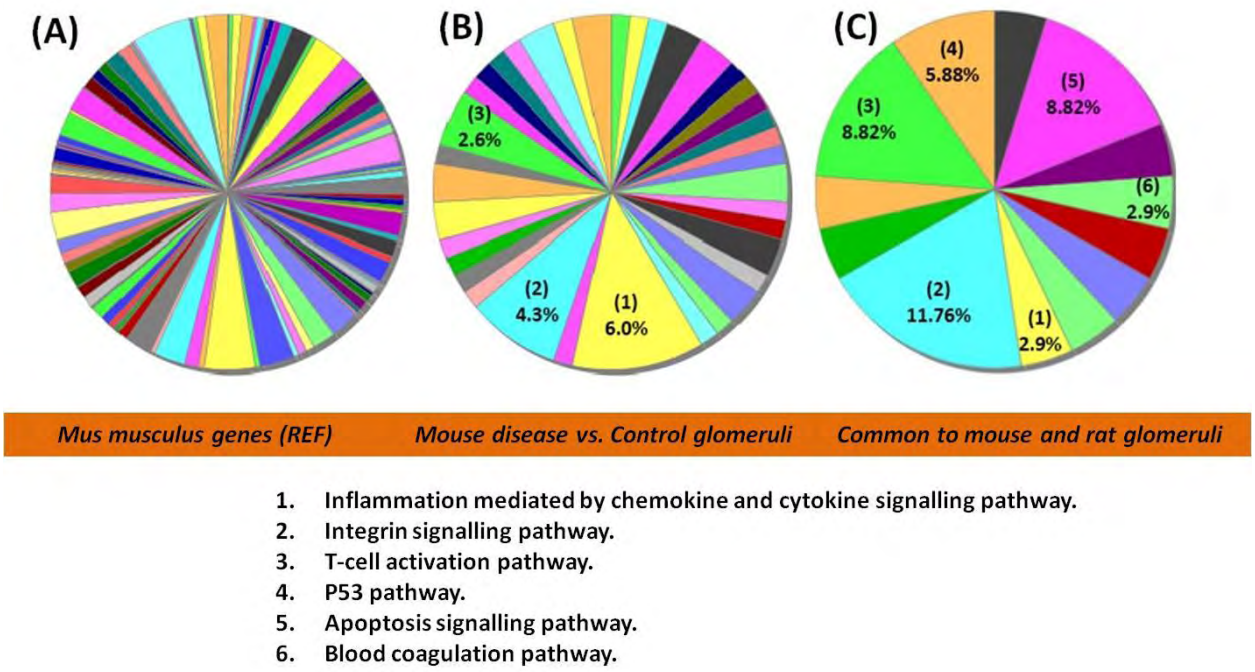

Figure 4.13: Pathway analysis. Upregulated genes in mouse glomeruli (B), mouse tubules (D), and upregulated genes common to both mouse and rat glomeruli (C) were sorted according to their different biological pathways. (A) The whole mouse genome divided into different pathways.

Genes associated with macrophage activation and recruitment

I found several upregulated genes that were associated with the trafficking and activation of macrophages. One of these genes was *CCR2*, which encodes the monocyte chemoattractant protein 1 (MCP-1) receptor. In addition, *CX3CR1*, a receptor of fractalkine, was upregulated in the mouse glomeruli and is known to be involved in macrophage recruitment. Furthermore, genes that are associated with macrophage activation such as *CXCL2*, which is also known as macrophage inflammatory protein 2-alpha, were upregulated. Some of these genes were associated with classically activated macrophages such as calprotectin (*S100a8* and *S100a9*) and *CxCl2*. Furthermore, genes known to be macrophage markers, such as *CD68* and EGF-like module-containing mucin-like hormone receptor-like 1(*Emr1*), which is also known as *F4/80* in the mouse, were also upregulated.

Genes common to the mouse, rat and humans

I compared the upregulated genes in mouse and rat glomeruli to those found in human glomeruli (human results obtained from ERCB, Dr. Clemens Cohen) (table 4.8). Again,

genes associated with macrophage accumulation in the kidney, such as *CD68* (a macrophage marker) and *EMR1* (also known as F4/80), were upregulated. Some of the other genes that were upregulated are part of the complement pathway, such as *C1qa* and *C1qc*.

Table 4.8: Upregulated genes common to mouse, rat and human glomeruli compared to the control glomeruli in each species.

Mouse gene symbol	Mouse gene title	Mouse P value	Mouse fold change	Rat gene symbol	Rat P value	Rat fold change	Human gene symbol
Lcn2	lipocalin 2	8.779E-05	8.705	Lcn2	5.49E-05	3.708	LCN2
Col3a1	collagen, type III, alpha 1	1.513E-04	4.898	Col3a1	3.81E-05	6.278	COL3A1
Fn1	fibronectin 1	1.143E-04	3.852	Fn1	1.37E-04	3.484	FN1
Cd44	CD44 antigen	1.078E-03	3.344	Cd44	6.97E-03	2.052	CD44
C1qa	complement component 1, q subcomponent, alpha polypeptide	2.666E-04	3.273	C1qa	1.01E-04	2.904	C1QA
C1qc	complement component 1, q subcomponent, C chain	2.253E-04	3.005	C1qc	6.92E-04	2.243	C1QC
Col3a1	collagen, type III, alpha 1	5.355E-05	2.963	Col3a1	3.81E-05	6.278	COL3A1
Egr2	early growth response 2	2.666E-03	2.880	Egr2	1.22E-03	2.499	EGR2
Clec7a	C-type lectin domain family 7, member a	1.350E-03	2.844	Clec7a	2.10E-04	3.415	CLEC7A
Il33	interleukin 33	2.391E-03	2.777	Il33	1.18E-03	2.269	IL33
Bcl2a1a /// Bcl2a1b /// Bcl2a1d	B-cell leukaemia/lymphoma 2-related protein A1a /// B-cell leukaemia/lymphoma 2-related protein A1b /// B-cell leukaemia/lymphoma 2-related protein A1d	3.244E-04	2.670	Bcl2a1d	3.20E-04	2.025	BCL2A1
Col1a1	collagen, type I, alpha 1	2.238E-03	2.662	Col1a1	5.23E-03	2.472	COL1A1
Col1a1	collagen, type I, alpha 1	2.238E-03	2.662	Col1a1	1.05E-02	2.160	COL1A1
H2-Aa	histocompatibility	3.425E-	2.636	RT1-Ba	2.89E-	2.651	HLA-

	2, class II antigen A, alpha	04			05		DQA1
Ms4a6d	membrane-spanning 4-domains, subfamily A, member 6D	6.743E-04	2.614	Ms4a11	4.79E-04	3.613	MS4A6A
H2-Ab1	histocompatibility 2, class II antigen A, beta 1	2.247E-03	2.585	RT1-Bb	3.61E-05	2.565	HLA-DQB1
Laptm5	lysosomal-associated protein transmembrane 5	1.543E-03	2.582	Laptm5	2.68E-04	2.304	LAPTM5
Egr2	early growth response 2	4.321E-03	2.557	Egr2	1.22E-03	2.499	EGR2
Ms4a6b	membrane-spanning 4-domains, subfamily A, member 6B	6.256E-05	2.495	Ms4a6b	2.84E-03	2.210	MS4A6A
H2-Ab1	histocompatibility 2, class II antigen A, beta 1	2.871E-04	2.475	RT1-Bb	3.61E-05	2.565	HLA-DQB1
H2-Eb1	histocompatibility 2, class II antigen E beta	9.155E-05	2.422	RT1-Db1	4.20E-04	2.580	HLA-DRB1
H2-Eb1	histocompatibility 2, class II antigen E beta	9.155E-05	2.422	RT1-Db1	3.60E-05	2.477	HLA-DRB1
Lgals3	lectin, galactose binding, soluble 3	2.540E-03	2.388	Lgals3	1.86E-04	3.623	LGALS3
Serpine1	serine (or cysteine) peptidase inhibitor, clade E, member 1	2.585E-03	2.323	Serpine1	1.07E-03	3.979	SERPINE1
Serpine1	serine (or cysteine) peptidase inhibitor, clade E, member 1	2.585E-03	2.323	Serpine1	5.91E-03	2.396	SERPINE1
Cd74	CD74 antigen (invariant polypeptide of major histocompatibility complex, class II antigen-associated)	2.342E-04	2.305	Cd74	7.14E-05	2.720	CD74
Lyz2	lysozyme 2	8.180E-04	2.272	Lyz2	8.90E-05	2.425	LYZ
Cd68	CD68 antigen	2.657E-02	2.247	Cd68	1.89E-02	2.080	CD68
H2-Ab1	histocompatibility 2, class II antigen A, beta 1	1.296E-04	2.243	RT1-Bb	3.61E-05	2.565	HLA-DQB1
Ctss	cathepsin S	1.415E-04	2.242	Ctss	1.36E-03	2.174	CTSS

Aif1	allograft inflammatory factor 1	8.242E-04	2.178	Aif1	2.41E-04	3.002	AIF1
Rgs10	regulator of G-protein signalling 10	3.649E-03	2.172	Rgs10	1.03E-05	2.933	RGS10
Spp1	secreted phosphoprotein 1	3.153E-03	2.129	Spp1	1.83E-06	5.812	SPP1
H2-Aa	histocompatibility 2, class II antigen A, alpha	1.585E-04	2.128	RT1-Ba	2.89E-05	2.651	HLA-DQA1
Lyz1	lysozyme 1	1.527E-03	2.096	Lyz2	8.90E-05	2.425	LYZ
Havcr1	hepatitis A virus cellular receptor 1	1.498E-02	2.087	Havcr1	7.88E-06	2.928	HAVCR1
Col6a1	collagen, type VI, alpha 1	6.592E-03	2.080	Col6a1	4.29E-05	2.537	no human homolog
Emr1	EGF-like module containing, mucin-like, hormone receptor-like sequence 1	3.499E-03	2.065	Emr1	2.86E-04	2.254	EMR1
Coro1a	coronin, actin binding protein 1A	2.929E-03	2.031	Coro1a	2.45E-04	2.186	CORO1A
Coro1a	coronin, actin binding protein 1A	4.238E-03	2.030	Coro1a	2.45E-04	2.186	CORO1A
Evi2a	ecotropic viral integration site 2a	2.183E-03	2.028	Evi2a	4.02E-03	2.102	EVI2A
Ptprc	protein tyrosine phosphatase, receptor type, C	2.157E-02	2.006	Ptprc	9.26E-04	2.132	PTPRC
Ptprc	protein tyrosine phosphatase, receptor type, C	2.157E-02	2.006	Ptprc	4.39E-03	2.039	PTPRC

4.3.4. The effect of liposomal clodronate on passively transferred antibodies

When I first started, I planned to use liposomal clodronate to deplete macrophages. However, we observed an effect on the level of passively transferred antibodies in clodronate-treated mice in the first pilot experiment. Clodronate and saline-treated mice received equal amounts of anti-MPO antibodies (100 µg/g) but the level of anti-MPO antibodies detected in clodronate-treated mice was significantly less than in saline-treated mice (Figure 4.14, A). This meant that, for some reason, some of the antibodies that were injected into the clodronate-treated mice were lost.

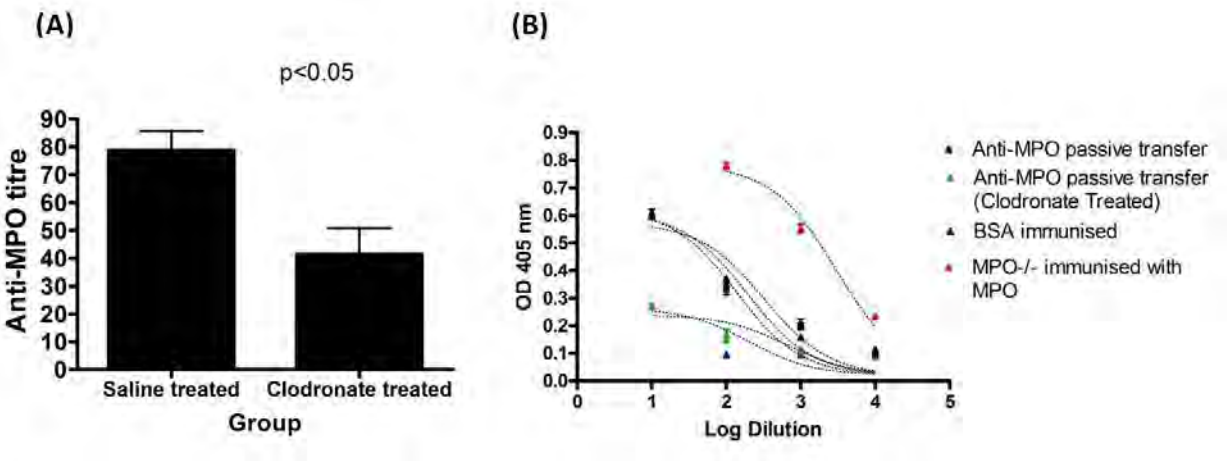

Figure 4.14: Anti-MPO antibodies in clodronate and saline-treated mice. A: A significant difference was found in the level of anti-MPO antibodies between clodronate and saline-treated mice (unpaired t-test). B: Dilution curve to calculate the anti-MPO antibody titre, which was EC_{50}=71-92 in saline-treated mice and EC_{50}=31-50 in clodronate-treated mice.

4.3.5. CD68 immunohistochemistry on mouse paraffin sections

Immunohistochemical staining for CD68 was used to check for the presence of macrophages in the liver, lung, kidney, and spleen in all of the mice that were used in the pilot MEV experiment. Macrophages were not seen in the kidney sections from either saline or clodronate-treated groups, which is consistent with the mild histological phenotype described above (Figure 4.15, C and D). In addition, the liver and lung sections from both groups were similar when analysed under the microscope after CD68 staining. On the other hand, there was a marked decrease in macrophages in spleen sections from clodronate-treated mice (Figure 4.15, B) compared to spleen sections from saline-treated mice (Figure 4.15, A). There were more stained cells in the control spleen sections.

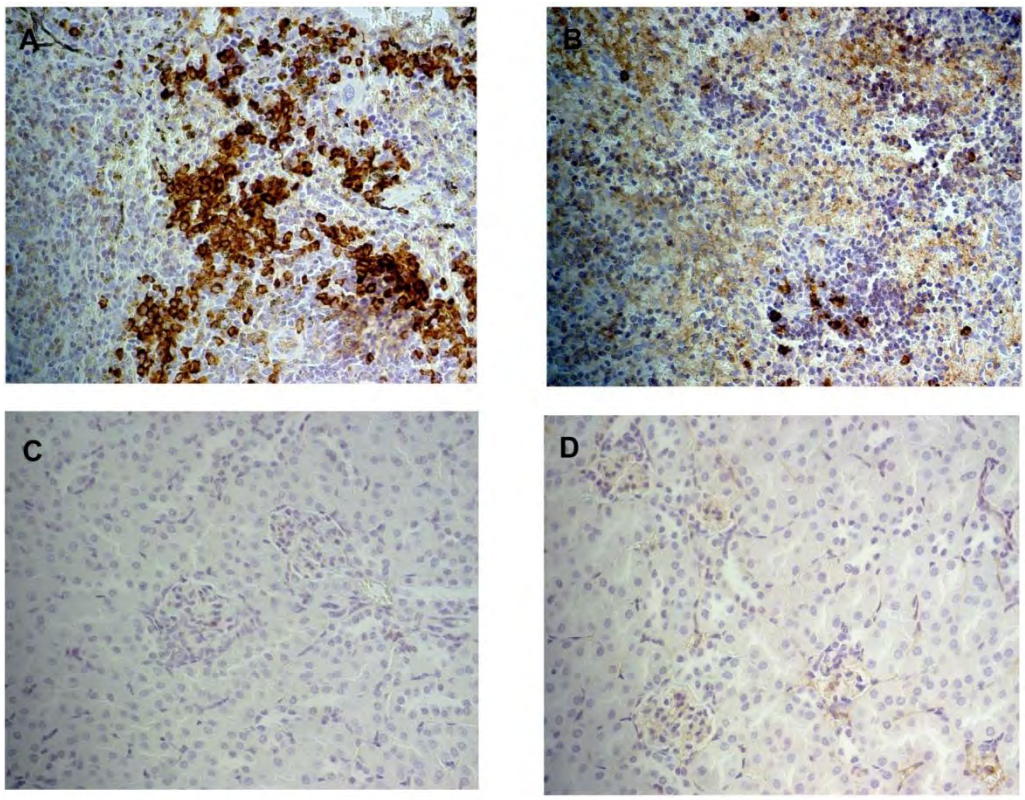

Figure 4.15: CD68 staining in mouse paraffin sections. The stained cells in these sections are macrophages. Some of these sections were treated with clodronate to deplete macrophages and staining was performed to see how effective clodronate was in depleting them. Staining was also performed to determine whether or not macrophages were present in the kidney after treating these mice with the anti-MPO antibody. A: spleen section from saline-treated mouse; B: spleen section from clodronate-treated mouse; C: kidney section from saline-treated mouse; D: kidney section from clodronate-treated mouse.

4.3.6. Depletion of macrophages using anti-mouse CCR2

Although clodronate was effective in depleting macrophages (as shown by IHC staining in the spleen), it had a negative effect on passively transferred antibodies for reasons that were not clear. As a result, I decided to use another method to deplete the macrophages: an anti-mouse CCR2 (MC-21) antibody. It was very effective in depleting blood monocytes that expressed CCR2. These cells were also Gr1+CD11b+ monocytes, as shown by flow cytometry. These blood monocytes differentiate into classically activated macrophages in the tissue and also into Tip-DCs (TNF/iNOS-producing cells), as mentioned above. The CCR2 marker was upregulated in mouse glomeruli, as shown by the Affymetrix array. Monocyte depletion was monitored throughout the experiment to make sure that the number of these cells stayed low (Figure 4.16, B). As a result, the number of Gr1+CD11b+ monocytes was

kept low throughout the experiment compared to mice from the control group (IgG2b treated) and untreated mice.

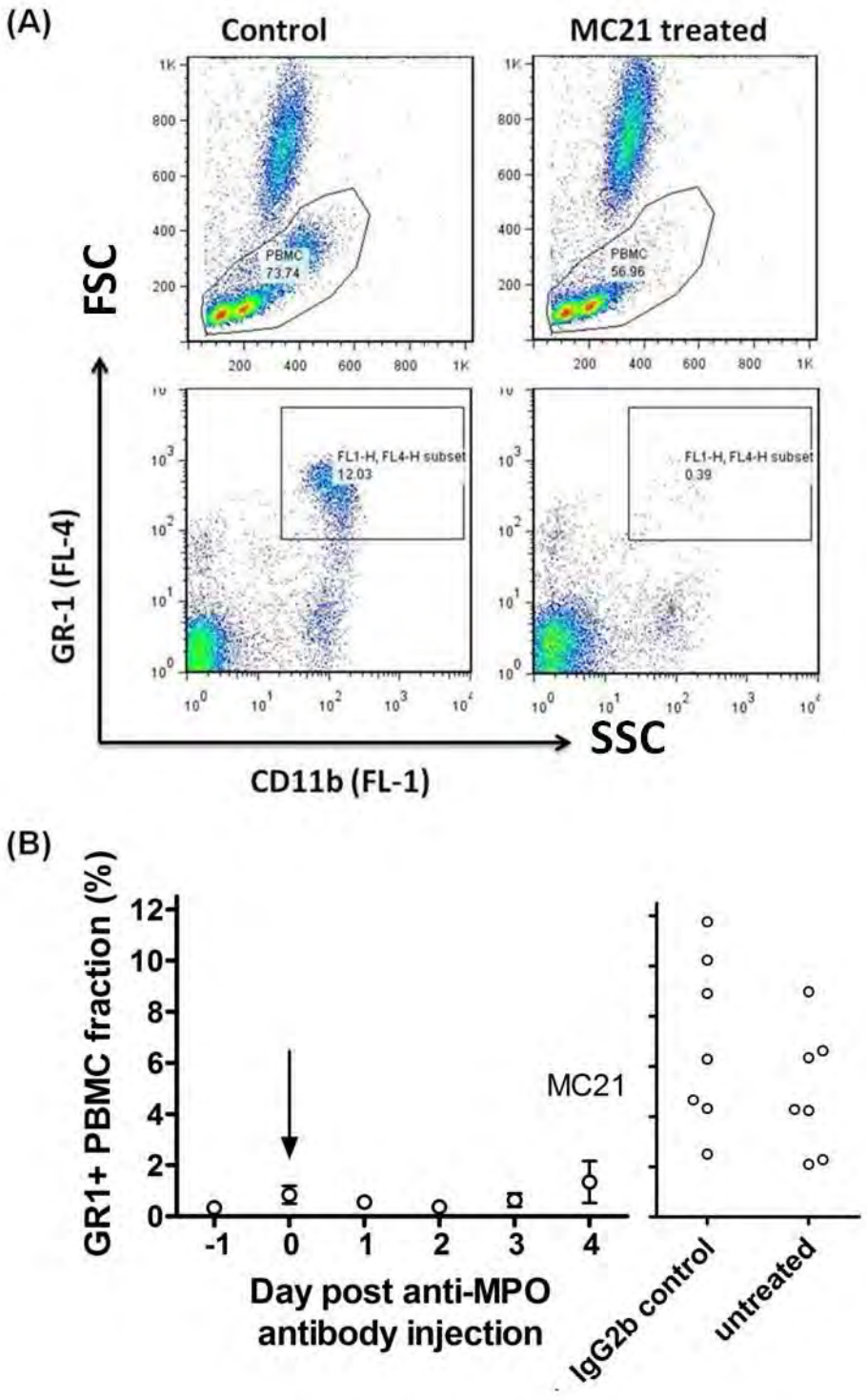

Figure 4.16: Monocyte depletion. The GR1+CD11b+ monocytes were depleted using 20 µg of anti-mouse CCR2. There was big reduction in the number of GR1+ monocytes on day 0 in the MC-21-treated mouse compared to the IgG2b-treated mouse, as shown by FACS analysis (A). Monocytes were monitored throughout the experiment and the number of these cells remained low in MC-21-treated mice (n=4) compared to IgG2b (n=4)-treated and untreated mice (B).

Induction of AAV in MC-21 and IgG2b-treated mice

These mice were injected with 75 µg/g of anti-MPO antibodies and urine was collected to assess the disease status. Urine was collected on days 1 and 6. All mice had haematuria on day 6, which was between +1 and +4 (Figure 4.17, A). In addition, no significant difference was found between the MC-21 and IgG2b-treated mice in terms of the albumin/creatinine ratio (Figure 4.17, B).

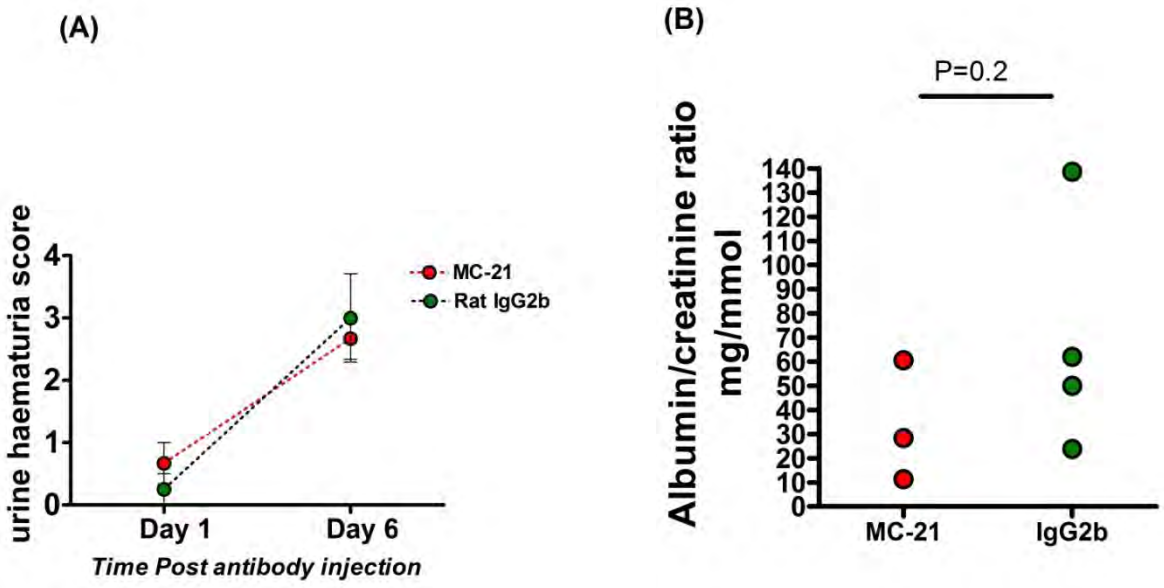

Figure 4.17: Urine analysis in the monocyte depletion experiment. The mice were negative for haematuria on day 1 and they had all developed urine haematuria by day 6 (A). The urine was collected from three MC-21-treated mice for technical reasons. No significant difference was found in the albumin/creatinine ratio (B); t-test (Mann-Whitney test).

Histological analysis

Histological sections were prepared in order to assess the disease in these mice. Kidney sections were used for the analysis and were stained with H&E or PAS. Mice from both groups (MC-21(figure 4.18 A and C) and IgG2b (figure 4.18 B) treated) had crescents, indicating a severe form of disease. However, no significant difference was found between MC-21 and IgG2b-treated mice in terms of the percentage of crescents (figure 4.18 D).

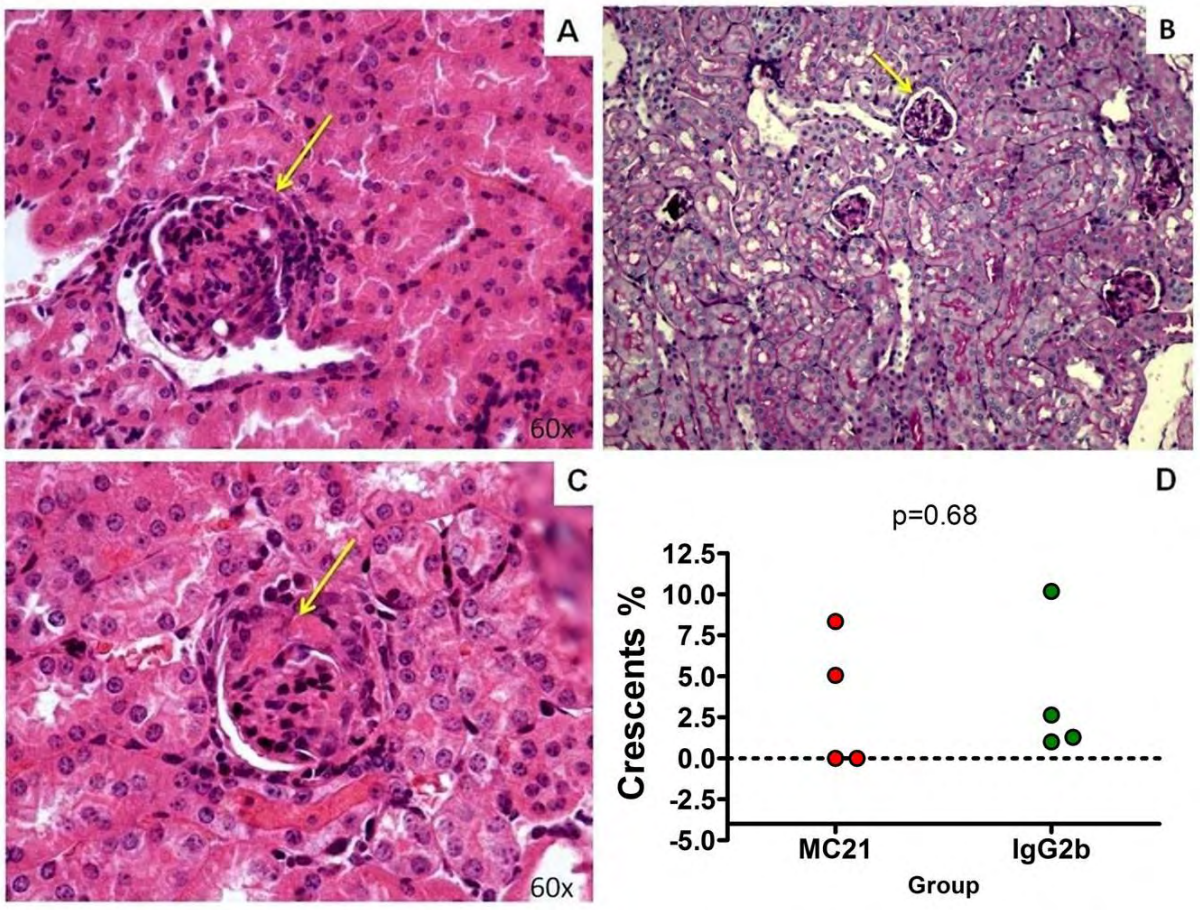

Figure 4.18: Histological analysis of the monocyte depletion experiment. Mice from both groups (MC-21 and IgG2b treated) developed crescents and necrosis (A and C). The arrows show crescents and necrosis in the glomeruli. No significant difference was found in the severity of the disease (estimated by the number of crescents), P=0.68 (D) using a t-test (Mann-Whitney test) analysis.

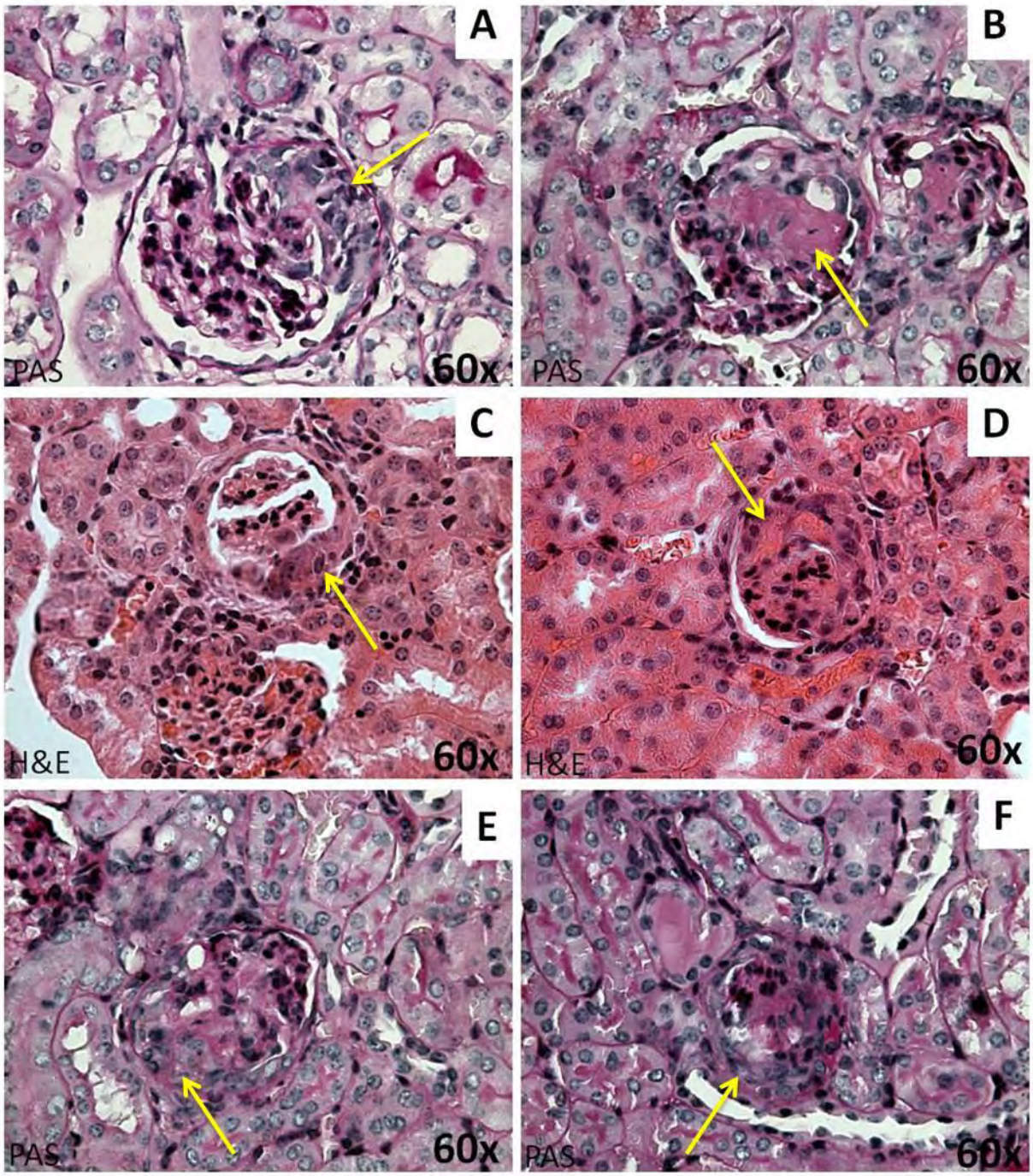

Figure 4.19: Histological sections from the anti-mouse CCR2 antibody experiment. Mice received 75 µg/g anti-MPO antibodies and 1,500 EU/g of LPS. They were treated with MC-21(F) or IgG2b (A, B, C, D, E). Mice from both groups developed crescents and necrosis. The arrows represent crescents and necrosis.

Immunohistochemical staining

The GR1+CD11b+ monocytes were depleted from the blood using anti-mouse CCR2, but CD68 staining in the frozen mouse sections showed the presence of some macrophages in

the kidney on day 6. Macrophages were detected in both IgG2b-treated (Figure 4.20, A and B) and MC-21-treated mice (Figure 4.20, D), and no significant difference was found in the total number of CD68-stained macrophages in the kidney between the two groups (Figure 4.20, D). This means that these macrophages could be resident macrophages or that some monocytes were still able to infiltrate to the kidney after anti-mouse CCR2 antibody treatment.

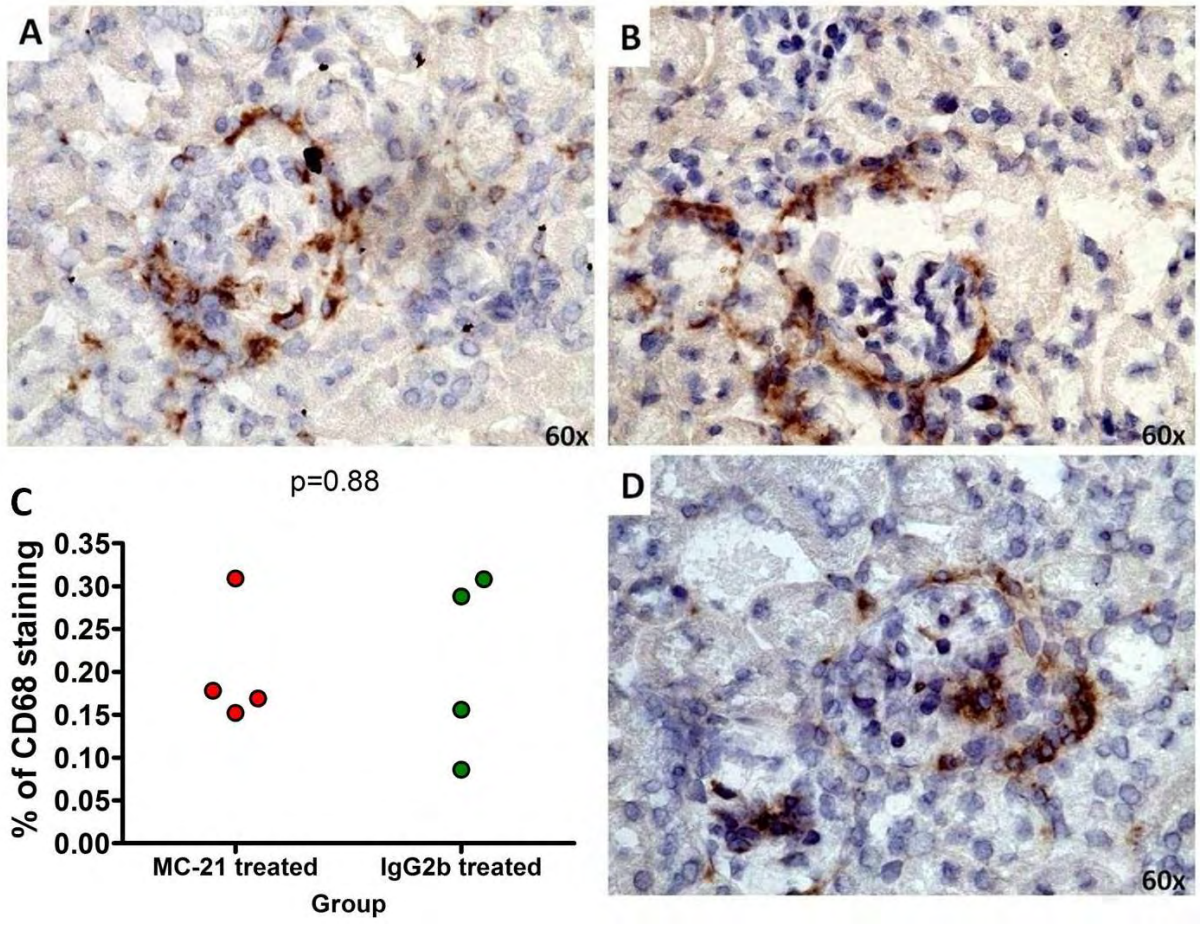

Figure 4.20: CD68 staining in the macrophage depletion experiment. Kidney sections from mice treated with MC-21 or IgG2b were stained for CD68. Macrophages were found in both MC-21 (D) and IgG2b (A and B)-treated mice. The number of macrophages is very low compared to the previous experiment. No significant difference in the total number of CD68-positive cells was found between the two groups (C); t-test (Mann-Whitney test) analysis.

4.4. Discussion

In this chapter, I studied different methods of depleting macrophages and the effect of this depletion on the development of vasculitis in mice. Although clodronate was effective in depleting macrophages, it also had a negative effect on the passively transferred antibodies. As a result, we used anti-mouse CCR2 to deplete the blood monocytes and we found no significant differences between MC-21 and IgG2b-treated mice in the percentage of crescents. We investigated the macrophage phenotype in anti-MPO and anti-BSA-treated mice. The staining of serial sections from the kidney showed different staining patterns for CD206 (M2 macrophage marker) and CD68. I concluded that the macrophages found in the crescents were M1 macrophages. In addition, I studied gene expression in the glomeruli and tubules from anti-MPO-treated mice compared to gene expression in anti-BSA-treated mice (in rats and mice). I found 146 genes that were upregulated in mouse glomeruli and 139 genes upregulated in rat glomeruli. I found 42 genes common to both rats and mice, including lipocalin-2 and hepatitis A virus cellular receptor 1, among others.

In order to understand the role of macrophages in the development of AAV, I investigated the phenotype of macrophages in anti-MPO-treated mice and compared it to those from anti-BSA treated-mice in both glomeruli and tubules. I found macrophages in the crescent areas of the glomeruli, as shown by CD68 staining. These cells did not express the mannose receptor, as shown by CD206 staining on serial kidney sections, although Chavele et al. (Chavele, Martinez-Pomares et al. 2010) showed the importance of the mannose receptor in the induction of crescentic glomerulonephritis in mice. They showed that animals were protected from the development of glomerulonephritis in mannose receptor-knockout mice (nephrotoxic nephritis model). They concluded that, through the mannose receptor (MR), mesangial cells underwent increased apoptosis and macrophages had diminished Fc-mediated function. They also concluded that FcR and MR could interact through binding to nephrotoxic globulin. In addition, macrophages from Mr-/- mice showed an anti-inflammatory

phenotype after ingesting apoptotic mesangial cells. I discovered that CD206 macrophages were either not found in the crescents or were found in small numbers, but I also found that CD206 is expressed by mesangial cells. I showed that most of the CD68-positive cells in the ANCA-associated vasculitis model did not express the mannose receptor and we concluded that these were M1 macrophages. We think that M1 macrophages are more involved in the development of vasculitis in mice than M2 macrophages. Macrophages show a variety of phenotypes (Gordon 2003), and it could be that these alternatively activated macrophages were different in our model to those in their model (Chavele, Martinez-Pomares et al. 2010). Another explanation could be that these M2 macrophages are important and are involved in the development of the disease by switching from M2 to M1-type macrophages. Another explanation could be that other factors or cells are affected by the absence of the mannose receptor and these could be involved in the development of the disease.

We know that the innate immune system is important for the initiation and amplification of inflammatory responses. This led me to further investigate the role of the innate immune system in ANCA-associated vasculitis by looking at the gene expression in animal models of vasculitis. We found genes that were upregulated in mouse and rat glomeruli compared to glomeruli from control animals. I found that some these genes are involved in complement activation. The importance of complement in renal disease has been reported in different studies. Brooimans et al reported the ability of proximal tubular epithelial cells from human kidny to synthesis complement (Brooimans, Stegmann et al. 1991). Xiao et al. showed the involvement of complement in the development of ANCA-associated vasculitis in mice (Xiao, Schreiber et al. 2007). They showed that the alternative complement pathway, rather than the classical pathway, was involved in development of the disease. In our study, complement components such as C1qa and C1qc were highly upregulated in both mice and rats, which suggests the involvement of a classical complement pathway. However, complement factor I (Cfi) was also upregulated in mice, and this complement component inhibits and regulates the formation of C3 convertase in all complement pathways. This

suggests the absence of complement involvement in our model. It could be that complement is only involved in the early stages of the disease, which is why C5 and factor B-knockout mice were protected.

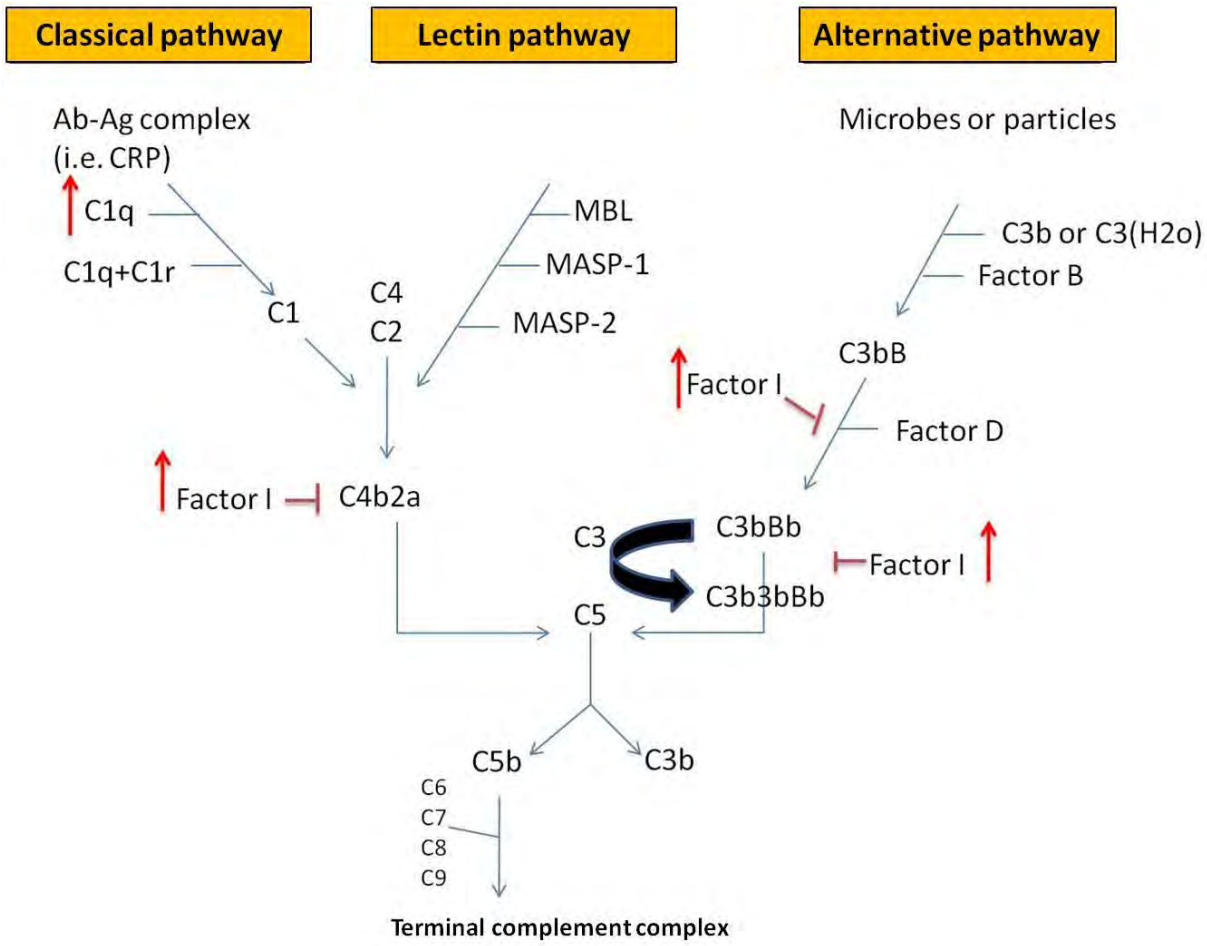

Figure 4.21: Complement pathways. There were some upregulated genes in the mouse glomeruli that were involved in complement activation, such as C1q, which is part of the classical complement pathway. However, there was an upregulation of complement factor I, which inhibits and regulates the formation of C3 convertase. The red arrows show the upregulated genes in mouse glomeruli.

In addition, I found that some of these upregulated genes were involved in macrophage activation. As a result, I wanted to investigate whether these genes would confirm my work on macrophage phenotyping. The upregulated genes in mouse glomeruli that were involved in macrophage activation included protein S100-A8 and protein S100-A9. These two proteins formed a complex called calprotectin. Fujiu et al. showed the ability of kruppel-like factor-5 (KLF5) to induce the expression of S100a8 and S100a9 in a unilateral ureteral obstruction model (Fujiu, Manabe et al. 2011). They showed the involvement of these

proteins in the recruitment of Ly6C+ inflammatory monocytes and then triggered the differentiation of these cells to M1-type macrophages. These cells were shown to accumulate in the kidney on days 1-4, at time when S100a8 and S100a9 expression peaked. This confirms the involvement of M1 macrophages in kidney injury and supports my macrophage phenotype work and the decision to deplete Ly6C+ monocytes to halt the disease. Fujiu et al. were able to recruit adaptively transferred Ly6C+ monocytes to the kidney following S100a8/a9 injection. Furthermore, there was an upregulation of chemokine receptors involved in monocyte and macrophage infiltration and accumulation. One of these receptors was CCR2, which is found on GR1+ monocytes that mature into inflammatory macrophages and dendritic cells in tissue (Auffray, Sieweke et al. 2009). This supports my hypothesis, which suggests that blocking CCR2 could be beneficial in preventing disease development.

I believe that macrophages are involved in renal vasculitis and that they are an important part of the development of this disease because large numbers of macrophages infiltrating the kidney have been reported in ANCA-associated vasculitis (Weidner, Carl et al. 2004; Xiao, Heeringa et al. 2005). In addition, macrophage depletion in other types of crescentic glomerulonephritis have provided protection against the disease. Over the years, many studies have been performed to investigate the cells involved in ANCA-associated vasculitis. I performed a pilot experiment to deplete macrophages from WT mice that were injected with anti-MPO antibody in order to assess the utility of liposomal clodronate in this approach. Clodronate has previously been used as a strategy to deplete macrophages and to study the function of macrophages *in vivo* (Van Rooijen and Sanders 1994). My results did not provide sufficient evidence to show that macrophages were important in the development of vasculitis because the disease was mild. Then, CD68 staining was performed on paraffin-fixed sections to investigate the presence of macrophages in the kidney and, specifically, in glomeruli. A few macrophages were detected by immunohistochemical staining in a saline-treated kidney, but they were only seen in tubules; this could have been because the

disease was very mild. Only one mouse showed crescents, in <1% of the glomeruli. However, my results showed that clodronate was very effective in depleting macrophages in the spleen. Claassen et al. showed that liposome-encapsulated clodronate was effective in depleting macrophages both *in vivo* and *in vitro* (Claassen I, Van Rooijen N et al. 1990). My results and the results of previous studies show that liposomal clodronate is effective in depleting macrophages, and I believe it is an important tool for studying the function of macrophages in glomerulonephritis in mice.

However, fewer anti-MPO antibodies were detected in the serum of mice that received clodronate compared to mice in the control group. All of these mice received similar amounts of anti-MPO antibodies, which suggests that they should have had the same level of anti-MPO antibodies in their serum. According to these results, I suggested that clodronate may have had an effect on the passively transferred antibodies. This effect could have been caused by macrophages engulfing clodronate and the antibodies as well. For this reason, I decided to investigate different methods of depleting macrophages and to determine whether previous studies performed using clodronate on antibody-induced disease were affected by this finding, or whether it was just specific to ANCA IgG. Huang et al. used liposomal clodronate to deplete macrophages in anti-GBM glomerulonephritis in rats (Huang, Tipping et al. 1997). They also used anti-T-cell antibodies and found that they reduced macrophage infiltration. They showed that the level of the anti-GBM antibody was not affected in rats when anti-T-cell antibodies were used, but they did not show the level of anti-GBM when the mice were treated with clodronate. There are other examples in the literature where clodronate was used. Cittera et al. showed a beneficial effect of the inhibition of rituximab on tumours following clodronate treatment. They suggested an important role of macrophages in rituximab treatment, but they were not able to observe any increase in the number of macrophages following treatment with rituximab (Cittera, Leidi et al. 2007). One would expect to see an increase in the number of macrophages following rituximab treatment if they were important. What I wanted to demonstrate by listing these studies on

clodronate is that it is very important to measure the level of passively transferred antibodies following clodronate treatment. We believe that this effect of clodronate on passively transferred antibodies should be investigated further.

Because clodronate had a negative effect on passively transferred antibodies, I decided to use anti-mouse CCR2 (MC-21) to deplete macrophages. The expression of CCR2 was upregulated in microdissected glomeruli from anti-MPO-treated mice. It was found that MC-21 depleted Gr1+CD11b+ blood monocytes and that this depletion was maintained throughout the experiment by injecting mice with 20 µg of MC-21 daily. GR1+ blood monocytes differentiate into tissue inflammatory macrophages, so these experiments should help answer the question as to the role of macrophages recruited from the circulation in acute vasculitic glomerulonephritis. I found that both MC-21 and IgG2b-treated mice developed crescents and that there was no significant difference between the two groups in terms of the percentage of crescents. All the mice had haematuria by day 6. Our results showed the development of crescents in mice even though we also showed a complete depletion of blood monocytes. One explanation is that tissue macrophages, rather than infiltrating monocytes, were involved in the pathogenesis of vasculitis. On the other hand, Furuichi et al. showed a reduction in acute tubular necrosis and interstitial cell infiltration in ischaemia-reperfusion injury following anti-mouse CCR2 treatment and also in CCR2-deficient mice (Furuichi, Wada et al. 2003). The difference between these two sets of results could be due to the macrophage phenotype that was still present in the kidney after depletion. In addition, these were different diseases induced by different methods. I could investigate this further by depleting resident macrophages in mice that express the diphtheria toxin receptor. This would allow me to determine the role of macrophages in ANCA-associated vasculitis. Finally, the form of disease in this experiment was mild, which limited my ability to draw definitive conclusions. Unfortunately, a sufficient amount of MC-21 was not available to repeat the experiment, and insufficient amounts of anti-MPO antibodies were available.

Chapter 5

Studying neutrophil degranulation in response to ANCA as another way of understanding the pathogenesis of ANCA and inhibition of degranulation by statins

5.1. Introduction

The mechanism of ANCA-induced injury is still unclear. The aim of these studies was to learn more about the disease and investigate the different factors involved in causing the disease. We looked at the role of macrophages in our previous work and wanted to investigate the response of neutrophils to ANCA *in vitro* because both of these cell types are part of the innate immune system, which is the focus of my work. I wanted to understand why some individuals develop vasculitis when they are ANCA negative. On the other hand, other individuals have ANCA IgG, but they do not develop the disease. This could mean that there are genetic and environmental factors involved in the development of the disease. It is important to understand what is happening on the cellular level. In this chapter, I focused on studying the variability in ANCA-induced neutrophil degranulation and neutrophil metabolomics following ANCA stimulation.

Small vessel systemic vasculitis is characterised by the presence of anti-neutrophil cytoplasm antibodies (ANCA), which are capable of disrupting normal neutrophil function (Falk, Terrell et al. 1990). These diseases have a wide spectrum of presentation with different disease kinetics and severity of inflammation ranging from upper respiratory disease to life-threatening renal failure and pulmonary haemorrhage. There is no obvious correlation between these phenotypes and either genetic or other factors. ANCA are usually directed against the neutrophil granule components myeloperoxidase (MPO) (Falk and Jennette 1988) and proteinase-3 (PR3) (Niles, McCluskey et al. 1989). The capacity of ANCA to dysregulate neutrophil function can be assessed using various assays. The most common assays use the ability of the purified antibody to induce superoxide release and

degranulation from purified TNF-α-primed neutrophils. This neutrophil activating capacity of ANCA lies at the heart of paradigms that propose mechanisms by which ANCA cause vascular injury in patients with vasculitis.

Anecdotally, it has been noted that the neutrophil activating capacity of IgG preparations from different patients with vasculitis vary in their ability to activate neutrophils. This phenomenon has not yet been studied formally. We looked at the results from previous experiments performed in our lab, which established a degree of variability in ANCA-induced neutrophil degranulation and superoxide release; however, these results were not investigated further. In addition, previous work was done on different days and at different time points which could introduce variability in the overall results. We looked at different variables that might have contributed to the variability seen in previous experiments. Some of this variability may be derived from the ANCA source, from neutrophil donors, or from the time at which the assay was done. These are all factors that we think contribute to the variability seen in ANCA-induced neutrophil degranulation and superoxide release. We used a general linear model to identify the factors that most influence variability. This approach incorporated a number of different statistical methods and was able to accommodate an enormous amount of information. Neutrophil donors and the ANCA source were found to be the main determinants of variability seen in previous work.

We sought to investigate the variability in the ability of ANCA to stimulate neutrophils from healthy donors and to assess whether this variability is primarily a function of the ANCA itself, or whether neutrophils from different individuals vary in their response to different ANCA samples. Furthermore, we aimed to investigate whether this variability was correlated with the clinical phenotype of the individuals from whom the samples were taken.

We also wanted to study neutrophil metabolomics after ANCA-induced neutrophil degranulation. The aim of this experiment was to investigate the variability in neutrophil degranulation from healthy donors in response to ANCA samples. Metabolomics could

provide some information regarding the variations seen here. This has not been done before, so the focus of this work was to see if this could be a viable approach. This can be done by studying neutrophil metabolomics following ANCA-induced neutrophil degranulation. We know that any biological process results in the generation or formation of specific metabolites that are considered to be the biological fingerprint of a cellular process. Metabolomics is the study of these metabolites and can be used to define changes in metabolites that are related to environmental, genetic and biological perturbation. Metabolomics has been used in human studies to define biomarkers related to human disease and also to study human responses to drug treatment and provide greater pathophysiological insight. The collection of all metabolites at the end of a cellular process in cells, tissues, or organs is called the metabolome. Unlike proteomic and RNA expression analyses, study of the metabolomic profile provides more details about the physiology of the cell. Different methods or technologies are used to identify and quantify these metabolites, including mass spectrometry (MS) and nuclear magnetic resonance (NMR). This can be achieved by transforming molecules in a sample into ionised fragments. These ions are then sorted by mass using electric and magnetic fields. The velocity of these charged molecules depends on their mass. Thus, the chemical composition of each molecule determines the mass-to-charge ratio and hence specifies different compounds.

This technology has been used in different applications such as toxicity assessments, functional genomics, and others. A metabolomic approach could help in understanding why neutrophils from healthy donors respond differently to the same ANCA sample. In addition, this could help clarify why some individuals develop severe vasculitis while the disease in some is mild. In addition, some individuals do not develop vasculitis, even though they are ANCA positive, which could be explained by our work. However, the aim of this approach was to see if it can be done as it has not been done before.

We hypothesised that ANCA-induced neutrophil degranulation can be blocked or reduced following anti-inflammatory treatment. Simvastatin is member of the statin family, which

includes inhibitors of 3-hydroxy-3-methylglutaryl CoA reductase. These compounds are widely used as cholesterol lowering agents. In addition to their role in blocking 3-hydroxy-3-methylglutaryl CoA reductase, their function is also mediated through blockage of the mevalonate pathway and the synthesis of isoprenoids (farnesyl pyrophosphate and geranylgeranyl pyrophosphate) (Henneman, van Cruchten et al. 2011). Isoprenoids are essential for the post-translational modification of several proteins involved in important signalling pathways. This in turn will affect different cellular functions, which explains the multifunctional aspect of statins, such as their anti-inflammatory, antioxidant, and endothelial cell protective effects, among others (Mason 2003; Mason 2005). In addition, simvastatin has been shown to play an anti-inflammatory role in arthritis (Leung, Sattar et al. 2003). In this study, we also investigated the effect of simvastatin on ANCA-induced neutrophil degranulation.

5.2. Methods

I have to mention here that the parallel superoxide experiments were done by Dr. Julie Williams but I prepared all IgG samples used in these experiments.

5.2.1. ANCA IgG isolation

Plasma exchange fluids were used as a source of human IgG; these were obtained from patients as a part of clinical patient care at University Hospital Birmingham. Plasma was stored at -20°C until use. Plasma samples were chosen from patients with ANCA-associated vasculitis (MPO or PR3), myeloma, Goodpasture's disease (anti-GBM), renal transplant, vasculitis with negative ANCA, and from healthy controls. These disease controls were chosen because the kidney is affected; additionally, the morphology of kidney injury is somewhat similar to that seen in AAV but without ANCA.

ANCA IgG was isolated from 5 ml of plasma. Plasma was filtered and then diluted 1:1 in loading buffer prior to protein G affinity purification as described in Chapter 2. Disease control and ANCA positive plasma samples were treated in the same manner in terms of storage and IgG isolation. IgG was then stored at 4ºC for no more than two weeks.

5.2.2. Neutrophil isolation and degranulation experiment

Neutrophils were isolated from human blood as previously described in Chapter 2. Healthy donors were used as the neutrophil source; all donors were Caucasians, from different age groups, and included both males and females. Neutrophil isolation from these donors was done on different days, which meant recruiting only two donors per day. In some cases, we isolated neutrophils from all individual donors in one day to eliminate this source of variability as shown below.

Neutrophil Donors	Time experiment was done	ANCA samples
110024 **110025** **110026** **110046** **110057** **110068**	Done on different days, using two donors each day. I used 12 ANCA each day + disease control + normal control.	26 ANCA IgG (MPO and PR3)
110024 **110057** **110016** **110068** **110025** **110046**	Done on the same day	8 ANCA IgG (MPO and PR3)

The aim of isolating these neutrophils was to test the variability in neutrophil degranulation from different donors to the same ANCA IgG samples. Neutrophil degranulation was measured as previously described in Chapter 2 using MPO ANCA, PR3 ANCA, disease control, and normal IgG.

ANCA IgG vs. Disease control IgG

We wanted to be sure that the response observed after treating neutrophils with ANCA was not mediated by endotoxin or other factors that might result from plasma handling, storage, and IgG preparation. As result, I compared neutrophil degranulation following stimulation with ANCA IgG and IgG from a disease control that was handled in the same manner as the ANCA sample. I used 20 ANCA IgG samples (10 MPO and 10 PR3) and 10 disease IgG control samples. IgG isolation and neutrophil degranulation was performed as described in Chapter 2.

General linear modelling of ANCA responses

In order to identify the factors involved in the variability of ANCA-induced neutrophil degranulation, we looked at various research projects that were done in the past. We

excluded some assays where the source of ANCA IgG and neutrophil donors could not be identified. We only included those healthy neutrophil donors that had been tested on at least 25 separate occasions (n=10 and 9 for superoxide and degranulation respectively), and only those ANCA IgG samples that had been tested on at least eight separate occasions (n=28 and 32 for superoxide and degranulation, respectively). To investigate the independent contribution of different factors to the observed variability, we then generated four linear models for each assay using the following parameters:

Model 1: ANCA source

Model 2: Neutrophil donor

Model 3: ANCA source + Neutrophil donor

Model 4: ANCA source + Neutrophil donor + Assay month (to control for variation in the assay over time)

Prospective assessment of variability in neutrophil responses resulting from variation in the ANCA source

One of the factors affecting variability in ANCA-induced neutrophil degranulation and superoxide release is the ANCA source. Based upon the observed variability in assay results in the general linear model, we estimated that testing ANCA IgG from 26 separate patients with vasculitis using the same neutrophil donors would provide a significant response for understanding superoxide release. Fewer samples would be required to demonstrate a significant difference in the degranulation assay, but we elected to use the same ANCA samples for both assays to aid in comparison. Therefore, plasma exchange samples from 26 patients with vasculitis were randomly selected from a pool of 143 samples, with stratification to ensure a roughly equal number of anti-PR3 and anti-MPO. We performed superoxide and degranulation assays in these 26 samples using the same six neutrophil donors. Assays were performed at different times. The anti-MPO and anti-PR3 levels in these 26 plasma exchange samples were measured by ELISA.

Prospective assessment of variability in neutrophil responses resulting from variation in the neutrophil donor

Another factor involved in assay variability is the source of neutrophils, so in some experiments we decided to fix the ANCA source. We selected eight ANCA samples (three high responder samples, three low responders and two intermediate) for testing with cells from seven different neutrophil donors. In order to minimise the effect of using different neutrophil preparations under variable atmospheric conditions, we sought to prepare neutrophils from the seven donors at the same time and to split them for testing into the superoxide and degranulation assays using the same IgG preparations in each. One of the degranulation assays was lost for technical reasons, so for the analysis of the degranulation assay, six of the seven donors were used.

5.2.3. Neutrophil metabolomics

This experiment was done at the Bioscience Department at the University of Birmingham in collaboration with Dr. Jennifer Kirwan. This occurred after testing the possibility of obtaining a clear signal from neutrophils isolated by me from human blood using the same approach.

I wanted to investigate why different healthy neutrophil donors vary in their response to the same ANCA IgG using a metabolomic approach. I used cells from six neutrophil donors, which were each treated with two ANCA IgG and disease control IgG samples. Neutrophils were isolated from six healthy donors as previously described. Neutrophils from each donor were divided into five tubes for five different treatments. First, 10 million cells were washed and snap frozen in liquid nitrogen (treatment 1). The remaining cells were treated with TNF-α and cytochalasin B for 15 minutes at 37ºC to stimulate the neutrophils and trigger the migration of antigens to the surface of neutrophils. The cells were then divided into four tubes from each donor (10 million cells per tube) as follows:

Table 5.1: Neutrophil donors and treatment groups in metabolomic experiment. Each sample was giving two numbers (e.g 1-1, 1-2, etc.), where the first number represents the donor and the second number represents treatment.

Neutrophil Donors	Treatment	
1. **110016**	1. Untreated (no stimulation with TNF-α and cytochalasin B)	
2. **110024**		
3. **110057**	2. PR3 ANCA treatment	Stimulation with TNF-α and cytochalasin B
4. **110025**	3. MPO-ANCA treatment	
5. **110068**	4. Anti-GBM IgG treatment	
	5. No treatment	

The cells were incubated with IgG for 15 minutes at 37ºC, then cells were centrifuged and the supernatant was taken to measure MPO release. Cells were washed with PBS and snap frozen in liquid nitrogen. Then, I transferred the samples to the Bioscience Department at the University of Birmingham to for metabolomics analysis. This was done by setting clean Precellys tubes on ice for each sample. These tubes contained beads that were used later for grinding the tissue. Then, 8 µl/mg of sample of MeOH and 2.5 µl/mg of H_2O were added to each tube. Next, frozen neutrophils were added to each tube and these tubes were put on the Precellys 24 homogeniser for 2 × 10 s bursts at 6,400 rpm. Next, the homogenised mixture was moved into clean 1.8 ml clean glass vials. Then, the glass vial was kept on ice and 8 µl/mg $CHCl_3$ and 4 µl/mg H_2O were added to each vial; each vial was vortexed for 30 s and placed on ice for 10 minutes. Glass vials were centrifuged at 3,000 rpm for 10 minutes at 4ºC and the samples were then left for 5 minutes at room temperature. Samples were biphasic at this point, with protein debris separating the upper (polar) and lower (non-polar) layers. 50 µl aliquots were taken from the upper and lower layers and transferred into 1.8 ml glass vials. All aliquots were dried using a Speed Vac concentrator for 1 hour with no heat. Samples were then stored at -80°C until needed.

Metabolite analysis using FT-ICR mass spectrometry:

Samples were run on a mass spectrometer (MS) at the Biosciences Department at the University of Birmingham. Metabolites were analysed using Fourier transform ion cyclotron resonance mass spectrometry (FT-ICR/MS). This was done by re-suspending the dried polar extracts (in five times their original volume) in a 80:20 methanol/water solution containing 0.25% formic acid. Samples were analysed in positive ion mode using a hybrid 7-T FT-ICR/MS (LTQ, Thermo Fisher Scientific, Bremen, Germany) with a chip-based direct infusion nanoelectrospray ionisation assembly (Triversa, Advion Biosciences, Ithaca, NY). The conditions of nanoelectrospray was controlled by ChipSoft software (version 8.1.0) and consisted of 0.3 psi backing pressure, 1.7 kV electrospray voltage, and a 200 nl/min flow rate. An automatic gain control setting of 1×10^6 and a mass resolution of 100,000 were used for mass spectrometry. Xcalibur software (version 2.0, Thermo Fisher Scientific) was used for analysis with 2.25 minutes of analysis time per technical replicate. Data were collected using the SIM-stitching FT-ICR metho detailed by Southam et al. (Southam, Payne et al. 2007) and Weber et al. (Weber, Southam et al. 2011) over a mass range of m/z 70-590. Each sample was analysed in triplicate; nine QC samples were analysed prior to analysis and a QC sample was analysed in triplicate every sixth sample.

Using custom written code in Matlab (version 7.9.0, The MathWorks), transient data (in the time domain) were collected and processed as described previously (Southam, Payne et al. 2007). Specifically, all the SIM windows were joined together using SIM stitching code (Southam, Payne et al. 2007) (version 1.16). This was done to reject peaks with a signal to noise ratio <3.5, and also to internally calibrate the mass spectra using a list of 13 pre-defined metabolites. Subsequently, only peaks that occurred in two or more of the three replicate measurements per sample were retained by applying a noise filtering algorithm (Payne, Southam et al. 2009). As a result, only peaks that were present in 50% or more of the samples were retained. Finally, data were normalised using the probabilistic quotient approach (Dieterle, Ross et al. 2006) after missing values were substituted as described by

Payne et al. This was followed by a generalised log transformation according to the approach reported by Persons et al (Parsons, Ludwig et al. 2007). This produced a final peak matrix that included a list of m/z values and their intensities across the samples.

Principle component analysis (PCA) and partial least square discriminate analysis (PLSDA)

Different factors could affect the analysis of metabolomics results; one of these is spray stability. Basically, the electrospray ionisation approach is used to transfer the sample into the mass spectrometer. Essentially, a liquid sample is passed into a charged needle which ionises the sample so that it comes out the other end as a very fine spray of ions. This spray can be measured in terms of its intensity by measuring the flow of ions. The intensity of this spray can change according to many factors, including the sample nature. The consistency of this spray is what is known as spray stability. This is measured by the relative standard deviation of the sample.

Principle component analysis (PCA) is an unsupervised multi-variant technique. PCA is a powerful tool for reducing a number of observed variables into a smaller number of artificial variables that account for most of variance in the data set. It works by reducing the dimensionality of the data while retaining most of the variation in the data set. This can be achieved by identifying directions called principle components along which variations in data are maximised. As a result, samples can be represented by relatively small numbers instead of thousands of variables by using a few components. This allowed us to plot the samples in a way that made it possible to assess the similarity and differences between samples.

On the other hand, partial least square discriminate analysis (PLSDA) is a supervised analysis which looks for maximum discrimination between groups. We used this approach because only partial separation was achieved on the PCA plot.

Finally, we used forward selection to improve the prediction capability of the model. In this approach, variables were added to the model one at a time and these variables were tested

for inclusion in the model. Finally, the most significant of these variables was added to the model. This resulted in a reduction in the number of final variables because the peaks that were most representative of the sample class were selected.

5.2.4. The effect of simvastatin on ANCA-induced neutrophil degranulation

We investigated the possibility of using simvastatin as a treatment for ANCA-associated vasculitis. We studied the effect of simvastatin on ANCA-induced neutrophil degranulation in vitro. Neutrophils were isolated from healthy donors and pre-incubated with 10 μM of the active form of simvastatin (Calbiochem, UK) for 20 min at 37ºC. Then, the neutrophil degranulation assay was performed as previously described using MPO and PR3 ANCA samples. Neutrophil survival was confirmed by trypan blue staining.

5.2.5. Confirming the survival of neutrophils following treatment with simvastatin

Neutrophils were treated with simvastatin, which was dissolved in DMSO. We wanted to be sure that this treatment did not cause neutrophil death. Stock simvastatin was dissolved in 100% DMSO to a final concentration of 10 mM. This was then diluted 1:1,000 in HBH buffer to 10 μM which was then used to treat neutrophils. We checked the viability of neutrophils following incubation with different concentrations of simvastatin (5, 10, 20, 50, and 100 μM). Cell viability was checked every 30 minutes using trypan blue for a period of 150 minutes.

Statistical analysis

The degree of the effect of different variables in the general linear models was assessed using the partial η^2. The goodness of fit of the model as a whole was assessed by calculating the r^2. Both of these parameters ranged from 0 to 1. The analysis result is in the appendix 7.5.

When comparing the responses from different ANCA samples (fixed donor) and from different neutrophil donors (fixed ANCA source), we used a matched two-way ANOVA. We

calculated the Spearman correlation coefficient to assess the correlation between superoxide and degranulation responses, and between assay results and clinical phenotype. The assay results for the 26 samples were compared across various dichotomous clinical variables using the Mann-Whitney test. To investigate the independent association of various clinical variables with the assay result for a given ANCA sample, we used multivariate logistic regression with forced variable entry.

5.3. Results

5.3.1. ANCA IgG vs. disease control

Plasma samples were stored at -20°C and were not tested for the presence of endotoxin prior to IgG purification. We wanted to confirm that the differences seen in neutrophil degranulation were due to the effect of ANCA and not to endotoxin or some other unmeasured factor. We used disease control IgG samples which were prepared from patients with different diseases such as anti-GBM, myeloma, and others; these included 20 ANCA IgG (MPO or PR3) and 10 disease control IgG samples. ANCA IgG and disease control IgG samples were purified from plasma exchange samples and were stored in the same way prior to IgG extraction. Neutrophils were isolated from healthy donors. There was a significant difference in neutrophil degranulation in response to ANCA IgG compared to disease control IgG (figure 5.1).

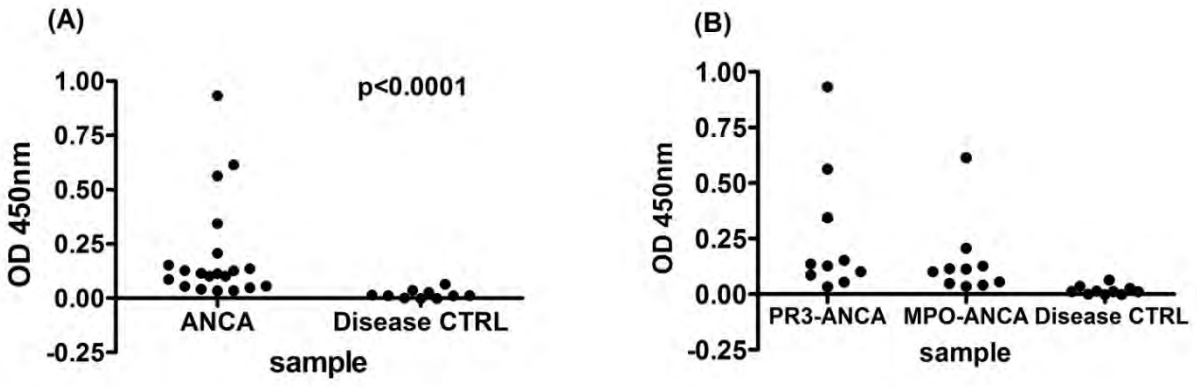

Figure 5.1: Neutrophil degranulation in response to ANCA IgG and disease control IgG. There was a significant difference in neutrophil degranulation between ANCA IgG and disease control (A). Both MPO and PR3 ANCA induced a significant increase in neutrophil degranulation compared to IgG from disease control samples (B). Mann-Whitney test.

5.3.2. ANCA IgG from different individuals with vasculitis vary in their ability to induce neutrophil superoxide release and degranulation

We observed marked variability in both the superoxide and degranulation neutrophil responses across ANCA samples from 26 different patients with vasculitis (Figure 5.2). It was not possible to comment specifically on the relative contribution of the ANCA source

and neutrophil donor in these experiments as the neutrophil donors were not randomly selected. However, the ANCA source appeared to contribute more to the variability in the degranulation assay (72.2%) than in the superoxide assay (40.4%). This was done by comparing all the results using a two-way ANOVA and assuming that donors had the same effect (if any) at all levels of ANCA.

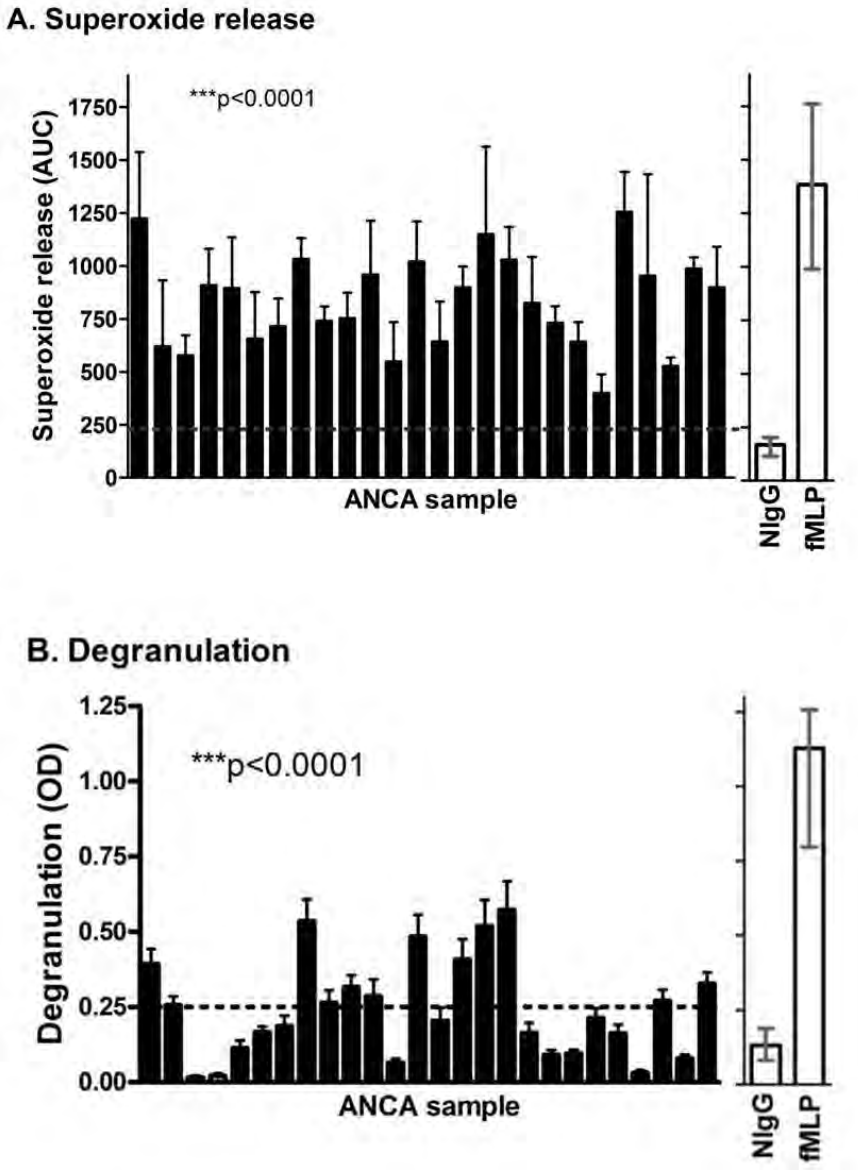

Figure 5.2: Variability in neutrophil responses to stimulation with ANCA IgG preparations from different patients. (A) IgG was purified from the plasma exchange fluid of 26 randomly selected patients and their ability to induce neutrophil superoxide release from the same nine donors was measured. (B) The neutrophil degranulation response to the same 26 IgG preparations was also measured in six of these neutrophil donors. The lines and bars depict the median and interquartile range, respectively. The p value represents the variation of the results as an effect of ANCA treatment using two-way ANOVA.

5.3.3. Neutrophils from different healthy donors vary in their response to ANCA stimulation

We went on to select eight ANCA samples from the previous experiments and measured responses in the same six or seven neutrophil donors. All assays were performed at the same time with the same neutrophil preparations. We again observed marked variability in both the superoxide and degranulation neutrophil responses across these donors, when tested using neutrophils from the same donors (Figure 5.3). Although I again cannot comment specifically on the relative contribution of the ANCA source and neutrophil donor in these experiments, it did appear that greater variability was derived from the donor in the superoxide assay (29.9% of the variability) than in the degranulation assay (8.1% of the variability).

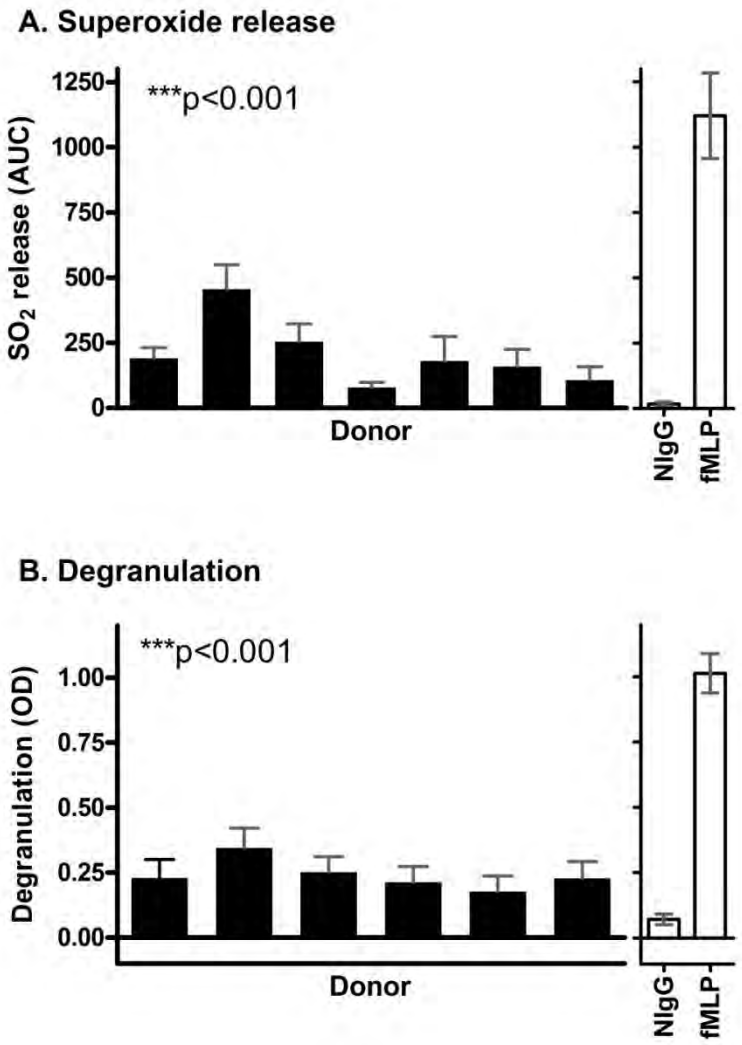

Figure 5.3: Variability in neutrophil responses to stimulation with ANCA IgG preparations using different neutrophil donors. (A) Eight IgG samples were selected from the previous pool of 26 samples and their ability to induce the release of superoxide from neutrophils from the same seven donors was measured. (B) The neutrophil degranulation response to the same eight IgG preparations was measured in six of the same seven neutrophil donors. Both assays were performed on the same day using the same neutrophil preparations. The p value calculated using two-way ANOVA.

5.3.4. Correlation between the degranulation and superoxide neutrophil responses to ANCA stimulation

As the experiments examining the contribution of the neutrophil donor to variability were all performed at the same time using the same neutrophil preparation for both the superoxide and degranulation assays, it was possible to assess the correlation between superoxide and degranulation responses for each ANCA-neutrophil pair. I observed that, in approximately two thirds of cases, both assays were concordant (i.e. either positive in both or negative in both, Figure 5.4). In the remaining one third, the assays were discordant

(either positive for superoxide or negative for degranulation in 25%, or vice versa in 8%). Overall, the two assays were moderately correlated (r=0.48), with the relationship best described by an exponential equation (r^2=0.55, Figure 5.4). Any measurement above two standard deviations (2SD) was considered positive in relation to measurements following incubation with a range of normal IgG preparations.

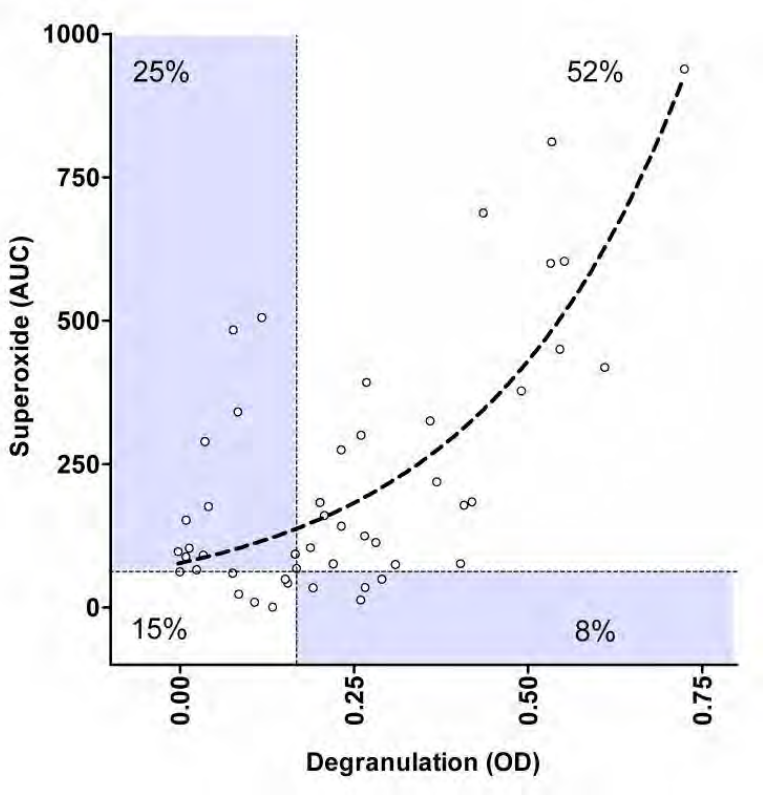

Figure 5.4: Concordance between neutrophil degranulation and superoxide release in paired samples. Each data point represents a paired degranulation/superoxide release assay performed using the same IgG preparation and donor, performed at the same time. The dashed line (----) depicts the best fit line described by the data and the dotted lines (┈┈) depict the mean+2SD following incubation with a range of control normal IgG preparations. The shaded areas describe values that are positive in one assay, but negative in another ("discordant") and the % values reflect the fraction of assays that lie within each quadrant. One third of the assays were discordant.

5.3.5. Confirming survival of neutrophils after treatment with a statin

Simvastatin was dissolved in dimethyl sulphoxide (DMSO), which could affect the survival of cells. The final concentration of DMSO was 10μM. We investigated the survival of neutrophils after treatment with the statin for 20 minutes using trypan blue. Cells were incubated with different concentrations of simvastatin for 150 minutes, which is much longer

than the time used in the experiment, but the total time required for the experiments, including treatment with ANCA IgG, takes about 150 minutes. There was little or no reduction in the percentage of viable cells after 150 minutes when the concentration was increased to 20μM. The number of viable cells started to decrease when the concentration was increased to 50 or 100μM, which is much higher than the concentration used in the experiment (10μM) (figure 5.5).

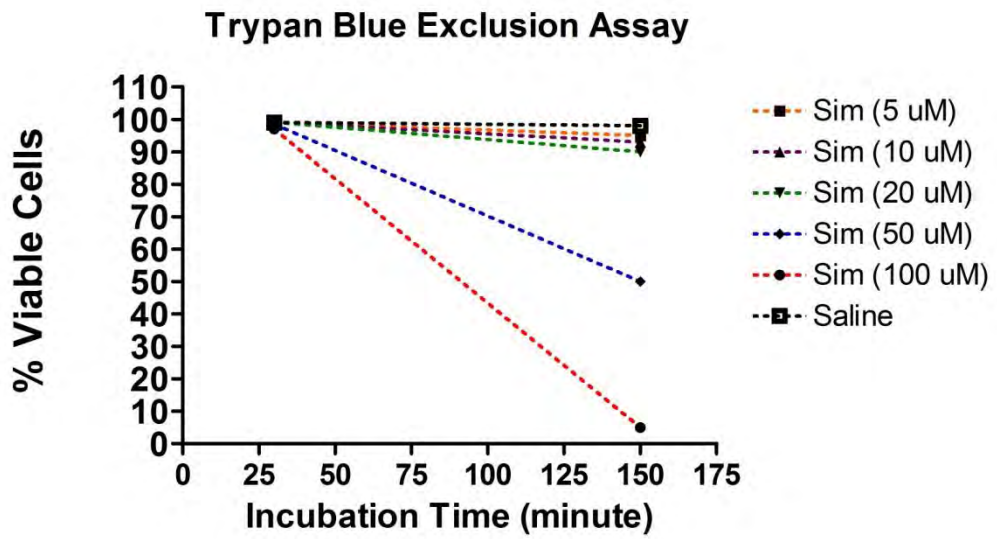

Figure 5.5: The effect of a statin (dissolved in DMSO) on cell survival. The number of viable cells was monitored for 150 minutes after treating the cells with different concentrations of the statin (5, 10, 20, 50, and 100 μm). There was no reduction in cell survival at concentrations up to 20 μM.

5.3.6. The effect of ANCA-induced neutrophil degranulation following treatment with simvastatin

We observed a significant difference in neutrophil degranulation following treatment with simvastatin. Simvastatin reduced ANCA induced neutrophil degranulation (Figure 5.6, A). The effect of simvastatin was also seen on fMLP (positive control) induced neutrophil degranulation. There was a reduction in both ANCA-PR3 and ANCA-MPO induced neutrophil degranulation in response to treatment with the statin (Figure 5.6, B), but this was only significant for ANCA-PR3.

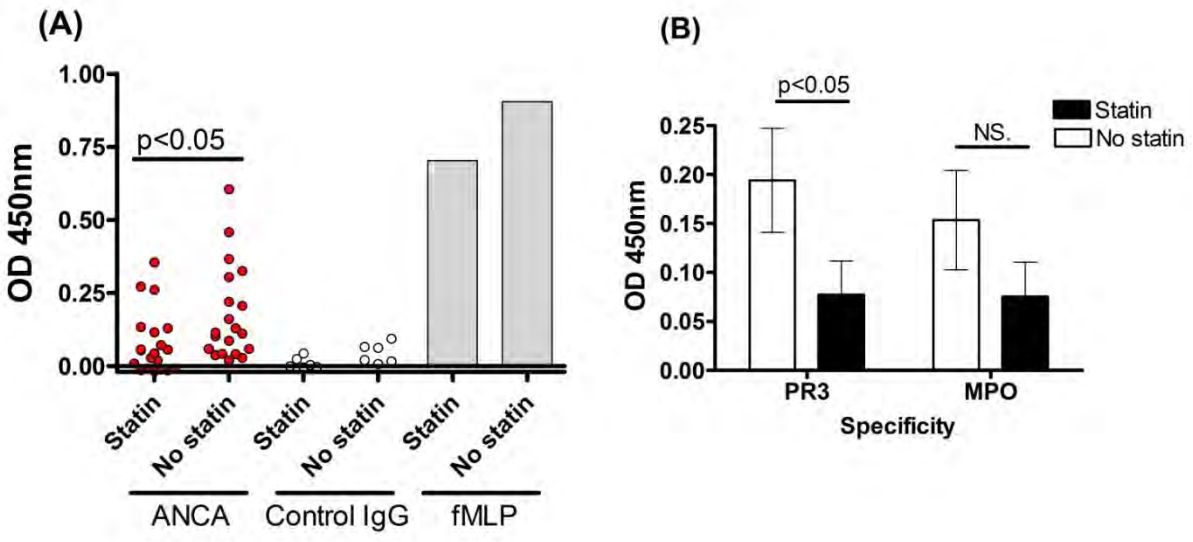

Figure 5.6: The effect of statin on ANCA-induced neutrophil degranulation. Treatment with a statin significantly induced a reduction in ANCA-induced neutrophil degranulation (A). This reduction was seen in both ANCA-PR3 and ANCA-MPO induced degranulation (B). Mann-Whitney test.

5.3.7. Neutrophil metabolomic analysis

Spray stability of sample

Spray stability, as measured by the relative standard deviation (RSD) of replicates, was higher than expected. 5_5 was especially high at 47%. This may have been due to the nature of the biological sample or the concentration of the sample.

Multivariate analysis

The RSD of the quality control (QC) samples had a median of 31%. Generally, the QCs did not cluster as well as was anticipated. This was probably linked to the poor spray stability noted previously. Additionally, despite the QCs being a combination of several samples, the QCs did not cluster at the centre of the PCA plot. Only treatment 1 clustered well, although treatment 4 appeared to cluster in PC1 with the exception of 5_4 (figure 5.7). This means that there was technical variation in this experiment of 31%; this was high compared to the expected value of <20%.

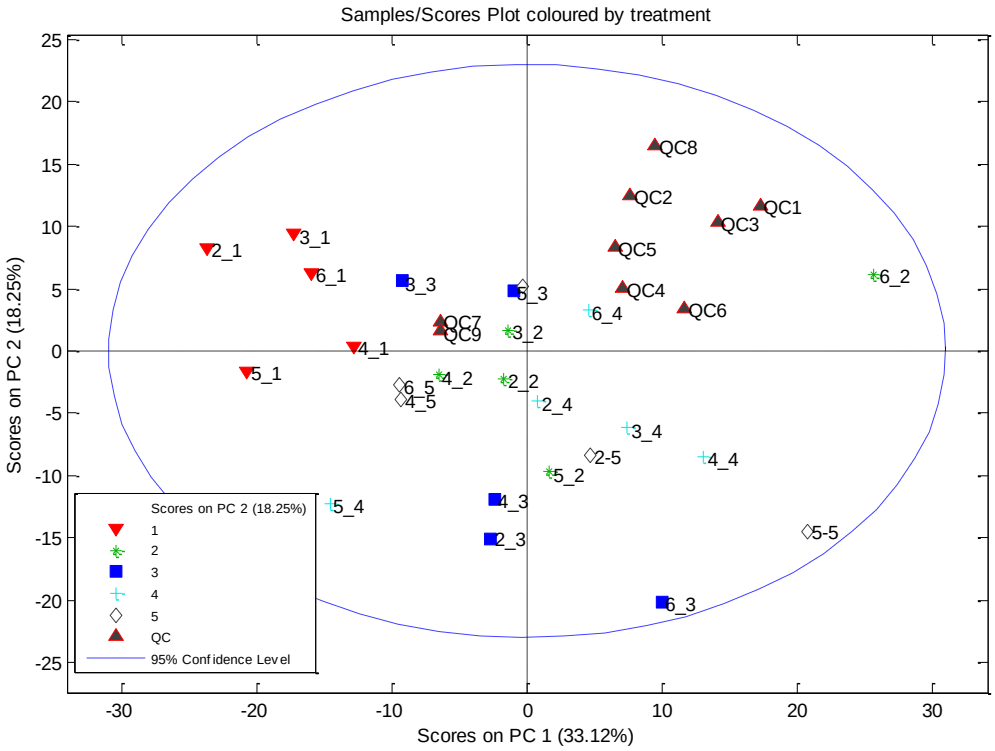

Figure 5.7: Unsupervised multivariate technique. Principle component analysis was the first approach used to separate the samples into related groups or clusters. Each point in the graph represents an individual donor and treatment (the first number is the donor number and the second number is the treatment number). For example 2_1 is donor 2 and treatment 1 (untreated neutrophils). Only treatment 1 clustered relatively well. Using this method, 33.12% of the variation in the data can be explained by PC1 and 18.25% can be explained by PC2.

PLSDA

Since there was only partial separation on the PCA scores plot, a supervised technique, PLSDA, was used to analyse the data. This technique is used to sharpen the separation between groups and works by rotating PCA components to allow maximum separation between classes. Again, only untreated neutrophils (treatment group 1) were well-differentiated from the other groups (Figure 5.8). On the other hand, none of the treated neutrophils clustered, even those neutrophils that only received TNF-α and cytochalasin B (no IgG treatment) (treatment 5).

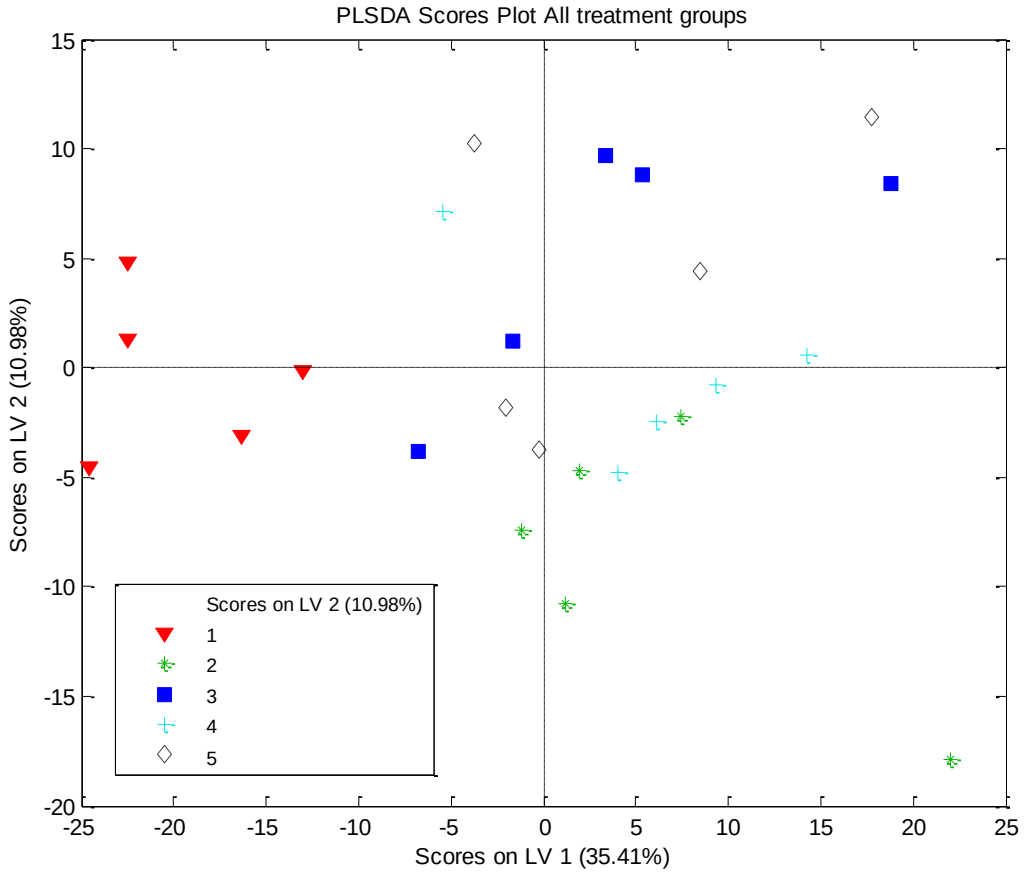

Figure 5.8: Partial least square discriminate analysis. This supervised technique is used to look for maximum discrimination between groups. Only untreated neutrophils (treatment 1) clustered well. Treated neutrophils, on the other hand, did not cluster.

In order to improve the prediction capability of the model, a forward selection procedure was carried out to select the peaks that were most predictive of sample class. Prior to forward selection, the classification errors were as follows:

Treatment group	Classification error (%)
1	8.5
2	44.0
3	42.4
4	44.1
5	57.1

Of these, only treatment group 1 (untreated neutrophils) was significant after permutation testing ($p<0.01$). Classification error represents the proportion of cases that are incorrectly predicted.

Following forward selection, which determined that 82 of the variables were more discriminatory, the classification errors improved as follows:

Treatment group	Classification error (%)
1	1.85
2	16.4
3	32.3
4	39.4
5	46.1

Of these, treatments 1, 2 and 3 were deemed significant after permutation testing ($p=<0.001$, $p=<0.001$ and $p=0.04$, respectively)

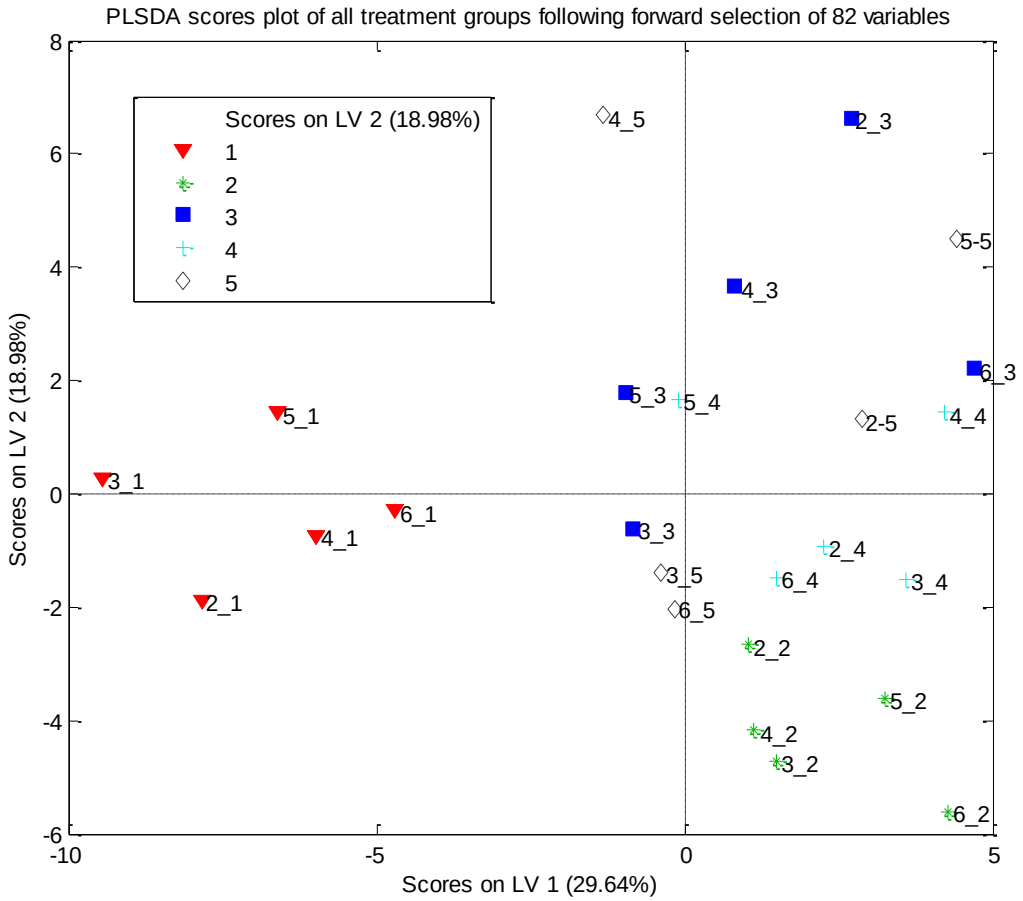

Figure 5.9: PLSDA of all treatment groups following forward selection. The classification errors improved following forward selection and it was relatively possible to see some clustering of treatment groups 1, 2, and 3; these had the lowest classification errors.

Metabolites detected following ANCA treatment

I identified some metabolites that were downregulated in ANCA-PR3 and ANCA-MPO compared to the control group (HBH buffer treated). These metabolites were slightly upregulated in relation to treatment 1 (untreated neutrophils), but when compared to treatment 5 (TNF-α, cytochalasin B, and HBH treated), these metabolites seemed to be downregulated in ANCA-PR3 treated cells. One of these metabolites was taurine, which has many biological roles such as antioxidation, osmoregulation, and modulation of calcium signalling. Aucubin was another metabolite that was downregulated following treatment with ANCA-PR3. It has various biological activities, including anti-inflammatory activities, blood pressure reduction, antimicrobial activity, and liver protection.

Fold change (in relation to treatment 1)				
Metabolite	ANCA-PR3	ANCA-MPO	TNF-α and cytochalasin B	p-value
Taurine	0.155	0.215	0.232	0.0075
Aucubin	0.151	0.246	0.225	0.0063

5.4. Discussion

I found variability in neutrophil degranulation in response to the same ANCA IgG. This was seen when the degranulation assay was done on different days using two donors each time and also when the assay was done on the same day using six donors and eight ANCA IgG. There was some variation in the release of superoxide between different donors when they were treated with the same ANCA IgG. I found that 2/3 of the cases were either positive for both assays (degranulation and superoxide) or negative for both. The effect of ANCA-induced neutrophil degranulation was specific to ANCA IgG because there was no or little neutrophil degranulation in response to IgG from disease control samples. In addition, simvastatin treatment significantly reduced ANCA-induced neutrophil degranulation.

Neutrophils are part of the innate immune system and they have been reported to have an important role in ANCA-associated vasculitis and necrotising crescentic glomerulonephritis (NCGN), causing tissue damage. Several studies have shown the ability of ANCA to activate TNF-α primed neutrophils, which results in the release of reactive oxygen radicals (Falk, Terrell et al. 1990; Charles, Caldas et al. 1991; Keogan, Esnault et al. 1992; Brouwer, Huitema et al. 1994; Mulder, Heeringa et al. 1994). The mechanisms that are involved in ANCA-induced neutrophil degranulation are not fully clear. We have shown here the variability in ANCA-induced neutrophil degranulation from healthy donors. Franssen et al. have shown differences in ANCA-induced neutrophil degranulation when they compared c-ANCA and p-ANCA (Franssen, Huitema et al. 1999). The variability that was found in our experiment could be caused by different factors. One reason could be the availability of the antigens (PR3 and MPO) on the surface of the neutrophils that were purified from healthy donors. This could explain the variability that we saw in ANCA-induced neutrophil degranulation from healthy donors when they were treated with the same ANCA IgG. We also noticed that some ANCA-IgG samples had the ability to induce greater neutrophil degranulation (as measured by ELISA) compared to other ANCA samples.

Different studies have shown the importance of the binding of ANCA to FcγRIIa in neutrophil activation (Mulder, Heeringa et al. 1994). It is possible that the binding of ANCA to the Fc receptor on the surface of neutrophils might be the reason why we observed differences in ANCA-induced neutrophil degranulation. This means that there might be more ANCA-IgG in a specific sample which would result in more receptor binding to induce a stronger response. The amount of ANCA in each sample was not known, and we only assessed the IgG concentration. This quantitative difference could result from the IgG preparation method. The use of a PR3 or MPO affinity column could be used to standardise the amount of ANCA in the preparations. Another explanation could be that there are differences in IgG subclass distributions in these ANCA samples. Pankhurst et al. have shown that IgG3 is the most effective subclass for inducing neutrophil adhesion and altered behaviour (Pankhurst, Nash et al. 2011).

In future experiments, I would like to study ANCA-induced neutrophil degranulation on cells from vasculitis patients. It would be interesting to see how neutrophils from these patients respond when treated with ANCA IgG from the same patient or different individuals.

We investigated the effect of simvastatin on ANCA-induced neutrophil degranulation and we found that it attenuated neutrophil degranulation in vitro. Statins are used as cholesterol lowering agents and recently have been proposed to have LDL cholesterol-independent anti-inflammatory properties. For example, pravastatin has been found to inhibit superoxide generation following neutrophil treatment with formyl-methionyl-leucyl-phenylalanine (fMLP) (Kanno, Abe et al. 1999). We know that the binding of ANCA to antigens on the surface of neutrophils is required to induce neutrophil degranulation and release reactive oxygen radicals. Choi et al. have shown that treatment with simvastatin or cerivastatin reduces the translocation of PR3 and MPO following TNF-α stimulation (Choi, Rolle et al. 2003). This could explain the reduction in neutrophil degranulation that we observed following treatment with simvastatin. This could be tested by performing immunofluorescence staining on these

neutrophils following treatment with simvastatin compared to untreated cells to check for antigens on the surface of neutrophils. In addition, a reduction has been shown in ANCA-induced respiratory burst activity in TNF-α primed neutrophils. It has been suggested that this inhibition could be explained in part by the ability of statins to inhibit the ERK pathway since previous experiments showed the involvement of p38 MAPK and ERK in the ANCA-induced neutrophil respiratory burst (Kettritz, Schreiber et al. 2001). These findings support previous work on statins suggesting that they could play an anti-inflammatory role. On the other hand, Al-Ani et al. were not able to find any effect of statins on ANCA-associated vasculitis in a rat model of vasculitis (Al-Ani, Al Nuaimi et al. 2011).

I also looked at the possibility of studying metabolites following ANCA-induced neutrophil degranulation. We used six healthy donors, and each donor sample underwent five different treatments (untreated, PR3-ANCA (ANCA1), MPO-ANCA (ANCA 28), disease control IgG, and TNF-α, and cytochalasin B). We were not able to observe clustering of the different donors with specific treatments, except for untreated samples. This could be due to technical variability or experimental design. We estimated the technical error to be 31%, which was much higher than anticipated. Another reason that these results did not cluster could be that they are biologically different. In other words, these healthy donors respond differently to the same ANCA IgG in terms of neutrophil degranulation. So, the experimental design could be incorrect. If I was to repeat this experiment, I would use only one healthy donor and treat these neutrophils with different ANCA samples (PR3 and MPO) to study the effect of ANCA on neutrophil degranulation and compare PR3-ANCA to MPO-ANCA. I think that we included too many variations in this experiment, including donor variation and treatment variation. I conclude that this approach was difficult to assess and interpret because of the variation in these biological samples. I would suggest repeating the experiment using only one ANCA IgG sample and one donor neutrophil. The aim of this experiment would be to only look at the differences in metabolites following ANCA IgG treatment.

Chapter 6

Overview Discussion

6.1. Project summary and application of results

The innate immune system is the first line of defence and it is crucial for initiating the inflammatory response. I wanted to investigate different components of the innate immune system and their involvement in ANCA-associated vasculitis (AAV). I was interested in studying the role of macrophages in AAV as this has not been investigated previously; specifically, I wished to determine if macrophage depletion could result in protection from the development of vasculitis. In addition, neutrophils are an important factor in AAV and studying the variability of ANCA-induced neutrophil degranulation was another one of my aims. I used a mouse model of vasculitis to study the role of macrophages; I also tried to improve this model. Furthermore, I looked at gene expression in animal models of AAV by comparing tissues from animals with vasculitis to those from control animals to find upregulated genes in the glomerulus.

Establishing and working to improve the mouse model

I started by establishing the animal model and establishing a MPO-/- mouse colony to raise anti-MPO antibodies. I cultured WEHI cells as a source of murine MPO and then tried using different methods such as MPO peptides, recombinant MPO, and MPO heavy chain to raise anti-MPO antibodies. These approaches resulted in the production of anti-MPO antibodies, but these antibodies showed a low affinity for murine MPO compared to the MPO used for immunisation. This was investigated by anti-MPO ELISA. In addition, I was not able to induce disease in WT mice using antibodies generated following immunisation with the antigens previously mentioned.

I tried inducing vasculitis in mice using anti-murine MPO antibodies, but I found that the form of the disease was very mild. I was able to induce a relatively severe form of the disease when I used LPS with anti-MPO antibodies. The mice developed crescentic glomerulonephritis with around 13% crescents.

Macrophages in AAV

I investigated macrophage infiltration into the kidney in mice treated with anti-MPO antibodies and LPS. I was able to show macrophage recruitment to the kidney following disease induction. Macrophages are mainly found in the crescent region of the kidney and there was also positive interstitial macrophage staining. I also investigated the type of macrophage infiltrating the kidney to determine whether these were M1 or M2-type macrophages. I found that the macrophages recruited into the crescent were mainly CD206 negative, which suggests that these cells are classically activated macrophages. In addition, I found strongly positive MHCII staining in the kidney.

Microarray and gene expression in AAV

I investigated gene expression in the glomerulus following disease induction, which is a novel approach. I found 42 upregulated genes common to both mouse and rat glomeruli. These genes are involved in macrophage activation, complement activation, cell adhesion, as well as antigen processing and presentation. In addition, there were some highly upregulated genes in mouse glomeruli such as lipocalin 2, also known as NGAL and the kidney injury molecule 1 (Kim 1). These genes are considered to be acute kidney injury biomarkers. Furthermore, there was an upregulation of collagen genes, especially collagen I, and these were found to be involved in most of the biological processes mentioned in Chapter 4. In addition, fibronectin 2 was upregulated in both mouse and rat glomeruli. There were other genes involved in cell adhesion and recruitment, such as CX3CR1 and CCR2, which are also involved in macrophage recruitment.

Macrophage depletion

I investigated the effect of macrophage depletion on disease development in mice following treatment with anti-MPO antibodies. I started by depleting macrophages using liposomal clodronate, which was effective in depleting macrophages. However, there was a significant reduction in the level of passively transferred antibodies in clodronate-treated mice compared to the control group. As a result, I used an anti-CCR2 antibody to prevent GR1+ monocytes from infiltrating the kidney. These are inflammatory monocytes which differentiate into inflammatory macrophages in the tissue. GR1+ cells were almost completely depleted in the blood, as shown by FACS throughout the experiment. However, no significant differences were found in crescent formation or in the percentage of CD68-positive cells in the kidney between the IgG2b and anti-CCR2-treated mice. The disease in this experiment was mild and I was not able to exclude the effect of macrophages in disease development.

The variability in neutrophil degranulation

I studied the variability in neutrophil degranulation in response to ANCA-IgG. Variability was shown in ANCA-induced neutrophil degranulation resulting from neutrophil donors and also in the source of ANCA. This was seen in both neutrophil degranulation and superoxide release. The effect seen on neutrophil degranulation was specific to ANCA-IgG, as IgG from control patients with diseases such as myeloma failed to induce neutrophil degranulation. I tried to investigate this variability using a metabolomics approach in order to study the metabolites following the degranulation experiment. This is a novel approach and the aim was to investigate whether using this approach was possible.

The effect of simvastatin on ANCA-induced neutrophil degranulation

Simvastatin is cholesterol-lowering agent known to have anti-inflammatory effect. There was a significant reduction in ANCA-induced neutrophil degranulation following treatment

with 10 μM simvastatin. This effect of simvastatin was seen on both PR3 and MPO-ANCA, but it was only significant on PR3-ANCA.

6.2. Different approaches for improving the mouse model of vasculitis

The mouse model of ANCA-associated vasculitis confirmed the pathogenicity of Anti-MPO antibodies and was also used to study the disease. The disease was induced by the i.v. administration of anti-murine MPO antibodies. There are some limitations of this model, which I will discuss here.

One of the limitations of this model is the source of murine MPO. The WEHI 3 cells are one source of murine MPO, but a large number of cells are required to generate a sufficient amount. This approach is not practical in most cases and it is also expensive. I tried different methods to find a reliable source of murine MPO. I used recombinant mouse MPO, MPO multi-antigenic peptides, and MPO heavy chain to immunise MPO-/- mice and investigated the possibility of producing antibodies that could induce vasculitis. These mice responded to immunisation and produced anti-MPO antibodies. However, these antibodies were antigen specific, as shown by ELISA, which means that they produced high titres when the plate was coated with the antigen used for immunisation but they produced relatively low titres when the plate was coated with murine MPO. This suggests that the antibodies produced following immunisation reacted poorly with murine MPO. This could explain the absence of disease when WT mice were injected with IgG from purified from the immunised animals. Apostolopoulos et al. used recombinant MPO to immunise MPO-/- mice; they detected the production of antibodies to native murine MPO (Apostolopoulos, Ooi et al. 2006). However, they did not report the antibody titre and they did not demonstrate the ability of these antibodies to induce disease in WT mice.

6.2.1. Why did the immunisation with non-native MPO not work?

There are several reasons that could explain why the use of recombinant MPO, MPO peptides, and MPO heavy chain was not as effect as native MPO in generating MPO antibodies. One explanation could be that whole MPO is required to generate an immune response in MPO-/- mice, which results in the production of anti-MPO antibodies. Furthermore, Erdbrugger et al. investigated the MPO epitopes recognised by ANCA and they identified what could be a target epitope on MPO heavy chain (Erdbrugger, Hellmark et al. 2006). However, they suggested that MPO-ANCAs target a number of regions of MPO rather than a single epitope. Another explanation could be that the native MPO differs from recombinant MPO as a result of post-translational modification and changes in protein folding, which affect the exposure of immunogenic epitopes. For example, different studies have shown that ANCA only binds to the MPO holoenzyme and not denatured MPO, which suggests a conformational nature of the target MPO epitopes (Falk, Becker et al. 1992; Tadros, Pozzi et al. 1993). As a result, antibodies generated following immunisation with MPO peptides or recombinant MPO are not necessarily as pathogenic as anti-murine MPO antibodies.

6.2.2. What was the idea behind the maternal transfer experiment?

The current model of vasculitis requires the immunisation of a large number of MPO-/- mice with murine MPO in order to raise anti-MPO antibodies, which can then be used to induce disease in WT mice. We thought that it would be possible to reduce the number of mice needed for immunisation if we could develop vasculitis in newborn mice from mothers immunised with MPO. One of the well-known pieces of clinical evidence of ANCA pathogenicity came when a neonate developed pulmonary-renal syndrome following transplacental transfer of MPO-ANCA from the mother (Bansal and Tobin 2004). I immunised MPO-/- females with MPO peptides and then mated them with WT males to produce heterozygous offspring. Although the newborn mice did not develop vasculitis, they showed detectable levels of anti-MPO peptides antibodies in ELISA. This is an encouraging

finding which shows that anti-MPO antibodies were transferred from the mother to offspring. The reason why these offspring did not develop vasculitis could be because MPO peptides and not native MPO was used to immunise the mothers. As I explained earlier, MPO peptides may not be sufficient to induce anti-murine MPO antibodies. The only way to confirm this is to use murine MPO for immunisation and then investigate if newborn mice develop vasculitis.

6.3. Macrophage phenotype

I investigated macrophage accumulation in the mouse kidney following disease induction. In addition, I studied the macrophage phenotype and whether they were classically or alternatively activated.

6.3.1. Macrophage infiltration into the kidney

I found strong positive staining of a macrophage marker (CD68) in the kidney following disease induction. There was a positive correlation between the number of macrophages and the percentage of crescents, which suggests the involvement of macrophages in the development of vasculitis. In addition, I found that most CD68+ macrophages were observed in the crescents. These results are in agreement with previous work performed by Xiao et al. (Xiao, Heeringa et al. 2005), where they showed an accumulation of neutrophils and macrophages as a result of anti-MPO-induced NGCN.

6.3.2. What are the phenotypes of accumulating macrophages?

I investigated the type of accumulated macrophage in the kidney using different markers that should identify M1 and M2 macrophages. The mannose receptor is a well-known M2 marker and I used it to identify alternatively activated macrophages. My results showed that most CD68+ macrophages in the crescents did not express the mannose receptor, which suggests that they were classically activated macrophages. Macrophages include different subsets of cells that differ in their functions and phenotypic plasticity. Their functions in renal

diseases are very diverse as they can be involved in both renal inflammation and fibrosis. On the other hand, they could have an anti-inflammatory role that involves tissue remodelling and wound healing (Wang and Harris 2011). The M2 macrophages secrete anti-inflammatory cytokines and are reported to reduce organ injury (Herbert, Holscher et al. 2004). The macrophages in our mouse model were most likely to be pro-inflammatory M1 macrophages as they lacked expression of the mannose receptor, which is an M2 marker. It would be more convincing if double staining was done to study macrophage phenotype. However, I was not able to do double staining because of the antibodies available as explained in Chapter 4. Nevertheless, serial sections that were used in my experiment can be used successfully to identify the same areas on the tissue and used to compare two different markers and whether they are on the same cells or different cells.

6.3.3. What genes are associated with macrophage activation in the glomeruli?

I wanted to investigate the characteristics of macrophages in the glomeruli by studying gene expression and whether or not there were any genes associated with macrophage activation. I found several genes that were associated with macrophage activation, such as calprotectin (S100a9 and S100a8), F4/80, CXCL2 and other genes. In addition, I found an upregulation of chemokine and cytokine receptors involved in macrophage infiltration, such as CCR2 and CX3CR1. In addition, Furuichi et al. demonstrated the involvement of CCR2 in ischaemia-reperfusion injury in the kidney (Furuichi, Wada et al. 2003). They also showed a reduction in the amount of macrophage infiltration in CCR2-deficient mice. Another chemokine receptor that could be involved in macrophage infiltration is CX3CR1, which was upregulated in mouse glomeruli. Auffray et al. showed an association between the commitment of myeloid progenitors to the monocyte/macrophage/DC lineage and CX3CR1 (Auffray, Fogg et al. 2009). Furthermore, Li et al. demonstrated the involvement of CCR2 and CX3CR1 in monocyte/macrophage infiltration during kidney ischaemia-reperfusion injury (Li, Huang et al. 2008). They found that CCR2 and CX3CR1 play an important role in inflamed monocyte recruitment in the kidney and they also showed that CX3CR1-deficient

mice are protected from ischaemia-reperfusion injury. I believe that CCR2 and CX3CR1 are involved in macrophage infiltration in ANCA-associated vasculitis. In my model, I think that macrophages are recruited to the kidney at an early stage of the disease via chemotactic gradient. Lipopolysaccharide stimulate macrophages to secrete TNF-α which results in the activation of macrophages and the expression of ANCA-antigens on the surface of neutrophils. This allows ANCA to bind to these antigens causing neutrophil degranulation and release of ROS and chemokines which results in the recruitment of CCR2+ monocytes. These monocytes differentiate in to classically activate macrophages and release pro-inflammatory cytokines such as TNF-α, IL-1, and TGF-β. I have observed 1.8 fold increases in the glomeruli for VCAM-1 which is an adhesion molecule critical for monocyte recruitment. In addition, macrophage adhesion to endothelium could be CD44-dependent as this antigen was upregulated in mouse glomeruli and shown previously to be involved in macrophage recruitment and adhesion (Hollingsworth, Li et al. 2007).

6.4. What function could macrophages have in ANCA-associated vasculitis?

Macrophages can be pro-inflammatory or anti-inflammatory depending on the type of activation. Classically activated macrophages (M1) secrete pro-inflammatory cytokines and are involved in tissue injury. On the other hand, alternatively activated macrophages secrete anti-inflammatory cytokines and could be involved in tissue repair. However, the function of macrophages is more complicated than that and there is evidence to suggest that macrophages do not stay committed to the same activation state. For example, M1 macrophages can change to M2-type macrophages following phagocytosis of apoptotic cells (Duffield 2003). Macrophage accumulation is a characteristic of most glomerular and interstitial kidney diseases. It is thought that macrophages initially accumulate to modulate the immune response and clear apoptotic cells. However, this function could later transform into an inflammatory role resulting in tissue destruction (Ricardo, van Goor et al. 2008).

I have shown some evidence via immunohistochemistry staining which indicates that classically activated macrophages were the dominant type in glomeruli (crescent). One of the genes upregulated in the glomeruli was collagen (Col1a1, Col1a2, Col3a1, Col5a1 and Col6a1) and the deposition of collagen can lead to fibrosis. Collagens and fibronectin are some of the extracellular matrix (ECM) proteins. Different factors could be responsible for collagen and fibronectin upregulation. One of these factors involves the action of transforming growth factor-beta 2 (TGF-β2) in the SMAD pathway (Zode, Sethi et al. 2011). Chaussepied et al. showed the ability of disease macrophages from Holstein-Friesian cattle to produce a high level of TGF-β2 (Chaussepied, Janski et al. 2010). It could be that macrophages accumulating in glomeruli produce TGF-β2, which then acts on the SMAD pathway to up-regulate the expression of collagens and fibronectin 1 by glomerular epithelial cells. Zode et al. demonstrated that TGF-β2 acts through SMAD2 and SMAD3 (Zode, Sethi et al. 2011). However, mice treated with anti-MPO antibodies did not develop fibrosis, which was opposite to what we expected. This could have been because the model represents the acute form of disease and only lasted 6 days; fibrosis may develop at a later stage of the disease. However, my results indicate that the fibrosis pathways are activated at a very early stage of disease, which may have therapeutic implications.

In addition, macrophages are thought to have a role in matrix destruction through the production of matrix metalloproteinases (MMPs) (Duffield 2003). There was slight upregulation (less than a two-fold increase) of MMP2, MMP12, MMP11 and MMP14 in mouse glomeruli. On the other hand, tissue inhibitor of metalloproteinase 1 (TIMP1), which has an inhibitory role against most of the known MMPs, was upregulated in mouse glomeruli by more than a 2-fold increase. Previous studies reported that the expression of TIMP-1 is predominant in the early stage of the disease (liver fibrosis) but that its expression decreases in later stages of liver fibrosis (Iredale, Benyon et al. 1998). In addition, Lin et al. showed the ability of TIMP-1 to inhibit rat mesangial cell apoptosis (Lin, Chen et al. 2002). It could be that we saw a high expression of TIMP-1 in mouse glomeruli because the

experiment was relatively short and the disease was still in its early stages. I observed a greater reduction in TIMP-1 expression in rat glomeruli while MMPs were still present. This could have been because the rat model has a relatively longer duration and this finding resembles what has been found in liver fibrosis explained earlier. The presence of TIMP-1 could inhibit the proteolytic activity of tissue macrophages, which could explain the absence of kidney fibrosis in our model.

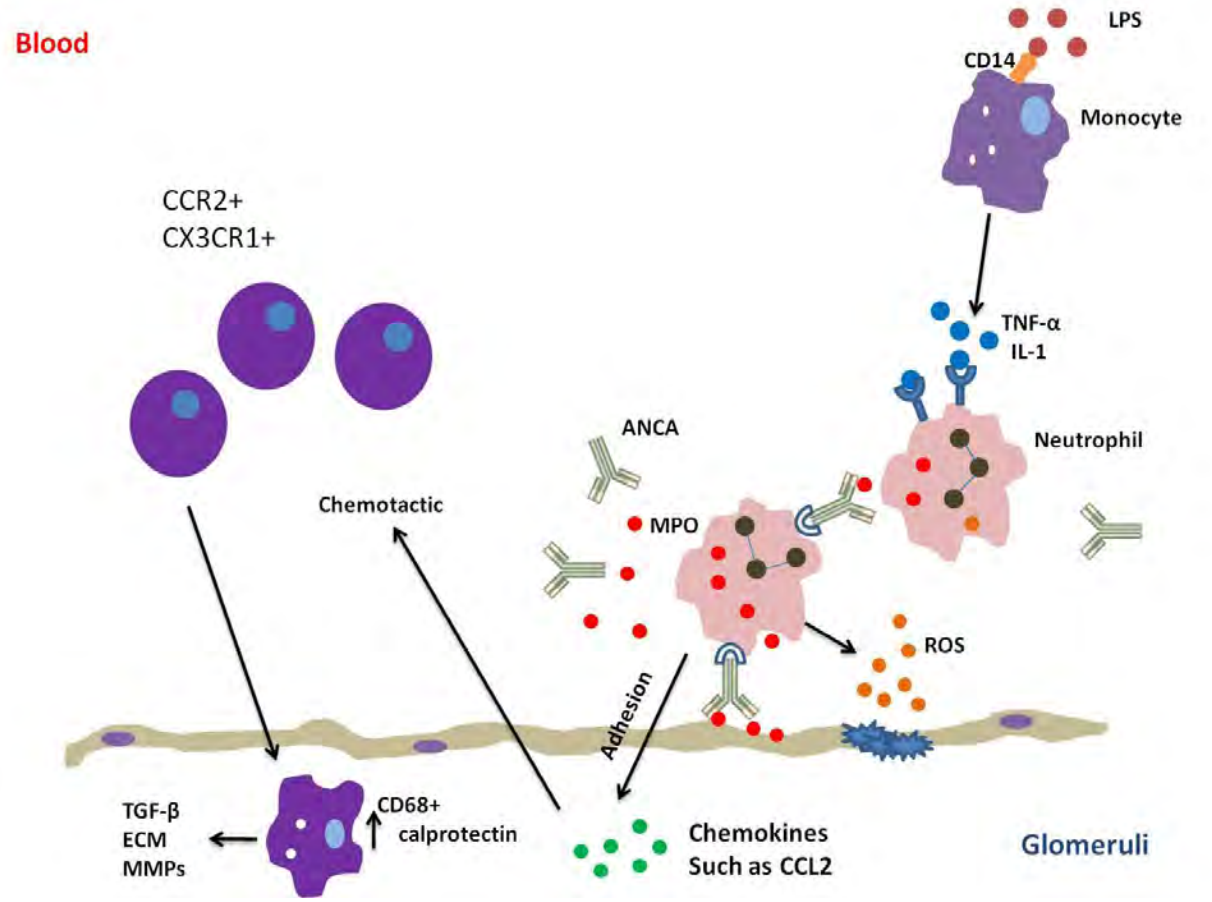

Figure 6.1: Proposed action of macrophages in crescentic glomerulonephritis. Neutrophils are stimulated by cytokines such as TNF-α which result in the migration of ANCA antigens to the surface allowing ANCA to bind to neutrophil. This results in neutrophil degranulation and release of ROS and also migration of neutrophils through the endothelium. Then, CCR2+ monocytes are recruited into the glomeruli following chemotactic gradient by CCL2. These monocytes are then differentiate in to macrophages in the tissue and secrete inflammatory cytokines such as TGF-β which result in formation of collagen and extracellular matrix (ECM) and matrix metalloproteinases (MMPs).

6.5. What are the effects of macrophage depletion on disease development?

I expected macrophages to be involved in the development of AAV in the mice as all of the evidence shown here suggests the presence of classically activated macrophages in the crescents. The logical approach of studying macrophage involvement in the disease was by either depleting them or preventing their accumulation in the kidney. The non-selective depletion of macrophages using clodronate was previously used to study the role of macrophages in different disease models (Jo, Sung et al. 2006). However, I found that clodronate had an effect on the passively transferred anti-MPO antibodies, as explained previously. I think it is very important to investigate this further as it could have affected the findings of previous work where clodronate was used in disease induced via the passive transfer of antibodies.

I have tried different approaches of studying macrophage involvement in AAV, for example, by blocking macrophage recruitment to the site of injury using anti-CCR2. However, the disease was mild and no difference was found in the percentage of crescents between anti-CCR2 treated mice and the control group. In addition, macrophages were detected in kidney sections from both the anti-CCR2 and control groups. This could mean that resident kidney macrophages were involved in the initiation of inflammation. Cailhier et al. demonstrated the importance of resident macrophages in initiating peritoneal inflammation in a peritonitis model (Cailhier, Partolina et al. 2005). However, the disease was mild in my experiment and it was difficult to reach any robust conclusions about the role of macrophages. I would suggest repeating the experiment and performing macrophage depletion using the diphtheria toxin approach, which was described in the introduction, or repeating the same experiment with anti-mouse CCR2.

6.6. What are the sources of variation in ANCA-induced neutrophil degranulation?

The severity of the disease and risk of relapse vary in patients with vasculitis (Jayne 2005). In addition, Little et al. showed that some rats are resistant to induced vasculitis, which suggests that genetic factors are involved in the development of this disease (Little, Smyth et al. 2009). Also, I found that the severity of this disease in mice varied after anti-MPO antibody injections. Furthermore, previous work in our laboratory showed a variation in ANCA-induced neutrophil degranulation and superoxide release. In addition, the severity of the disease, as measured by the level of serum creatinine, correlates with the number of activated intraglomerular neutrophils (Brouwer, Huitema et al. 1994). I wanted to investigate this further in order to understand more about the role of the innate immune system in vasculitis. I found variations in ANCA-induced neutrophil degranulation and that the sources of these variations mainly depended on the source of neutrophils and the ANCA source. Different factors can affect the variability of ANCA-induced neutrophil degranulation in healthy donors. One of these factors could be the availability of antigens on the surface of neutrophils. Muller Kobold et al. showed a correlation between disease activity and the expression of PR3 by neutrophils in Wegener's Granulomatosis (WG) (Muller Kobold, Kallenberg et al. 1998). I wanted to understand the mechanism behind the variability observed in our assays by studying the metabolomic profile of neutrophils following treatment with ANCA IgG. This is a novel approach and the aim was to investigate whether or not it was feasible in our samples. The advantage of this approach is that it is unbiased and looked at the effect in the whole cell. However, we found technical variations, as previously described in Chapter 5.

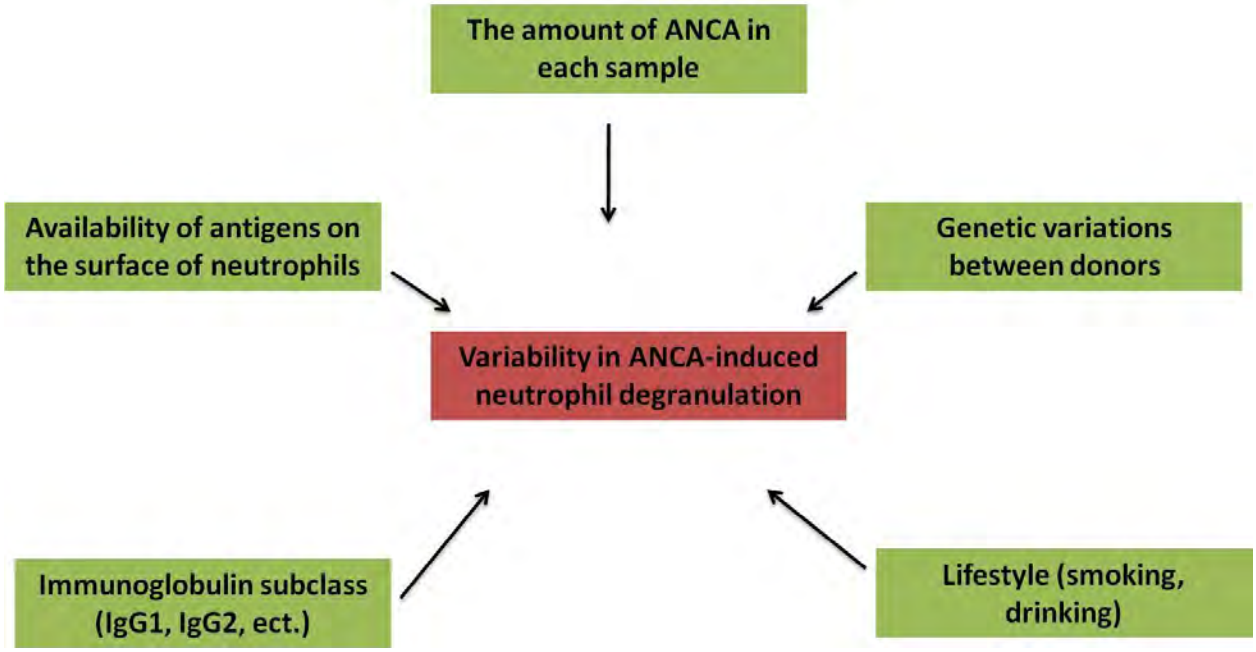

Figure 6.2: potential factors in the variability of ANCA-induced neutrophil degranulation. There are different factors that could contribute to the variations seen on my degranulation experiments.

Different factors may have contributed to the variations observed in our experiments. One of these factors could have been the biological nature of our samples which includes the variation in the lifestyle of different donors such as smoking and also the health of each donor and if they had an infection on that day. In addition, we introduced multiple factors in our experiment, such as donors and treatment variations; this made it difficult to study and compare neutrophil metabolomics. I think it is important to minimise the number of variables, at least at the start of the project, in order to understand how the samples behave and to make it easier to analyse. For future experiments, the neutrophils should be isolated from one healthy donor only and then treated with ANCA or normal IgG, which will reduce the number of variables.

6.7. What is the effect of simvastatin on ANCA-induced neutrophil degranulation?

We investigated the effect of the active form of simvastatin on ANCA-induced neutrophil degranulation *in vitro*. The idea came from my colleague Bahjat Al-Ani who was interested to see the effect of simvastatin vasculitis. Simvastatin significantly reduced ANCA-induced

neutrophil degranulation. Statin is an anti-inflammatory agent that has been reported to inhibit the upregulation of pro-inflammatory cytokines such as TNF-α and IFN-γ in the anti-GBM rat model (Fujita, Shimizu et al. 2010). Furthermore, it has been shown that neutrophil stimulation with TNF-α is necessary to cause ANCA-induced neutrophil degranulation *in vitro*. Tumor necrosis factor-α stimulates antigens to migrate to the surface of neutrophils, thus allowing ANCA to bind to them, triggering neutrophil degranulation. Simvastatin might act by blocking or inhibiting the action of TNF-α, which could result in the inhibition or a reduction in the level of antigen presentation on the surface of neutrophils. We hypothesised that simvastatin might result in the reduction of crescentic glomerulonephritis in rats. My colleague Bahjat Al-Ani treated rats that were immunised with human MPO with simvastatin. However, these rats developed crescentic glomerulonephritis and they were not protected following simvastatin treatment (Al-Ani, Al Nuaimi et al. 2011). A simvastatin suspension, which is used as a human drug, was used for this experiment; furthermore, it is known that simvastatin needs to be activated in the human liver. However, we do not know whether it became activated when given to the rats. On the other hand, the active form of simvastatin was used for the *in vitro* experiment. This could explain the absence of a simvastatin effect *in vivo*.

6.8. Future work

This thesis has led to some interesting findings and it would be useful to follow these further. First of all, I have shown that anti-recombinant MPO can be transferred from the mother to the newborn mice in maternal transfer experiment. It would be useful to investigate this further by using murine MPO instead of recombinant MPO to immunise MPO-/- female mice. I think that this experiment is worth repeating because it could help to reduce the number of mice needed for immunisation and it could also reduce the amount of MPO required.

In addition, it would be useful to increase the number of animals in macrophage depletion experiment to draw a final conclusion. However, I would use C57 mice if I was to repeat the experiment, as I have shown that we can induce a good disease in these mice. Anti-CCR2 was very effective in depleting GR1+ monocytes and it can be used in future experiments.

I would also like to further investigate the effect of clodronate on passively injected antibodies. We showed a significant reduction in the level of passively transferred antibodies following treatment with clodronate. This experiment could be repeated using either anti-MPO antibodies or other antibodies such as the anti-GBM antibody and then measure the level of the antibody in the serum following clodronate treatment.

Furthermore, it would be useful to further investigate the variability of ANCA-induced neutrophil degranulation. I would like to isolate neutrophils from patients with AAV and then stimulate the neutrophils with ANCA from the same patient or different vasculitis patients. This would help understand whether ANCA from certain patients is highly pathogenic or whether these patients are just more susceptible than others. I would also further investigate the possibility of studying neutrophil metabolomics, but I would consider minimising the number of variables in the experiment. I would start by isolating neutrophils from one healthy donor and then treating them with MPO-ANCA, PR3-ANCA or normal IgG. This would allow us to investigate the variability in neutrophil degranulation due to ANCA treatment only and not due to donor variations.

7. Appendix

7.1. Buffers for MPO isolation

Stock solutions

Stock solutions	g/mol	Weight (g)	Volume (ml)	Mol/L
$CaCl_2.2H_2O$	147	5.373	36.55	1.0
$MgCl_2.6H_2O$	203.3	8.444	41.6	1.0
CETAB		20	200	10%
$MnCl_2.4H_2O$	197.9	8.09	40.86	1.0
α-Methyl D-mannopyranoside	194.18	38.8	200	1.0
PMSF	174.2	0.871	50	0.1
Sodium acetate pH 6.0	136.1	68.05	500	1.0
Sodium acetate pH 6.3	136.1	68.05	500	1.0
NaCl	58.44	58.5	500	2.0

Buffer A (100 ml)

solutions	Stock (M)	End Concentration	Volume (ml)
Sodium acetate pH 6.0	1.0	0.0067	0.67
$MgCl_2.6H_2O$	1.0	0.003	0.30
NaCl	2.0	0.003	0.15
CETAB			10.00
PMSF			0.5
			Total: 11.62 + 88.38 H_2O

Buffer B (1 L)

solutions	Stock (M)	End Conc. (M)	Volume (ml)
Sodium acetate pH 6.3	1.0	0.1	100
NaCl	2.0	0.1	50
			Total: 150 + 850 H_2O

Buffer B Con A (100 ml)

Solutions	Stock (M)	End Conc. (M)	Volume (ml)
Sodium acetate pH 6.3	1.0	0.1	10.0
NaCl	2.0	0.1	5.0
$CaCl_2.2H_2O$	1.0	0.001	0.1
$MgCl_2.6H_2O$	1.0	0.001	0.1
$MnCl_2.4H_2O$	1.0	0.001	0.1
			Total: 15.3 + 84.7 H_2O

Buffer B Elution (100 ml)

Solutions	Stock Conc. (M)	End Conc. (M)	Volume (ml)
Sodium acetate pH 6.3	1.0	0.1	10.0
NaCl	2.0	0.1	5.0
$CaCl_2.2H_2O$	1.0	0.001	0.1
$MgCl_2.6H_2O$	1.0	0.001	0.1
$MnCl_2.4H_2O$	1.0	0.001	0.1
α-Methyl D-mannopyranoside	1.0	0.75	75.0
			Total: 90.3 + 9.7 H_2O

Buffer D

Solutions	Stock (M)	End Conc. (M)	Volume (ml)
Sodium Acetate PH 8.9	1.0	0.05	50
NaCl	2.0	0.1	50
			Total: 100 + 900 H_2O

Buffer E

Solutions	Stock (M)	End Conc. (M)	Volume (ml)
Sodium Acetate PH 8.9	1.0	0.05	50
NaCl	2.0	1.0	500
			Total: 550 + 450 H_2O

7.2. SDS-Page

10 % gel

% Gel	10%
Acrylamide	2.5 ml
Bis-acrylamide	650 µl
Tris PH 8.8	3.73 ml
10% SDS	100 µl
10% APS	100.5 µl
TEMED	7.5 µl
H_2O	2.948 ml

Stacking gel

% Gel	5 %
Acrylamide	500 µl
Bis-acrylamide	260 µl
Tris PH 6.8	500 µl
10% SDS	40 µl
10% APS	40 µl
TEMED	4 µl
H_2O	2.656 ml

7.3. Buffers for neutrophil isolation

7.3.1. ACD

4.2 g Disodium hydrogen citrate

5.0 g D-glucose

200 ml pyrogen-free water

7.3.2. Dextran 2 %

9.0 g NaCl

20 g Dextran T500

1 L pyrogen-free water

7.3.3. HBH

500 ml Hanks buffered salt solution

5 ml 1M HEPES

7.4. Buffers for anti-MPO ELISA

7.4.1. Carbonate buffer (0.015 M)

0.795 g Na_2CO_3

1.465 g sodium hydrogen carbonate

500 ml H_2O

7.5. General linear modelling results of chapter 5

Table 7.1: General linear modelling of the factors contributing to variability in superoxide (n=345) and degranulation (n=343) assays. The R^2 value reflects how well the model accounts for the observed variability in the data (maximum=1) and the Partial η^2 value reflects how much each factor contributes to the observed variability (maximum=1).

	Model R^2	Partial η^2		Model R^2	Partial η^2
Superoxide release			**Degranulation**		
Model 1	0.18		Model 1	0.46	
ANCA source		0.18	ANCA source		0.46
Model 2	0.40		Model 2	0.18	
Neutrophil donor		0.40	Neutrophil donor		0.18
Model 3	0.77		Model 3	0.91	
ANCA source		0.38	ANCA source		0.66
Neutrophil donor		0.64	Neutrophil donor		0.83
Model 4	0.99		Model 4	0.97	
ANCA source		0.95	ANCA source		0.91
Neutrophil donor		0.92	Neutrophil donor		0.83
Assay month		0.95	Assay month		0.04

8. References

Aird, W. C. (2007). "Phenotypic heterogeneity of the endothelium: II. Representative vascular beds." Circ Res **100**(2): 174-90.

Aitman, T. J., R. Dong, et al. (2006). "Copy number polymorphism in Fcgr3 predisposes to glomerulonephritis in rats and humans." Nature **439**(7078): 851-5.

Al-Ani, B., H. Al Nuaimi, et al. (2011). "The beneficial effects of statin therapy may not apply to all forms of crescentic glomerulonephritis." Am J Pathol **178**(5): 2447; author reply 2447-8.

Al-Ani, B., H. Al Nuaimi, et al. (2010). Inhibition of ANCA-induced neutrophil stimulation by simvastatin. Renal Association. Manchester**:** 425.

Alves-Rosa, F., C. Stanganelli, et al. (2000). "Treatment with liposome-encapsulated clodronate as a new strategic approach in the management of immune thrombocytopenic purpura in a mouse model." Blood **96**(8): 2834-40.

Anders, H. J., M. Frink, et al. (2003). "CC chemokine ligand 5/RANTES chemokine antagonists aggravate glomerulonephritis despite reduction of glomerular leukocyte infiltration." J Immunol **170**(11): 5658-66.

Anderson, C. F. and D. M. Mosser (2002). "Cutting edge: biasing immune responses by directing antigen to macrophage Fc gamma receptors." J Immunol **168**(8): 3697-701.

Anderson, C. F. and D. M. Mosser (2002). "A novel phenotype for an activated macrophage: the type 2 activated macrophage." J Leukoc Biol **72**(1): 101-6.

Andrews, P. C., C. Parnes, et al. (1984). "Comparison of myeloperoxidase and hemi-myeloperoxidase with respect to catalysis, regulation, and bactericidal activity." Arch Biochem Biophys **228**(2): 439-42.

Apostolopoulos, J., J. D. Ooi, et al. (2006). "The isolation and purification of biologically active recombinant and native autoantigens for the study of autoimmune disease." J Immunol Methods **308**(1-2): 167-78.

Atkins, R. C., S. R. Holdsworth, et al. (1976). "The macrophage in human rapidly progressive glomerulonephritis." Lancet **1**(7964): 830-2.

Auffray, C., D. K. Fogg, et al. (2009). "CX3CR1+ CD115+ CD135+ common macrophage/DC precursors and the role of CX3CR1 in their response to inflammation." J Exp Med **206**(3): 595-606.

Auffray, C., M. H. Sieweke, et al. (2009). "Blood monocytes: development, heterogeneity, and relationship with dendritic cells." Annu Rev Immunol **27**: 669-92.

Bagchus, W. M., M.F.Jeunink, et al. (1990). "The mesangium in anti-Thy-1 nephritis. Influx of macrophages, mesangial cell hypercellularity, and macromolecular accumulation." Am J Pathol. **137**(1): 9.

Balding, C. E., A. J. Howie, et al. (2001). "Th2 dominance in nasal mucosa in patients with Wegener's granulomatosis." Clin Exp Immunol **125**(2): 332-9.

Ballieux, B. E., P. S. Hiemstra, et al. (1994). "Detachment and cytolysis of human endothelial cells by proteinase 3." Eur J Immunol **24**(12): 3211-5.

Bansal, P. J. and M. C. Tobin (2004). "Neonatal microscopic polyangiitis secondary to transfer of maternal myeloperoxidase-antineutrophil cytoplasmic antibody resulting in neonatal pulmonary hemorrhage and renal involvement." Ann Allergy Asthma Immunol **93**(4): 398-401.

Behmoaras, J., G. Bhangal, et al. (2008). "Jund is a determinant of macrophage activation and is associated with glomerulonephritis susceptibility." Nat Genet **40**(5): 553-9.

Belge, K. U., F. Dayyani, et al. (2002). "The proinflammatory CD14+CD16+DR++ monocytes are a major source of TNF." J Immunol **168**(7): 3536-42.

Boomsma, M. M., C. A. Stegeman, et al. (2000). "Prediction of relapses in Wegener's granulomatosis by measurement of antineutrophil cytoplasmic antibody levels: a prospective study." Arthritis Rheum **43**(9): 2025-33.

Booth, A. D., M. K. Almond, et al. (2003). "Outcome of ANCA-associated renal vasculitis: a 5-year retrospective study." Am J Kidney Dis **41**(4): 776-84.

Border, W. A. and N. A. Noble (1994). "Transforming growth factor beta in tissue fibrosis." N Engl J Med **331**(19): 1286-92.

Border, W. A. and N. A. Noble (1997). "TGF-beta in kidney fibrosis: a target for gene therapy." Kidney Int **51**(5): 1388-96.

Boswell, J. M., M. A. Yui, et al. (1988). "Increased tumor necrosis factor and IL-1 beta gene expression in the kidneys of mice with lupus nephritis." J Immunol **141**(9): 3050-4.

Boyce, N. W., P. G. Tipping, et al. (1989). "Glomerular macrophages produce reactive oxygen species in experimental glomerulonephritis." Kidney Int **35**(3): 778-82.

Brooimans, R. A., A. P. Stegmann, et al. (1991). "Interleukin 2 mediates stimulation of complement C3 biosynthesis in human proximal tubular epithelial cells." J Clin Invest **88**(2): 379-84.

Brouwer, E., M. G. Huitema, et al. (1993). "Antimyeloperoxidase-associated proliferative glomerulonephritis: an animal model." J Exp Med **177**(4): 905-14.

Brouwer, E., M. G. Huitema, et al. (1994). "Neutrophil activation in vitro and in vivo in Wegener's granulomatosis." Kidney Int **45**(4): 1120-31.

Brouwer, E., J. J. Weening, et al. (1993). "Induction of an humoral and cellular (auto) immune response to human and rat myeloperoxidase(MPO) in Brown-Norway(BN), Lewis and Wistar Kyoto(WKY) rat strains." Adv Exp Med Biol **336**: 139-42.

Bruhl, H., J. Cihak, et al. (2007). "Targeting of Gr-1+,CCR2+ monocytes in collagen-induced arthritis." Arthritis Rheum **56**(9): 2975-85.

Cailhier, J. F., M. Partolina, et al. (2005). "Conditional macrophage ablation demonstrates that resident macrophages initiate acute peritoneal inflammation." J Immunol **174**(4): 2336-42.

Cattell, V. (1994). "Macrophages in acute glomerular inflammation." Kidney Int **45**(4): 945-52.

Cecchini, M. G., M. G. Dominguez, et al. (1994). "Role of colony stimulating factor-1 in the establishment and regulation of tissue macrophages during postnatal development of the mouse." Development **120**(6): 1357-72.

Charles, L. A., M. L. Caldas, et al. (1991). "Antibodies against granule proteins activate neutrophils in vitro." J Leukoc Biol **50**(6): 539-46.

Chaussepied, M., N. Janski, et al. (2010). "TGF-b2 induction regulates invasiveness of Theileria-transformed leukocytes and disease susceptibility." PLoS Pathog **6**(11): e1001197.

Chavele, K. M., L. Martinez-Pomares, et al. (2010). "Mannose receptor interacts with Fc receptors and is critical for the development of crescentic glomerulonephritis in mice." J Clin Invest **120**(5): 1469-78.

Chen, M. and C. G. Kallenberg (2010). "ANCA-associated vasculitides--advances in pathogenesis and treatment." Nat Rev Rheumatol **6**(11): 653-64.

Chen, M. and C. G. Kallenberg (2010). "The environment, geoepidemiology and ANCA-associated vasculitides." Autoimmun Rev **9**(5): A293-8.

Chen, S., K. B. Bacon, et al. (1998). "In vivo inhibition of CC and CX3C chemokine-induced leukocyte infiltration and attenuation of glomerulonephritis in Wistar-Kyoto (WKY) rats by vMIP-II." J Exp Med **188**(1): 193-8.

Chen, Y. and K. J. Wood (2007). "Interleukin-23 and TH17 cells in transplantation immunity: does 23+17 equal rejection?" Transplantation **84**(9): 1071-4.

Cho, R. J. and M. J. Campbell (2000). "Transcription, genomes, function." Trends Genet **16**(9): 409-15.

Choi, M., S. Rolle, et al. (2003). "Extracellular signal-regulated kinase inhibition by statins inhibits neutrophil activation by ANCA." Kidney Int **63**(1): 96-106.

Cittera, E., M. Leidi, et al. (2007). "The CCL3 family of chemokines and innate immunity cooperate in vivo in the eradication of an established lymphoma xenograft by rituximab." J Immunol **178**(10): 6616-23.

Claassen I, Van Rooijen N, et al. (1990). "A new method for removal of mononuclear phagocytes from heterogeneous cell populations in vitro, using the liposome-mediated macrophage 'suicide' technique." J Immunol Methods. **134**(2): 9.

Claassen, I., N. Van Rooijen, et al. (1990). "A new method for removal of mononuclear phagocytes from heterogeneous cell populations in vitro, using the liposome-mediated macrophage 'suicide' technique." J Immunol Methods **134**(2): 153-61.

Cockwell, P., C. J. Brooks, et al. (1999). "Interleukin-8: A pathogenetic role in antineutrophil cytoplasmic autoantibody-associated glomerulonephritis." Kidney Int **55**(3): 852-63.

Cockwell, P., A. J. Howie, et al. (1998). "In situ analysis of C-C chemokine mRNA in human glomerulonephritis." Kidney Int **54**(3): 827-36.

Cook, H. T., S. J. Singh, et al. (1999). "Interleukin-4 ameliorates crescentic glomerulonephritis in Wistar Kyoto rats." Kidney Int **55**(4): 1319-26.

Cook, H. T., J. Smith, et al. (1989). "Functional characteristics of macrophages in glomerulonephritis in the rat. O2- generation, MHC class II expression, and eicosanoid synthesis." Am J Pathol **134**(2): 431-7.

Cotch, M. F., A. S. Fauci, et al. (1995). "HLA typing in patients with Wegener granulomatosis." Ann Intern Med **122**(8): 635.

Csernok, E., M. Ernst, et al. (1994). "Activated neutrophils express proteinase 3 on their plasma membrane in vitro and in vivo." Clin Exp Immunol **95**(2): 244-50.

Csernok, E., C. H. Szymkowiak, et al. (1996). "Transforming growth factor-beta (TGF-beta) expression and interaction with proteinase 3 (PR3) in anti-neutrophil cytoplasmic antibody (ANCA)-associated vasculitis." Clin Exp Immunol **105**(1): 104-11.

Dai, X. M., G. R. Ryan, et al. (2002). "Targeted disruption of the mouse colony-stimulating factor 1 receptor gene results in osteopetrosis, mononuclear phagocyte deficiency, increased primitive progenitor cell frequencies, and reproductive defects." Blood **99**(1): 111-20.

Davies, D. J., J. E. Moran, et al. (1982). "Segmental necrotising glomerulonephritis with antineutrophil antibody: possible arbovirus aetiology?" Br Med J (Clin Res Ed) **285**(6342): 606.

Day, C. J., P. Hewins, et al. (2003). "New developments in the pathogenesis of ANCA-associated vasculitis." Clin Exp Rheumatol **21**(6 Suppl 32): S35-48.

de Lind van Wijngaarden, R. A. F., L. van Rijn, et al. (2008). "Hypotheses on the etiology of antineutrophil cytoplasmic autoantibody associated vasculitis: The cause is hidden, but the result is known." Clin J Am Soc Nephrol **3**(1): 237-252.

Deguchi, Y., N. Shibata, et al. (1990). "Enhanced expression of the tumour necrosis factor/cachectin gene in peripheral blood mononuclear cells from patients with systemic vasculitis." Clin Exp Immunol **81**(2): 311-4.

Devey, L., D. Ferenbach, et al. (2009). "Tissue-resident macrophages protect the liver from ischemia reperfusion injury via a heme oxygenase-1-dependent mechanism." Mol Ther **17**(1): 65-72.

Diamond, J. R. and I. Pesek-Diamond (1991). "Sublethal X-irradiation during acute puromycin nephrosis prevents late renal injury: role of macrophages." Am J Physiol **260**(6 Pt 2): F779-86.

Dieterle, F., A. Ross, et al. (2006). "Probabilistic quotient normalization as robust method to account for dilution of complex biological mixtures. Application in 1H NMR metabonomics." Anal Chem **78**(13): 4281-90.

Dijstelbloem, H. M., J. G. van de Winkel, et al. (2001). "Inflammation in autoimmunity: receptors for IgG revisited." Trends Immunol **22**(9): 510-6.

Doyle, A. G., G. Herbein, et al. (1994). "Interleukin-13 alters the activation state of murine macrophages in vitro: comparison with interleukin-4 and interferon-gamma." Eur J Immunol **24**(6): 1441-5.

Duffield, J. S. (2003). "The inflammatory macrophage: a story of Jekyll and Hyde." Clin Sci (Lond) **104**(1): 27-38.

Duffield, J. S., P. G. Tipping, et al. (2005). "Conditional Ablation of Macrophages Halts Progression of Crescentic Glomerulonephritis." Am J Pathol **167**(5): 1207-1219.

Eddy, A. A. (2005). "Progression in chronic kidney disease." Adv Chronic Kidney Dis **12**(4): 353-65.

Eiserich, J. P., S. Baldus, et al. (2002). "Myeloperoxidase, a leukocyte-derived vascular NO oxidase." Science **296**(5577): 2391-4.

Eiserich, J. P., M. Hristova, et al. (1998). "Formation of nitric oxide-derived inflammatory oxidants by myeloperoxidase in neutrophils." Nature **391**(6665): 393-7.

Erdbrugger, U., T. Hellmark, et al. (2006). "Mapping of myeloperoxidase epitopes recognized by MPO-ANCA using human-mouse MPO chimers." Kidney Int **69**(10): 1799-805.

Ewert, B. H., J. C. Jennette, et al. (1992). "Anti-myeloperoxidase antibodies stimulate neutrophils to damage human endothelial cells." Kidney Int **41**(2): 375-83.

Falk, R. J., M. Becker, et al. (1992). "Anti-myeloperoxidase autoantibodies react with native but not denatured myeloperoxidase." Clin Exp Immunol **89**(2): 274-8.

Falk, R. J. and J. C. Jennette (1988). "Anti-neutrophil cytoplasmic autoantibodies with specificity for myeloperoxidase in patients with systemic vasculitis and idiopathic necrotizing and crescentic glomerulonephritis." N Engl J Med **318**(25): 1651-7.

Falk, R. J., P. H. Nachman, et al. (2000). "ANCA glomerulonephritis and vasculitis: a Chapel Hill perspective." Semin Nephrol **20**(3): 233-43.

Falk, R. J., R. S. Terrell, et al. (1990). "Anti-neutrophil cytoplasmic autoantibodies induce neutrophils to degranulate and produce oxygen radicals in vitro." Proc Natl Acad Sci U S A **87**(11): 4115-9.

Faurschou, M. and N. Borregaard (2003). "Neutrophil granules and secretory vesicles in inflammation." Microbes Infect **5**(14): 1317-27.

Fenton, M. J., J. A. Buras, et al. (1992). "IL-4 reciprocally regulates IL-1 and IL-1 receptor antagonist expression in human monocytes." J Immunol **149**(4): 1283-8.

Ferenbach, D. A., N. C. Nkejabega, et al. (2011). "The induction of macrophage hemeoxygenase-1 is protective during acute kidney injury in aging mice." Kidney Int.

Finkielman, J. D., P. A. Merkel, et al. (2007). "Antiproteinase 3 Antineutrophil Cytoplasmic Antibodies and Disease Activity in Wegener Granulomatosis." Ann Intern Med **147**(9): 611-619.

Flory, C. M., M. L. Jones, et al. (1993). "Pulmonary granuloma formation in the rat is partially dependent on monocyte chemoattractant protein 1." Lab Invest **69**(4): 396-404.

Fogg, D. K., C. Sibon, et al. (2006). "A clonogenic bone marrow progenitor specific for macrophages and dendritic cells." Science **311**(5757): 83-7.

Frankenberger, M., T. Sternsdorf, et al. (1996). "Differential cytokine expression in human blood monocyte subpopulations: a polymerase chain reaction analysis." Blood **87**(1): 373-7.

Franssen, C. F., M. G. Huitema, et al. (1999). "In vitro neutrophil activation by antibodies to proteinase 3 and myeloperoxidase from patients with crescentic glomerulonephritis." J Am Soc Nephrol **10**(7): 1506-15.

Fujita, E., A. Shimizu, et al. (2010). "Statin attenuates experimental anti-glomerular basement membrane glomerulonephritis together with the augmentation of alternatively activated macrophages." Am J Pathol **177**(3): 1143-54.

Fujiu, K., I. Manabe, et al. (2011). "Renal collecting duct epithelial cells regulate inflammation in tubulointerstitial damage in mice." J Clin Invest.

Furtmuller, P. G., M. Zederbauer, et al. (2006). "Active site structure and catalytic mechanisms of human peroxidases." Arch Biochem Biophys **445**(2): 199-213.

Furuichi, K., T. Wada, et al. (2003). "CCR2 signaling contributes to ischemia-reperfusion injury in kidney." J Am Soc Nephrol **14**(10): 2503-15.

Geissmann, F., S. Jung, et al. (2003). "Blood monocytes consist of two principal subsets with distinct migratory properties." Immunity **19**(1): 71-82.

Ginhoux, F., F. Tacke, et al. (2006). "Langerhans cells arise from monocytes in vivo." Nat Immunol **7**(3): 265-73.

Gordon, S. (2002). "Pattern recognition receptors: doubling up for the innate immune response." Cell **111**(7): 927-30.

Gordon, S. (2003). "Alternative activation of macrophages." Nat Rev Immunol **3**(1): 23-35.

Gordon, S. and P. R. Taylor (2005). "Monocyte and macrophage heterogeneity." Nat Rev Immunol **5**(12): 953-64.

Griffith, M. E., J. U. Lovegrove, et al. (1996). "C-antineutrophil cytoplasmic antibody positivity in vasculitis patients is associated with the Z allele of alpha-1-antitrypsin, and P-antineutrophil cytoplasmic antibody positivity with the S allele." Nephrol Dial Transplant **11**(3): 438-43.

Guchhait, P., M. F. Tosi, et al. (2003). "The murine myeloid cell line 32Dcl3 as a model system for studying neutrophil functions." J Immunol Methods **283**(1-2): 195-204.

Gueler, F., J. K. Park, et al. (2007). "Statins attenuate ischemia-reperfusion injury by inducing heme oxygenase-1 in infiltrating macrophages." Am J Pathol **170**(4): 1192-9.

Guilpain, P., A. Servettaz, et al. (2007). "Pathogenic effects of antimyeloperoxidase antibodies in patients with microscopic polyangiitis." Arthritis Rheum **56**(7): 2455-63.

Hamour, S., A. D. Salama, et al. (2010). "Management of ANCA-associated vasculitis: Current trends and future prospects." Ther Clin Risk Manag **6**: 253-64.

Hara, M., S. R. Batsford, et al. (1991). "Complement and monocytes are essential for provoking glomerular injury in passive Heymann nephritis in rats. Terminal

complement components are not the sole mediators of proteinuria." Lab Invest **65**(2): 168-79.

Harper, L., Y. Ren, et al. (2000). "Antineutrophil cytoplasmic antibodies induce reactive oxygen-dependent dysregulation of primed neutrophil apoptosis and clearance by macrophages." Am J Pathol **157**(1): 211-20.

Heeringa, P., E. Brouwer, et al. (1998). "Animal models of anti-neutrophil cytoplasmic antibody associated vasculitis." Kidney Int **53**(2): 253-63.

Heeringa, P. and J. W. Tervaert (2004). "Pathophysiology of ANCA-associated vasculitides: are ANCA really pathogenic?" Kidney Int **65**(5): 1564-7.

Hellmich, B., E. Csernok, et al. (2000). "Granulocyte-macrophage colony-stimulating factor (GM-CSF) but not granulocyte colony-stimulating factor (G-CSF) induces plasma membrane expression of proteinase 3 (PR3) on neutrophils in vitro." Clin Exp Immunol **120**(2): 392-8.

Henneman, L., A. G. van Cruchten, et al. (2011). "Inhibition of the isoprenoid biosynthesis pathway; detection of intermediates by UPLC-MS/MS." Biochim Biophys Acta **1811**(4): 227-33.

Herbert, D. R., C. Holscher, et al. (2004). "Alternative macrophage activation is essential for survival during schistosomiasis and downmodulates T helper 1 responses and immunopathology." Immunity **20**(5): 623-35.

Hewins, P., M. D. Morgan, et al. (2006). "IL-18 is upregulated in the kidney and primes neutrophil responsiveness in ANCA-associated vasculitis." Kidney Int **69**(3): 605-15.

Hogan, S. L., K. K. Satterly, et al. (2001). "Silica exposure in anti-neutrophil cytoplasmic autoantibody-associated glomerulonephritis and lupus nephritis." J Am Soc Nephrol **12**(1): 134-42.

Holdsworth, S. R. and T. J. Neale (1984). "Macrophage-induced glomerular injury. Cell transfer studies in passive autologous antiglomerular basement membrane antibody-initiated experimental glomerulonephritis." Lab Invest **51**(2): 172-80.

Holdsworth, S. R., T. J. Neale, et al. (1981). "Abrogation of macrophage-dependent injury in experimental glomerulonephritis in the rabbit. Use of an antimacrophage serum." J Clin Invest **68**(3): 686-98.

Holle, J. U. and W. L. Gross (2009). "ANCA-associated vasculitides: pathogenetic aspects and current evidence-based therapy." J Autoimmun **32**(3-4): 163-71.

Hollingsworth, J. W., Z. Li, et al. (2007). "CD44 regulates macrophage recruitment to the lung in lipopolysaccharide-induced airway disease." Am J Respir Cell Mol Biol **37**(2): 248-53.

Huang, X. R., P. G. Tipping, et al. (1997). "Mechanisms of T cell-induced glomerular injury in anti-glomerular basement membrane (GBM) glomerulonephritis in rats." Clin Exp Immunol **109**(1): 134-42.

Huffnagle, G. B., R. M. Strieter, et al. (1995). "The role of monocyte chemotactic protein-1 (MCP-1) in the recruitment of monocytes and CD4+ T cells during a pulmonary Cryptococcus neoformans infection." J Immunol **155**(10): 4790-7.

Hulett, M. D. and P. M. Hogarth (1994). "Molecular basis of Fc receptor function." Adv Immunol **57**: 1-127.

Huugen, D., H. Xiao, et al. (2005). "Aggravation of Anti-Myeloperoxidase Antibody-Induced Glomerulonephritis by Bacterial Lipopolysaccharide: Role of Tumor Necrosis Factor-{alpha}." Am J Pathol **167**(1): 47-58.

Ikezumi, Y., L. A. Hurst, et al. (2003). "Adoptive transfer studies demonstrate that macrophages can induce proteinuria and mesangial cell proliferation." Kidney Int **63**(1): 83-95.

Iredale, J. P., R. C. Benyon, et al. (1998). "Mechanisms of spontaneous resolution of rat liver fibrosis. Hepatic stellate cell apoptosis and reduced hepatic expression of metalloproteinase inhibitors." J Clin Invest **102**(3): 538-49.

Iwasaki, H. and K. Akashi (2007). "Myeloid lineage commitment from the hematopoietic stem cell." Immunity **26**(6): 726-40.

Jakubzick, C., E. S. Choi, et al. (2003). "Impact of interleukin-13 responsiveness on the synthetic and proliferative properties of Th1- and Th2-type pulmonary granuloma fibroblasts." Am J Pathol **162**(5): 1475-86.

Jakubzick, C., F. Tacke, et al. (2008). "Blood monocyte subsets differentially give rise to CD103+ and CD103- pulmonary dendritic cell populations." J Immunol **180**(5): 3019-27.

Jayne, D. (2005). "How to induce remission in primary systemic vasculitis." Best Pract Res Clin Rheumatol **19**(2): 293-305.

Jayne, D., N. Rasmussen, et al. (2003). "A randomized trial of maintenance therapy for vasculitis associated with antineutrophil cytoplasmic autoantibodies." N Engl J Med **349**(1): 36-44.

Jayne, D. R., A. P. Weetman, et al. (1991). "IgG subclass distribution of autoantibodies to neutrophil cytoplasmic antigens in systemic vasculitis." Clin Exp Immunol **84**(3): 476-81.

Jennette, J. C., H. Xiao, et al. (2006). "Pathogenesis of vascular inflammation by anti-neutrophil cytoplasmic antibodies." J Am Soc Nephrol **17**(5): 1235-42.

Jiang, W., M. S. Anderson, et al. (2005). "Modifier loci condition autoimmunity provoked by Aire deficiency." J Exp Med **202**(6): 805-15.

Jo, S. K., S. A. Sung, et al. (2006). "Macrophages contribute to the initiation of ischaemic acute renal failure in rats." Nephrol Dial Transplant **21**(5): 1231-9.

Johnson, R. J., W. G. Couser, et al. (1987). "New mechanism for glomerular injury. Myeloperoxidase-hydrogen peroxide-halide system." J Clin Invest **79**(5): 1379-87.

Jordan, M. B., N. van Rooijen, et al. (2003). "Liposomal clodronate as a novel agent for treating autoimmune hemolytic anemia in a mouse model." Blood **101**(2): 594-601.

Kain, R., M. Exner, et al. (2008). "Molecular mimicry in pauci-immune focal necrotizing glomerulonephritis." Nat Med **14**(10): 1088-96.

Kallenberg, C. G. and H. Tadema (2008). "Vasculitis and infections: contribution to the issue of autoimmunity reviews devoted to "autoimmunity and infection"." Autoimmun Rev **8**(1): 29-32.

Kanno, T., K. Abe, et al. (1999). "Selective inhibition of formyl-methionyl-leucyl-phenylalanine (fMLF)-dependent superoxide generation in neutrophils by pravastatin, an inhibitor of 3-hydroxy-3-methylglutaryl coenzyme A (HMG-CoA) reductase." Biochem Pharmacol **58**(12): 1975-80.

Karkar, A. M., J. Smith, et al. (2001). "Prevention and treatment of experimental crescentic glomerulonephritis by blocking tumour necrosis factor-alpha." Nephrol Dial Transplant **16**(3): 518-24.

Keogan, M. T., V. L. Esnault, et al. (1992). "Activation of normal neutrophils by anti-neutrophil cytoplasm antibodies." Clin Exp Immunol **90**(2): 228-34.

Kessenbrock, K., M. Krumbholz, et al. (2009). "Netting neutrophils in autoimmune small-vessel vasculitis." Nat Med **15**(6): 623-5.

Kettritz, R., J. C. Jennette, et al. (1997). "Crosslinking of ANCA-antigens stimulates superoxide release by human neutrophils." J Am Soc Nephrol **8**(3): 386-94.

Kettritz, R., A. Schreiber, et al. (2001). "Role of mitogen-activated protein kinases in activation of human neutrophils by antineutrophil cytoplasmic antibodies." J Am Soc Nephrol **12**(1): 37-46.

Kitagawa, K., T. Wada, et al. (2004). "Blockade of CCR2 ameliorates progressive fibrosis in kidney." Am J Pathol **165**(1): 237-46.

Klebanoff, S. J. (1970). "Myeloperoxidase: contribution to the microbicidal activity of intact leukocytes." Science **169**(950): 1095-7.

Kluth, D. C., L. P. Erwig, et al. (2004). "Multiple facets of macrophages in renal injury." Kidney Int **66**(2): 542-57.

Kluth, D. C. and A. J. Rees (1999). "New approaches to modify glomerular inflammation." J Nephrol **12**(2): 66-75.

Koch, C. (1974). "Effect of sodium azide upon normal and pathological granulocyte function." Acta Pathol Microbiol Scand B Microbiol Immunol **82**(1): 136-42.

Kocher, M., J. C. Edberg, et al. (1998). "Antineutrophil cytoplasmic antibodies preferentially engage Fc gammaRIIIb on human neutrophils." J Immunol **161**(12): 6909-14.

Koldingsnes, W. and H. Nossent (2000). "Epidemiology of Wegener's granulomatosis in northern Norway." Arthritis Rheum **43**(11): 2481-7.

Kuligowski, M. P., R. Y. Kwan, et al. (2009). "Antimyeloperoxidase antibodies rapidly induce alpha-4-integrin-dependent glomerular neutrophil adhesion." Blood **113**(25): 6485-94.

Kurihara, T., G. Warr, et al. (1997). "Defects in macrophage recruitment and host defense in mice lacking the CCR2 chemokine receptor." J Exp Med **186**(10): 1757-62.

Landsman, L. and S. Jung (2007). "Lung macrophages serve as obligatory intermediate between blood monocytes and alveolar macrophages." J Immunol **179**(6): 3488-94.

Landsman, L., C. Varol, et al. (2007). "Distinct differentiation potential of blood monocyte subsets in the lung." J Immunol **178**(4): 2000-7.

Laudanna, C., G. Constantin, et al. (1994). "Sulfatides trigger increase of cytosolic free calcium and enhanced expression of tumor necrosis factor-alpha and interleukin-8 mRNA in human neutrophils. Evidence for a role of L-selectin as a signaling molecule." J Biol Chem **269**(6): 4021-6.

Lee, S., S. Huen, et al. (2011). "Distinct macrophage phenotypes contribute to kidney injury and repair." J Am Soc Nephrol **22**(2): 317-26.

Lehrer, R. I. (1971). "Inhibition by sulfonamides of the candidacidal activity of human neutrophils." J Clin Invest **50**(12): 2498-505.

Leigh, J., H. Wang, et al. (1997). "Silica-induced apoptosis in alveolar and granulomatous cells in vivo." Environ Health Perspect **105 Suppl 5**: 1241-5.

Leung, B. P., N. Sattar, et al. (2003). "A novel anti-inflammatory role for simvastatin in inflammatory arthritis." J Immunol **170**(3): 1524-30.

Li, L., L. Huang, et al. (2008). "The chemokine receptors CCR2 and CX3CR1 mediate monocyte/macrophage trafficking in kidney ischemia-reperfusion injury." Kidney Int **74**(12): 1526-37.

Lin, H., X. Chen, et al. (2002). "Inhibition of apoptosis in rat mesangial cells by tissue inhibitor of metalloproteinase-1." Kidney Int **62**(1): 60-9.

Liston, A., S. Lesage, et al. (2004). "Generalized resistance to thymic deletion in the NOD mouse; a polygenic trait characterized by defective induction of Bim." Immunity **21**(6): 817-30.

Little, M. A., G. Bhangal, et al. (2006). "Therapeutic effect of anti-TNF-alpha antibodies in an experimental model of anti-neutrophil cytoplasm antibody-associated systemic vasculitis." J Am Soc Nephrol **17**(1): 160-9.

Little, M. A., C. L. Smyth, et al. (2005). "Antineutrophil cytoplasm antibodies directed against myeloperoxidase augment leukocyte-microvascular interactions in vivo." Blood **106**(6): 2050-8.

Little, M. A., L. Smyth, et al. (2009). "Experimental autoimmune vasculitis: an animal model of anti-neutrophil cytoplasmic autoantibody-associated systemic vasculitis." Am J Pathol **174**(4): 1212-20.

Lloyd, C. M., M. E. Dorf, et al. (1997). "Role of MCP-1 and RANTES in inflammation and progression to fibrosis during murine crescentic nephritis." J Leukoc Biol **62**(5): 676-80.

Lloyd, C. M., A. W. Minto, et al. (1997). "RANTES and monocyte chemoattractant protein-1 (MCP-1) play an important role in the inflammatory phase of crescentic nephritis, but only MCP-1 is involved in crescent formation and interstitial fibrosis." J Exp Med **185**(7): 1371-80.

Lote, C. J. (2000). Principles of Renal Physiology, Kluwer Academic Publishers.

Luedke, E. S. and J. L. Humes (1989). "Effect of tumor necrosis factor on granule release and LTB4 production in adherent human polymorphonuclear leukocytes." Agents Actions **27**(3-4): 451-4.

Mack, M., J. Cihak, et al. (2001). "Expression and characterization of the chemokine receptors CCR2 and CCR5 in mice." J Immunol **166**(7): 4697-704.

Martinez, F. O., A. Sica, et al. (2008). "Macrophage activation and polarization." Front Biosci **13**: 453-61.

Mason, J. C. (2003). "Statins and their role in vascular protection." Clin Sci (Lond) **105**(3): 251-66.

Mason, J. C. (2005). "The statins--therapeutic diversity in renal disease?" Curr Opin Nephrol Hypertens **14**(1): 17-24.

Matteson, E. L., K. N. Gold, et al. (1996). "Long-term survival of patients with Wegener's granulomatosis from the American College of Rheumatology Wegener's Granulomatosis Classification Criteria Cohort." Am J Med **101**(2): 129-34.

Miller, A., N. Basu, et al. (2008). "Assessment of systemic vasculitis." Autoimmun Rev **8**(2): 170-5.

Mulder, A. H., P. Heeringa, et al. (1994). "Activation of granulocytes by anti-neutrophil cytoplasmic antibodies (ANCA): a Fc gamma RII-dependent process." Clin Exp Immunol **98**(2): 270-8.

Muller Kobold, A. C., C. G. Kallenberg, et al. (1998). "Leucocyte membrane expression of proteinase 3 correlates with disease activity in patients with Wegener's granulomatosis." Br J Rheumatol **37**(8): 901-7.

Nahrendorf, M., F. K. Swirski, et al. (2007). "The healing myocardium sequentially mobilizes two monocyte subsets with divergent and complementary functions." J Exp Med **204**(12): 3037-47.

Naito, M., H. Nagai, et al. (1996). "Liposome-encapsulated dichloromethylene diphosphonate induces macrophage apoptosis in vivo and in vitro." J Leukoc Biol **60**(3): 337-44.

Ng-Sikorski, J., R. Andersson, et al. (1991). "Calcium signaling capacity of the CD11b/CD18 integrin on human neutrophils." Exp Cell Res **195**(2): 504-8.

Niles, J. L., R. T. McCluskey, et al. (1989). "Wegener's granulomatosis autoantigen is a novel neutrophil serine proteinase." Blood **74**(6): 1888-93.

Nishida, M., Y. Okumura, et al. (2005). "Adoptive transfer of macrophages ameliorates renal fibrosis in mice." Biochem Biophys Res Commun **332**(1): 11-6.

Nishikawa, K., Y. J. Guo, et al. (1993). "Antibodies to intercellular adhesion molecule 1/lymphocyte function-associated antigen 1 prevent crescent formation in rat autoimmune glomerulonephritis." J Exp Med **177**(3): 667-77.

Nolan, S. L., N. Kalia, et al. (2008). "Mechanisms of ANCA-mediated leukocyte-endothelial cell interactions in vivo." J Am Soc Nephrol **19**(5): 973-84.

Noronha, I. L., C. Kruger, et al. (1993). "In situ production of TNF-alpha, IL-1 beta and IL-2R in ANCA-positive glomerulonephritis." Kidney Int **43**(3): 682-92.

Ohlsson, S., O. Bakoush, et al. (2009). "Monocyte chemoattractant protein 1 is a prognostic marker in ANCA-associated small vessel vasculitis." Mediators Inflamm **2009**: 584916.

Pankhurst, T., G. Nash, et al. (2011). "Immunoglobulin subclass determines ability of immunoglobulin (Ig)G to capture and activate neutrophils presented as normal human IgG or disease-associated anti-neutrophil cytoplasm antibody (ANCA)-IgG." Clin Exp Immunol **164**(2): 218-26.

Papiha, S. S., G. E. Murty, et al. (1992). "Association of Wegener's granulomatosis with HLA antigens and other genetic markers." Ann Rheum Dis **51**(2): 246-8.

Parsons, H. M., C. Ludwig, et al. (2007). "Improved classification accuracy in 1- and 2-dimensional NMR metabolomics data using the variance stabilising generalised logarithm transformation." BMC Bioinformatics **8**: 234.

Payne, T. G., A. D. Southam, et al. (2009). "A signal filtering method for improved quantification and noise discrimination in fourier transform ion cyclotron resonance mass spectrometry-based metabolomics data." J Am Soc Mass Spectrom **20**(6): 1087-95.

Pendergraft, W. F., 3rd, G. A. Preston, et al. (2004). "Autoimmunity is triggered by cPR-3(105-201), a protein complementary to human autoantigen proteinase-3." Nat Med **10**(1): 72-9.

Peveri, P., A. Walz, et al. (1988). "A novel neutrophil-activating factor produced by human mononuclear phagocytes." J Exp Med **167**(5): 1547-59.

Pfister, H., M. Ollert, et al. (2004). "Anti-neutrophil cytoplasmic autoantibodies (ANCA) against the murine homolog of proteinase 3 (Wegener's autoantigen) are pathogenic in vivo." Blood **104**(5): 1411-8.

Popa, E. R., C. A. Stegeman, et al. (2002). "Staphylococcus aureus and Wegener's granulomatosis." Arthritis Res **4**(2): 77-9.

Porges, A. J., P. B. Redecha, et al. (1994). "Anti-neutrophil cytoplasmic antibodies engage and activate human neutrophils via Fc gamma RIIa." J Immunol **153**(3): 1271-80.

Radford, D. J., J. M. Lord, et al. (1999). "The activation of the neutrophil respiratory burst by anti-neutrophil cytoplasm autoantibody (ANCA) from patients with systemic vasculitis requires tyrosine kinases and protein kinase C activation." Clin Exp Immunol **118**(1): 171-9.

Radford, D. J., J. M. Lord, et al. (1999). "The activation of the neutrophil respiratory burst by anti-neutrophil cytoplasm autoantibody (ANCA) from patients with systemic vasculitis requires tyrosine kinases and protein kinase C activation." Clin Exp Immunol **118**(1): 171-9.

Radford, D. J., N. T. Luu, et al. (2001). "Antineutrophil cytoplasmic antibodies stabilize adhesion and promote migration of flowing neutrophils on endothelial cells." Arthritis Rheum **44**(12): 2851-61.

Radford, D. J., C. O. Savage, et al. (2000). "Treatment of rolling neutrophils with antineutrophil cytoplasmic antibodies causes conversion to firm integrin-mediated adhesion." Arthritis Rheum **43**(6): 1337-45.

Rarok, A. A., P. C. Limburg, et al. (2003). "Neutrophil-activating potential of antineutrophil cytoplasm autoantibodies." J Leukoc Biol **74**(1): 3-15.

Reumaux, D., P. J. Vossebeld, et al. (1995). "Effect of tumor necrosis factor-induced integrin activation on Fc gamma receptor II-mediated signal transduction: relevance for activation of neutrophils by anti-proteinase 3 or anti-myeloperoxidase antibodies." Blood **86**(8): 3189-95.

Ricardo, S. D., H. van Goor, et al. (2008). "Macrophage diversity in renal injury and repair." J Clin Invest **118**(11): 3522-30.

Roach, J. P., E. E. Moore, et al. (2009). "Heme oxygenase-1 induction in macrophages by a hemoglobin-based oxygen carrier reduces endotoxin-stimulated cytokine secretion." Shock **31**(3): 251-7.

Rovin, B. H., N. Doe, et al. (1996). "Monocyte chemoattractant protein-1 levels in patients with glomerular disease." Am J Kidney Dis **27**(5): 640-6.

Rovin, B. H., M. Rumancik, et al. (1994). "Glomerular expression of monocyte chemoattractant protein-1 in experimental and human glomerulonephritis." Lab Invest **71**(4): 536-42.

Saitoh, A., K. Sekizuka, et al. (1998). "Detection of urinary MCP-1 in patients with diabetic nephropathy." Nephron **80**(1): 99.

Savage, C. O. (2001). "ANCA-associated renal vasculitis." Kidney Int **60**(4): 1614-27.

Savage, C. O., G. Gaskin, et al. (1993). "Anti-neutrophil cytoplasm antibodies can recognize vascular endothelial cell-bound anti-neutrophil cytoplasm antibody-associated autoantigens." Exp Nephrol **1**(3): 190-5.

Savage, C. O., L. Harper, et al. (2000). "ABC of arterial and vascular disease: vasculitis." BMJ **320**(7245): 1325-8.

Savage, C. O., B. E. Pottinger, et al. (1992). "Autoantibodies developing to myeloperoxidase and proteinase 3 in systemic vasculitis stimulate neutrophil cytotoxicity toward cultured endothelial cells." Am J Pathol **141**(2): 335-42.

Schlieben, D. J., S. M. Korbet, et al. (2005). "Pulmonary-renal syndrome in a newborn with placental transmission of ANCAs." Am J Kidney Dis **45**(4): 758-61.

Schreiber, A., A. Busjahn, et al. (2003). "Membrane expression of proteinase 3 is genetically determined." J Am Soc Nephrol **14**(1): 68-75.

Schreiber, A., F. C. Luft, et al. (2004). "Membrane proteinase 3 expression and ANCA-induced neutrophil activation." Kidney Int **65**(6): 2172-83.

Schreiber, A., H. Xiao, et al. (2009). "C5a receptor mediates neutrophil activation and ANCA-induced glomerulonephritis." J Am Soc Nephrol **20**(2): 289-98.

Schreiner, G. F., R. S. Cotran, et al. (1978). "A mononuclear cell component in experimental immunological glomerulonephritis." J Exp Med **147**(2): 369-84.

Segerer, S., Y. Cui, et al. (2000). "Expression of the chemokine monocyte chemoattractant protein-1 and its receptor chemokine receptor 2 in human crescentic glomerulonephritis." J Am Soc Nephrol **11**(12): 2231-42.

Sengelov, H., L. Kjeldsen, et al. (1993). "Control of exocytosis in early neutrophil activation." J Immunol **150**(4): 1535-43.

Serbina, N. V., T. Jia, et al. (2008). "Monocyte-mediated defense against microbial pathogens." Annu Rev Immunol **26**: 421-52.

Serbina, N. V. and E. G. Pamer (2006). "Monocyte emigration from bone marrow during bacterial infection requires signals mediated by chemokine receptor CCR2." Nat Immunol **7**(3): 311-7.

Southam, A. D., T. G. Payne, et al. (2007). "Dynamic range and mass accuracy of wide-scan direct infusion nanoelectrospray fourier transform ion cyclotron resonance mass spectrometry-based metabolomics increased by the spectral stitching method." Anal Chem **79**(12): 4595-602.

Spencer, S. J., A. Burns, et al. (1992). "HLA class II specificities in vasculitis with antibodies to neutrophil cytoplasmic antigens." Kidney Int **41**(4): 1059-63.

Springer, T. A. (1994). "Traffic signals for lymphocyte recirculation and leukocyte emigration: the multistep paradigm." Cell **76**(2): 301-14.

Stegeman, C. A., J. W. Tervaert, et al. (1994). "Association of chronic nasal carriage of Staphylococcus aureus and higher relapse rates in Wegener granulomatosis." Ann Intern Med **120**(1): 12-7.

Stein, M., S. Keshav, et al. (1992). "Interleukin 4 potently enhances murine macrophage mannose receptor activity: a marker of alternative immunologic macrophage activation." J Exp Med **176**(1): 287-92.

Sunderkotter, C., T. Nikolic, et al. (2004). "Subpopulations of mouse blood monocytes differ in maturation stage and inflammatory response." J Immunol **172**(7): 4410-7.

Swirski, F. K., M. Nahrendorf, et al. (2009). "Identification of splenic reservoir monocytes and their deployment to inflammatory sites." Science **325**(5940): 612-6.

Tadros, M., C. Pozzi, et al. (1993). "Characterization of anti-myeloperoxidase antibodies in vasculitis." Adv Exp Med Biol **336**: 291-4.

Taekema-Roelvink, M. E., C. van Kooten, et al. (1998). "Effect of anti-neutrophil cytoplasmic antibodies on proteinase 3- induced apoptosis of human endothelial cells." Scand J Immunol **48**(1): 37-43.

Tam, F. W., J. Smith, et al. (1999). "Development of scarring and renal failure in a rat model of crescentic glomerulonephritis." Nephrol Dial Transplant **14**(7): 1658-66.

Tang, W. W., M. Qi, et al. (1996). "Monocyte chemoattractant protein 1 mediates glomerular macrophage infiltration in anti-GBM Ab GN." Kidney Int **50**(2): 665-71.

Thomas, R. (2010). "The balancing act of autoimmunity: central and peripheral tolerance versus infection control." Int Rev Immunol **29**(2): 211-33.

Tipping, P. G., T. W. Leong, et al. (1991). "Tumor necrosis factor production by glomerular macrophages in anti-glomerular basement membrane glomerulonephritis in rabbits." Lab Invest **65**(3): 272-9.

Tzima, S., P. Victoratos, et al. (2009). "Myeloid heme oxygenase-1 regulates innate immunity and autoimmunity by modulating IFN-beta production." J Exp Med **206**(5): 1167-79.

van de Wiel, B. A., K. M. Dolman, et al. (1992). "Interference of Wegener's granulomatosis autoantibodies with neutrophil Proteinase 3 activity." Clin Exp Immunol **90**(3): 409-14.

van de Winkel, J. G. and P. J. Capel (1993). "Human IgG Fc receptor heterogeneity: molecular aspects and clinical implications." Immunol Today **14**(5): 215-21.

van der Geld, Y. M., T. Hellmark, et al. (2007). "Rats and mice immunised with chimeric human/mouse proteinase 3 produce autoantibodies to mouse Pr3 and rat granulocytes." Ann Rheum Dis **66**(12): 1679-82.

van der Veen, B. S., M. Chen, et al. (2011). "Effects of p38 mitogen-activated protein kinase inhibition on anti-neutrophil cytoplasmic autoantibody pathogenicity in vitro and in vivo." Ann Rheum Dis **70**(2): 356-65.

van der Veen, B. S., A. H. Petersen, et al. (2009). "Spatiotemporal expression of chemokines and chemokine receptors in experimental anti-myeloperoxidase antibody-mediated glomerulonephritis." Clin Exp Immunol **158**(1): 143-53.

van der Woude, F. J., N. Rasmussen, et al. (1985). "Autoantibodies against neutrophils and monocytes: tool for diagnosis and marker of disease activity in Wegener's granulomatosis." Lancet **1**(8426): 425-9.

van Rooijen, N., N. Kors, et al. (1989). "Macrophage subset repopulation in the spleen: differential kinetics after liposome-mediated elimination." J Leukoc Biol **45**(2): 97-104.

Van Rooijen, N. and A. Sanders (1994). "Liposome mediated depletion of macrophages: mechanism of action, preparation of liposomes and applications." J Immunol Methods **174**(1-2): 83-93.

van Rooijen, N. and A. Sanders (1997). "Elimination, blocking, and activation of macrophages: three of a kind?" J Leukoc Biol **62**(6): 702-9.

van Rooijen, N., A. Sanders, et al. (1996). "Apoptosis of macrophages induced by liposome-mediated intracellular delivery of clodronate and propamidine." J Immunol Methods **193**(1): 93-9.

van Rooijen, N. and R. van Nieuwmegen (1984). "Elimination of phagocytic cells in the spleen after intravenous injection of liposome-encapsulated dichloromethylene diphosphonate. An enzyme-histochemical study." Cell Tissue Res **238**(2): 355-8.

Varol, C., L. Landsman, et al. (2007). "Monocytes give rise to mucosal, but not splenic, conventional dendritic cells." J Exp Med **204**(1): 171-80.

von Muhlen, C. A. and E. M. Tan (1995). "Autoantibodies in the diagnosis of systemic rheumatic diseases." Semin Arthritis Rheum **24**(5): 323-58.

Wada T, Furuichi K, et al. (1999). "MIP-1alpha and MCP-1 contribute to crescents and interstitial lesions in human crescentic glomerulonephritis." Kidney Int. **56**(3): 9.

Wada T, Yokoyama H, et al. (1996). "Intervention of crescentic glomerulonephritis by antibodies to monocyte chemotactic and activating factor (MCAF/MCP-1)." FASEB J. **10**(12): 8.

Wang, Y. and D. C. Harris (2011). "Macrophages in renal disease." J Am Soc Nephrol **22**(1): 21-7.

Wang, Y., Y. P. Wang, et al. (2007). "Ex vivo programmed macrophages ameliorate experimental chronic inflammatory renal disease." Kidney Int **72**(3): 290-9.

Waskow, C., K. Liu, et al. (2008). "The receptor tyrosine kinase Flt3 is required for dendritic cell development in peripheral lymphoid tissues." Nat Immunol **9**(6): 676-83.

Watts, R. A., S. E. Lane, et al. (2001). "Epidemiology of vasculitis in Europe." Ann Rheum Dis **60**(12): 1156-7.

Watts, R. A. and D. G. Scott (2003). "Epidemiology of the vasculitides." Curr Opin Rheumatol **15**(1): 11-6.

Weber, R. J., A. D. Southam, et al. (2011). "Characterization of isotopic abundance measurements in high resolution FT-ICR and Orbitrap mass spectra for improved confidence of metabolite identification." Anal Chem **83**(10): 3737-43.

Weidner, S., M. Carl, et al. (2004). "Histologic analysis of renal leukocyte infiltration in antineutrophil cytoplasmic antibody-associated vasculitis: importance of monocyte and neutrophil infiltration in tissue damage." Arthritis Rheum **50**(11): 3651-7.

Westman, K. W., P. G. Bygren, et al. (1998). "Relapse rate, renal survival, and cancer morbidity in patients with Wegener's granulomatosis or microscopic polyangiitis with renal involvement." J Am Soc Nephrol **9**(5): 842-52.

Williams, J. M., A. Ben-Smith, et al. (2003). "Activation of the G(i) heterotrimeric G protein by ANCA IgG F(ab')2 fragments is necessary but not sufficient to stimulate the recruitment of those downstream mediators used by intact ANCA IgG." J Am Soc Nephrol **14**(3): 661-9.

Williams, J. M., L. Kamesh, et al. (2005). "Translating basic science into patient therapy for ANCA-associated small vessel vasculitis." Clin Sci (Lond) **108**(2): 101-12.

Winterbourn, C. C., M. C. Vissers, et al. (2000). "Myeloperoxidase." Curr Opin Hematol **7**(1): 53-8.

Xiao, H. (2009). Genetic control of the severity of experimental anti-MPO necrotizing and crescentic glomerulonephritis. the 14th International Vasculitis and ANCA workshop, Sweden, APMIS.

Xiao, H., P. Heeringa, et al. (2002). "Antineutrophil cytoplasmic autoantibodies specific for myeloperoxidase cause glomerulonephritis and vasculitis in mice." J Clin Invest **110**(7): 955-63.

Xiao, H., P. Heeringa, et al. (2005). "The Role of Neutrophils in the Induction of Glomerulonephritis by Anti-Myeloperoxidase Antibodies." Am J Pathol **167**(1): 39-45.

Xiao, H., A. Schreiber, et al. (2007). "Alternative Complement Pathway in the Pathogenesis of Disease Mediated by Anti-Neutrophil Cytoplasmic Autoantibodies." Am J Pathol **170**(1): 52-64.

Yang, J., A. Reutzel-Selke, et al. (2003). "Targeting of macrophage activity by adenovirus-mediated intragraft overexpression of TNFRp55-Ig, IL-12p40, and vIL-10 ameliorates adenovirus-mediated chronic graft injury, whereas stimulation of macrophages by overexpression of IFN-gamma accelerates chronic graft injury in a rat renal allograft model." J Am Soc Nephrol **14**(1): 214-25.

Yang, J. J., R. Kettritz, et al. (1996). "Apoptosis of endothelial cells induced by the neutrophil serine proteases proteinase 3 and elastase." Am J Pathol **149**(5): 1617-26.

Yang, Z. F., D. W. Ho, et al. (2005). "Allograft inflammatory factor-1 (AIF-1) is crucial for the survival and pro-inflammatory activity of macrophages." Int Immunol **17**(11): 1391-7.

Yokoo, T., T. Ohashi, et al. (1999). "Prophylaxis of antibody-induced acute glomerulonephritis with genetically modified bone marrow-derived vehicle cells." Hum Gene Ther **10**(16): 2673-8.

Yoshida, T., S. S. Tang, et al. (2002). "Global analysis of gene expression in renal ischemia-reperfusion in the mouse." Biochem Biophys Res Commun **291**(4): 787-94.

Yoshimura, T., K. Matsushima, et al. (1987). "Purification of a human monocyte-derived neutrophil chemotactic factor that has peptide sequence similarity to other host defense cytokines." Proc Natl Acad Sci U S A **84**(24): 9233-7.

Zode, G. S., A. Sethi, et al. (2011). "Transforming growth factor-beta2 increases extracellular matrix proteins in optic nerve head cells via activation of the Smad signaling pathway." Mol Vis **17**: 1745-58.